

TECHNICAL REPORT

Agricultural Systems in the San Joaquin Valley: Development of Emissions Estimates for Nitrogen Oxides

Contract Number: 94-732

Principal Investigators:

Pamela Matson
Mary Firestone

Prepared for:

State of California Air Resources Board
and the California Environmental Protection Agency

Prepared by:

Pamela Matson
Mary Firestone
Donald Herman
Tina Billow
Nancy Kiang
Tracy Benning
Josephine Burns

LIBRARY
CALIFORNIA AIR RESOURCES BOARD
P.O. BOX 2815
SACRAMENTO, CA 95812

Department of Environmental Science, Policy and Management
151 Hilgard Hall
University of California
Berkeley, CA 94305-3110
510 643-9880
FAX 510 643-5098

Disclaimer

The statements and conclusions on this report are those of the contractor and not necessarily those of the California Air Resources Board. The mention of commercial products, their source, or their use in connection with material reported herein is not to be construed as actual or implied endorsement of such products.

Acknowledgments

Tasks I and II of this project happened thanks to contributions of numerous scientists. We would first like to thank all the contributors in Appendix 1 who took time from their busy schedules to answer questions about crop distribution and management. We also owe a debt of gratitude to Fred Swanson (Superintendent of the Kearney Agricultural Center), Jimmie Ross (Superintendent of West Side Research Center), and Louis Whitendatle (Superintendent of Lindcove Field Station) for expediting the process of our proposals to conduct research at U.C. research centers; Jean Chevalier (Superintendent of Agriculture, Kearney Agricultural Center), Richard Schetter (Superintendent of Agriculture, West Side Agricultural Center), and Walter Stuttzman Superintendent of Agriculture, Lindcove Agricultural Center) for coordinating use of on-station facilities and sites; Pete Christiansen (Viticulture Specialist, Kearney Agriculture Center), Nick Dokoozlian (Viticulture Specialist, Kearney Agriculture Center) and Don May (Fresno County Farm Advisor); for use of their U.C. station research plots; Scott Johnson (Pomologist, Kearney Agriculture Center), Daniel Monk (Fresno County Farm Advisor), Carol Frate (Tulare County Farm Advisor), Thomas Johnson (Spreckels Sugar), Manuel Cunha (Nisei Farmer League), and Roger Isom (California Cotton Growers Association) for recruiting growers and arranging off-station sampling sites.

We are grateful to David Major, Adam Davis, Claire Eustace, Farhad Ghodrati, Ulysses Hillard, Steve Lindblom, Toby Sprunk, and Anna Thompson for technical support in field, laboratory, and data management operations.

This report was submitted in fulfillment of ARB 94-732: Agricultural Systems in the San Joaquin Valley: Development of Emissions Estimates for Nitrogen Oxides by the University of California, Berkeley under the sponsorship of the California Air Resources Board. Funds for M.K. Firestone and P.A. Matson from the California Agricultural Experiment Station and the USDA also contributed to the accomplishment of this project. Specifically, salaries for Firestone, Matson, Herman and Billow were covered by these latter sources. Work was completed as of January 31, 1997.

Abstract

The objective of this study was to estimate emissions of nitrogen oxides (NO_x) from agricultural systems in the San Joaquin Valley of California during the late summer period of maximum tropospheric ozone development. Nitrogen oxide fluxes were measured during July, August, and early September of 1995. Field sites that were utilized for sampling represented the most important crop types and the dominant fertilizer and irrigation management practices for the area. Hourly and daily flux data along with a spatial data base of crop type areas were used to extrapolate fluxes to county and Valley scales. Soil, climatic, and management factors that were important in controlling the rate and timing of NO_x flux from soil were identified.

Information on crop acreage for eight San Joaquin Valley counties was used to identify nine dominant crop types including: alfalfa, citrus, corn, cotton, grapes, irrigated pasture, stonefruits, sugar beets, vegetables, and other. Twenty-eight agricultural systems were identified that represented the most important crop types and the dominant fertilizer and irrigation management practices of the area. Diel measurements were carried out at least once on four sites; thirteen sites were sampled repeatedly over several week periods in order to estimate variation in fluxes within sites over time.

Soil water filled pore space (WFPS), soil temperature, air temperature, soil ammonium and nitrate, total soil organic nitrogen and organic carbon, soil pH, and soil texture were determined for all sites. Net and gross nitrogen mineralization and nitrification, and nitrification potentials were also measured for a subset of the sites.

There was substantial variability in NO_x fluxes among crops (crop mean fluxes at mid-day ranging from 1.0-9.1 $\text{ng-N cm}^{-2} \text{h}^{-1}$), with irrigated pastures, almonds, and tomatoes having generally high mean fluxes relative to the other crops. Variation among different fields of the same crop type was also very large (e.g., 0.13-17.53 $\text{ng-N cm}^{-2} \text{h}^{-1}$ for cotton, 0.16-15.69 $\text{ng-N cm}^{-2} \text{h}^{-1}$ for corn) and appeared to be related to proximity in time to a fertilizer application and soil moisture characteristics. The low fluxes measured from many of the sites during the July-August period reflected the management practices for that period of time. There was relatively little application of fertilizer to crops during this mid-summer period. Sites sampled during or immediately after fertilizer application (one each of almonds, corn, and cotton) showed substantially higher NO_x flux values than did the same fields or other fields of the same crop type when they were not sampled soon after fertilization.

Two types of regression models were developed to relate NO_x fluxes to environmental or soil variables: 1) Point-predictive model, which is

driven by information on crop type, WFPS, soil texture, soil temperature, soil NO_3^- and NH_4^+ , total soil C and N, and field position. 2) Management model, which is driven by crop type, fertilizer characteristics, WFPS, pH, and air temperature. The management model was designed to utilize more generally available data for the development of regional emissions estimates. By incorporating important controllers of NO_x flux from soil, especially WFPS and temperature, the management model developed and evaluated here improves our capacity to predict NO_x fluxes under a variety of cropping and management regimes as compared to single-factor empirical models.

GIS-based data on major crop types in the San Joaquin Valley was used to calculate hourly and daily NO_x flux by crop type and county, which could then be summed to estimate total flux for the Valley. Cotton, which had an intermediate mean mid-day hourly flux in comparison with other crops, had the highest total Valley hourly flux (232120.9 g-N h^{-1}) due to a large total acreage. Grapes were calculated to have the next largest total flux when summed over the Valley. Total flux values however can mask the spatial component of the fluxes which may be critical in determining air chemistry. Spatial distribution of NO_x fluxes was presented for seven San Joaquin Valley counties. Total mid-day hourly flux ranged from 60265 to 188422 g-N h^{-1} , with the counties with the highest to lowest fluxes following this sequence: Fresno, Kern, Tulare, San Joaquin, Merced, Kings, Madera.

Agricultural Systems in the San Joaquin Valley: Development of Emissions Estimates for Nitrogen Oxides

Table of Contents

List of Figures

List of Tables

Executive Summary

1. Project Objectives

2. Tasks: Methods and Results

2.1 Task I. Systematic Sampling plan.

2.1.1 Methods.

2.1.2 Results.

2.2 Task II. Field Studies.

2.2.1 Methods.

2.2.1.1 Field Methods.

2.2.1.2 Laboratory Methods.

2.2.1.3 Data Management.

2.2.1.4 Estimation of Diel Fluxes.

2.2.2 Results.

2.2.2.1 Diel Flux Calculation Results.

2.2.2.2 Daily Maximum Fluxes for NO_x .

2.2.2.3 Soils and Process Data.

2.2.2.4 Results Summary.

2.3 Task III. Soil Emissions.

2.3.1 Extrapolation Approach.

2.3.1.1 GIS-Based Crop Maps and Extrapolation Approaches.

2.3.1.2 Results.

2.3.2 Statistical Model Development.

2.3.2.1 Approach.

2.3.2.2 Results.

2.3.2.2.1 Application of Williams' Model.

2.3.2.2.2 Point Predictive Model.

2.3.2.2.3 Management Model.

2.3.2.2.4 Comparison of models.

2.3.2.2.5 Comparison of Davidson Model (CASA) and San Joaquin Valley NO_x data.

2.3.3 Discussion.

2.4 Task IV. Integrated Field Measurement Program.

3.0 Summary and Conclusions

List of Figures

- Figure 1. Targeted crop systems, indicating typical fertilization and irrigation practices in the San Joaquin Valley.
- Figure 2. Tactical display of sites sampled for NO_x emissions in the San Joaquin Valley, July-September, 1995.
- Figure 3a. Diel plots: time of day vs. measured NO_x flux by crop, site, position, and date (corn and grapes).
- Figure 3b. Diel plots: time of day vs. measured NO_x flux by crop, site, position, and date (almonds).
- Figure 3c. Diel plots: time of day vs. measured NO_x flux by crop, site, position, and date (cotton).
- Figure 4a. Diel plots: time of day vs. measured NO_x flux, with 95% confidence interval (corn and grapes).
- Figure 4b. Diel plots: time of day vs. measured NO_x flux, with 95% confidence interval (almonds).
- Figure 4c. Diel plots: time of day vs. measured NO_x flux, with 95% confidence interval (cotton).
- Figure 5. Diel characteristic curves: means and 95% confidence envelopes by crop and position, with dates averaged.
- Figure 6a. NO_x flux and associated soil parameters: Site B, flood-irrigated almonds, Parlier, CA.
- Figure 6b. NO_x flux and associated soil parameters: Site C, drip-irrigated almonds, Parlier, CA.
- Figure 6c. NO_x flux and associated soil parameters: Site D, cotton, San Joaquin, CA.
- Figure 6d. NO_x flux and associated soil parameters: Site I, corn, Tulare, CA.
- Figure 6e. NO_x flux and associated soil parameters: Site J, corn, Plainview, CA.
- Figure 6f. NO_x flux and associated soil parameters: Site K, corn, Waukena, CA.
- Figure 6g. NO_x flux and associated soil parameters: Site Q, drip-irrigated grapes, Kearney Agricultural Center.
- Figure 6h. NO_x flux and associated soil parameters: Site R, flood-irrigated grapes, Kearney Agricultural Center.
- Figure 6i. NO_x flux and associated soil parameters: Site T, oranges, U.C. Lindcove Field Station.
- Figure 6j. NO_x flux and associated soil parameters: Site V, peaches, Wawona, CA.
- Figure 6k. NO_x flux and associated soil parameters: Site W, irrigated pasture, Bonadelle Ranchos, CA.

- Figure 6l. NO_x flux and associated soil parameters: Site X irrigated pasture, Bonadelle Ranchos, CA.
- Figure 6m. NO_x flux and associated soil parameters: Site Y, cotton, U.C. West Side Field Station.
- Figure 6n. NO_x flux and associated soil parameters: Site Z, tomatoes, U.C. West Side Field Station.
- Figure 7. Mean mid-day NO_x fluxes averaged for each crop measured in the San Joaquin Valley, July-September, 1995.
- Figure 8. Mean mid-day NO_x fluxes for sites sampled in the San Joaquin Valley, July-September, 1995.
- Figure 9. Comparison of NO_x flux measured in the San Joaquin Valley, July-September 1995, to predictions of NO_x flux estimated from water-filled pore space by the Davidson CASA model.
- Figure 10. Relationship of NO_x flux to nitrification potential.
- Figure 11. Relationship of NO_x flux to gross nitrate production.
- Figure 12a. Estimated NO_x emissions: Fresno County.
- Figure 12b. Estimated NO_x emissions: Kern County.
- Figure 12c. Estimated NO_x emissions: Kings County.
- Figure 12d. Estimated NO_x emissions: Madera County.
- Figure 12e. Estimated NO_x emissions: Merced County.
- Figure 12f. Estimated NO_x emissions: San Joaquin County.
- Figure 12g. Estimated NO_x emissions: Tulare County.
- Figure 13a. "A" factors fitted to San Joaquin Valley NO_x data for Williams' Model, using data collected at individual chambers.
- Figure 13b. "A" factors fitted to San Joaquin Valley NO_x data for Williams' Model, using site means for all data.
- Figure 14. Alternating Conditional Expectations (ACE) transformations to the variables used in the point-predictive model, developed using NO_x emissions and site- and chamber-level variables measured in the San Joaquin Valley, July-September, 1995.
- Figure 15a. Coefficients derived from fitting point predictive model to NO_x flux data: Crop interaction with soil temperature.
- Figure 15b. Coefficients derived from fitting point predictive model to NO_x flux data: Crop Effects.
- Figure 15c. Coefficients derived from fitting point predictive model to NO_x flux data: Soil Texture Effects.
- Figure 15d. Coefficients derived from fitting point predictive model to NO_x flux data: Position Effects.
- Figure 16. Alternating Conditional Expectations (ACE) transformations to the variables used in the management model, developed using NO_x emissions and site-level variables measured in the San Joaquin Valley, July-September, 1995.

- Figure 17a. Coefficients derived from fitting management model to NO_x flux data: Crop Interaction with Air Temperature.
- Figure 17b. Coefficients derived from fitting management model to NO_x flux data: Crop Effects.
- Figure 17c. Coefficients derived from fitting management model to NO_x flux data: Soil Texture Effects.
- Figure 17d. Coefficients derived from fitting management model to NO_x flux data: Effect of Fertilizer.

List of Tables

- Table 1. Acreages of San Joaquin Valley agricultural crops obtained from the 1993 County Agricultural Report Data.
- Table 2. Index of sites sampled for NO_x emissions, July-September 1995 in the San Joaquin Valley.
- Table 3. Code, crop, location, date of fertilization, and nitrogen fertilization record for San Joaquin Valley sites sampled for NO_x emissions July-September 1995.
- Table 4. Crop type, soil texture, fertilization type, irrigation type, and number of NO_x flux measurements at each site.
- Table 5. Dates and numbers of observations for NO_x emissions measured at each site in the San Joaquin Valley, July-September 1995.
- Table 6. Summary of: (a) fitted diel curves; and (b) characteristic diel curves for each crop type at sites located in the San Joaquin Valley measured July-September 1995.
- Table 7. Mid-day NO_x flux and total daily NO_x flux (predicted from diel curves) measured in the San Joaquin Valley, July-September 1995.
- Table 8. Mean hourly NO_x fluxes for each crop type, based on measurements taken mid-day in each site.
- Table 9. Comparison of crop categories used by the 1993 County Agricultural Commissioners's report and the Department of Water Resources Database for the San Joaquin Valley.
- Table 10. Area (ha) occupied by major land use types in San Joaquin Valley counties.
- Table 11a. Area occupied by surveyed crops, mean measured mid-day NO_x fluxes (ng-N km⁻² h⁻¹) for each crop weighted by position, and total NO_x flux for each crop summed over 7 San Joaquin Valley counties made July-September, 1995.
- Table 11b. Total NO_x flux for each crop within 7 San Joaquin Valley counties.

Executive Summary

The objective of this study was to estimate emissions of nitric oxide and nitrogen dioxide (together referred to as NO_x) from agricultural systems in the San Joaquin Valley of California during the months of July and August (periods of maximum tropospheric ozone development). We measured NO_x fluxes in agricultural systems representing the most important crop types, and utilizing the dominant fertilizer and irrigation management practices. We used hourly and daily flux data along with a spatial data base of crop types to extrapolate fluxes to the area of the Valley. We also identified the factors that control the rate and timing of NO_x fluxes, and we suggest ways that this information can be used in the development of spatially explicit models.

The project was organized around four sequential tasks. In the following paragraphs, we will summarize the approach and results of each.

Task I. Determine the most important crop/management practices in the San Joaquin Valley (in terms of area extent of crop type and amounts of fertilizer used) and use this information to develop a systematic sampling plan.

Utilizing information from the "1993 Agricultural Commissioners' Report Data" and the "1990 Engineering Science Design Research Planning Final Report to the Environmental Protection Agency (EPA): Leaf Biomass Density and Land Use Data for Estimating Vegetative Emissions", we tabulated crop acreage for the eight San Joaquin Valley counties. We identified nine dominant types, including alfalfa, citrus, corn, cotton, grapes, irrigated pasture, stonefruits, sugar beets, vegetables, and other. We identified 28 agricultural systems representing the most important crop types and the dominant fertilizer and irrigation management practices. Diel measurements (measurements carried out over a 24 hour period) were carried out at least once on 4 agricultural systems; 13 of the 28 were sampled repeatedly over several week periods in order to estimate means and variation in fluxes within sites over time.

Task II. Carry out field studies of soil NO_x fluxes measured simultaneously with measurements of environmental and edaphic (soil) characteristics of importance in regulating NO_x emission, and carry out laboratory analyses of soil samples collected simultaneously with NO_x flux.

We measured soil surface NO_x fluxes, water-filled pore space (WFPS), soil temperature, air temperature, ammonium and nitrate in the soil, total soil nitrogen and carbon, pH, and soil texture for all of the sites. Soil characteristics were measured for the top 10 cm of soil. In a subset of the sites, we carried out measurements of net and gross nitrogen mineralization and nitrification and nitrification potentials. In general, there was substantial variability in mean midday NO_x fluxes among crops (range 1.0-9.1 $\text{ng-N cm}^{-2} \text{h}^{-1}$), with irrigated pastures, almonds, and tomatoes having generally high fluxes relative to the other crops (crop mean mid-day fluxes of 9.1, 6.4, and 7.2 $\text{ng-N cm}^{-2} \text{h}^{-1}$ for pastures, almonds, and tomatoes respectively; range for other crops: 1.0 - 5.8 $\text{ng-N cm}^{-2} \text{h}^{-1}$). In the case of almonds and irrigated pasture, mean fluxes were consistently high from site to site and date to date. However, for some of the other crops, variation among different fields or sampling dates were very large (e.g., 0.13-17.53 $\text{ng-N cm}^{-2} \text{h}^{-1}$ for cotton, 0.16-15.69 $\text{ng-N cm}^{-2} \text{h}^{-1}$ for corn) and appeared to be related to proximity in time of our measurements to a fertilizer event and to water-filled pore space at the time of sampling. Within a given site, mean fluxes for different days varied by over an order of magnitude, apparently as a consequence of changes in soil inorganic N and in water filled pore space. This temporal variation at the scale of individual fields suggests that estimation of fluxes on a daily or hourly basis, as is needed for air quality and chemical transport models, will be difficult without information on the temporal and spatial distribution of fertilizer and irrigation as well as the more easily obtained information on air temperature.

Task III. Develop soils emissions statistical models based on the field and laboratory study data, and develop spatially and temporally explicit estimates of NO_x flux at the soil-air interface for the San Joaquin Valley for the months of July, August and early September, 1995.

We developed two sets of regression models relating NO_x flux to other variables measured in the field.

a) Models that require more detailed soil variables and that will be useful in process modeling frameworks ("Point-predictive model"). e.g. $\text{NO}_x = f(\text{crop type, \%WFPS, soil texture, soil temperature, soil } \text{NO}_3^-, \text{NO}_2^-, \text{ and } \text{NH}_4^+ \text{ concentrations, total organic carbon concentration, total organic nitrogen concentration, position within the field -- under canopy/open and furrow/ridge})$.

b) Models that can be applied at a regional scale using spatial data bases of crop type, soils and climate ("Management model"). e.g. $\text{NO}_x =$

f(crop type, air temperature, soil texture, soil pH, an index of fert amount, type and timing, and mean WFPS).

We compared the outputs of our models to those of the Williams model, which uses air temperature as well as an empirically-derived "A value" to drive predictions of NO_x flux. The Point-predictive model and the Management model both substantially improved the prediction of NO_x fluxes across a variety of crops and sites, in contrast to the Williams model. In fact, for most crops, WFPS was as important as temperature in the prediction of NO_x emissions.

We also compared our NO_x flux data to the Davidson model of NO_x flux as a function of soil WFPS (the functional relationship used in the CASA model). There was reasonably good agreement between the summer '95 San Joaquin Valley NO_x flux vs. soil WFPS and that predicted by Davidson. Both show maximum NO_x fluxes occurring at about 50% WFPS; however the San Joaquin Valley data show significant NO_x fluxes occurring at very low water contents (WFPS 1-3 %), a result not predicted by previous models but which has been reported in other measurement studies.

GIS-based data on major crop types in the San Joaquin Valley were used in combination with measured mid-day mean fluxes and calculated daily fluxes for each crop type, in order to calculate hourly and daily NO_x flux by crop type, county, and for the entire San Joaquin Valley area that the GIS data covered. Cotton, which had an intermediate mean mid-day flux in relation to other crops, had the highest Valley-scale flux (232120.9 g/h) due to its large total acreage. Grapes were calculated to have the next largest mid-day hourly flux when summed over the Valley (142936.1 g/h). Among San Joaquin Valley counties, Fresno county had the highest flux summed over the crop types we measured (188422 g-N h⁻¹), while Madera county had the lowest (60265 g-N h⁻¹). The estimated spatial distribution of NO_x flux (which may be an important factor in air chemistry) is presented in map and tabular format.

Task IV. Once the systems with greatest soil fluxes have been identified, begin planning for integrated field studies (to take place in 1996 or later) in several sites to determine the role of vegetation canopies and boundary layer chemistry and dynamics in controlling the contributions and role of soil NO_x emissions in ozone formation.

Planning for integrated field studies should begin with estimation of the potential role of soil NO_x fluxes via air chemistry modeling. Given the range in variability in fluxes measured in our sites during the July-August period, we suggest that air quality modeling experiments be carried out

utilizing the highest and lowest site means measured for the different crops, in addition to the average flux by crop. If such modeling experiments reveal circumstances under which agricultural soils play a critical role in air chemistry, multi-disciplinary studies that couple soil and canopy-scale flux measurements with atmospheric chemistry studies may be appropriate. For such studies, we suggest emphasizing regions with relatively homogeneous expanses of crops with high flux characteristics, such as irrigated pasture or almonds, and as appropriate, with concurrent use of fertilizer.

Overall Conclusions

The San Joaquin Valley is an highly complex agricultural system, composed of at least nine dominant crop types (alfalfa, citrus, corn, cotton, grapes, irrigated pasture, stonefruits, sugar beets, vegetables) as well as other crops, grown on a range of soils and managed under a number of different fertilizer and irrigation management practices. Because NO_x fluxes are potentially influenced by the types of plants growing in the fields as well as by the soils being cropped and by the ways those crops are managed, NO_x fluxes should be expected to show a large degree of spatial and temporal variation within the Valley. The data presented in this document substantiate this expected large range of variation.

The implications of this variability are several. First, it suggests that carrying out a field sampling program that encompasses that variability is a very difficult task. Fluxes change from field to field, crop to crop, and day to day. Therefore, while our flux estimates for given sites and days are accurate, their extrapolation to all sites within a given crop and to all dates within the July-August time-frame must be viewed as rough approximations rather than reality. On the other hand, our data do indicate some consistencies. For example, they indicate that almonds and irrigated pasture have typically higher fluxes than other crops we measured, whereas the other crops have greater ranges in fluxes from time to time or site to site. Also, our data quite clearly suggest that NO_x fluxes in the San Joaquin Valley in July and August 1995 were not remarkably high in comparison with the range of values published in the literature. (We note, however, that we cannot draw conclusions about the relative importance of agricultural soil NO_x emissions in atmospheric chemistry in the San Joaquin Valley by simply looking at these flux values, and we leave it to air quality modelers within the California Air Resources Board to develop that analysis.)

The large potential for spatial and temporal variability in the Valley agricultural system also suggests that, given the difficulties inherent in NO_x measurements and the cost of the instruments used to measure NO_x

flux at the soil-air or canopy-air interface, detailed spatial monitoring of those fluxes (even for a short period) is logistically impossible. We believe a viable alternative for estimation of NO_x in complex systems like the San Joaquin Valley is the development and use of predictive models that can utilize spatially and temporally-varying data on crops, soils, climate/weather, and management. We have developed such models as part of this project. One critical conclusion drawn from the model development task is that accurate prediction for most crop types in the Valley require more than just temperature, the variable used in the only other commonly used NO_x model (Williams et al 1992). Rather, our point-based "Point-predictive model" and the site-based "Management model" both indicate that soil moisture (described here as %WFPS) is at least as important as temperature, and that variables describing either soil inorganic nitrogen concentrations or fertilization activity are also important. Given our process-based understanding of the interactive controls of nitrogen, water, and temperature on NO_x production and emission, we find these results entirely consistent.

While our models are ready for use at the site level, their application at the scale of the Valley will require several additional steps. First, while spatially-explicit data bases on crop type, soil characteristics like texture, organic C, organic N and pH, and meteorological station data such as air temperature and precipitation are generally available, spatially-explicit data bases on fertilizer type, rate, and time of application, and on irrigation use and thus change in water-filled pore space in the soil, are not available. What may be more available are county-wide monthly data on fertilizer use and on allocation of water for irrigation. Short of doing detailed farm-by-farm surveys of fertilizer and water use, we believe it may be possible to develop models of irrigation and fertilizer applications that distribute county totals as a function of crop type and weather conditions. Once such models have been developed and the NO_x models run at the scale of the Valley, validation through measurements of soil-air and canopy-air exchange of NO_x at select sites would be required. These tasks are outside the scope of this project.

Finally, it is worthwhile to note that our analysis of San Joaquin soils fluxes reflects the current management framework for the Valley, that is, there is relatively little application of fertilizer to crops during the July-August period. Any changes in management practices that lead to increased application of fertilizer during or immediately preceding this July-August time frame may lead to very significant increases in NO_x flux from soils. Thus, the importance of San Joaquin Valley agricultural soils as contributors to air quality in California cannot be assumed to be

constant year to year, but rather will change as a function of the crop type, fertilizer and irrigation employed in the valley.

1. Project Objectives

The objective of this study was to estimate emissions of nitric oxide and nitrogen dioxide, together referred to as NO_x , from agricultural systems in the San Joaquin Valley of California during the months of July and August (periods of maximum tropospheric ozone development). We measured NO_x fluxes in agricultural systems representing the most important crop types, and utilizing the dominant fertilizer and irrigation management practices. We used hourly and daily flux data along with a spatial data base of crop types to extrapolate fluxes to the area of the Valley. We also identified the factors that control the rate and timing of NO_x fluxes, and suggest ways that this information can be used in the development of spatially explicit models.

Background

Growth and productivity of crops are most frequently limited by the availability of nitrogen; nitrogen, therefore, accounts for the bulk of fertilizer applied worldwide. Today, over 80 Tg (80×10^{12} g) of nitrogen are produced and applied globally each year, an amount equivalent to the natural inputs of nitrogen via biological nitrogen fixation in terrestrial ecosystems (Vitousek and Matson 1993). California alone applies over 0.5 Tg of N annually (California Department of Food and Agriculture 1994).

Numerous studies have demonstrated that nitrogen fertilization in temperate agriculture leads both to increased leaching of nitrate to ground and surface water (e.g., Turner and Rabalais 1991) and to increased emissions of nitrous oxide, a greenhouse gas, to the atmosphere (see Eichner 1990 for a review). The consequences of fertilizer use on nitric oxide (NO) and/or nitrogen dioxide (NO_2) emissions have received much less attention. Nitric oxide is produced by biological and chemical processes in the soil, including nitrification and denitrification -- the same microbial processes that produce nitrous oxide (Firestone and Davidson 1989, Hutchinson and Davidson 1993). While NO is an intermediate in denitrification, NO_x flux from soils in which denitrification is occurring is generally very low. It is likely that in field situations with conditions of high soil moisture that are conducive to denitrification, any NO_x that is produced is consumed before it can diffuse through the soil (Remde et al 1989, Williams et al 1992a). The production of NO_x during nitrification is poorly understood, but the soil studies that have been done suggest that NO_x production via nitrification is far greater than rates of N_2O production (Tortoso and Hutchinson 1990, Davidson 1992, Davidson et al. 1993); thus, relatively large losses of NO_x are expected when substrate for

nitrification (i.e., ammonium) is available and when soil conditions are aerobic and moist but not saturated.

In the atmosphere, NO_x is reactive, with a lifetime of hours to days; consequently, its effects are regional in scale. Nitric oxide plays key roles in regulating the concentration of the main oxidizing agent in the atmosphere, the hydroxyl radical, and contributes, often in a rate-limiting way, to the photochemical formation of tropospheric ozone, a major atmospheric pollutant (Jacob and Wofsy 1990, Williams et al. 1992a). Moreover, it is a precursor to nitric acid, a principal component of acid deposition. Nitric acid deposition represents one pathway by which nitrogen applied in agricultural systems can be transferred to natural systems (Melillo et al. 1989). Thus, agricultural systems that lose fertilizer nitrogen in the form of NO_x may be significant non-point sources of air pollution (Vitousek and Matson 1993, Hall et al. in press).

Despite its potential importance, there are currently very few published estimates of NO_x flux in agricultural systems (none in California), but these studies indicate significant effects of fertilization on NO_x fluxes (Johansson and Granat 1984, Williams et al. 1988, Hutchinson and Brams 1992, Shepard et al. 1991, Williams et al. 1992a, Williams et al. 1992b, Keller and Matson 1994, Matson et al. in press, Hall et al. in press). Williams et al. (1992b) used an empirical model based on relationships between NO_x and soil nitrate and temperature to derive continental scale estimates of NO_x flux from natural and agricultural systems; they estimate that agricultural lands account for 66% of the land source of NO_x in the United States, and suggest that NO_x fluxes in agricultural areas may have a significant effect on atmospheric mixing ratios, ozone production, and acid deposition. Because of the dearth of field data, no statistical analysis of the role of crop, fertilizer type or management has been possible. We developed a data base for NO_x emissions for the San Joaquin Valley, California.

2. Tasks: Methods and Results

We utilized a systematic, phased study in which we addressed the following tasks:

Task I. Determine the most important crop/management practices in the San Joaquin Valley (in terms of area extent of crop type and amounts of fertilizer used) and use this information to develop a systematic sampling plan;

Task II. Carry out field studies of NO_x fluxes measured simultaneously with measurements of environmental and edaphic variables of

importance, and carry out laboratory analyses of soil samples collected during the field studies;

Task III. Develop soils emissions statistical models based on the field study data, and develop spatially and temporally explicit estimates of NO_x flux at the soil-air interface for the San Joaquin Valley for the months of July and August, 1995.

Task IV. Once the systems with greatest soil fluxes have been identified, begin planning for integrated field studies (to take place in 1996 or later) in several sites to determine the role of vegetation canopies and boundary layer chemistry and dynamics in controlling the contributions and role of soil NO_x emissions in ozone formation.

2.1 Task I. Systematic Sampling plan.

2.1.1 Methods.

Task I involved: (i) identifying the dominant San Joaquin Valley crops, as well as common soil types and management practices for each crop; and (ii) selecting sampling sites representing the dominant crop-soil-management types.

We tabulated crop acreage in each of the eight San Joaquin Valley counties using 1993 County Agricultural Commissioners' Report Data (California Department of Food and Agriculture) (Appendix C), and Engineering Science Design Research Planning's final Report to the U.S. Environmental Protection Agency: Leaf Biomass Density and Land Use Data for Estimating vegetative emissions (1990). Not including nonirrigated rangeland, we identified nine dominant crop types (Table 1).

We next identified the major nitrogen fertilizer types, rates, and application methods used for various crops, and the dominant irrigation types. Sources included: (i) the Radian Corporation's Final Report: AUSPEX Ammonia Emission Inventory / Data Collection Effort (1992); (ii) Fertilizing Materials Tonnage Report, January - June, 1994 (California Department of Food and Agriculture); (iii) interviews with twenty-two county farm advisors, extension specialists, and University of California, Davis faculty (Appendix B). The interviews were particularly useful to identify management practices (including fertilizer use) *currently* being implemented.

Soils on the west side of the valley lie predominantly on the Coast Range alluvial fans; the Tulare lake basin and various stream channels characterize soils along the center of the valley; and Sierran alluvial fan soils are common on the east side of the valley. The

Table 1. Acreage of San Joaquin Valley agricultural crops obtained from the 1993 County Agricultural Report Data (California Dept. of Food and Agriculture).

County	Alfalfa	Citrus	Corn	Cotton	Grapes	Irrig. Pasture
San Joaquin	64,000		81,600			23,700
Stanislaus	40,200		42,700		17,200	75,500
Merced	75,220		50,540	79,200	14,338	80,000
Madera	31,800		12,800	51,400	81,644	20,000
Fresno	66,000	23,218	24,200	377,700	208,228	40,000
Tulare	76,900	103,357	70,700	148,065	73,580	12,400
Kings	27,457		25,598	266,315	3,905	11,000
Kern	78,568	34,835		300,759	73,719	10,000
Total	460,145	161,410	308,138	1,223,439	472,614	272,600

County	Prunus (including almonds)	Sugar Beets	Vegetables	Other ¹
San Joaquin	36,100	36,800	28,624	118,196
Stanislaus	88,100	3,870	69,905	106,518
Merced	76,711	19,100	46,600	122,646
Madera	42,454	3,700	7,991	63,339
Fresno	80,586	33,200	209,045	181,075
Tulare	63,915	3,600	19,677	207,666
Kings	10,111	2,016	20,894	144,448
Kern	79,453	10,650	74,093	167,742
Total	477,430	112,936	476,829	1,111,630

¹ "Other" crops include rice, safflower, seeds, onions, garlic, olives, sorghum, hay (other than alfalfa), silage (other than corn), and other fruits and nuts.

alluvial fan soils have various loamy textures, and the basin and stream channel soils range from shallow, poorly drained clayey soils to well-drained sandy soils. We identified boundaries of these materials using Geologic Maps of California (United States Geological Survey). While interviewing farm advisors for fertilizer and irrigation usage, we also queried them for soil characteristics that particular crops favor.

Criteria for selecting crop systems involved identifying the dominant crops in the valley, soils on which they were grown, and their dominant management regimes (Figure 1). Crops selected were planted to a total of 100,000 acres in eight San Joaquin Valley counties. Both the alluvial fan soils and basin soils were selected for crops commonly grown on both soils; otherwise only the dominant soil for a given crop was selected. Likewise, several irrigation or fertilization types were selected for crops commonly managed under several regimes, otherwise only the dominant practice was selected.

Crop	Soil	Irrigation	Fertilization Rates (kg N/ha)	Fertilizer Types [‡]	Codes [§]
cotton	fan	flood	200	anhydrous NH ₃ , UN-32	
		sprinkler	200	UN-32	
		furrow	120-280	urea, UN-32	Y*
	basin	furrow	180-250	UN-32	D*E*F [†]
		sprinkler	250	UN-32, NH ₃ , foliar	G [†]
alfalfa	fan	border check	0		O [†]
			20	11-52-0, UN-32, (NH ₄) ₂ SO ₄	P [†]
	basin	border check	0		A [†]
			20	UN-32, (NH ₄) ₂ SO ₄	
citrus	fan	drip	110-140	Ca(NO ₃) ₂ , urea	T*
stonefruits	fan	flood	100-300	CAN-17, UN-32, (NH ₄) ₂ SO ₄ , NH ₄ NO ₃	B*V*
		drip	150-300	NH ₄ NO ₃ , UN-32, CAN-17	C*
	basin	drip	150-250	CAN-17	

corn	fan	furrow	150-435	11-52-0, NH ₃ , UN-32	J*K*
	basin	furrow	200-435	11-52-0, NH ₃ , UN-32	I*
grapes	fan	flood	20-100	aqua NH ₃ , NH ₄ NO ₃ , UN-32	L*R*
		drip	20-100	CAN-17	Q*
irrig. pasture	fan	border check	0	Dairy Manure Disposal	M [†]
			High		
	basin	border check	0		W [†] X [†]
vegetables	fan	furrow	60-600	11-52-0, urea, aqua NH ₃	Z*
sugar beets	basin	furrow	125-350	10-34-0, 11-52-0, UN-32, NH ₃	H [†] N [†] S [†] U [†]
	fan	furrow	120-180	UN-32, anhydrous NH ₃	

Figure 1. Targeted crop systems, indicating typical fertilization and irrigation practices in the San Joaquin Valley in 1995.

* indicates sites sampled intensively, [†] indicates sites sampled extensively, § site codes are explained in Table 2, ‡UN-32 is a urea-nitrate fertilizer, and CAN-17 is a calcium-ammonium-nitrate fertilizer.

2.1.2 Results.

Selecting field sites for targeted crops systems was more difficult than expected. Seven sites were located on University of California agricultural research stations, the remaining 19 were on private lands ranging from Kings to Madera counties (Figure 2, Table 2). Sites on U.C. research stations were only included if they were managed as typical of nearby off-station growers (for example, check plots or experimental controls). Numerous prospective sites on U.C. research stations were rejected because they were receiving experimental treatments or otherwise managed atypically. In selecting sites, we achieved a broad spectrum of nitrogen fertilization types, rates, and application methods (Table 3).

As noted in Table 3, only cotton, corn, and alfalfa were fertilized during the study period. According to our interviews and survey, these are the only crops typically fertilized during July and August. For this study, we purposefully followed the NO_x response to fertilization in two fields; our soil sampling, however, suggests that the effects of previous fertilization on soil inorganic nitrogen were evident in several other sites.

Since soil texture may be a controlling factor for NO_x emissions, we sampled on several different soil textures for many crops. Growers reported whether their soils were "light," "medium," or "heavy." We subsequently located their sites on United States Soil Conservation Service soil surveys, and looked up textures. Soil survey data was occasionally at variance with growers' reports, and preliminary spot tests of soil texture have revealed that growers' reports tend to be accurate. Thus, textural analysis was conducted for soils from each site.

Table 4 provides an inventory of the data taken for all sites. Table 5 is a calendar indicating when measurements were taken, giving the number of observations by field site (the different positions are not shown). Diel observations are marked in bold boxes. Other data are "routine" data from both intensive and extensive study sites, with observations made only at midday, when NO_x flux is expected to be highest.

2.2 Task II. Field Studies.

2.2.1 Methods.

The second task involved the measurement of NO_x emissions and related soil properties and processes. Field studies were preceded by the hiring and training of 6 field assistants with 3-month appointments, 1 with a 6 month appointment, and 1 with an

Figure 2. Tactical display of sites sampled for NO_x emissions in the San Joaquin Valley, July- September, 1995.

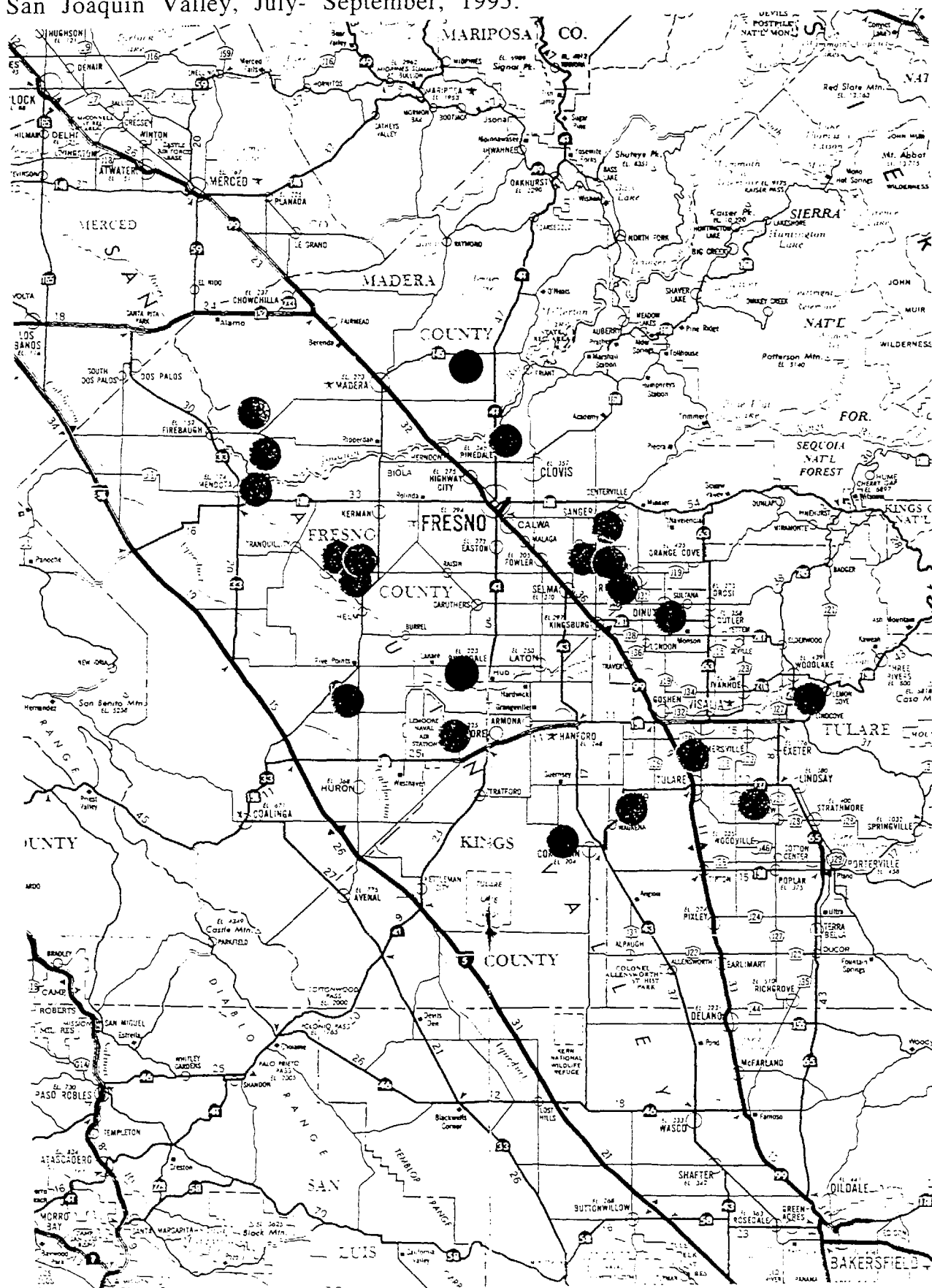


Table 2. Index of sites sampled for NO_x emissions July-September 1995 in San Joaquin Valley.

Code	Crop	Location	Soil	Soil texture ⁵	Irrigation
A	Alfalfa	Firebaugh	Basin	sandy loam	Border Check
B	Almonds ^{2,3}	Parlier	Fan	sandy loam	Flood
C	Almonds ²	Parlier	Fan	sandy loam	Drip
D	Cotton ²	San Joaquin ¹	Basin	sandy clay loam	Furrow
E	Cotton	San Joaquin ¹	Basin	sandy loam	Furrow
F	Cotton	Tranquillity ¹	Basin	clay loam	Furrow
G	Cotton	Riverdale	Basin	fine clay	Sprinkler
H	Sugar Beets	Mendota	Basin	sandy loam	Furrow
I	Corn ²	Tulare	Basin	loam	Furrow
J	Corn ^{2,3}	Plainview	Fan	fine loam	Furrow
K	Corn ²	Waukena	Fan	loam	Furrow
L	Grapes	Firebaugh	Fan	loamy sand	Flood
M	Irrigated Pasture	Sanger	Fan	sandy loam	Border Check
N	Sugar Beets	Mendota	Basin	loam	Furrow
O	Alfalfa	Kearney ⁴	Fan	fine sandy loam	Border Check, unfertilized
P	Alfalfa	Kearney ⁴	Fan	fine sandy loam	Border Check
Q	Grapes ^{2,3}	Kearney ⁴	Fan	sandy loam	Drip
R	Grapes ²	Kearney ⁴	Fan	fine sandy loam	Flood
S	Sugar Beets	Corcoran	Basin	sandy loam	Furrow
T	Orange ²	Lindcove ⁴	Fan	sandy loam	Drip
U	Sugar Beets	San Joaquin	Basin	sandy loam	Furrow
V	Peaches ²	Clovis	Fan	sandy loam	Flood
W	Irrigated Pasture ²	Bonadelle Ranchos	Basin	loam	Border Check
X	Irrigated Pasture ²	Bonadelle Ranchos	Basin	loam	Border Check
Y	Cotton ^{2,3}	West Side ⁴	Fan	sandy clay loam	Furrow
Z	Tomatoes ²	West Side ⁴	Fan	clay loam	Furrow

⁵ Textures determined by the sedimentation-hydrometer method (Day, 1965)

¹ Site arranged by Daniel Munk

² Intensive sampling site

³ Diel measurements were performed at this site.

⁴ University of California Agricultural Research Center

Table 3. Code, crop, location, date of fertilization, and nitrogen fertilization record for San Joaquin Valley sites sampled for NO_x emissions July-September, 1995.

Code	Crop	Location	Date	Rate and Form*	How Applied†
A	Alfalfa	Firebaugh	n a	None	n a
B	Almonds	Parlier	Mar 13	80 lb N/ac as CAN17	Water-Run
			May 5	80 lb N/ac as UN32	Surface
			July 10	80 lb N/ac as CAN17	Water-Run
C	Almonds	Parlier	Mar 13	80 lb N/ac as NH ₄ NO ₃	Broadcast
			May 5	80 lb N/ac as UN32	Surface
			July 7	50 lb N/ac as NH ₄ NO ₃	Broadcast
D	Cotton	San Joaquin	May	160 lb N/ac	Side-Dressed
			June	89 lb N/ac	Water-Run
E	Cotton	San Joaquin	May	160 lb N/ac	Side-Dressed
			June	81 lb N/ac	Water-Run
F	Cotton	Tranquillity	May	160 lb N/ac	Side-Dressed
			June	55 lb N/ac	Water-Run
G	Cotton	Riverdale	June 7	180 lb N/ac as NH ₃	Injection
			July 11	30 lb N/ac as UN32	Water-Run
			July 18	10 lb N/ac as Unocal	Foliar
				Plus	
			July 25	30 lb N/ac as UN32	Water-Run
H	Sugar Beets	Mendota	Apr. 15	28 lb N/ac as 11-52-0	Sub-Soil Shank
			June 10	97 lb N/ac as UN32	Sub-Soil Shank
I	Corn	Tulare	Preplant	18 lb N/ac as 11-52-0	
J	Corn	Plainview	Apr-May	275 lb N/ac as NH ₃	Side-Dressed
			July 27	150 lb N/ac as UN32	Shanked In
K	Corn	Waukena	Preplant	18 lb N/ac as 11-52-0	
			Apr-May	275 lb N/ac as NH ₃	Side-Dressed
			July 27	150 lb N/ac as UN32	Shanked In
L	Grapes	Firebaugh	Oct /94	20 lb N/ac as aqua	Injected
			Feb.	NH ₃	
				20 lb N/ac as aqua	Injected
M	Irrigated Pasture	Sanger	n a	None	n a
N	Sugar Beets	Mendota	Feb. 5	24 lb N/ac as 10-34-0	Soil Injection
			Apr. 24	100 lb N/ac as UN34	Soil Injection
			June 15	40 lb N/ac as aqua	Water-Run
O	Alfalfa	Kearney	n a	None	n a
P	Alfalfa	Kearney	Apr. 25	20 lb N/ac as 11-52-0	Broadcast
Q	Grapes	Kearney	Mar. 30	30 lb N/ac as CAN17	Water-Run
			June 15	30 lb N/ac as CAN17	Water-Run
R	Grapes	Kearney	May 18	60 lb N/ac as NH ₄ NO ₃	Broadcast
S	Sugar Beets	Corcoran	n a	n a	n a
T	Orange	Lindcove	Mar. 15	109 lb N/a as Ca(NO ₃) ₂	Broadcast
			May 2	14 lb N/ac as Urea	Foliar Spray
U	Sugar Beets	San Joaquin	Dec/94	24 lb N/ac as 10-34-0	Soil Injection
			June 1	100 lb N/ac as UN32	Sub-Soil Injection

V	Peaches	Clovis	Sep/94 Mar	60 lb N/ac as NH_4NO_3 40 lb N/ac as (NH_4) $_2\text{SO}_4$	Banded in Banded in
W	Irrigated Pasture	Bonadelle Ranchos	n a	None	n a
X	Irrigated Pasture	Bonadelle Ranchos	n a	None	n a
Y	Cotton	West Side	Feb. May	11 lb N/ac as 11-52-0 180 lb N/ac as urea	Drilled in Side-Dressed
Z	Tomatoes	West Side	May	180 lb N/ac as urea	Side-Dressed

*UN-32 is a urea-nitrate fertilizer, and CAN-17 is a calcium-ammonium-nitrate fertilizer.

†Side-dressed, banded, shanked, drilled, and injected applications are directly incorporated into the soil; broadcast fertilizer is applied to the soil surface; and water-run fertilizer is applied in irrigation water.

Table 4. Crop type, soil texture, fertilization type, irrigation type and number of NOx flux measurements at each site. Total number of flux measurements are presented by irrigation regime, field position and sampling protocol.

location	crop	soil textural class	fertilizer type	texture [%Sa/Si/C]*	Irrigation				Position				Protocol		total number of measurements
					border check	drip	flood	furrow	canopy	furrow	open	ridge	Diel	Routine	
A	Firebaugh	alfalfa	Sandy Loam	NA	72/19/9			20				20			20
B	Parlier	almonds	Hanford Sandy Loam	CAN-17, UN32	77/16/7			660	340		320	500	160		660
C	Parlier	almonds	Sandy Loam	NH5NO3	64/28/8		80		40		40		80		80
D	San Joaquin	cotton	Sandy Clay Loam	UN32	50/23/27					30	30		60		60
E	San Joaquin	cotton	Sandy Loam	UN32	59/22/19			40		20	20		40		40
F	Tranquillity	cotton	Clay Loam	UN32	42/26/32			40		20	20		40		40
G	Riverdale	cotton	Fine Clay Loam	UN32	16/32/52			20		10	10		20		20
H	Mendota	sugar beets	Sandy Loam	NH3	65/23/72			40		20	20		40		40
I	Tulare	corn	Loam	NH3	51/37/12			60		30	30		60		60
J	Plainview	corn	Fine Loam	UN32	35/40/25			180		90	90	100	80		180
K	Waukena	corn	Loam	NH3	37/45/18			90		40	10	40	90		90
L	Firebaugh	grapes	Loamy Sand	UN32	81/10/9			40		20	20		40		40
M	Sanger	irrig pasture	Sandy Loam	11-52-0	59/30/11	10					10		10		10
N	Mendota	sugar beets	Loam	CAN-17	32/50/18			40		20	20		40		40
O	Kearney	alfalfa	Hanford Fine Sandy Loam	NA	60/30/10			20			20		20		20
P	Kearney	alfalfa	Hanford Fine Sandy Loam	11-52-0	60/30/10			20			20		20		20
Q	Kearney	grapes	Hanford Sandy Loam	CAN-17	70/24/6		120			60	60		120		120
R	Kearney	grapes	Hanford Fine Sandy Loam	NH4NO3	59/31/10			390		200	190	370	20		390
S	Corcoran	sugar beets	Sandy Loam partially drained	NA	67/22/11			10			10		10		10
T	Lindcove	oranges	San Joaquin Sandy Loam	urea	71/19/10		80		40		40		80		80
U	San Joaquin	sugar beets	Sandy Loam	UN32	65/23/12			40		20	20		40		40
V	Clovis	peaches	Visalia Sandy Loam Clay Loam	(NH4)2SO4	70/20/10			80	40		40		80		80
W	Bonadelle Ranchos	irrig pasture	Loam	NA	50/38/13			40			40		40		40
X	Bonadelle Ranchos	irrig pasture	Loam	NA	50/38/13			40			40		40		40
Y	West Side	cotton	Sandy Clay Loam	urea	52/22/26			470		235	235	350	120		470
Z	West Side	tomatoes	Panoche Clay Loam	urea	44/25/31			160		80	80		160		160

*[%Sa/Si/C]=percent Sand/Silt/Clay

Fertilizer categories: NH4 fertilizer: 11-52-0, (NH4)2SO4, NH3, aqua NH, urea

Mixed fertilizer: CAN-17, NH4NO3, UN32

2850

Table 5. Dates and numbers of observations for NOx emissions measured at each site in the San Joaquin Valley, July through September 1995.

Fertilized	I	J	K	A	L	D	E	F	G	S	P	O	Q	R	T	U	B	N	C	H	M	Bonadelle Ramblas		V	Z	Y	
	5/1		5/1		2/28					4/25		6/15	5/18	5/2	6/1		6/10		6/15				3/1	5/15	5/15		
Location	Tulare	Plainview	Waukena	Firebaugh	Firebaugh	San Joaquin	San Joaquin	Tranquility	Riverdale	Corcoran	Kearney	Kearney	Kearney	Kearney	Lindcove	San Joaquin	Parlier	Mendota	Parlier	Mendota	Sanger	Bonadelle Ramblas	Bonadelle Ramblas	Clovis	West Side	West Side	
7/06/95																	127										
7/07/95																	53		F								
7/08/95																											
7/09/95																											
7/10/95																	F										
7/11/95											10						20										70
7/12/95										10							20								20		70
7/13/95																	20							20	20		20
7/14/95																	20		20					20	20		20
7/15/95																	20							20	20		20
7/16/95																	20		20					20	20		20
7/17/95																	20		20					20	20		20
7/18/95																	20		20					20	20		20
7/19/95																		20						20	20		20
7/20/95																		20						20	20		20
7/21/95																	20		20					20	20		20
7/22/95																	20		20					20	20		20
7/23/95																											
7/24/95																											
7/25/95									F																		
7/26/95																											
7/27/95		F				20								20													
7/28/95							20	20														10					
7/29/95														90													
7/30/95																	130										
7/31/95																											110
8/01/95						20		20																			
8/02/95						20	20																				
8/03/95																	110										
8/04/95			20																								
8/05/95	20																										
8/06/95			20																								
8/07/95																											
8/08/95		20																									
8/09/95		20	20																								
8/10/95		20	20																		20						
8/11/95															20	20					20						
8/12/95		20								10			20		20												
8/13/95	20		10																								
8/14/95													20														
8/15/95	20																										
8/16/95															20												
8/17/95																20											
8/18/95													20														
8/19/95												10	20														
8/20/95													20		20												
8/21/95				10	20						10	20															
8/22/95				10	20																						
8/23/95																							10	10			
8/24/95																							10	10			
8/25/95																							10	10			
8/26/95																											
8/27/95				10																			10	10			
8/28/95																											
8/29/95																											
8/30/95																											
8/31/95																											
9/01/95																											
9/02/95																											
9/03/95																											
9/04/95																											
9/05/95																											
9/06/95														100													
9/07/95																	80										
9/08/95		100																									
9/09/95																											
9/10/95																											100
9/11/95									20																		

Diel data
 F - Fertilized
 Dates and number of data observations

11 month appointment. To acquire laboratory facilities for the field work, we requested and received permission to use laboratory space and to sample in fields at the University of California Kearney Agricultural Center. We utilized analytical balances and ovens as well as bench space at the Center.

Research teams were in the field July 5-8, July 10-23, July 26-August 4, August 7-13, August 18-29, and September 5-11. The assistants were divided into two teams and carried out research following three broad protocols: 1) diel sampling; 2) intensive sampling (repeated measures for 3-10 days in a site); and 3) extensive sampling (once or twice only).

The first protocol was a diel sampling in which single fields were measured repeatedly from morning through evening. In some cases, these diel measurements ran from predawn hours until after midnight. Personnel measured soil and chamber temperatures with each NO_x flux, and sampled for soil moisture and inorganic nitrogen content at each chamber each day. Bulk density, pore space, pH, and total N was sampled once at each location. For diel measurements we grouped crops into structural types which collectively share similar patterns in the variation of ambient factors such as temperature and shading. These were grouped as tree crops, vine crops, and row crops, and were represented by almonds, grapes, cotton and corn (Table 2). Diel measurements were repeated in late summer to evaluate seasonal effects such as shorter day lengths.

The second protocol was the intensive protocol, in which individual fields were measured repeatedly over the course of five to ten days. The objective of this protocol was to identify patterns in the change of NO_x flux in relation to fertilization and/or irrigation events. Based on results of the diel measurements, NO_x measurements for the intensive and extensive protocols were performed between 9:30 AM and 3:00 PM to capture peak midday fluxes. In addition to ancillary measurements described above, nitrification potential and *in situ* gross nitrification assays were performed in 13 sites. These allow subsequent correlation of NO_x flux with these measures of the process thought to be the source of NO_x emission. We were able to sample 1 to 2 intensive sites for each targeted crop system.

The third protocol was an extensive protocol, with the objective of identifying spatial and crop-specific patterns of NO_x flux. All of the ancillary measurements performed for the diel measurements were also performed under the extensive protocol.

2.2.1.1 Field Methods.

Field measurements of NO_x (nitric oxide (NO) plus nitrogen dioxide (NO_2)) at the soil-air interface were carried out using a two-piece molded plastic chamber (Matson et al. 1991, 1992) in which a 25 cm diameter PVC base was inserted before measurement, and was capped with a vented ABS plastic cover at the time of sampling. Nitric oxide was measured in the field using a Scintrex LMA-3 luminol chemoluminescence detector modified for field measurements (Appendix D; Davidson et al. 1991, 1993b). With this system, gas fluxes are measured over a short (3-5 minute) time period, thereby reducing chamber effects on exchange dynamics. Our system has been compared with the NO/O_3 chemoluminescence detector (Williams and Davidson 1993); the authors concluded that measurements from the two systems were comparable, that the luminol system suffers an approximate 7% decrease in signal under high (>50%) humidity, but that the luminol system is capable of sampling more points per time and thus better able to estimate spatial variability and accurate site means. Such chamber-based measurements are useful only for measuring flux at the soil-air interface; some NO_2 may be taken up by the crop canopy before it is lost to the atmosphere.

Data collected by the chemoluminescence detector allow calculation of NO_x concentrations within the chambers over time. Measurements (mV) were collected every 30 seconds with data loggers and down-loaded to computers for further calculations. Logged data were imported to Excel 4.0 worksheets, and converted to concentrations using the calibration curves developed in the field (see below). Baseline subtractions were performed, and chamber volumes and temperatures were used with NO_x concentrations in the ideal gas law equation to determine the mass of NO_x in the chamber at each time point. Regressions were performed to determine the linear increase in chamber NO_x over time. Quality assurance was carried out at several points. Transcription errors were checked by verifying that data used in calculations agreed with logged data. Each flux calculation was checked to insure that the correct leading and trailing baseline points were used for baseline subtraction, and that the correct groups of points were used in the regression calculations. Flux calculations and quality control were performed by different personnel.

Calibration curves were run in the field at the beginning and end of each sample run (e.g., every 10-20 samples). The response of the chemiluminescent detector (Scintrex, Ltd., Ontario, Canada) is first calibrated by mixing known flows of ambient air and standard gas (Scott-Marin, Inc., Riverside, CA) through the detector. By varying the proportions of ambient air and standard gas, a calibration curve is developed. The standard gas is supplied as NO; NO in the gas-air mixture is oxidized to NO_2 in a CrO_3 converter, so that NO_2 is the N species actually

detected. Bypassing the CrO_3 converter assays NO_2 only; NO is determined by subtracting NO_2 from $(\text{NO} + \text{NO}_2)$. In most agricultural systems where we have worked, NO is by far the dominant gas emitted from soils, normally contributing over 90% of the total NO_x flux. In this study, we did not distinguish NO and NO_2 , and this we refer to as NO_x .

Hutchinson and Livingston (1993) define a minimum detectable flux based upon the flux standard error:

$$\text{minimum detectable flux} = (t)(SE)$$

with $n-2$ degrees of freedom and $1 - \alpha$ significance level. At $\alpha = 0.05$, we determined our minimum detectable flux during the first course of measurements to be $0.655 \text{ ng-N cm}^{-2} \text{ h}^{-1}$.

At each gas sampling site, soil cores were collected down to 10 cm depth and placed in plastic bags; soils were held on ice until laboratory processing (within 8 h). Soil and chamber air temperatures also were collected concomitantly with flux measurements; soil temperature at 2 cm depth was collected with field thermometers. Temperatures within the chambers were collected at the end of each measurement; these within-chamber air temperature measurements were required for the calculation of NO_x flux.

Due to an oversight in field sampling, air temperatures outside of the chamber were not taken. In order to estimate outside air temperatures, we used the mean value of the within-chamber air temperatures from the four coolest chambers at each sampling time (these were shaded chambers). In other words, we assumed that the air temperature inside shaded chambers would not be different than air temperature in the shade outside. We utilized met station air temperature data from the Kearney Agricultural Center in comparison with field temperature estimates from our nearby study site to test the accuracy of this assumption. By paired t-test, differences were not significant ($P > 0.05$; standard deviation was 0.7 C). We report these shaded chamber air temperatures as "air temperature" in the data analysis.

2.2.1.2. Laboratory Methods.

Total N and C content of soils were measured using a Carlo Erba NA1500 automated nitrogen-carbon analyzer on 25 mg samples of soil milled to a fine powder. Soil bulk density was measured by extracting an 8 cm diameter by 9 cm depth soil core (452 cm^3), then weighing after oven-drying to constant weight (overnight) at 105 C .

Soil textural classifications were originally obtained from Soil Conservation Service soil survey maps; however, the resolution of the maps proved too coarse to derive textures for soils from specific fields. Spot tests identified discrepancies between textures reported on the maps and textures measured in our laboratory. Therefore we

performed particle size analysis using the sedimentation-hydrometer method (Day, 1965) on soils collected from each site we visited.

With each NO_x flux measured, a soil core was taken and extracted for inorganic N pool size determinations. Fresh soil weights were measured in the field, but pool sizes are usually expressed on an oven-dry soil basis. To convert fresh weights to oven-dry weight equivalents, as well as to determine WFPS, soil moisture measurements were made. Soil moisture was measured using subsamples of soils collected for inorganic N pool size determinations. After obtaining fresh weights, 10 g samples of soil were dried overnight at 105°C and reweighed. After reweighing, soils were wet-sieved to remove > 2 mm particles, and moisture was determined on the < 2 mm fraction.

For analysis of inorganic nitrogen in field soils, 10 g subsamples of soil were placed in 100 mL 2N KCl and shaken for 1 hour; 10 mL aliquots of the supernatant were stored in vials and refrigerated until colorimetric analysis of inorganic ions. Quantification of NH_4^+ , NO_2^- , and NO_3^- in soil extracts was completed in February, 1996, using a Lachat autoanalyzer (Lachat Instruments, Milwaukee, WI). Ammonium was analyzed by reacting NH_3 with sodium salicylate in the presence of hypochlorite (an oxidizing reagent). Sodium nitroprusside catalyzes the reaction, and EDTA complexes cations which would otherwise form interfering precipitates in the reaction. Nitrite is analyzed by reacting it with sulfanilimide (a diazotizing reagent), then treated with a coupling reagent [*N*-(1-naphthyl)-ethylenediamine] to form a red azo compound. Nitrate is analyzed by first passing the extract through a copperized cadmium column to reduce NO_3^- to NO_2^- . It is then determined as $(\text{NO}_2^- + \text{NO}_3^-)$ minus NO_2^- .

Having performed the inorganic nitrogen analyses and measured soil weights and moisture contents, soil inorganic nitrogen pool sizes were computed. Fresh weights of soils sampled in the field were adjusted for measured moisture content to an oven dry weight equivalent. Solution volumes were divided by oven dry soil weight equivalent and multiplied by solution concentrations to derive NH_4^+ , NO_2^- , and NO_3^- pools on the basis of $\mu\text{g N}$ per gram of oven dry soil.

For *in situ* nitrification rates, soil samples were labeled in the field with ^{15}N - NO_3^- solutions. Soil samples (approximately 500 g) were placed in plastic bags; a ^{15}N solution ($30 \mu\text{g N mL}^{-1}$ at 25 atom% excess ^{15}N) was applied by spraying; subsamples of the soils were extracted in KCl as described above for measurement of initial ^{15}N concentration. The remaining soil was replaced in the holes from which they were cored. After 6 hour *in situ* incubations, soil extracts were again taken. Extracts were first analyzed for $\text{NO}_2^- + \text{NO}_3^-$ as

described above. Then they were prepared for mass spectrometry by reducing the NO_2^- and NO_3^- to NH_4^+ , and diffusing the NH_4^+ onto acidified paper disks. The $^{15}\text{N}/^{14}\text{N}$ ratio on the disks was measured using automated nitrogen-carbon analyzer - isotope ratio mass spectrometer (Europa Scientific, Crewe, U.K.). The NO_2^- and NO_3^- pool sizes and isotope ratios measured at the beginning and end of the incubation were used in an isotope dilution model to calculate the gross rate of NO_3^- production in the field (Hart et al. 1994).

Nitrification potential was also measured. Nitrification potential is an assay which measures the activity of soil nitrifying enzymes under standardized laboratory conditions and which has been found to correlate with soil NO_x emissions. Field soil samples were collected and 10 g of each sample were weighed into Erlenmeyer flasks. A buffered NH_4^+ supply (100 mL) was added to each flask, and flasks were orbitally shaken. Spaced over the course of 24 hour incubations, four aliquots (10 mL each) of the soil slurries were drawn and centrifuged. Supernatants were colorimetrically analyzed for NO_2^- and NO_3^- as described above. Potential rate of nitrification was calculated from the regression of NO_2^- and NO_3^- concentrations during the 24 hour incubation.

Water filled pore space was calculated by the following formula:

$$\% \text{WFPS} = [100 \times (\theta_g \times \text{BD})] / [1 - (\text{BD}/\text{PD})]$$

where

θ_g = gravimetric soil water content

BD = bulk density

PD = particle density (2.65 g cm^{-2} for most soils)

(Davidson and Schimel, 1995).

2.2.1.3 Data Management.

For each NO_x flux measurement, we also have information on soil temperature, soil moisture, calculated water filled pore space, and nitrate, nitrite, and ammonium concentrations. For each field, we have one-time data for pH, total C and N as well as bulk density and texture. These data were managed using Microsoft Excel 4.0. Statistical analysis are described in the sections below.

2.2.1.4 Estimation of Diel Fluxes.

This summary explains the methods used for estimating:

1) Diel NO_x flux from diel-measured data, for mean chamber results by site, position, and date (refer to Table 4 for data collection layout).

- 2) Normalized diel NO_x flux curves to represent the hourly distribution of NO_x flux, for estimating diel curves for different levels of peak NO_x flux.
- 3) Diel NO_x flux from routine-measured data (where measurements were collected only once a day), for mean chamber results by crop, site, position, and date.
- 4) Diel NO_x flux for whole field crops (position area-weighted average of mean chamber results)

The statistical software S-Plus (MathSoft, 1993), based on the S statistical language developed at At&T's Bell Laboratories, is used to perform all statistical analysis and estimations.

For background on the data set, Appendix A provides a listing and description of the data taken for all sites. Note that the "site" distinguishes categories of conditions at the spatial level of a whole agricultural field (crop, soil texture, bulk density, percent canopy cover, irrigation method), while temperature, moisture, NO_x data, and position within a field's plow pattern are distinguished at the level of a NO_x flux chamber. From here on, "data point" will mean the set of data collected at a point in time from a chamber; places will be referred to as field "sites."

Table 5 is a calendar of when data measurements were taken, giving the number of observations by field site (the different positions are not shown). Diel observations are marked in bold boxes. Other data are "routine" data, with observations made only at midday, when NO_x flux is expected to be highest. Fertilization dates before July 1, 1995 are marked in the second row, and fertilization dates during the study period (July through August 1995) are marked with an "F."

The estimations here make use of both the more detailed but less frequently conducted diel measurements and also the more frequent routine measurements. Calculations are made of mean daily NO_x fluxes based on actual data, rather than on a predictive model with explanatory parameters. The time of day is the only "explanatory" variable, in that it tracks the changes in soil conditions over time and therefore NO_x flux during the course of a day. More complex investigation of explanatory variables is provided in a separate analysis.

The general strategy for NO_x flux estimation here is to make use of the subset of observations that covered NO_x flux over the course of a day to fit curves that represent the relationship between the time of day and NO_x flux in ng-N cm⁻² h⁻¹. This simple correlation is chosen to incorporate the full range of variability in NO_x flux (due to e.g. soil temperature, soil moisture, NH₄⁺, others),

including that due to unknown conditions. These "diel curves" can then be used to calculate the mean daily NO flux per unit area of the study site. In addition, these curves can be used to approximate the diel distribution of NO_x flux at field sites where NO_x was measured less frequently (at midday only). The methods used in each kind of estimation will be described in detail in the following pages, and are stated in brief below:

- 1) Derive diel curves of time of day versus chamber NO_x flux via local regression on NO_x data, generating distinct curves by crop, site, position, irrigation method, and date.
- 2) Derive normalized diel curves to represent the hourly distribution of NO flux, generating distinct curves by crop, site, position, and irrigation method, grouping different dates together. These curves can then be scaled to generate diel curves for different levels of peak NO_x flux.
- 3) Estimate daily chamber NO_x flux at field sites where only midday measurements were made ("routine" measurements), deriving diel curves from a) the normalized diel curves that were produced from the diel-measured data, and b) the mean routine-measured midday flux.

Step 1). Diel NO_x flux curves from diel-measured data, by crop, site, position, and date.

Individual curves of diel NO_x flux are calculated for each crop, field site, position, and date for which diel data were taken. At each field site for which diel data were recorded, there were ten replicate chambers for each field position. These ten chambers were visited several times over the course of a day, providing sets of 10 data points for NO flux measurements at different hours. To predict mean hourly fluxes, the data from these ten replicates for a particular day and position are used to estimate a curve of time of day vs. NO_x flux [ng-N/cm²/hour], using local trend surface fitting to derive curves from the replicate data (see Figure 3 for plots of data and fitted curves).

The local trend surface fitting method used here involves local regression with the S-Plus function loess. This function produces a curve that is effectively a "smooth" of the data via weighted least squares to make nearby (by time of day) points more influential. Given n data points, a span parameter $\alpha < 1$, and $q = \alpha * n$,

Figure 3a. Diel plots: time of day vs. measured NOx flux [ng-N/cm²/hour], with loess-estimated curves and integrated daily total NOx flux [ng-N/cm²/day]. By crop, site, position, and date. Corn and Grapes.

Each point is an individual flux measurement (minimum detectable flux = 0.66 ng/cm²/hour; see section 2.2.1.1)
Data collected in San Joaquin Valley, July-September, 1995

solid line: loess curve; dashed line: extrapolation (see Appendix E for method)

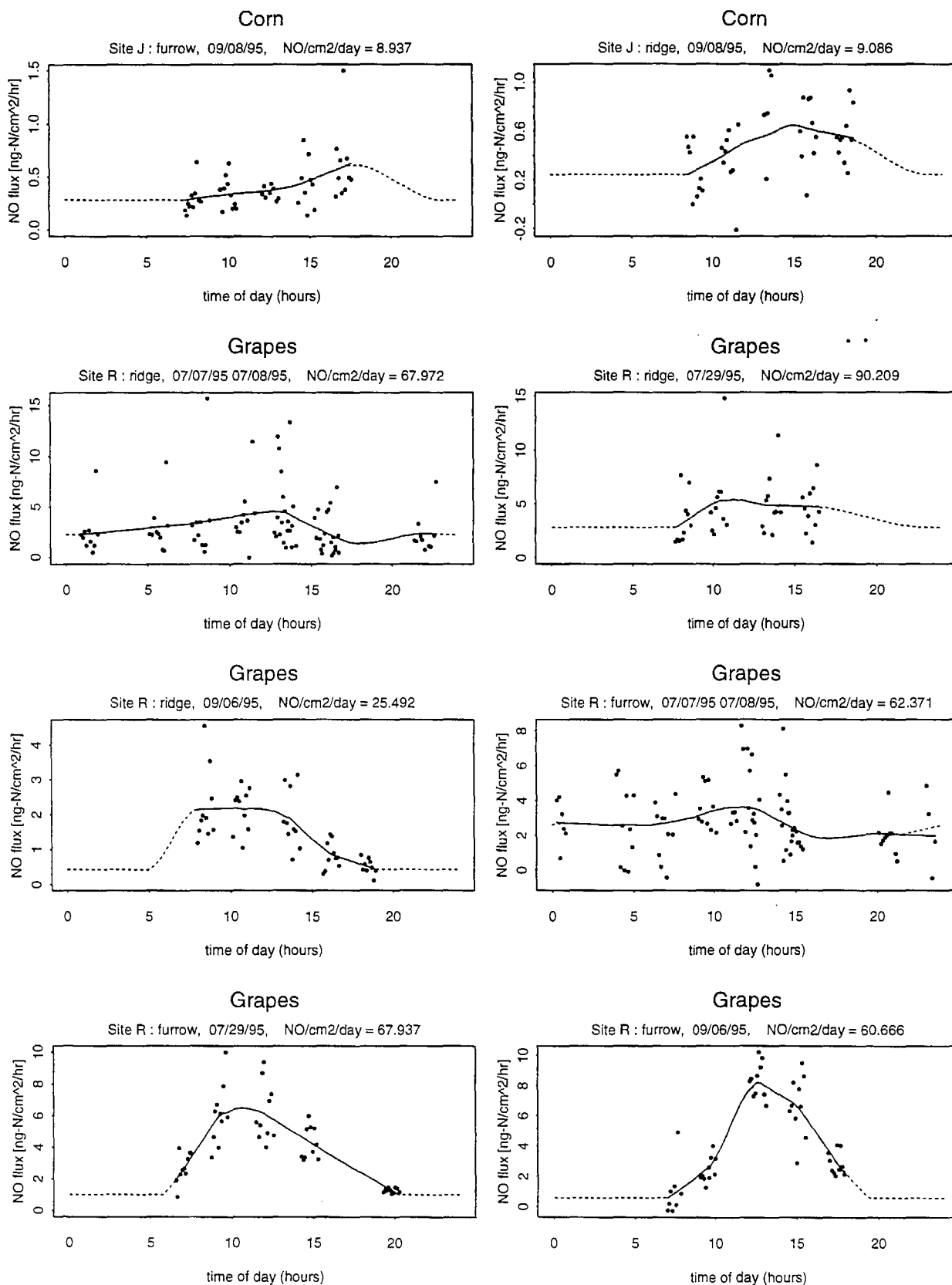


Figure 3b. Diel plots: time of day vs. measured NO_x flux [ng-N/cm²/hour], with loess-estimated curves and integrated daily total NO_x flux [ng-N/cm²/day]. By crop, site, position, and date. Almonds.

Each point is an individual flux measurement (minimum detectable flux = 0.66 ng/cm²/hour; see section 2.2.1.1)
Data collected in San Joaquin Valley, July-September, 1995

solid line: loess curve; dashed line: extrapolation (see Appendix E for method)

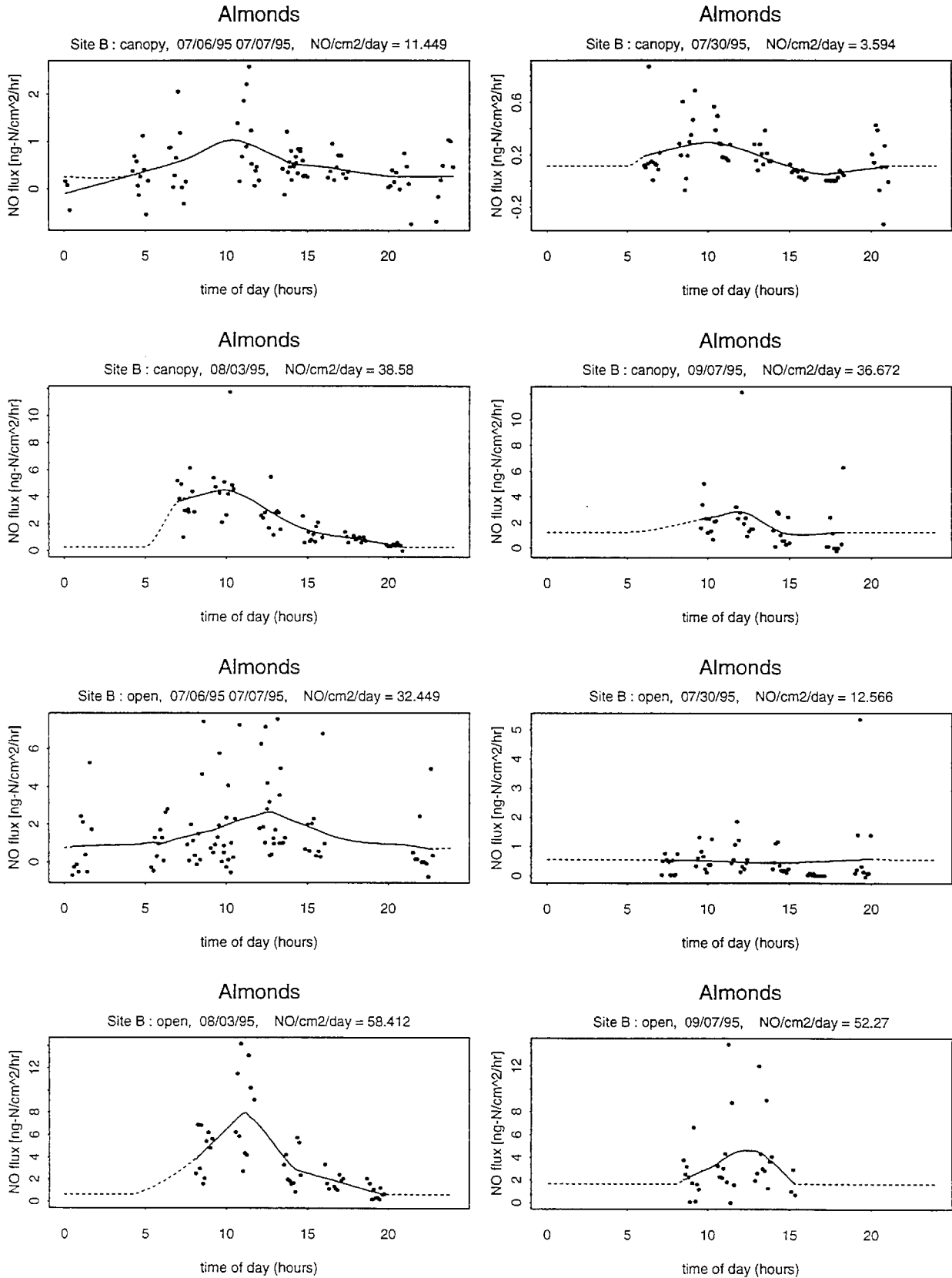
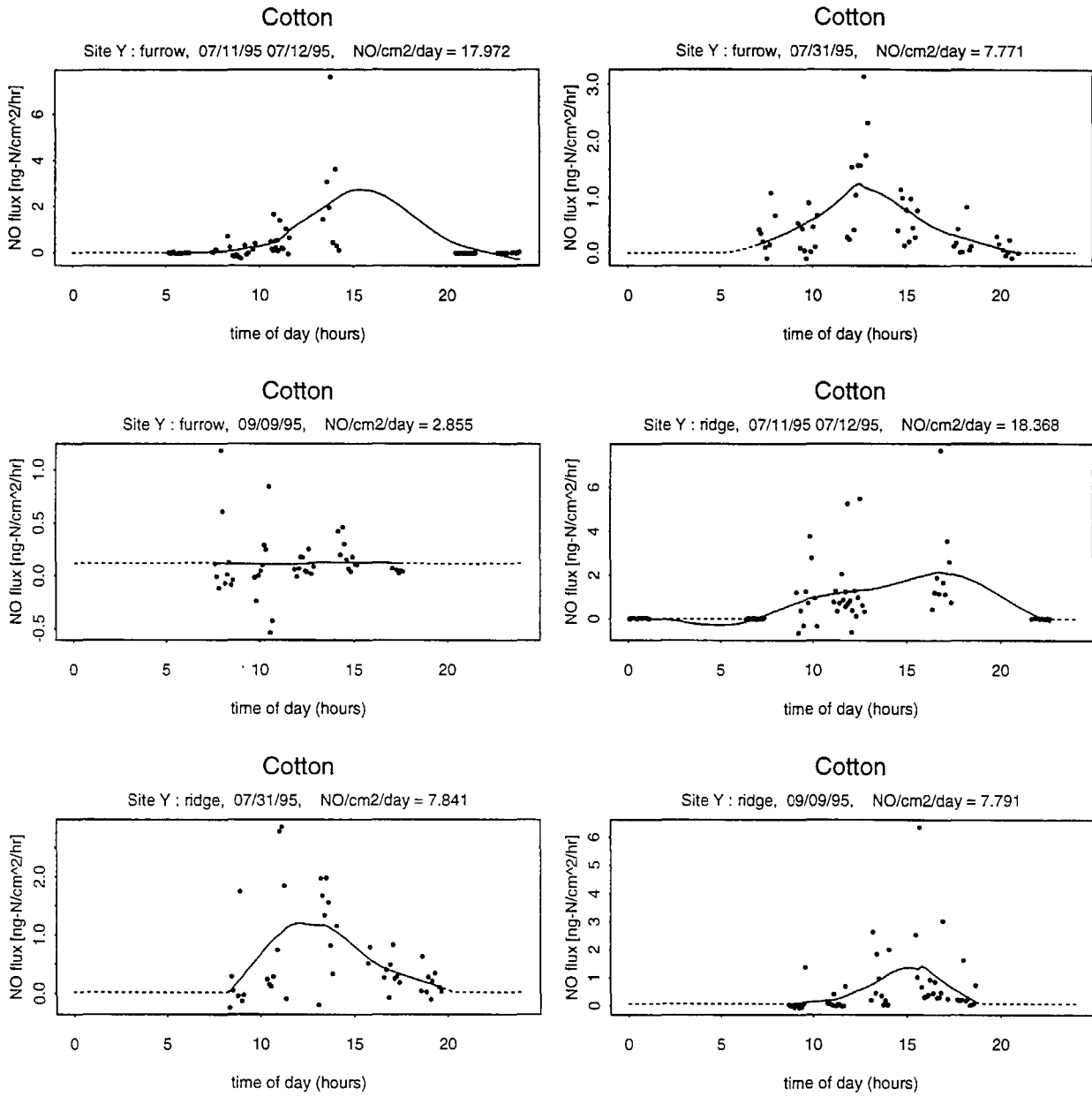


Figure 3c. Diel plots: time of day vs. measured NO_x flux [ng-N/cm²/hour], with loess-estimated curves and integrated daily total NO_x flux [ng-N/cm²/day]. By crop, site, position, and date. Cotton.

Each point is an individual flux measurement (minimum detectable flux = 0.66 ng/cm²/hour; see section 2.2.1.1)
 Data collected in San Joaquin Valley, July-September, 1995

solid line: loess curve; dashed line: extrapolation (see Appendix E for method)



letting delta equal the distance to the qth nearest point to x, then for observation xi, the weights are:

$w_i = [1 - (d(x, x_i)/\delta)^3]^3 [^+]$ where $[^+]$ denotes the positive part

The span parameter must be subjectively chosen, depending on the degree of smoothing desired. Details for loess are provided by Cleveland, et.al. (1992).

We ran these local regressions assuming a normal distribution of the data. Although NO_x flux is commonly considered to be approximately lognormally distributed, the distribution is not strict, because NO_x flux can be negative, for instance, due to microbial uptake. Since there are no sound transformations to compensate for negative observations of an otherwise lognormally-distributed variable, we ran the regressions assuming normally-distributed data and calculated the associated standard errors.

Since some of the diel data do not span a full twenty-four hours (usually NO_x was not measured during the hours around midnight), combination of spline and lower bounds on NO_x flux is used to interpolate NO_x flux for the missing hours. The mean standard error and mean confidence interval are taken for bounds on interpolated points. Integration of the diel curve over 24 hours yields an estimate of the daily NO_x flux. The NO_x flux is interpolated as follows:

- 1.) The NO_x flux is known to be periodic on daily cycles, and it is assumed that adjacent days have similar absolute NO_x fluxes. Therefore, repeating the loess curves from the available data in cycles of 3 consecutive days allows splining in of the missing hours.
- 2.) If the fitted loess curve is very steep, the splined NO_x values may drop very low, yielding an unrealistic interpolation. In such cases, the lowest predicted value from the loess fit of the data (or zero, whichever is largest) is used as a lower bound for NO_x flux.
- 3.) When splined values (i.e. no data taken during those hours) fall during the night-time hours of 11 PM to 5 am, the interpolated NO_x flux is held to the minimum of the fitted data, or zero, whichever is larger.

A procedure for calculating the confidence intervals from the standard errors is described in Chapter 6 of the *S-Plus Guide to Statistical and Mathematical Analysis* (Statistical Sciences, 1993).

Step 2) Normalized diel NO_x flux curves to represent the hourly distribution of NO_x flux, for estimating diel curves for different levels of peak NO_x flux.

It is assumed that the basic shape of the distribution of NO flux over a day stays the same, although absolute NO_x levels may change. The curve shape, as evidenced by the plots in Figures 3 and 4, is generally a bell shape, peaking around midday and dropping to a minimum in the nighttime.

In order to derive a general curve for the same crop, site, position, and irrigation method, the diel curves obtained in (1) are normalized to a [0,1] range of NO_x flux, and these normalized curves are averaged together by site (crop) and position, combining different dates. The ratios between the original curves' amplitudes and maximum fitted fluxes are averaged to characterize the amplitude/maximum ratio of the averaged curve. This step is a necessary simplification in lieu of more data on how the minimum and maximum NO_x flux from a site may vary together. The final average characteristic diel curve is then obtained by a rescaling of the average normal curve (range [0,1]) and translation upward so that the maximum is maintained at 1:

$$\begin{aligned} &\text{characteristic normalized NO} \\ &= \text{average normalized} * \text{ratio} + 1 - \text{ratio} \end{aligned}$$

More detail on the methodology for calculating characteristic diel curves by crop and position is provided in Appendix E. Figure 5 shows the mean characteristic curves, scaled by the amplitude/maximum ratio (preserving a peak of 1), and with 95% simultaneous confidence envelopes. The two almond and cotton plots with very flat, near-zero NO_x flux curves were excluded from the calculation of the means, and also the data extending over less than 10 hours were excluded.

Standard errors for these mean characteristic curves are obtained by propagating the (scaled to [0,1]) standard errors of the original curves and scaling by the characteristic amplitude/maximum ratio. The simultaneous confidence envelopes are calculated as in the *S-Plus Guide*, by accounting for the equivalent number of parameters and number of observations of each curve in the average in calculating the F-distributed confidence envelopes.

Figure 4a. Diel plots: time of day vs. diel-measured NO_x flux with loess curves and 95% confidence intervals. By crop, site, position, and date. Corn and Grapes.

Each point is an individual flux measurement (minimum detectable flux = 0.66 ng/cm²/hour; see section 2.2.1.1). Data collected in San Joaquin Valley, July-September, 1995.

solid line: fitted means; dashed line: mean diel from normalized curves; dotted lines: 95% confidence intervals

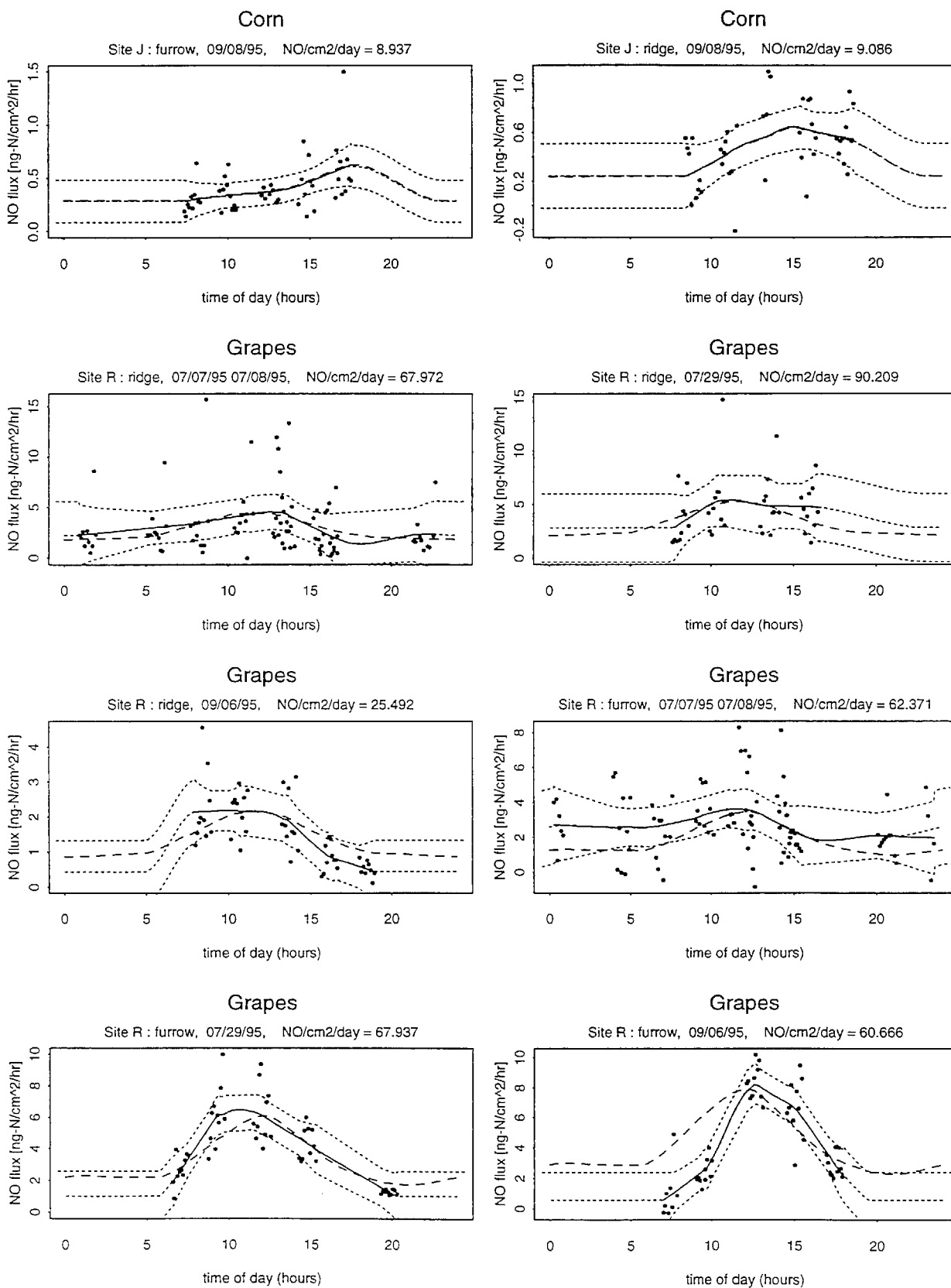


Figure 4b. Diel plots: time of day vs. diel-measured NO_x flux with loess curves and 95% confidence intervals. By crop, site, position, and date. Almonds.

Each point is an individual flux measurement (minimum detectable flux = 0.66 ng/cm²/hour; see section 2.2.1.1). Data collected in San Joaquin Valley, July-September, 1995.

solid line: fitted means; dashed line: mean diel from normalized curves; dotted lines: 95% confidence intervals

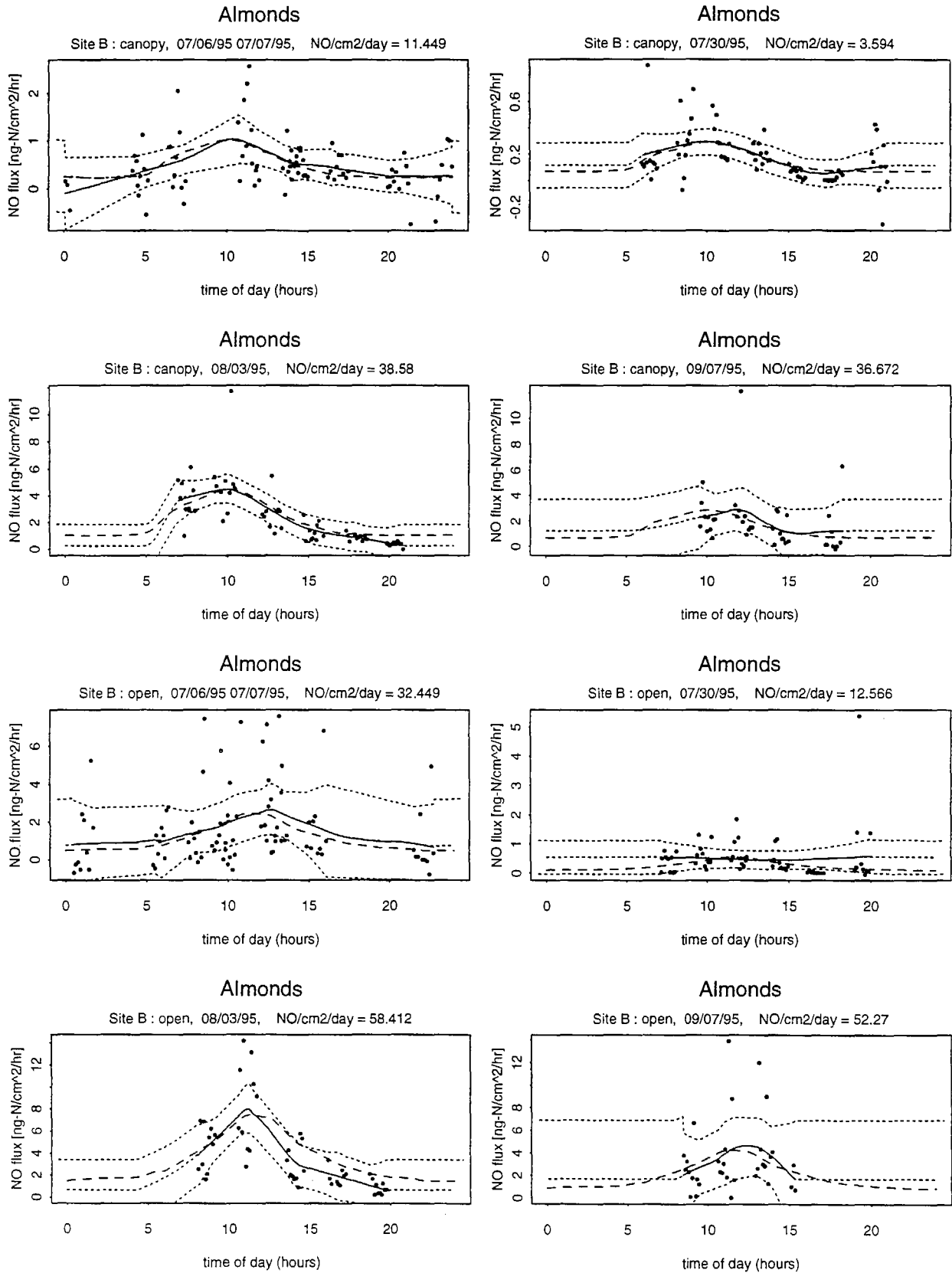


Figure 4c. Diel plots: time of day vs. diel-measured NO_x flux with loess curves and 95% confidence intervals. By crop, site, position, and date. Cotton.

Each point is an individual flux measurement (minimum detectable flux = 0.66 ng/cm²/hour; see section 2.2.1.1). Data collected in San Joaquin Valley, July-September, 1995.

solid line: fitted means; dashed line: mean diel from normalized curves; dotted lines: 95% confidence intervals

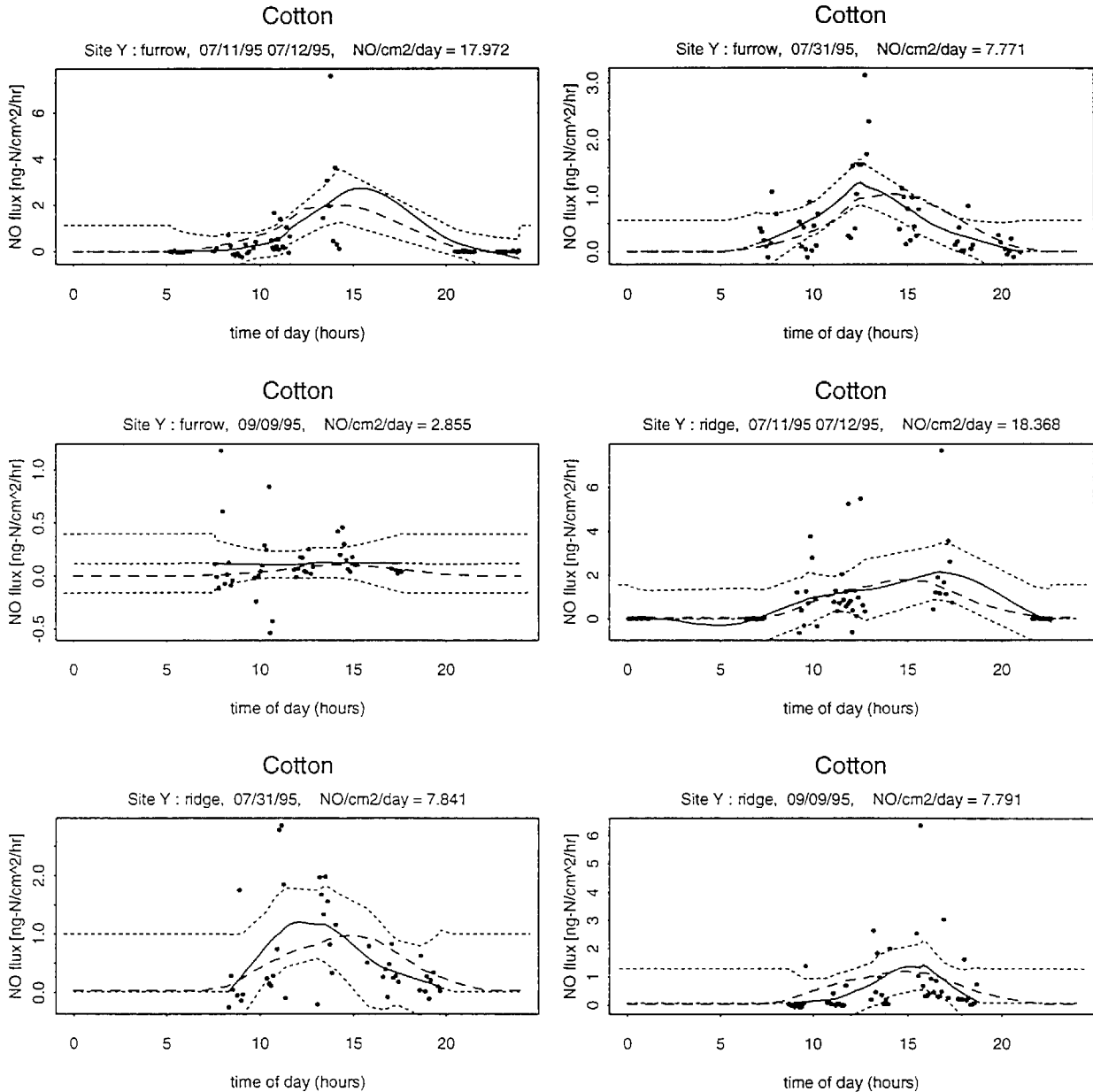
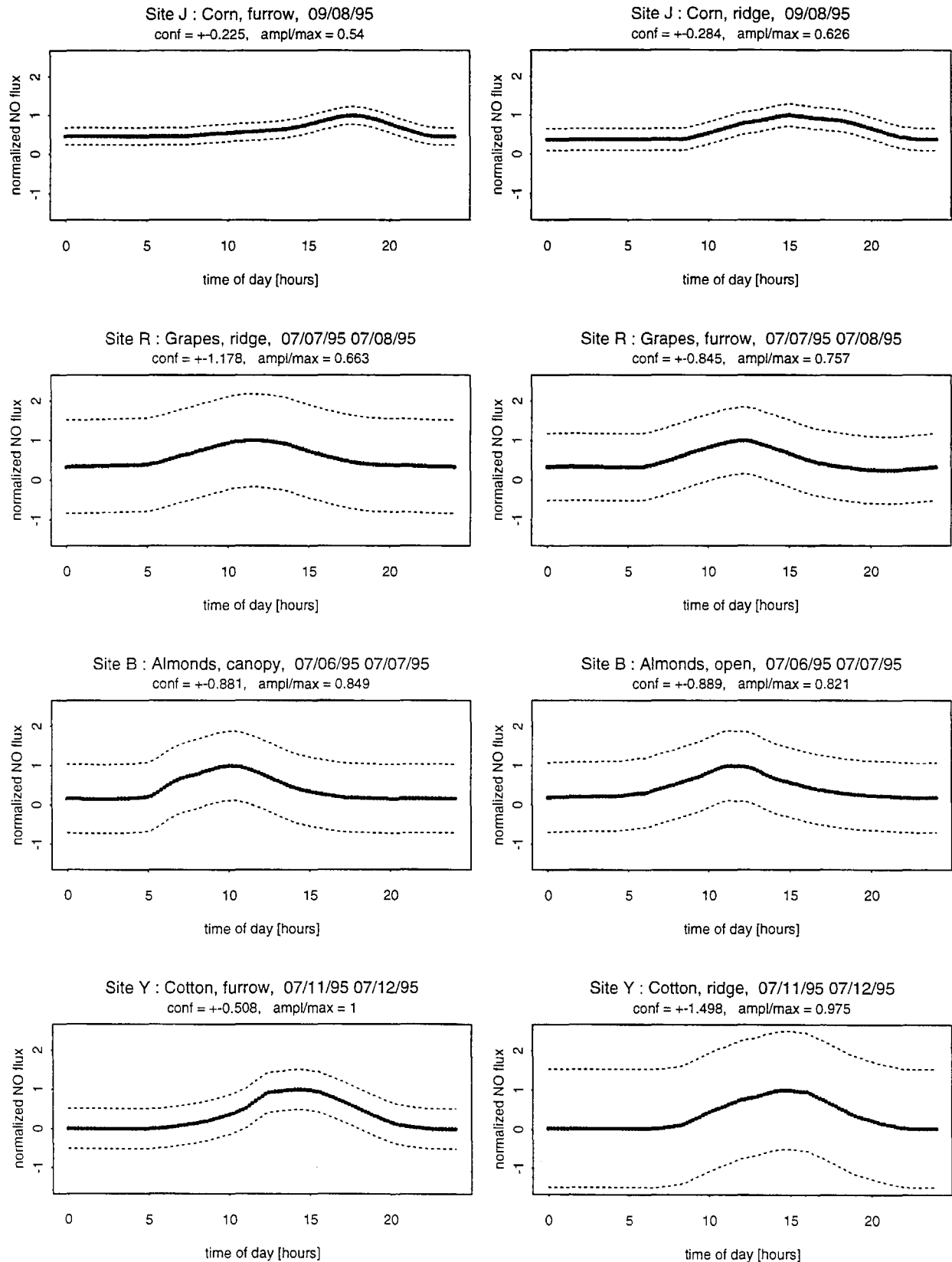


Figure 5. Diel characteristic curves: means and 95% confidence envelopes.
By crop and position.

Estimated by averaging normalized diel plots (from Figures 3a-3c) for all days by crop and position (see Appendix 5 for method).
Data collected in San Joaquin Valley, July-September, 1995.

loess smoother, spline for interpolated points



Step 3). Calculation of diel NO_x flux from routine-measured data, for mean chamber results by crop, site, position, and date.

To estimate daily chamber NO_x flux at field sites where only midday measurements were made ("routine" measurements), it is assumed that the basic shape of the distribution of NO_x flux over a day stays the same, although the maximum NO_x flux levels may change. The associated diel curves are derived from a) the characteristic diel curves that were produced from the diel-measured data with similar crop type in Step 2 above, and b) the mean routine-measured flux.

The characteristic curves calculated in Step 2 are taken to represent the general distribution of NO_x during a day, for any absolute flux levels for relevant crop types. The ratio of the amplitude to the maximum is assumed to remain constant; this assumption is considered reasonable, as inspection of the data shows the amplitude of the diel flux to be approximately proportional to the maximum flux. The average routine-measured flux, taken around midday, is assumed to be the mean maximum flux for that day, and is used to scale the normalized curve and to estimate the amplitude of the derived diel curve. The times of day for routine data ranged from 9:30 am - 3:00 pm; NO_x flux values taken within this time window routinely fall within the 95% confidence interval for the peak flux predicted by the diel curve (See Figure 4.) Therefore, given:

meanNOmax = peak NO flux level from routine data

C = a relevant characteristic diel curve with:

NOcharacteristic = the value in [0, 1] of C

then

NO = meanNOmax * NOcharacteristic

The integral of the new diel curve provides an estimate of the total daily NO_x flux for the routine-measured site. Standard errors are propagated by taking into account the standard errors in the meanNOmax and in NOcharacteristic. The propagation of standard error is therefore:

$$\begin{aligned}
 \text{s.e.}(\text{NO}) &= \sqrt{\left(\frac{d\text{NO}}{d\text{meanNOmax}} * \text{s.e.}(\text{meanNOmax}) \right)^2 + \left(\frac{d\text{NO}}{d\text{NOcharacteristic}} * \text{s.e.}(\text{NOcharacteristic}) \right)^2 } \\
 &= \sqrt{\left[\text{NOcharacteristic} * \text{s.e.}(\text{meanNOmax}) \right]^2 + \left[\text{meanNOmax} * \text{s.e.}(\text{NOcharacteristic}) \right]^2}
 \end{aligned}$$

Since full diel data were not taken for all crop types, certain crop types are used as proxy for similar crops:

<u>Crop with diel data</u>	<u>as proxy for</u>	<u>similar crops</u>
corn		corn
grapes		grapes
almonds		tree crops: almonds, peaches, oranges
cotton		row crops: alfalfa, irrigated pasture, sugar beets, tomatoes

2.2.2. Results.

2.2.2.1. Diel Flux Calculation Results.

Figure 3 shows the results of the curve-fitting and interpolation from step 1. The titles for each plot give the total NO_x flux as the 24-hour integral of the curve. Figure 4 shows the results of rescaling the normalized curves to the original diel curves with 95% confidence intervals (F-distribution). There is generally good approximation of the original diels, but in the case of Kearney flood, grapes, furrow, there are very wide differences in the amplitude/maximum ratio due to averaging this ratio for the normalized curve; the steepest and the flattest curves are poorly approximated. Ideally, one should know both the maximum and minimum fluxes at those sites where only routine data were taken, rather than extrapolating from a constant ratio. However, minimum flux levels were not measured, because this would have required an additional nighttime measurement, for which the necessary labor was not available. Characteristics of the normalized individual diel curves from Step 2 and their mean characteristic curves (scale [0,1]) are provided in Table 6. The results for Step 3 field NO_x flux for all

Table 6. Summary of diel curves: a. fitted diel curves, and b. characteristic diel curves for each crop type at sites located in the San Joaquin Valley measured July-September 1995. Flux measurements are presented by irrigation regime and field position. Minimum and maximum NO fluxes represent minimum and maximum points of the fitted diel curves for each site and day; total fluxes are integrated values for the 24-h period.

a. Fitted diel curves.

code	crop	location	position	irrigation	date	[ng-N/cm2/h]				[ng-N/cm2/day]	
						Min. NOx	Max. NOx	Standard Error	95% Confidence Interval	Total NOx	95% Confidence Interval
J	Corn	Plainview	furrow	Furrow	09/08/95	0.280	0.610	0.051	0.143	8.937	3.422
J	Corn	Plainview	ridge	Furrow	09/08/95	0.242	0.647	0.068	0.192	9.086	4.609
R	Grapes	Kearney	ridge	Flood	07/07/95 07/08/95	1.343	4.542	0.642	2.072	67.972	49.722
R	Grapes	Kearney	ridge	Flood	07/29/95	2.813	5.415	0.815	2.473	90.209	59.358
R	Grapes	Kearney	ridge	Flood	09/06/95	0.428	2.189	0.212	0.685	25.492	16.447
R	Grapes	Kearney	furrow	Flood	07/07/95 07/08/95	1.820	3.612	0.398	1.288	62.371	30.913
R	Grapes	Kearney	furrow	Flood	07/29/95	1.009	6.471	0.387	1.252	67.937	30.045
R	Grapes	Kearney	furrow	Flood	09/06/95	0.565	8.226	0.413	1.341	60.666	32.190
B	Almonds	Parlier	canopy	Flood	07/06/95 07/07/95	0.228	1.038	0.117	0.384	11.449	9.208
B	Almonds	Parlier	canopy	Flood	07/30/95	0.051	0.294	0.037	0.112	3.594	2.697
B	Almonds	Parlier	canopy	Flood	08/03/95	0.269	4.510	0.354	1.130	38.580	27.124
B	Almonds	Parlier	canopy	Flood	09/07/95	1.023	2.864	0.624	1.880	36.672	45.128
B	Almonds	Parlier	open	Flood	07/06/95 07/07/95	0.733	2.655	0.477	1.607	32.449	38.569
B	Almonds	Parlier	open	Flood	07/30/95	0.447	0.567	0.150	0.396	12.566	9.506
B	Almonds	Parlier	open	Flood	08/03/95	0.648	7.933	0.672	2.159	58.412	51.813
B	Almonds	Parlier	open	Flood	09/07/95	1.654	4.631	0.990	2.998	52.270	71.951
Y	Cotton	West Side	furrow	Furrow	07/11/95 07/12/95	0.000	2.752	0.231	0.746	17.972	17.897
Y	Cotton	West Side	furrow	Furrow	07/31/95	0.000	1.220	0.124	0.373	7.771	8.942
Y	Cotton	West Side	furrow	Furrow	09/09/95	0.107	0.130	0.063	0.167	2.855	4.007
Y	Cotton	West Side	ridge	Furrow	07/11/95 07/12/95	0.000	2.153	0.357	1.224	18.368	29.372
Y	Cotton	West Side	ridge	Furrow	07/31/95	0.019	1.202	0.215	0.701	7.841	16.822
Y	Cotton	West Side	ridge	Furrow	09/09/95	0.080	1.372	0.273	0.870	7.791	20.870

b. Characteristic diel curves.

crop	position	Amplitude/Max	Max	Curve.se	Curve.conf	Crops represented by curve
Corn	furrow	0.540	1.000	0.027	0.225	corn
Corn	ridge	0.626	1.000	0.042	0.284	
Grapes	ridge	0.663	1.000	0.622	1.178	grapes
Grapes	furrow	0.757	1.000	0.382	0.845	
Almonds	canopy	0.849	1.000	0.347	0.881	tree crops:
Almonds	open	0.904	1.000	0.707	0.889	almonds, peaches, oranges
Cotton	furrow	1.000	1.000	0.263	0.508	row crops: alfalfa, tomatoes
Cotton	ridge	0.975	1.000	0.489	1.498	irrigated pasture, sugar beets

field sites (with diel data, with routine data, different crop type) are provided in Table 7.

The hourly and daily NO fluxes in Table 7 show, for corn crops, very low fluxes ($<1 \text{ ng-N cm}^{-2} \text{ h}^{-1}$), due most likely to very dry conditions, except for the site located at Plainview (site code J), which was fertilized during the study period. The fluxes for this site decrease markedly over time (Figure 6e). Grape crops show consistently higher fluxes in the furrow rather than ridge position. The almond crop at site B, like the corn crop at site J, was also fertilized during the study period and show marked increases then decreases over time in both canopy and open positions (Figure 6a.). Among all tree crops, there is no consistent NO_x flux difference between canopy and open positions. Cotton crop and other row crops (sugar beets, tomatoes) exhibit a high degree of variability over time that is not clearly related to either time since fertilization or position. Especially the intensively sampled sites can show orders of magnitude differences in fluxes over two to three consecutive days. Tree crops also exhibit some of this variability, but with row crops there does not appear to be other strong trends related to the variables listed. More explanation of these NO_x flux characteristic follows.

The methods used here to estimate daily NO_x fluxes are bottom-up in nature and provide more detailed estimation than has been available to date. Caveats are in order, of course:

- (1) Local regression that takes into account lognormality and also negative NO_x fluxes would be most ideal for fitting diel curves; unfortunately, the negative fluxes preclude the possibility of a data transformation that would preserve lognormality.
- (2) It is not known how the amplitude of a diel curve varies with the mean peak NO_x flux or even the overall maximum NO_x flux at a site; therefore, a characteristic curve may not necessarily remain the same in shape over time and under different conditions;
- (3) The diel curves derived for routine data make use of the assumption that the routine data collected all were at the time of peak NO_x flux during the day. For these "routine" data, it cannot be known from the data when peak NO_x actually occurred; maximum solar insolation and hence maximum soil temperature would be required when peak conditions occur. This driving data was not available to us. Moreover, flux measurements taken at "peak conditions" are statistically indistinguishable from values used.
- (4) The confidence bounds on the diel curves, incorporating the standard error of the fitted diel curve) integrate to produce extremely large integral (daily flux) differences from the mean

Table 7. Mid-day NOx flux (mean of all NOx measurements per site and day) and total daily NOx flux (predicted from diel curves) measured in the San Joaquin Valley, July-September, 1995. Fluxes were computed from diel curves derived from: a. corn, b. grapes, c. almonds, d. cotton, e. cotton, ridge. Flux measurements are presented by irrigation regime and field position.

*For diel-measured data, the standard error columns are simultaneous confidence bounds rather than standard errors.

Table 7a. Diel fluxes derived from Site J, Corn diel data

diel/routine	site code	crop	location	position	irrigation method	date	mid-day NOx flux		total daily NOx flux	
							mean [ng-N/cm2/h]	std. error [ng-N/cm2/h]	mean [ng-N/cm2/day]	std. error [ng-N/cm2/day]
d	J	Corn	Plainview	furrow	Furrow	09/08/95	0.610	0.143	8.9	3.4
d	J	Corn	Plainview	ridge	Furrow	09/08/95	0.647	0.192	9.1	4.6
r	J	Corn	Plainview	furrow	Furrow	08/08/95	13.483	22.084	197.5	1521.1
r	J	Corn	Plainview	furrow	Furrow	08/09/95	9.741	11.055	142.7	767.1
r	J	Corn	Plainview	furrow	Furrow	08/10/95	8.655	6.013	126.8	416.3
r	J	Corn	Plainview	furrow	Furrow	08/12/95	7.601	6.237	111.3	431.1
r	J	Corn	Plainview	ridge	Furrow	08/08/95	52.411	33.161	735.6	2306.9
r	J	Corn	Plainview	ridge	Furrow	08/09/95	39.485	29.955	554.2	2076.3
r	J	Corn	Plainview	ridge	Furrow	08/10/95	12.116	9.238	170.1	640.3
r	J	Corn	Plainview	ridge	Furrow	08/12/95	12.142	11.484	170.4	793.6
r	I	Corn	Tulare	furrow	Furrow	08/05/95	0.041	0.067	0.6	4.6
r	I	Corn	Tulare	furrow	Furrow	08/13/95	-0.007	0.281	0.0	0.0
r	I	Corn	Tulare	furrow	Furrow	08/16/95	0.276	0.272	4.0	18.7
r	I	Corn	Tulare	ridge	Furrow	08/05/95	0.202	0.113	2.8	7.9
r	I	Corn	Tulare	ridge	Furrow	08/13/95	0.129	0.436	1.8	30.0
r	I	Corn	Tulare	ridge	Furrow	08/16/95	0.351	0.678	4.9	46.7
r	K	Corn	Waukena	furrow	Furrow	08/04/95	0.064	0.225	0.9	15.5
r	K	Corn	Waukena	furrow	Furrow	08/06/95	0.480	0.691	7.0	47.6
r	K	Corn	Waukena	furrow	Furrow	08/09/95	1.013	0.880	14.8	60.8
r	K	Corn	Waukena	furrow	Furrow	08/10/95	0.095	0.126	1.4	8.7
r	K	Corn	Waukena	ridge	Furrow	08/04/95	0.383	0.271	5.4	18.8
r	K	Corn	Waukena	ridge	Furrow	08/06/95	0.557	0.233	7.8	16.5
r	K	Corn	Waukena	ridge	Furrow	08/09/95	0.523	0.388	7.3	26.9
r	K	Corn	Waukena	ridge	Furrow	08/10/95	0.112	0.120	1.6	8.3

Table 7b. Diel fluxes derived from Site R, Grapes diel data

diel/routine	site code	crop	location	position	irrigation method	date	mid-day NOx flux		total daily NOx flux	
							mean [ng-N/cm2/h]	std. error [ng-N/cm2/h]	mean [ng-N/cm2/day]	std. error [ng-N/cm2/day]
d	R	Grapes	Kearney	ridge	Flood	07/07/95	4.542	2.072	68.0	49.7
d	R	Grapes	Kearney	ridge	Flood	07/29/95	5.415	2.473	90.2	59.4
d	R	Grapes	Kearney	ridge	Flood	09/06/95	2.189	0.685	25.5	16.4
d	R	Grapes	Kearney	furrow	Flood	07/07/95	3.612	1.288	62.4	30.9
d	R	Grapes	Kearney	furrow	Flood	07/29/95	6.471	1.252	67.9	30.0
d	R	Grapes	Kearney	furrow	Flood	09/06/95	8.226	1.341	60.7	32.2
r	R	Grapes	Kearney	ridge	Flood	07/27/95	4.607	2.251	66.3	289.6
r	R	Grapes	Kearney	furrow	Flood	07/27/95	7.800	1.860	93.9	270.5
r	L	Grapes	Firebaugh	furrow	Flood	08/22/95	20.451	20.584	246.1	2463.3
r	L	Grapes	Firebaugh	furrow	Flood	08/23/95	16.450	6.177	198.0	805.6
r	L	Grapes	Firebaugh	ridge	Flood	08/22/95	2.517	3.083	36.2	363.6
r	L	Grapes	Firebaugh	ridge	Flood	08/23/95	0.906	0.618	13.0	75.5
r	Q	Grapes	Kearney	furrow	Drip	08/12/95	2.116	0.611	25.5	83.9
r	Q	Grapes	Kearney	furrow	Drip	08/15/95	3.391	1.816	40.8	225.0
r	Q	Grapes	Kearney	furrow	Drip	08/19/95	2.751	0.866	33.1	116.5
r	Q	Grapes	Kearney	furrow	Drip	08/20/95	3.663	1.739	44.1	218.2
r	Q	Grapes	Kearney	furrow	Drip	08/21/95	3.815	1.724	45.9	217.6
r	Q	Grapes	Kearney	furrow	Drip	08/22/95	3.184	2.151	38.3	261.8
r	Q	Grapes	Kearney	ridge	Drip	08/12/95	0.939	0.525	13.5	66.3
r	Q	Grapes	Kearney	ridge	Drip	08/15/95	1.146	0.577	16.5	73.8
r	Q	Grapes	Kearney	ridge	Drip	08/19/95	1.180	0.589	17.0	75.5
r	Q	Grapes	Kearney	ridge	Drip	08/20/95	1.215	0.644	17.5	81.5
r	Q	Grapes	Kearney	ridge	Drip	08/21/95	1.168	0.691	16.8	86.0
r	Q	Grapes	Kearney	ridge	Drip	08/22/95	0.639	0.400	9.2	49.4

Table 7c. Diel fluxes derived from Site B, Almonds diel data

diel/routine	site code	crop	location	position	irrigation method	date	mid-day NOx flux		total daily NOx flux	
							mean [ng-N/cm2/h]	std. error [ng-N/cm2/h]	mean [ng-N/cm2/day]	std. error [ng-N/cm2/day]
d	B	Almonds	Parlier	canopy	Flood	07/06/95	1.038	0.384	11.4	9.2
d	B	Almonds	Parlier	canopy	Flood	07/30/95	0.294	0.112	3.6	2.7
d	B	Almonds	Parlier	canopy	Flood	08/03/95	4.510	1.130	38.6	27.1
d	B	Almonds	Parlier	canopy	Flood	09/07/95	2.864	1.880	36.7	45.1
d	B	Almonds	Parlier	open	Flood	07/06/95	2.655	1.607	32.4	38.6
d	B	Almonds	Parlier	open	Flood	07/30/95	0.567	0.396	12.6	9.5
d	B	Almonds	Parlier	open	Flood	08/03/95	7.933	2.159	58.4	51.8
d	B	Almonds	Parlier	open	Flood	09/07/95	4.631	2.998	52.3	72.0
r	B	Almonds	Parlier	canopy	Flood	07/11/95	15.558	14.181	165.2	1678.1
r	B	Almonds	Parlier	canopy	Flood	07/12/95	15.600	13.528	165.7	1604.1
r	B	Almonds	Parlier	canopy	Flood	07/13/95	25.269	20.546	268.4	2443.2
r	B	Almonds	Parlier	canopy	Flood	07/14/95	16.455	13.786	174.8	1637.1
r	B	Almonds	Parlier	canopy	Flood	07/15/95	36.300	26.885	385.5	3231.6
r	B	Almonds	Parlier	canopy	Flood	07/16/95	2.414	2.168	25.6	256.7
r	B	Almonds	Parlier	canopy	Flood	07/18/95	6.374	5.192	67.7	617.4
r	B	Almonds	Parlier	canopy	Flood	07/21/95	3.473	2.593	36.9	309.8
r	B	Almonds	Parlier	open	Flood	07/11/95	0.646	0.645	6.4	68.2
r	B	Almonds	Parlier	open	Flood	07/12/95	4.327	1.847	42.8	212.1
r	B	Almonds	Parlier	open	Flood	07/13/95	5.461	2.081	54.0	244.7
r	B	Almonds	Parlier	open	Flood	07/14/95	2.863	1.828	28.3	198.7
r	B	Almonds	Parlier	open	Flood	07/15/95	8.007	4.042	79.1	451.5
r	B	Almonds	Parlier	open	Flood	07/16/95	0.479	0.345	4.7	37.3
r	B	Almonds	Parlier	open	Flood	07/18/95	1.329	0.695	13.1	77.3
r	B	Almonds	Parlier	open	Flood	07/21/95	1.862	0.929	18.4	103.9
r	C	Almonds	Parlier	canopy	Drip	07/14/95	7.265	9.444	77.2	1121.9
r	C	Almonds	Parlier	canopy	Drip	07/16/95	3.651	9.006	38.8	1047.9
r	C	Almonds	Parlier	canopy	Drip	07/18/95	0.206	0.238	2.2	28.4
r	C	Almonds	Parlier	canopy	Drip	07/21/95	9.355	15.937	99.4	1859.8
r	C	Almonds	Parlier	open	Drip	07/14/95	9.940	7.767	98.2	841.7
r	C	Almonds	Parlier	open	Drip	07/16/95	4.862	3.372	48.1	363.7
r	C	Almonds	Parlier	open	Drip	07/18/95	0.196	0.317	1.9	33.2
r	C	Almonds	Parlier	open	Drip	07/21/95	9.635	4.050	95.2	466.5
r	T	Oranges	Lindcove	canopy	Drip	08/11/95	0.855	0.918	9.1	108.0
r	T	Oranges	Lindcove	canopy	Drip	08/12/95	2.140	2.898	22.7	339.3
r	T	Oranges	Lindcove	canopy	Drip	08/17/95	1.590	1.346	16.9	159.8
r	T	Oranges	Lindcove	canopy	Drip	08/21/95	1.480	1.711	15.7	200.9
r	T	Oranges	Lindcove	open	Drip	08/11/95	0.796	1.728	7.9	179.5

Table 7c. Diel fluxes derived from Site B, Almonds diel data, cont'd.

diel/routine	site code	crop	location	position	irrigation method	date	mid-day NOx flux		total daily NOx flux	
							mean [ng-N/cm2/h]	std. error [ng-N/cm2/h]	mean [ng-N/cm2/day]	std. error [ng-N/cm2/day]
r	T	Oranges	Lindcove	open	Drip	08/12/95	1.323	1.128	13.1	120.0
r	T	Oranges	Lindcove	open	Drip	08/17/95	1.573	1.389	15.5	147.5
r	T	Oranges	Lindcove	open	Drip	08/21/95	1.822	1.507	18.0	160.6
r	V	Peaches	Clovis	canopy	Flood	07/13/95	2.117	1.139	22.5	139.6
r	V	Peaches	Clovis	canopy	Flood	07/15/95	0.438	0.489	4.7	57.5
r	V	Peaches	Clovis	canopy	Flood	07/19/95	0.046	0.047	0.5	5.6
r	V	Peaches	Clovis	canopy	Flood	07/20/95	0.418	0.497	4.4	58.4
r	V	Peaches	Clovis	open	Flood	07/13/95	3.626	2.261	35.8	246.3
r	V	Peaches	Clovis	open	Flood	07/15/95	0.561	0.486	5.5	51.9
r	V	Peaches	Clovis	open	Flood	07/19/95	0.060	0.026	0.6	2.9
r	V	Peaches	Clovis	open	Flood	07/20/95	0.654	0.428	6.5	46.4

Table 7d. Diel fluxes derived from Site Y, Cotton diel data

diel/routine	site code	crop	location	position	irrigation method	date	mid-day NOx flux		total daily NOx flux	
							mean [ng-N/cm ² /h]	std. error [ng-N/cm ² /h]	mean [ng-N/cm ² /day]	std. error [ng-N/cm ² /day]
d	Y	Cotton	West Side	furrow	Furrow	07/11/95	2.752	0.746	18.0	17.9
d	Y	Cotton	West Side	furrow	Furrow	07/31/95	1.220	0.373	7.8	8.9
d	Y	Cotton	West Side	furrow	Furrow	09/09/95	0.130	0.167	2.9	4.0
d	Y	Cotton	West Side	ridge	Furrow	07/11/95	2.153	1.224	18.4	29.4
d	Y	Cotton	West Side	ridge	Furrow	07/31/95	1.202	0.701	7.8	16.8
d	Y	Cotton	West Side	ridge	Furrow	09/09/95	1.372	0.870	7.8	20.9
r	Y	Cotton	West Side	furrow	Furrow	07/13/95	0.281	0.231	1.8	22.8
r	Y	Cotton	West Side	furrow	Furrow	07/15/95	0.942	0.692	6.1	68.4
r	Y	Cotton	West Side	furrow	Furrow	07/16/95	0.273	0.433	1.8	42.3
r	Y	Cotton	West Side	furrow	Furrow	07/18/95	0.082	0.204	0.5	19.9
r	Y	Cotton	West Side	furrow	Furrow	07/19/95	0.157	0.133	1.0	13.2
r	Y	Cotton	West Side	furrow	Furrow	07/21/95	0.005	0.078	0.0	7.7
r	Y	Cotton	West Side	ridge	Furrow	07/13/95	0.783	0.764	5.4	95.7
r	Y	Cotton	West Side	ridge	Furrow	07/15/95	2.899	1.742	19.9	233.1
r	Y	Cotton	West Side	ridge	Furrow	07/16/95	0.698	0.452	4.8	59.7
r	Y	Cotton	West Side	ridge	Furrow	07/18/95	0.550	0.367	3.8	48.1
r	Y	Cotton	West Side	ridge	Furrow	07/19/95	0.484	0.277	3.3	37.4
r	Y	Cotton	West Side	ridge	Furrow	07/21/95	0.246	0.197	1.7	25.2
r	D	Cotton	San Joaquin	furrow	Furrow	07/27/95	65.404	58.199	421.8	5730.2
r	D	Cotton	San Joaquin	furrow	Furrow	08/01/95	8.074	4.940	52.1	491.6
r	D	Cotton	San Joaquin	furrow	Furrow	08/02/95	6.160	3.991	39.7	396.3
r	D	Cotton	San Joaquin	ridge	Furrow	07/27/95	10.194	3.874	70.1	591.1
r	D	Cotton	San Joaquin	ridge	Furrow	08/01/95	10.278	4.538	70.6	656.9
r	D	Cotton	San Joaquin	ridge	Furrow	08/02/95	5.074	1.657	34.9	269.5
r	E	Cotton	San Joaquin	furrow	Furrow	07/28/95	0.917	0.862	5.9	84.8
r	E	Cotton	San Joaquin	furrow	Furrow	08/02/95	3.096	6.837	20.0	667.7
r	E	Cotton	San Joaquin	ridge	Furrow	07/28/95	1.438	1.311	9.9	168.9
r	E	Cotton	San Joaquin	ridge	Furrow	08/02/95	3.003	2.500	20.6	319.8
r	F	Cotton	Tranquillity	furrow	Furrow	07/28/95	2.339	3.454	15.1	338.0
r	F	Cotton	Tranquillity	furrow	Furrow	08/01/95	2.072	0.677	13.4	70.7
r	F	Cotton	Tranquillity	ridge	Furrow	07/28/95	2.088	1.261	14.3	168.5
r	F	Cotton	Tranquillity	ridge	Furrow	08/01/95	3.282	1.230	22.6	188.7
r	G	Cotton	Riverdale	furrow	Furrow	09/11/95	0.057	0.145	0.4	14.2
r	G	Cotton	Riverdale	ridge	Furrow	09/11/95	0.208	0.177	1.4	22.5
r	H	Sugar beets	Mendota	furrow	Furrow	08/10/95	0.967	0.380	6.2	38.9
r	H	Sugar beets	Mendota	furrow	Furrow	08/11/95	0.757	0.585	4.9	57.8
r	H	Sugar beets	Mendota	ridge	Furrow	08/10/95	0.451	0.285	3.1	37.8
r	H	Sugar beets	Mendota	ridge	Furrow	08/11/95	0.678	0.439	4.7	57.9

Table 7d. Diel fluxes derived from Site Y, Cotton diel data, cont'd.

diel/routine	site code	crop	location	position	irrigation method	date	mid-day NOx flux		total daily NOx flux	
							mean [ng-N/cm2/h]	std. error [ng-N/cm2/h]	mean [ng-N/cm2/day]	std. error [ng-N/cm2/day]
r	N	Sugar beets	Mendota	furrow	Furrow	07/19/95	0.406	0.185	2.6	18.7
r	N	Sugar beets	Mendota	furrow	Furrow	07/20/95	0.806	0.276	5.2	28.7
r	N	Sugar beets	Mendota	ridge	Furrow	07/19/95	1.346	1.089	9.3	139.0
r	N	Sugar beets	Mendota	ridge	Furrow	07/20/95	1.201	1.215	8.3	151.7
r	S	Sugar beets	Corcoran	open	Furrow	08/12/95	0.086	0.110	0.6	13.6
r	U	Sugar beets	San Joaquin	furrow	Furrow	08/11/95	7.968	5.736	51.4	571.1
r	U	Sugar beets	San Joaquin	furrow	Furrow	08/18/95	3.670	2.090	23.7	208.6
r	U	Sugar beets	San Joaquin	ridge	Furrow	08/11/95	3.786	1.489	26.0	224.3
r	U	Sugar beets	San Joaquin	ridge	Furrow	08/18/95	4.765	2.700	32.7	365.8
r	Z	Tomatoes	West Side	furrow	Furrow	07/12/95	4.967	3.125	32.0	312.5
r	Z	Tomatoes	West Side	furrow	Furrow	07/13/95	3.418	1.630	22.0	164.3
r	Z	Tomatoes	West Side	furrow	Furrow	07/14/95	2.502	1.118	16.1	113.2
r	Z	Tomatoes	West Side	furrow	Furrow	07/15/95	20.732	10.462	133.7	1050.9
r	Z	Tomatoes	West Side	furrow	Furrow	07/16/95	0.757	0.229	4.9	24.2
r	Z	Tomatoes	West Side	furrow	Furrow	07/18/95	8.005	1.866	51.6	206.4
r	Z	Tomatoes	West Side	furrow	Furrow	07/20/95	16.150	3.433	104.2	388.4
r	Z	Tomatoes	West Side	furrow	Furrow	07/21/95	1.157	0.247	7.5	27.9
r	Z	Tomatoes	West Side	ridge	Furrow	07/12/95	9.317	4.565	64.0	641.0
r	Z	Tomatoes	West Side	ridge	Furrow	07/13/95	8.912	12.129	61.3	1486.7
r	Z	Tomatoes	West Side	ridge	Furrow	07/14/95	2.193	0.994	15.1	142.7
r	Z	Tomatoes	West Side	ridge	Furrow	07/15/95	10.545	4.119	72.5	624.5
r	Z	Tomatoes	West Side	ridge	Furrow	07/16/95	1.111	0.470	7.6	68.9
r	Z	Tomatoes	West Side	ridge	Furrow	07/18/95	12.685	4.084	87.2	668.6
r	Z	Tomatoes	West Side	ridge	Furrow	07/20/95	12.329	4.054	84.7	657.3
r	Z	Tomatoes	West Side	ridge	Furrow	07/21/95	1.152	0.189	7.9	47.2

Table 7e. Open crops: Diel flux derived from Site Y, Cotton, ridge

diel/routine	site code	crop	location	position	irrigation method	date	mid-day NOx flux		total daily NOx flux	
							mean [ng-N/cm2/h]	std. error [ng-N/cm2/h]	mean [ng-N/cm2/day]	std. error [ng-N/cm2/day]
r	A	Alfalfa	Firebaugh	open	Flood	08/22/95	6.948	4.283	97.5	315.8
r	A	Alfalfa	Firebaugh	open	Flood	08/23/95	3.545	1.675	49.8	117.6
r	O	Alfalfa	Kearney	open	Flood	08/20/95	1.342	0.637	18.8	44.7
r	O	Alfalfa	Kearney	open	Flood	08/22/95	0.396	0.246	5.6	17.1
r	P	Alfalfa	Kearney	open	Flood	07/11/95	2.399	0.542	33.7	40.7
r	P	Alfalfa	Kearney	open	Flood	07/12/95	2.546	0.946	35.7	67.3
r	M	Irrigated pasture	Sanger	open	Border Check	07/28/95	10.956	12.195	153.8	846.6
r	W	Irrigated pasture	Bonadelle Ranchos	open	Flood	08/24/95	13.169	23.102	184.8	1590.3
r	W	Irrigated pasture	Bonadelle Ranchos	open	Flood	08/25/95	6.984	7.606	98.0	524.9
r	W	Irrigated pasture	Bonadelle Ranchos	open	Flood	08/26/95	10.786	9.876	151.4	682.7
r	W	Irrigated pasture	Bonadelle Ranchos	open	Flood	08/28/95	6.898	9.602	96.8	661.6
r	X	Irrigated pasture	Bonadelle Ranchos	open	Flood	08/24/95	6.953	14.169	97.6	975.0
r	X	Irrigated pasture	Bonadelle Ranchos	open	Flood	08/25/95	10.771	29.313	151.2	2015.9
r	X	Irrigated pasture	Bonadelle Ranchos	open	Flood	08/26/95	4.755	1.769	66.7	133.0
r	X	Irrigated pasture	Bonadelle Ranchos	open	Flood	08/28/95	4.836	10.888	67.9	749.0

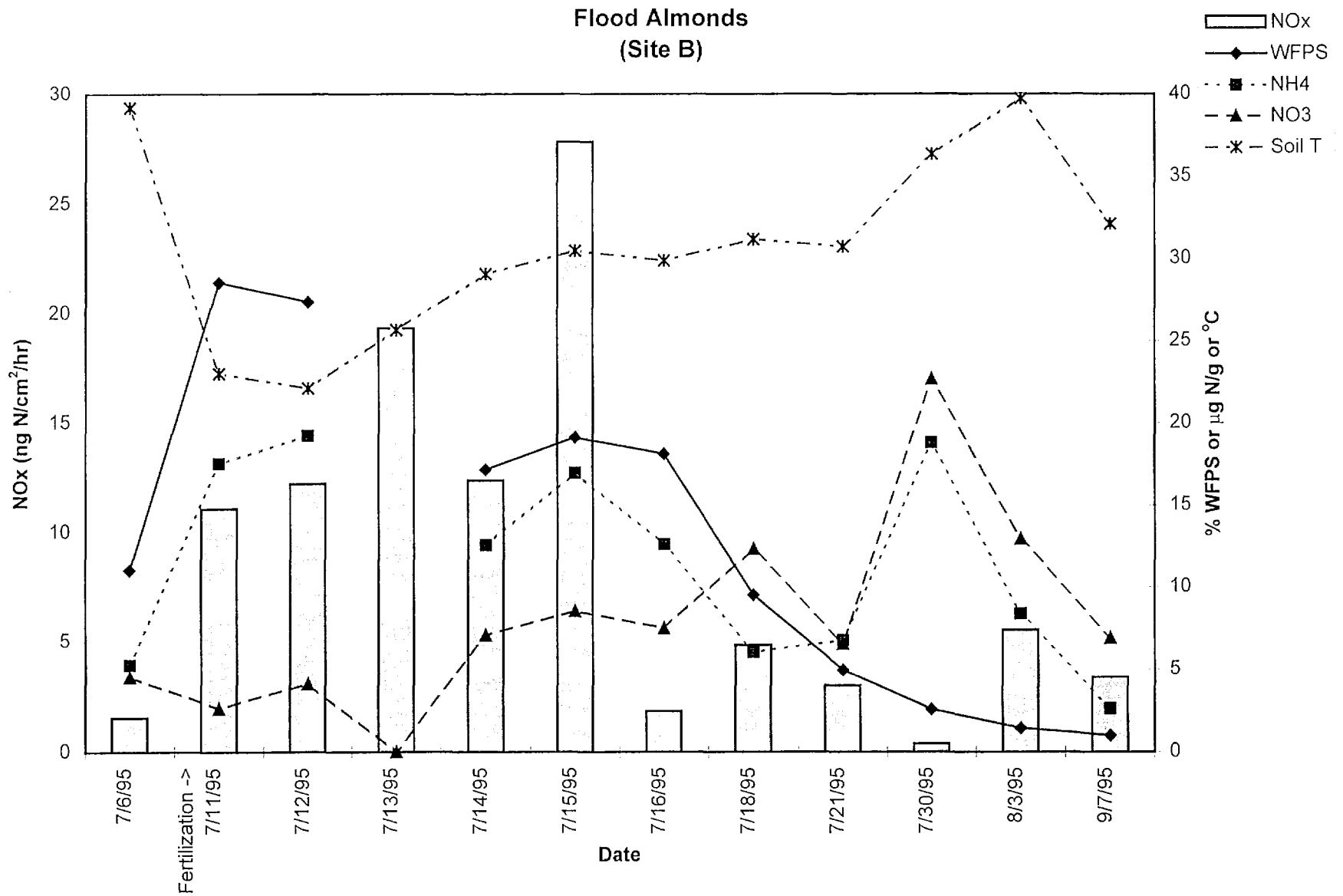


Figure 6a. NO_x fluxes and associated soil parameters measured at site B (flood almonds), Parlier, CA, July-September, 1995. Each bar or point is a mean of 20 observations.

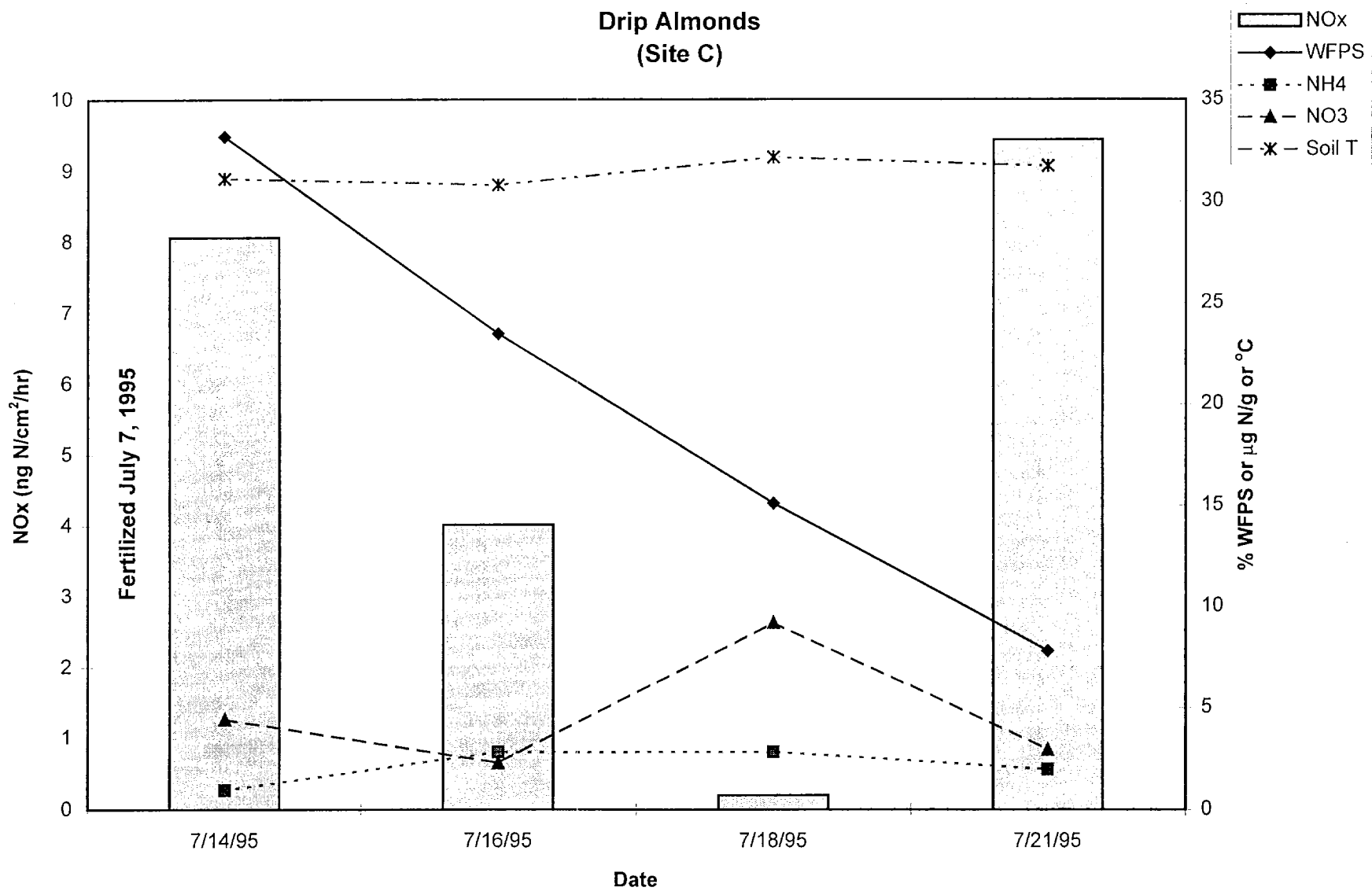


Figure 6b. NOx fluxes and associated soil parameters measured at site C (drip almonds), Parlier, CA, July, 1995. Each bar or point is a mean of 20 observations.

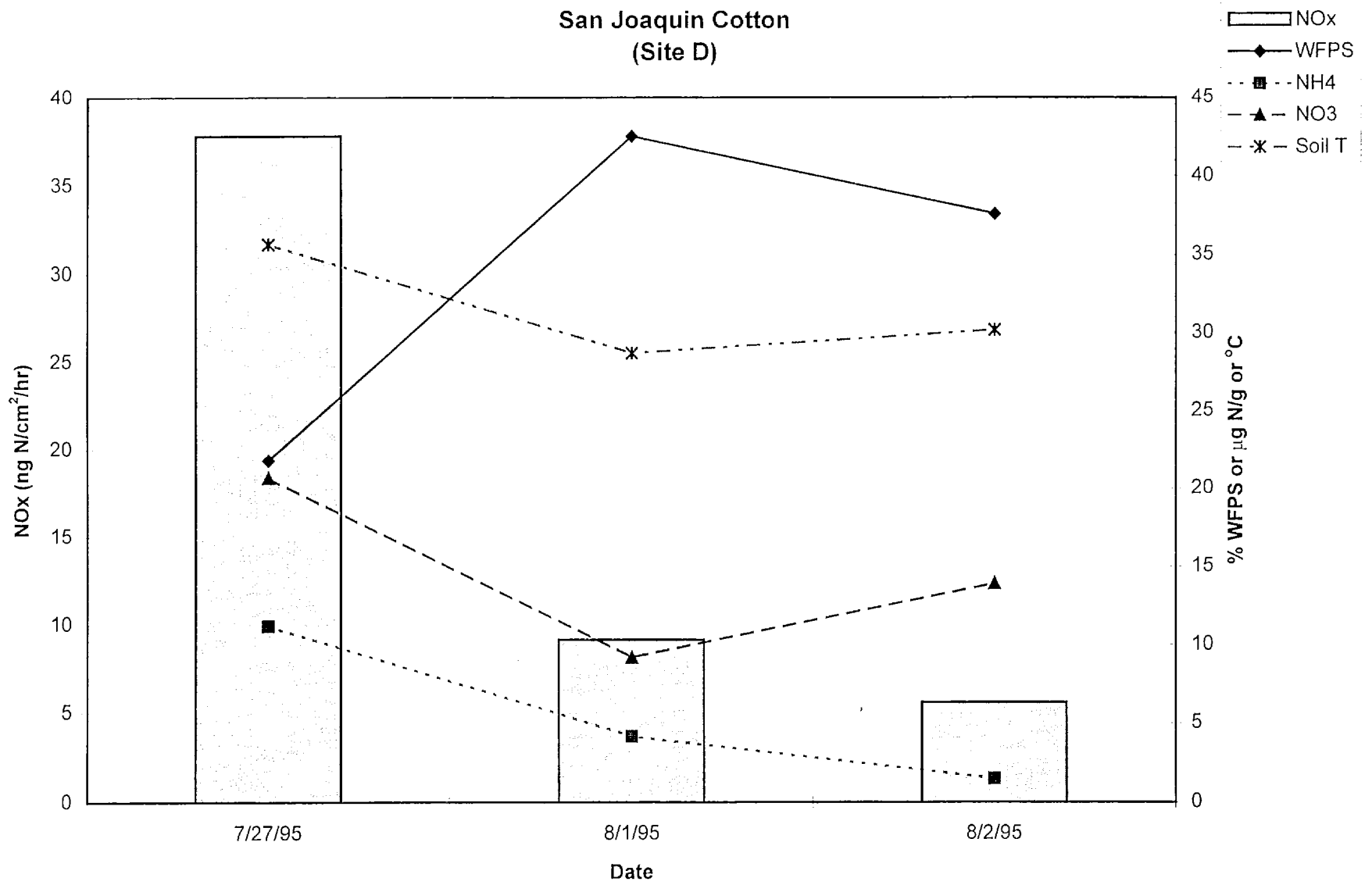


Figure 6c. NO_x fluxes and associated soil parameters measured at site D (cotton), San Joaquin, CA, July-August, 1995. Each bar or point is a mean of 20 observations.

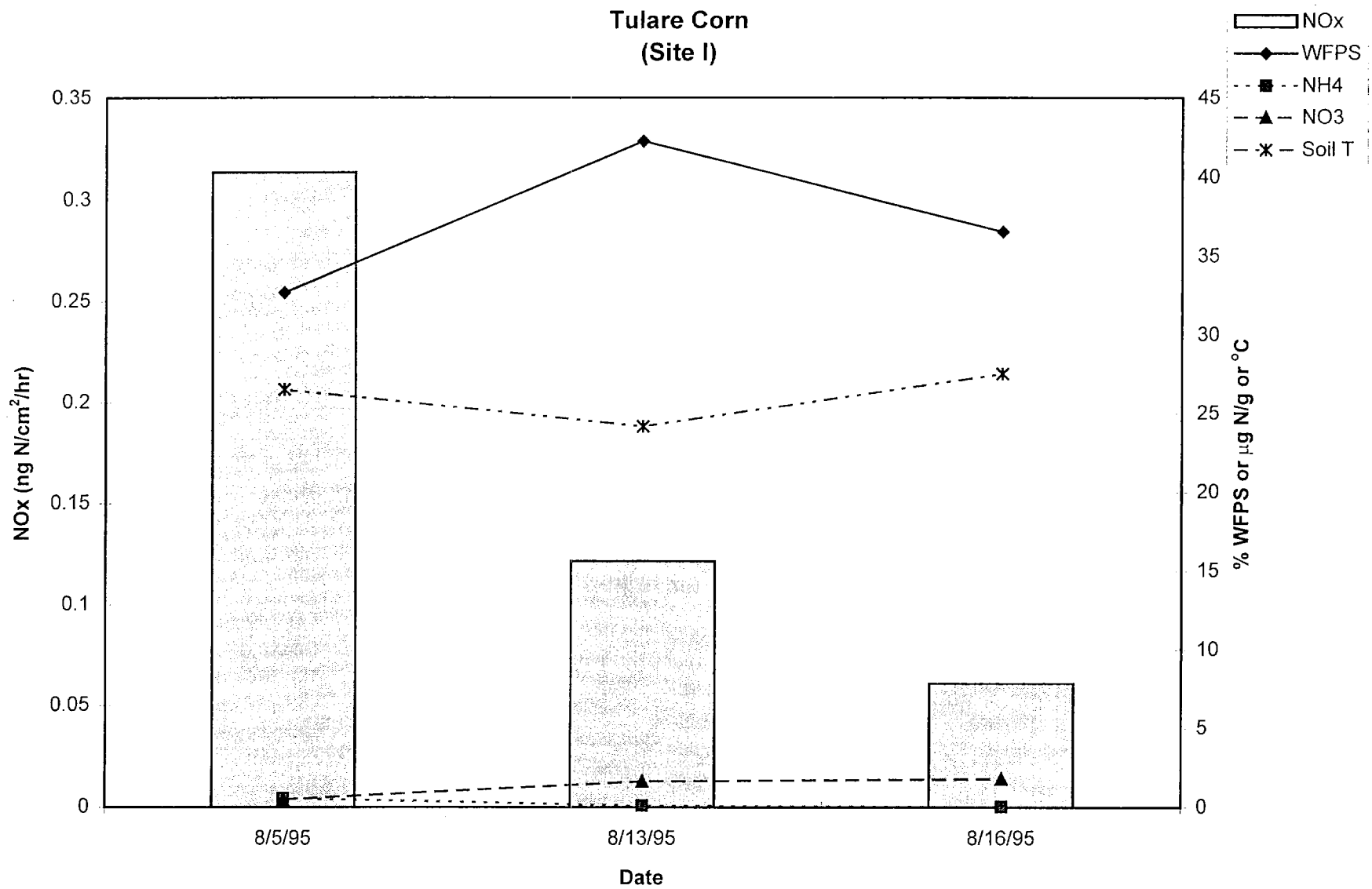


Figure 6d. NOx fluxes and associated soil parameters measured at site I (corn), Tulare, CA, August, 1995. Each bar or point is a mean of 20 observations..

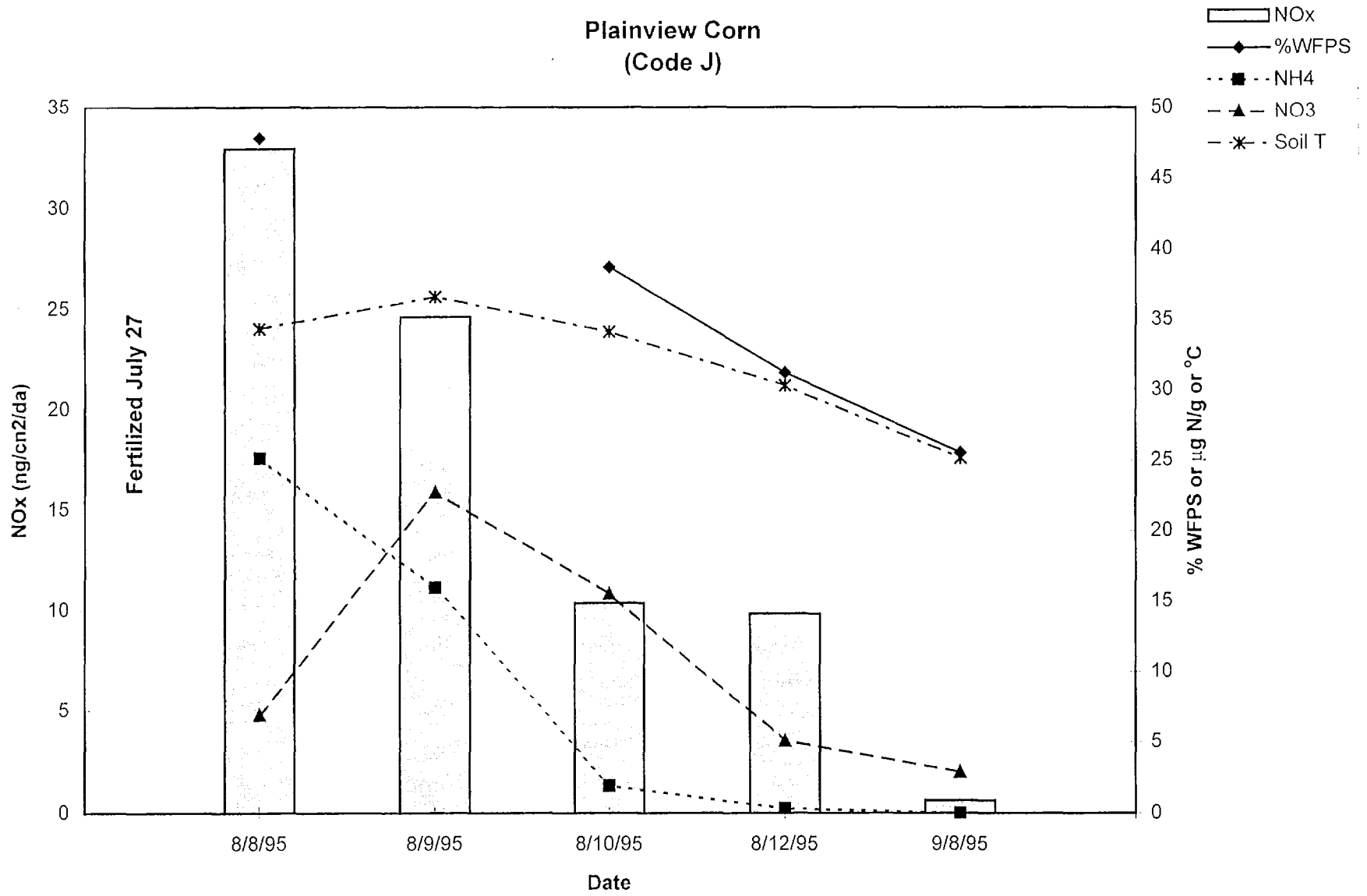


Figure 6e. NOx fluxes and associated soil parameters measured at site J (corn), Plainview, CA August, 1995. Each bar or point is a mean of 20 observations.

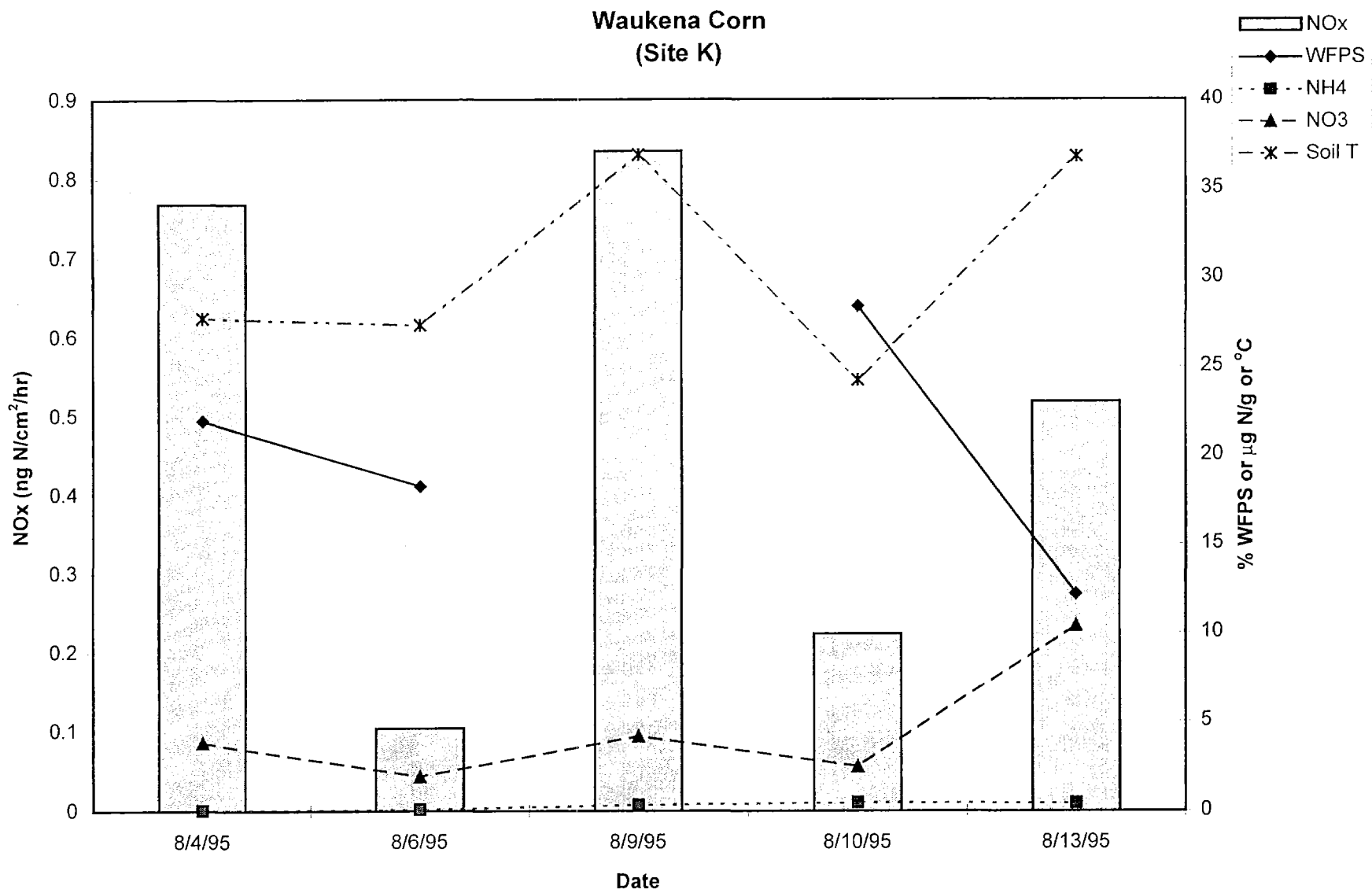


Figure 6f. NOx fluxes and associated soil parameters measured at site K (corn), Waukena, CA, August, 1995. Each bar or point is a mean of 20 observations.

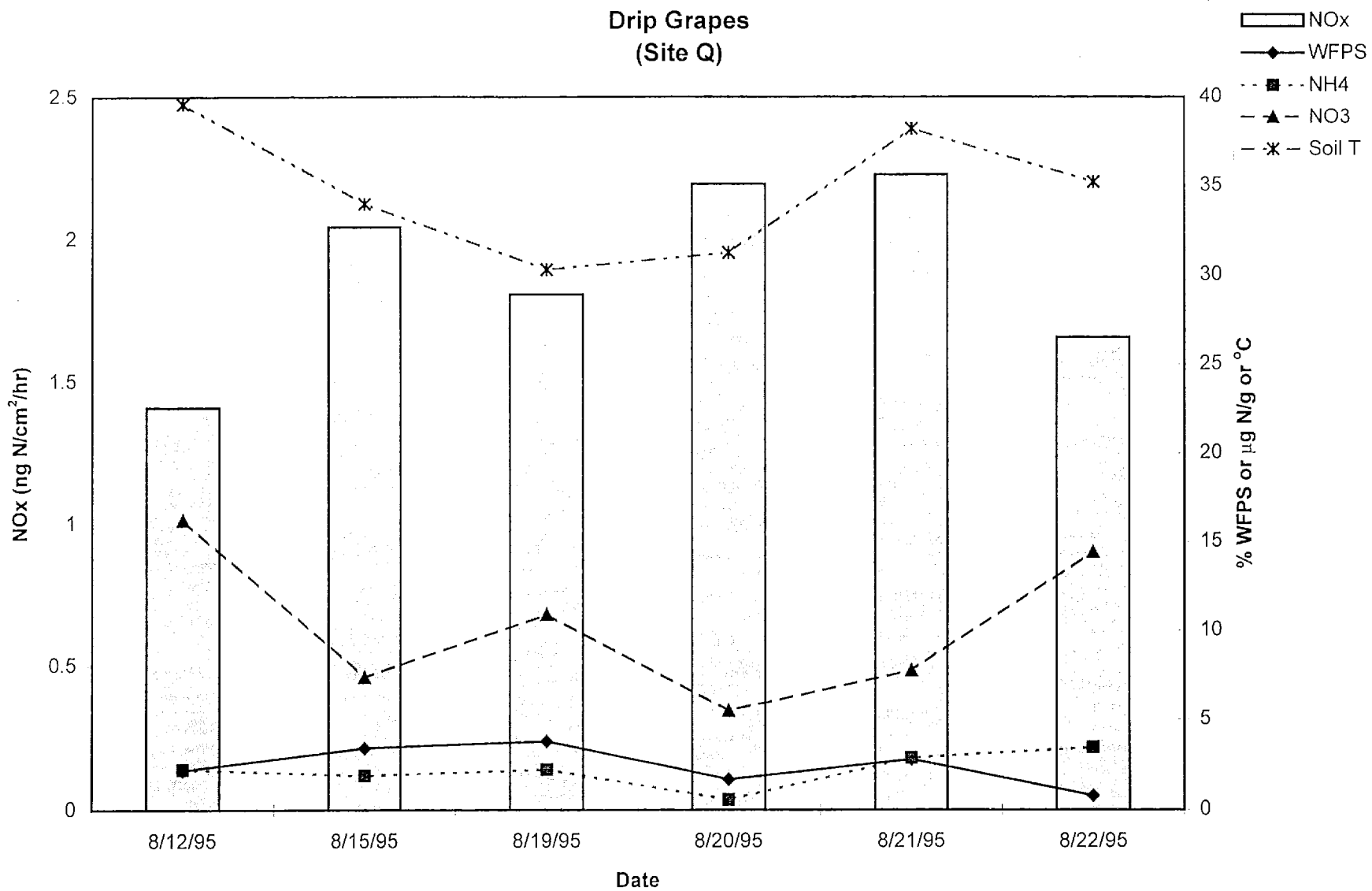


Figure 6g. NO_x fluxes and associated soil parameters measured at site Q (drip grapes), Kearney Ag Center, August, 1995. Each bar or point is a mean of 20 observations.

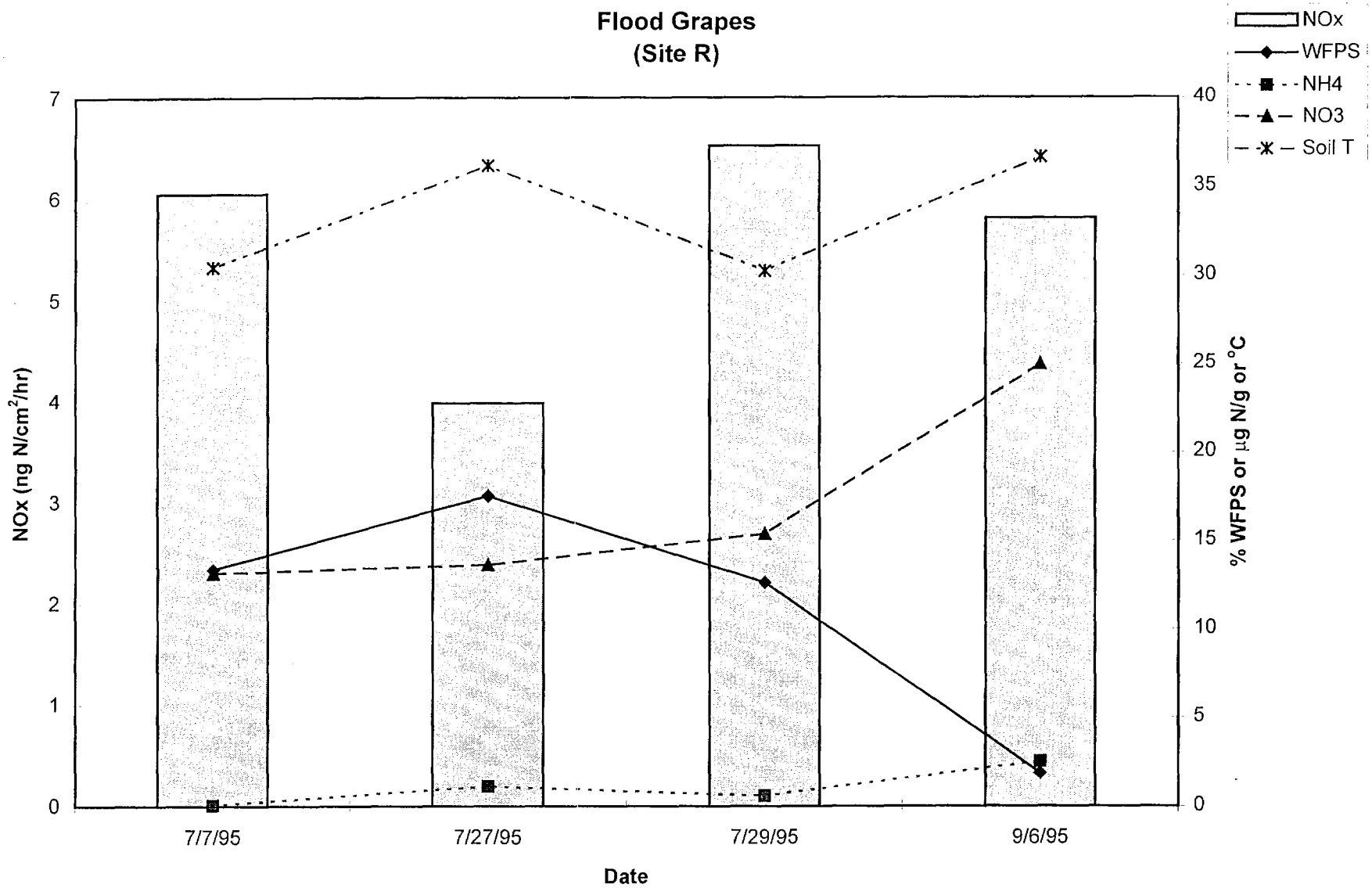


Figure 6h. NO_x fluxes and associated soil parameters measured at site R (flood grapes), Kearney Agricultural Center, July-September, 1995. Each bar or point is a mean of 20 observations.

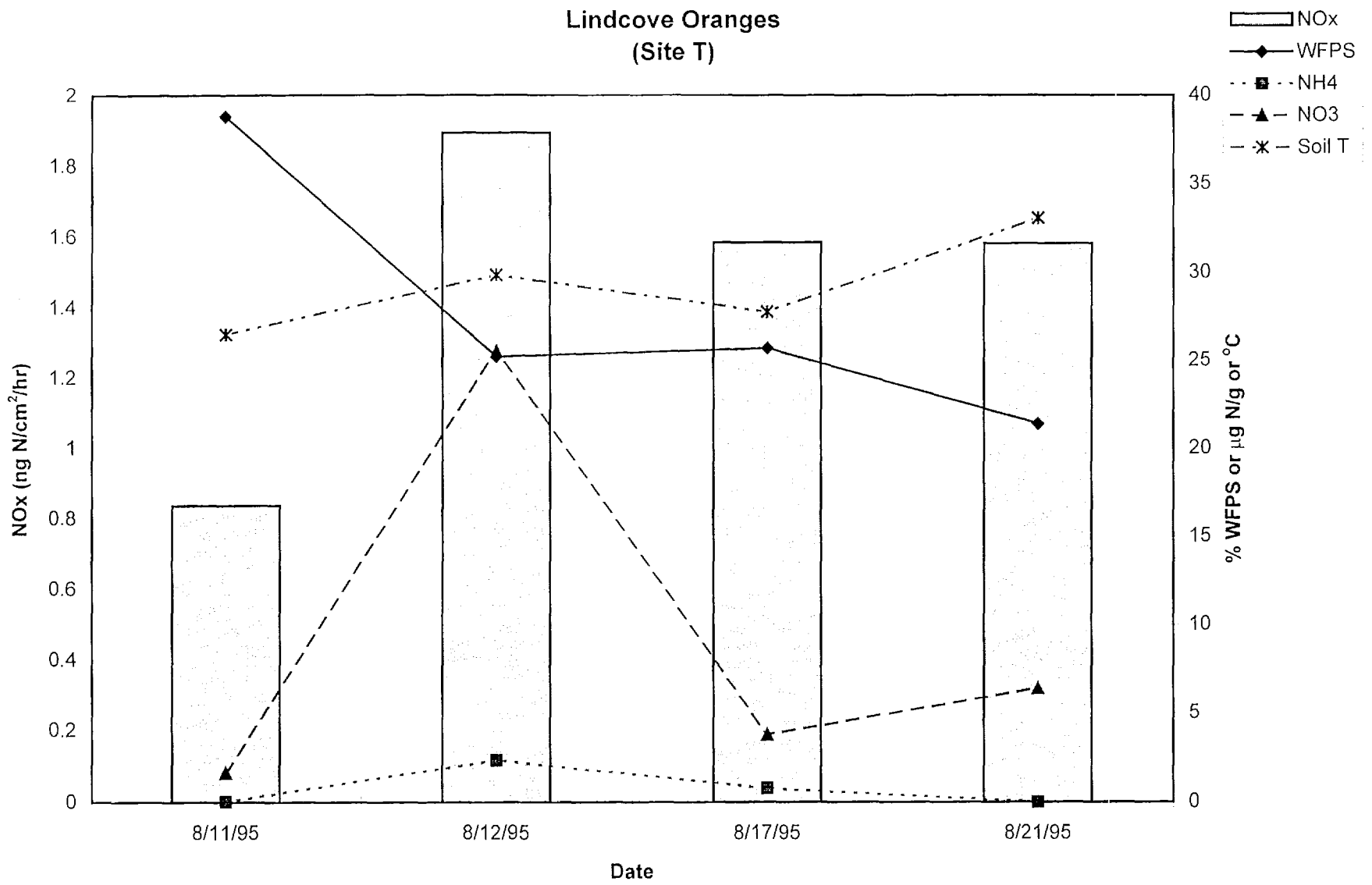


Figure 6i. NO_x fluxes and associated soil parameters measured at site T (oranges), Lindcove, CA, August, 1995. Each bar or point is a mean of 20 observations.

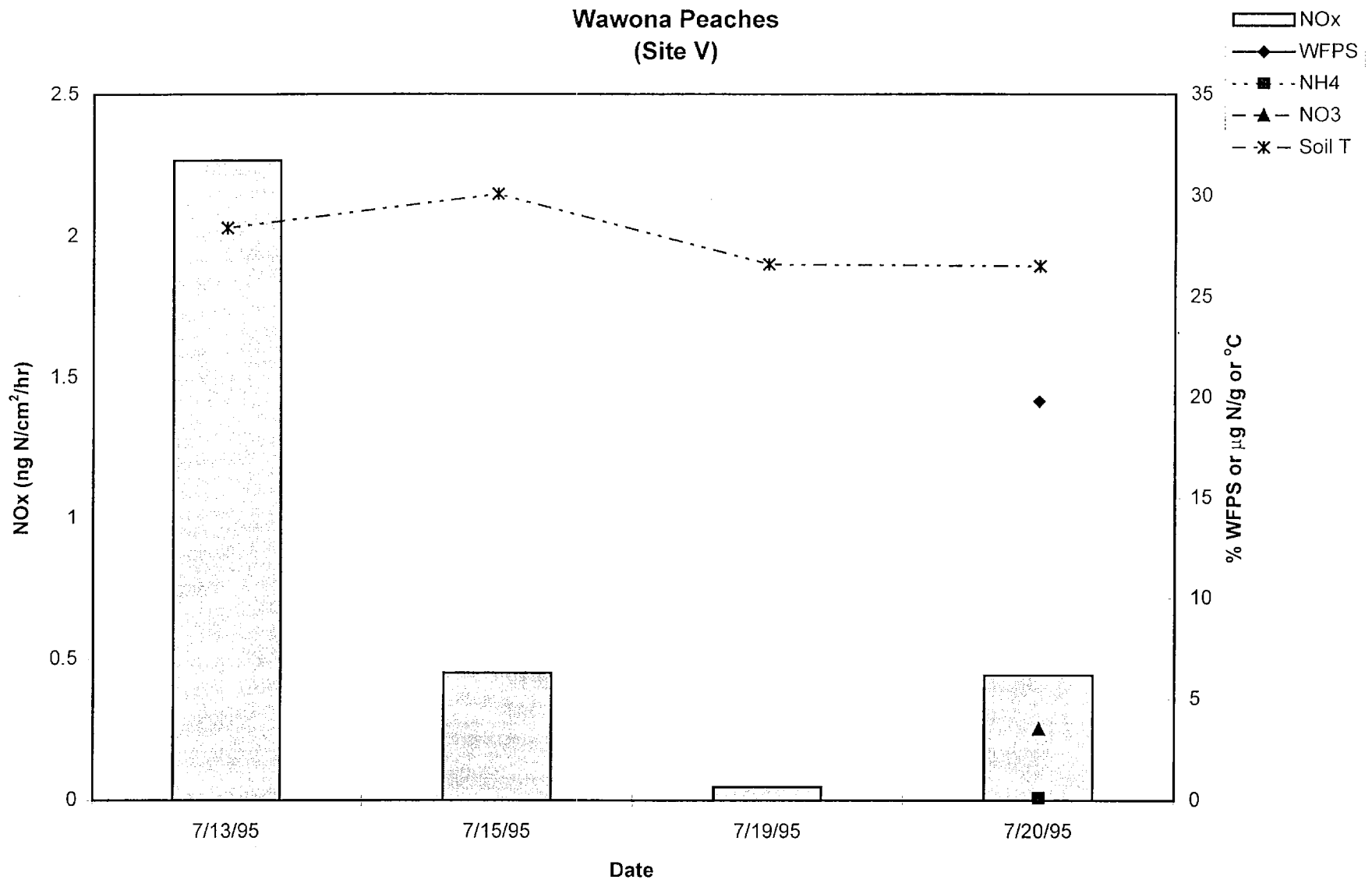


Figure 6j. NO_x fluxes and associated soil parameters measured at site V (peaches), Wawona, CA, July, 1995. Each bar or point is a mean of 20 observations.

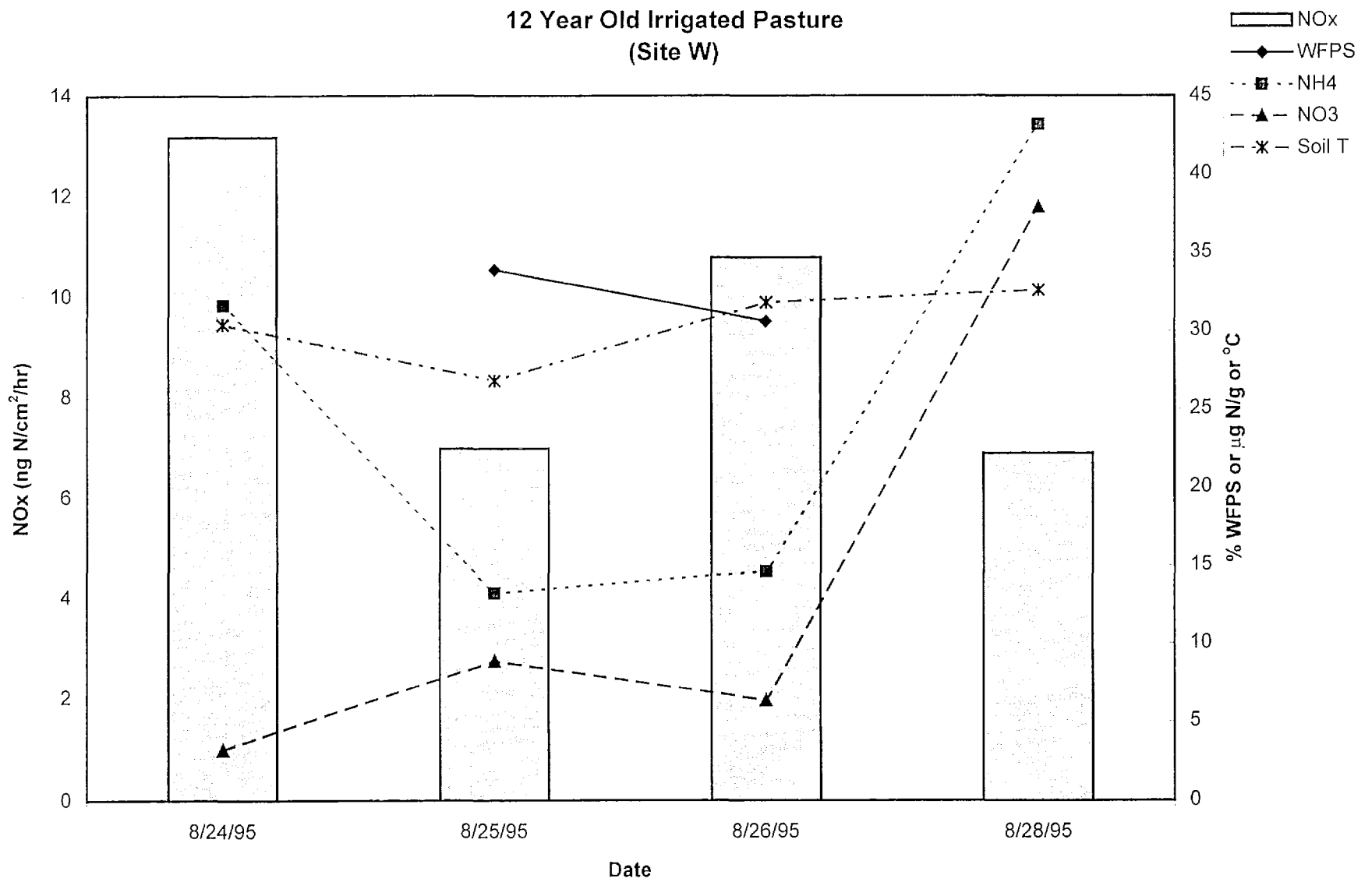


Figure 6k. NOx fluxes and associated soil parameters measured at site W (irrigated pasture), Bonadelle Ranchos, CA, August, 1995. Each bar or point is a mean of 10 observations.

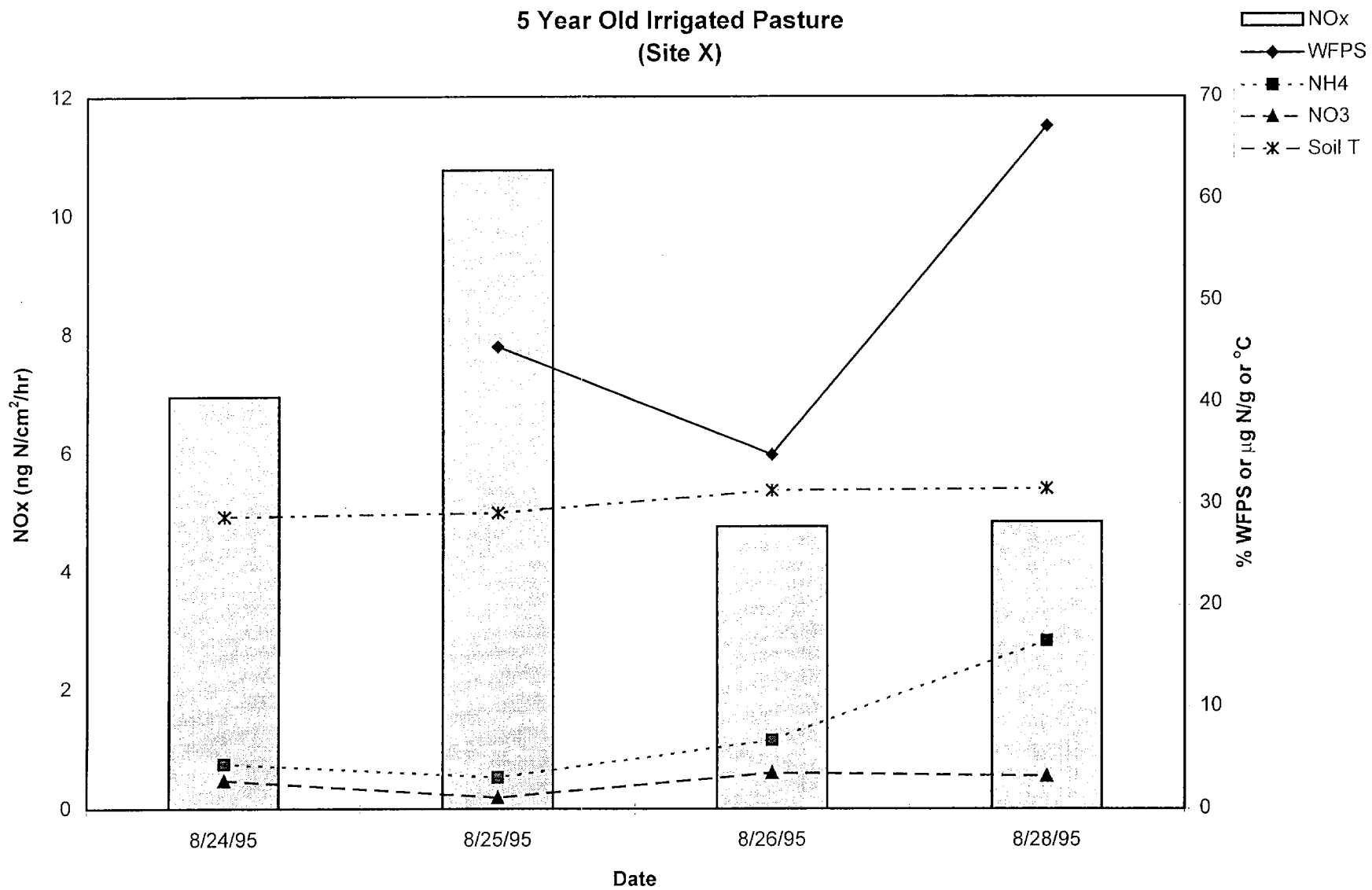


Figure 6I. NO_x fluxes and associated soil parameters measured at site T (irrigated pasture), Bonadelle Ranchos, CA, August, 1995. Each bar or point is a mean of 10 observations.

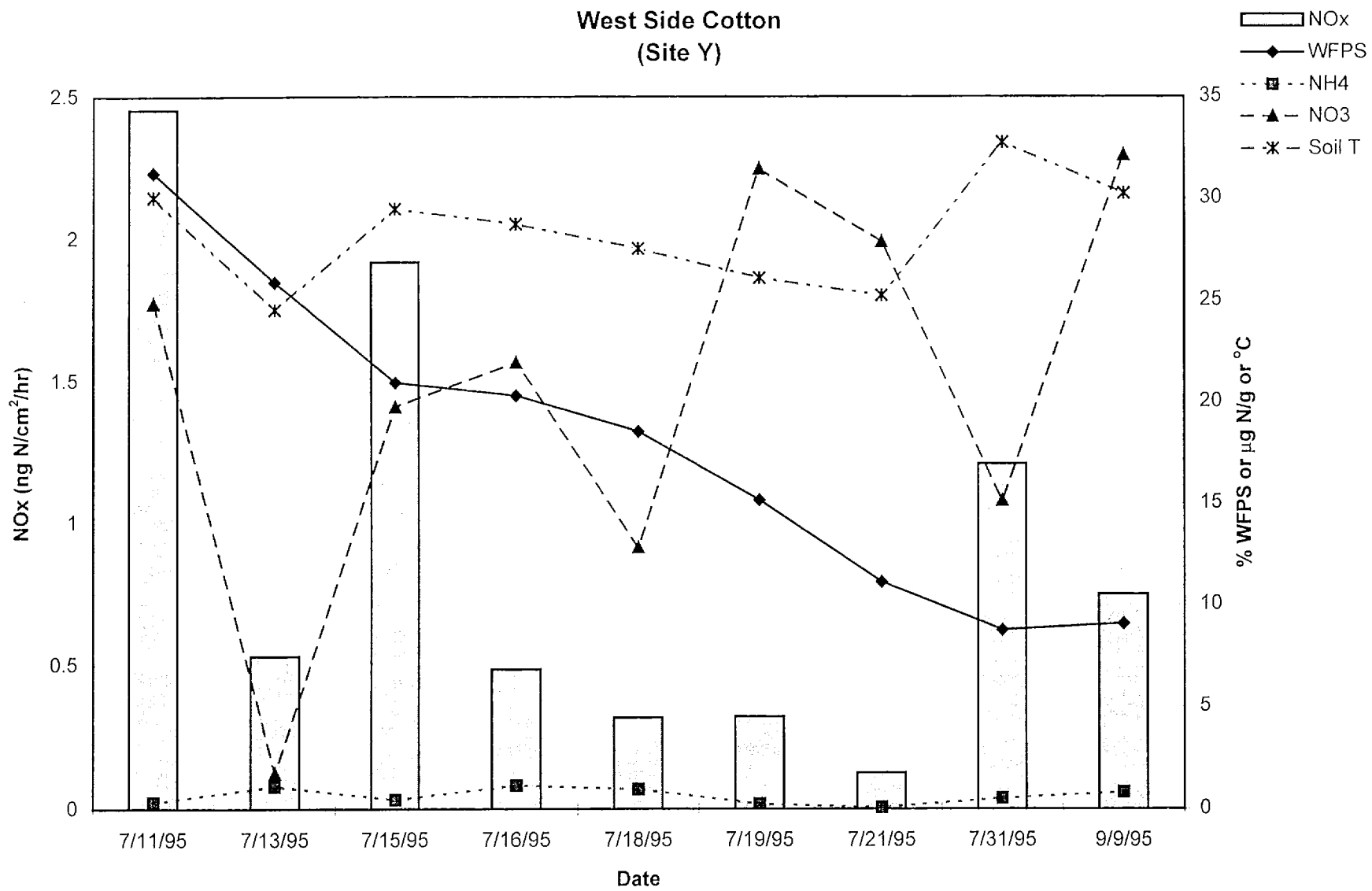


Figure 6m. NO_x fluxes and associated soil parameters measured at site Y (cotton), West Side Field Station, July-September, 1995. Each bar or point is a mean of 20 observations.

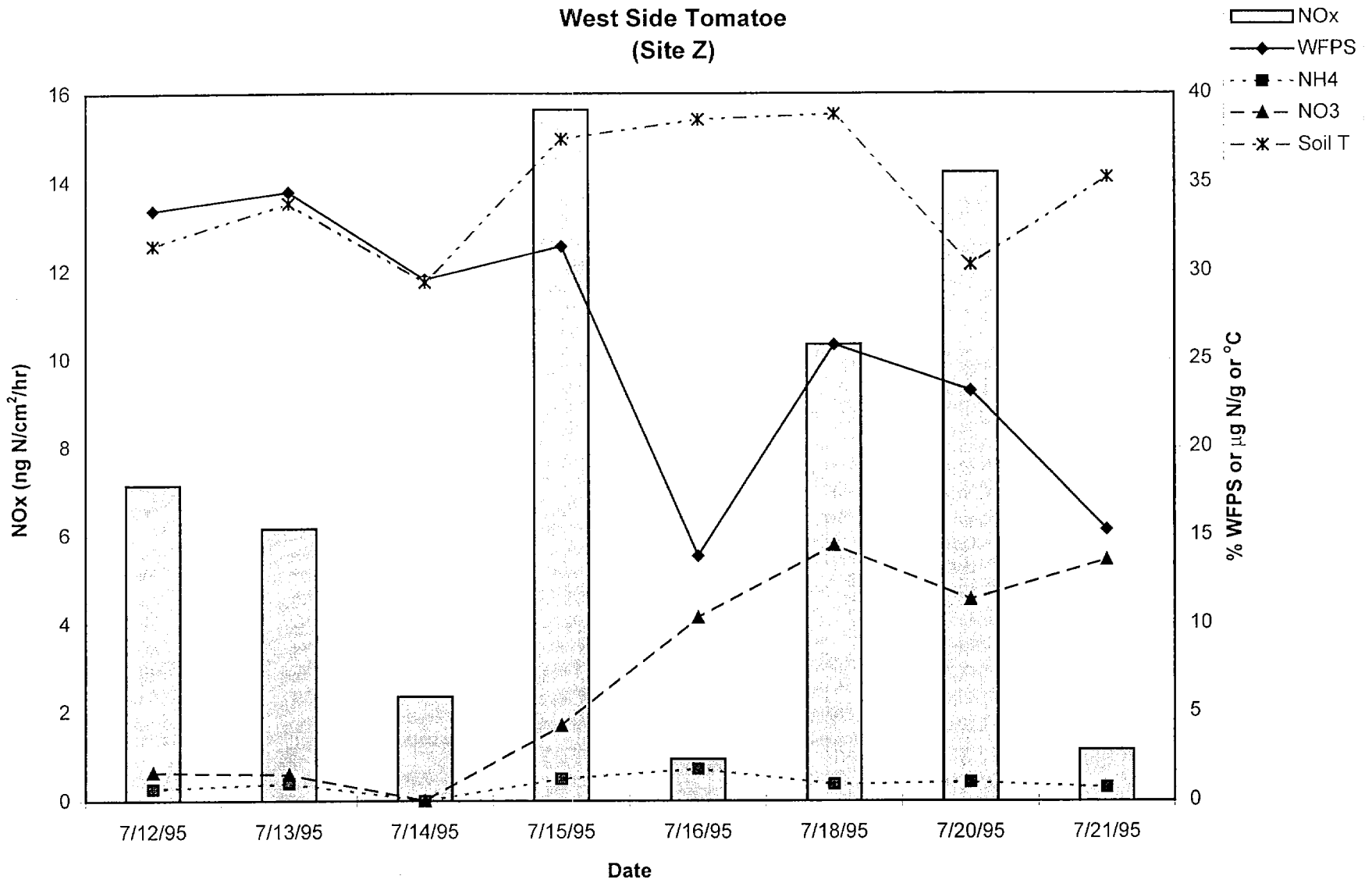


Figure 6n. NOx fluxes and associated soil parameters measured at site Z (tomatoes), West Side Field Station, July, 1995. Each bar or point is a mean of 20 observations.

curve, larger than six times the mean in some cases. This is partly because the normal rather than lognormal distribution was assumed in order to include the negative and zero value fluxes; a log normal distribution would yield smaller confidence intervals for the integral. Also, confidence bounds for interpolated data could only be imputed from the mean standard error of the data.

Despite these simplifying assumptions, the detail of the above methods for estimating hourly and daily NO_x fluxes makes use of the general observed behavior of these fluxes out in the field, and the flux amounts calculated here for different crop type, sites, irrigation methods, positions within a field, and dates can allow formation of hypotheses about other factors controlling NO_x flux. Using the diel relationships developed and described above, fluxes for any hour of any day can be estimated based on the application of the curve to a measured or estimated maximum hourly flux. Values for the curves are provided in a computer file (Appendix H.; Diskette 2; File: Diel.xls)

2.2.2.2 Daily Maximum Fluxes for NO_x .

In our original sampling plan, we developed a stratified sampling scheme that would maximize variation in what, based on the literature and our own experience, we expected to be the major controls on NO_x flux -- crop type, soil type, and fertilization/irrigation effects on soil inorganic N and water filled pore space. Using this sampling design, we can ask:

- 1) Do crops differ with respect to NO_x flux?
- 2) Do site means differ on the basis of broad soil types (basin vs. fan)?
- 3) Do site means differ within a crop based on soil type or fertilization/irrigation regime?
- 4) Are our intensive study sites representative of the extensive sites within the crop type?

Analyses of variance and means comparisons were performed using daily maximum NO_x fluxes averaged for each crop-site-date combination, and weighted by position (e.g. % ridge vs. % furrow). Differences in means were considered to be significant at $P < 0.05$.

To determine if there were differences among crops in NO_x flux, a one way ANOVA was performed using crop as a factor, and all sites and dates within a given crop as replicates. The model was weighted by the number of dates that each site was sampled. While Figure 7 shows substantial differences in maximum NO_x fluxes among crop types, the variability within crop was so large and nonuniformly distributed among crops, that no significant differences among crops could be detected using parametric statistics. However

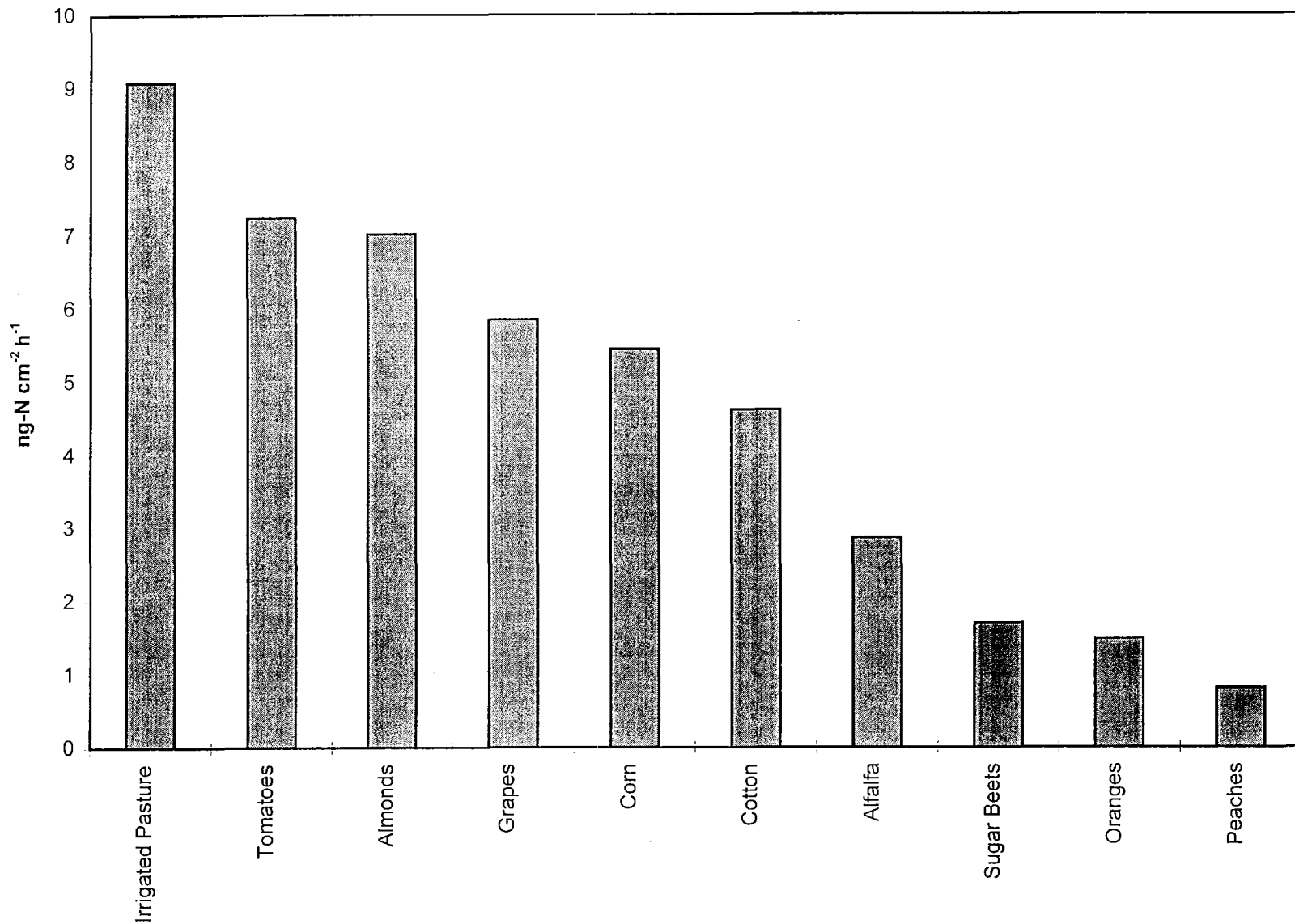


Figure 7. Mean mid-day NO_x fluxes averaged for each crop measured in the San Joaquin Valley, July-September, 1995. Values are means of 1 - 5 sites per crop type (see Figure 8); 10 - 660 chamber measurements were performed at each site.

the non-parametric Kruskal-Wallis Rank Sum Comparison among crops identified significant differences among crops ($P < 0.01$, Figure 7). Figure 8 clearly shows the large and nonuniform variability within a crop.

To determine distinguishable differences among the sites we sampled (not categorized on basis of crop) a one way ANOVA was performed with site as the factor and date as replication. Tukey's honestly significant difference (HSD) test was performed to identify specific differences. Site J (corn) was different from sites K (corn), Q (grapes), and Y (cotton), and site D (cotton) was different from site Y (cotton) (Figure 8). All other comparisons were indistinguishable.

To determine if basin and fan soils yielded different NO_x fluxes, a 2-way ANOVA was performed. Crop type was treated as a blocking factor and soil type as the treatment effect. The model was weighted by the number of dates each site was sampled. No significant effects were detected. While no differences in soil type could be detected from simple ANOVA analysis of basin vs. fan soils, the soil texture variable was found to be important in regression model analysis (see 2.3.3.2).

To determine if site means differed within a crop and if our intensive sites were representative of their crops, we performed separate ANOVAs for each crop. Each ANOVA was a one-way design using site as the factor and date as the replication. Means were compared using Tukey's HSD (honestly significant difference) test. Orange, peach, and tomato crops were only sampled at one site each. For the crops sampled at multiple sites, there were no site differences for alfalfa, almonds, cotton, or irrigated pasture (Figure 8). For corn, site J was higher than site K; site J had been fertilized shortly before sampling while sites I and K had not. For grapes, all three sites were different from each other, in the order $L > R > Q$. Site L had an oat and vetch cover crop planted in alternating rows the previous October. In February the grower manured the cover crop rows and ripped the other rows. The management of site L resulted in high NO_3^- concentrations (37-47 $\mu\text{g-N g}^{-1}$) during the summer sampling period. Sites R and Q were both at Kearney, but site R was flood irrigated and site Q was drip irrigated. The flood irrigated site, Q, had numerous observations with WFPS greater than 8% which generally corresponded to high NO_x fluxes. The drip irrigated WFPS were mostly less than 3% and generally had low but measurable NO_x fluxes. This association of low but measurable NO_x fluxes with very dry soils is notable in the overall data set (see Figure 9). Sugar beet site U was different from H, N, and S but this difference could not be

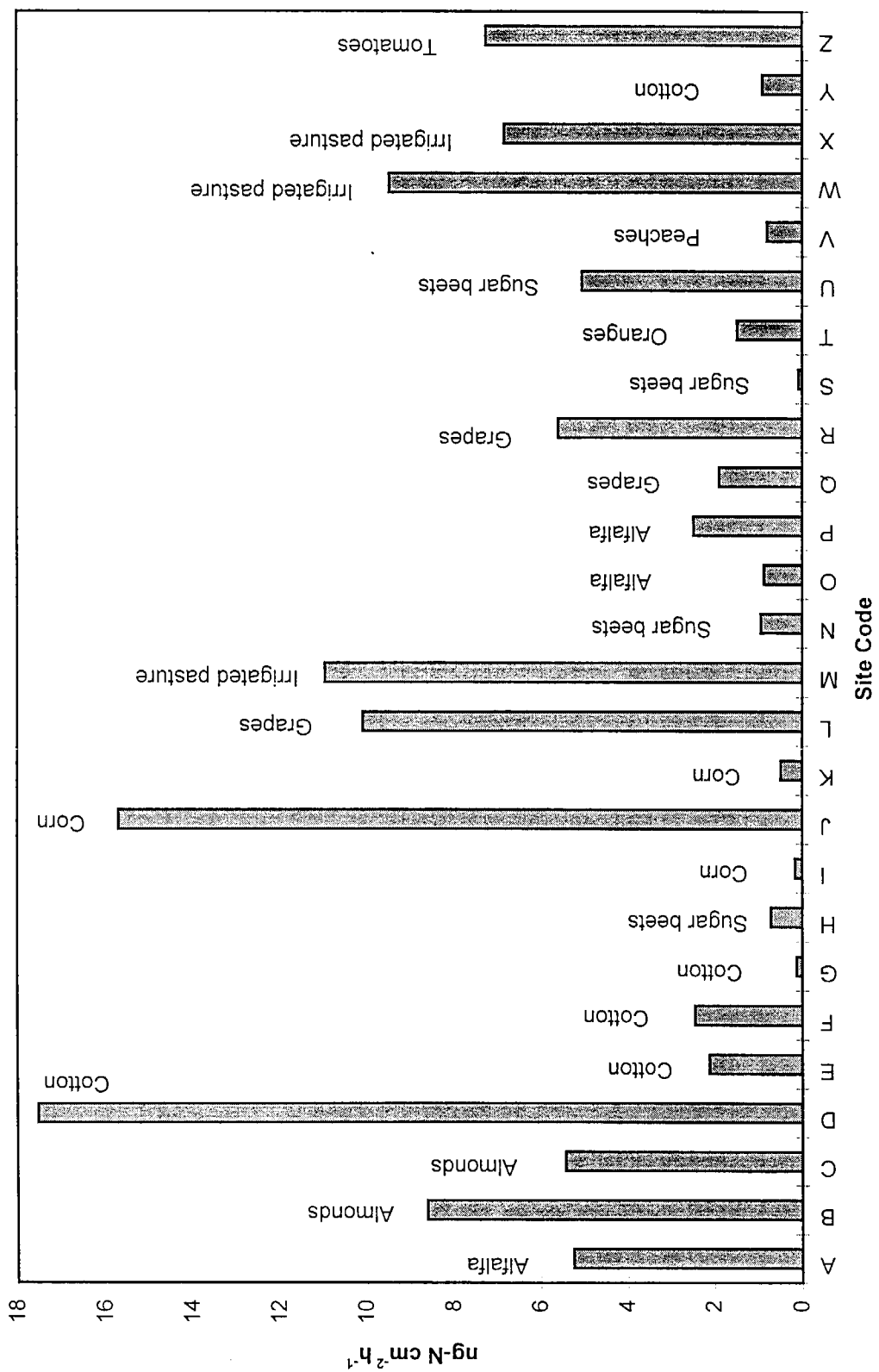


Figure 8. Mean mid-day NOx fluxes for sites sampled in the San Joaquin Valley, July-September, 1995. Each value is the mean of 10 - 660 chamber measurements per site. See Table 3 for site descriptions.

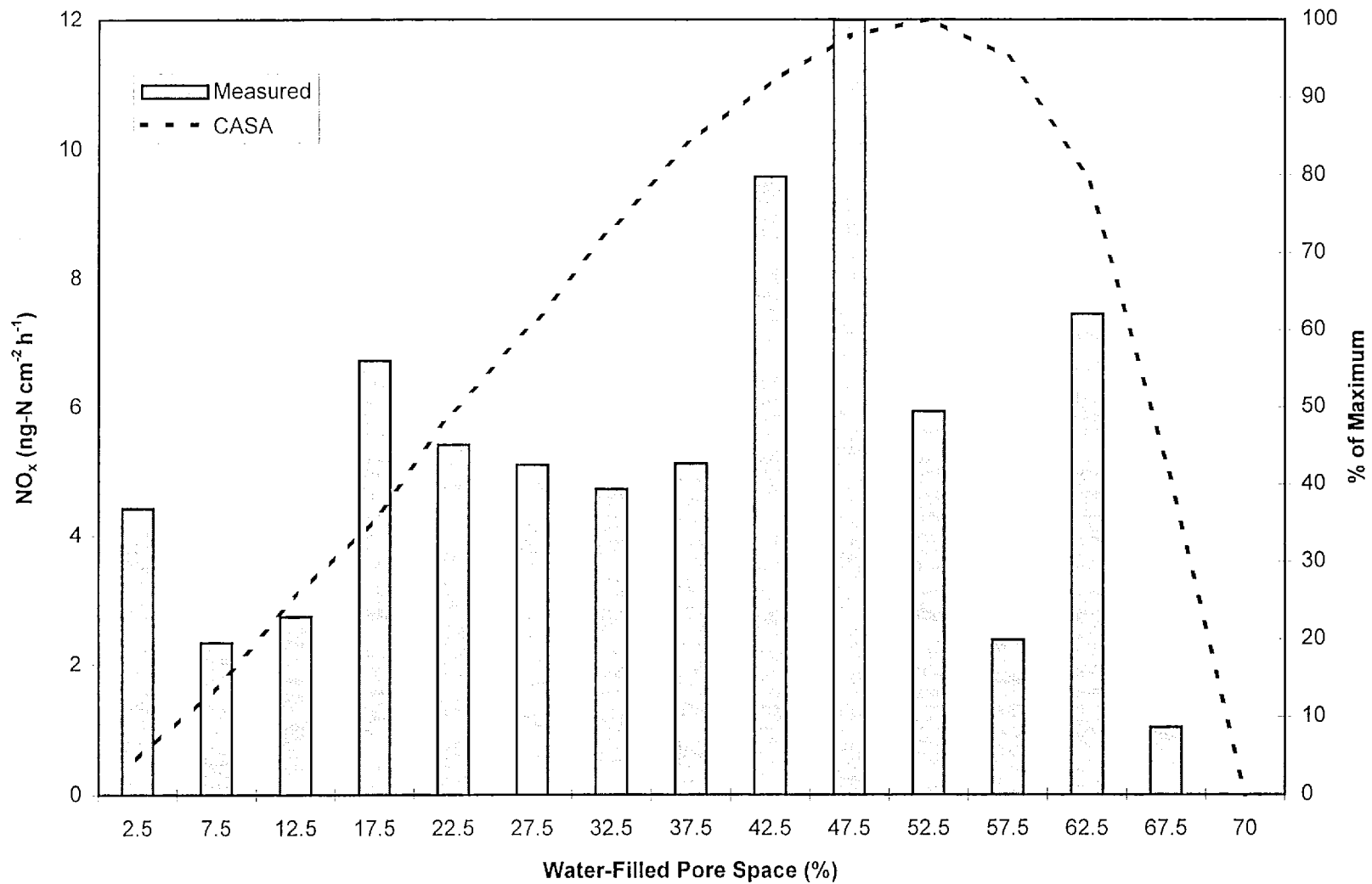


Figure 9. Comparison of NO_x flux (ng-N cm⁻² hr⁻¹) measured in the San Joaquin Valley, July-September, 1995 to predictions of NO_x flux estimated by the Davidson CASA model from water-filled pore space.

simply related to soil type or texture, fertilization or irrigations or WFPS.

We performed intensive and extensive sampling on only one crop type, cotton, for which two sites were sampled intensively and two extensively. Based on daily maximum NO_x fluxes, the sites extensively sampled were not distinguishable from the sites intensively sampled.

2.2.2.3 Soils and Process Data.

Figures 6a through 6n provide summaries of NO_x fluxes from intensively sampled sites and the associated inorganic N, temperature, and soil water parameter (WFPS). Fertilization events are noted in the sampling time frame for sites B, C, and J (Figures 6a, b, and e). Regression analyses for NO_x and these soil variables are presented in 2.3.3.2.

NO_x flux was not significantly correlated with either nitrification potential or gross nitrate production (correlation coefficients of -0.0005 and +0.023 for nitrification potential and gross nitrate production, respectively). See Figures 10 and 11 for scatter plots.

2.2.2.4 Results Summary.

In general, there was substantial variability in NO_x fluxes among crops, with irrigated pastures, almonds, and tomatoes having high fluxes relative to other crops (Table 8). For some crops variability within crop was quite large, yet in other crops substantially less. Due to the high and nonuniform variability within crops, crop differences could not be detected by ANOVA analysis. A nonparametric test did, however, confirm significant differences between crop types. Variation among different fields of single crop types was also large, sometimes significant, and appeared to be related to close temporal proximity to a fertilizer event and WFPS; time from fertilization seemed to be important within a 2-3 week window after fertilization. Over the summer sampling schedule, three sites were sampled within three weeks of a fertilization event (B, C, and J); all three sites showed elevated NO_x fluxes after fertilization which declined with time from fertilization application. Within a given site, fluxes varied more than a factor of 10 over time, probably as a consequence of combined changes in soil inorganic N and in water filled pore space.

2.3 Task III. Soils Emissions.

The approach taken above (emphasizing systematic studies spanning a range of crop, soil, and management conditions) allows development of emissions estimates for the San Joaquin Valley using several different approaches. In the following sections we describe the

Table 8. Mean hourly NO_x fluxes, based on measurements taken mid-day in each site. Site means include 10 - 660 chamber measurements, weighted by area of each position. Crop means are means of 1 - 5 site means.

Crop	Site	Site mean	Overall crop	Overall crop
		(ng-N cm ⁻² h ⁻¹)	mean (ng-N cm ⁻² h ⁻¹)	mean (g-N ha ⁻¹ hr ⁻¹)
Corn	J*	15.689	5.4	0.54
Corn	I	0.165		
Corn	K	0.404		
Grapes	R	5.358	5.8	0.58
Grapes	L	10.081		
Grapes	Q	2.100		
Almonds	B*	7.121	6.4	0.64
Almonds	C*	5.639		
Oranges	T	1.447	1.4	0.14
Peaches	V	0.990	1.0	0.10
Cotton	Y	0.902	4.6	0.46
Cotton	D	17.530		
Cotton	E	2.113		
Cotton	F	2.445		
Cotton	G	0.132		
Sugar beets	H	0.713	1.7	0.17
Sugar beets	N	0.940		
Sugar beets	S	0.086		
Sugar beets	V	5.047		
Tomatoes	Z	7.246	7.2	0.72
Alfalfa	A	5.247	2.9	0.29
Alfalfa	D	0.869		
Alfalfa	P	2.473		
Irrigated pasture	M	10.956	9.1	0.91
Irrigated pasture	W	9.459		
Irrigated pasture	X	6.829		

*Average values include measurements taken within two weeks following fertilization (See Table 3 for fertilizer schedule, and Figures 6 a, b, and e for changes in NO_x flux following fertilization).

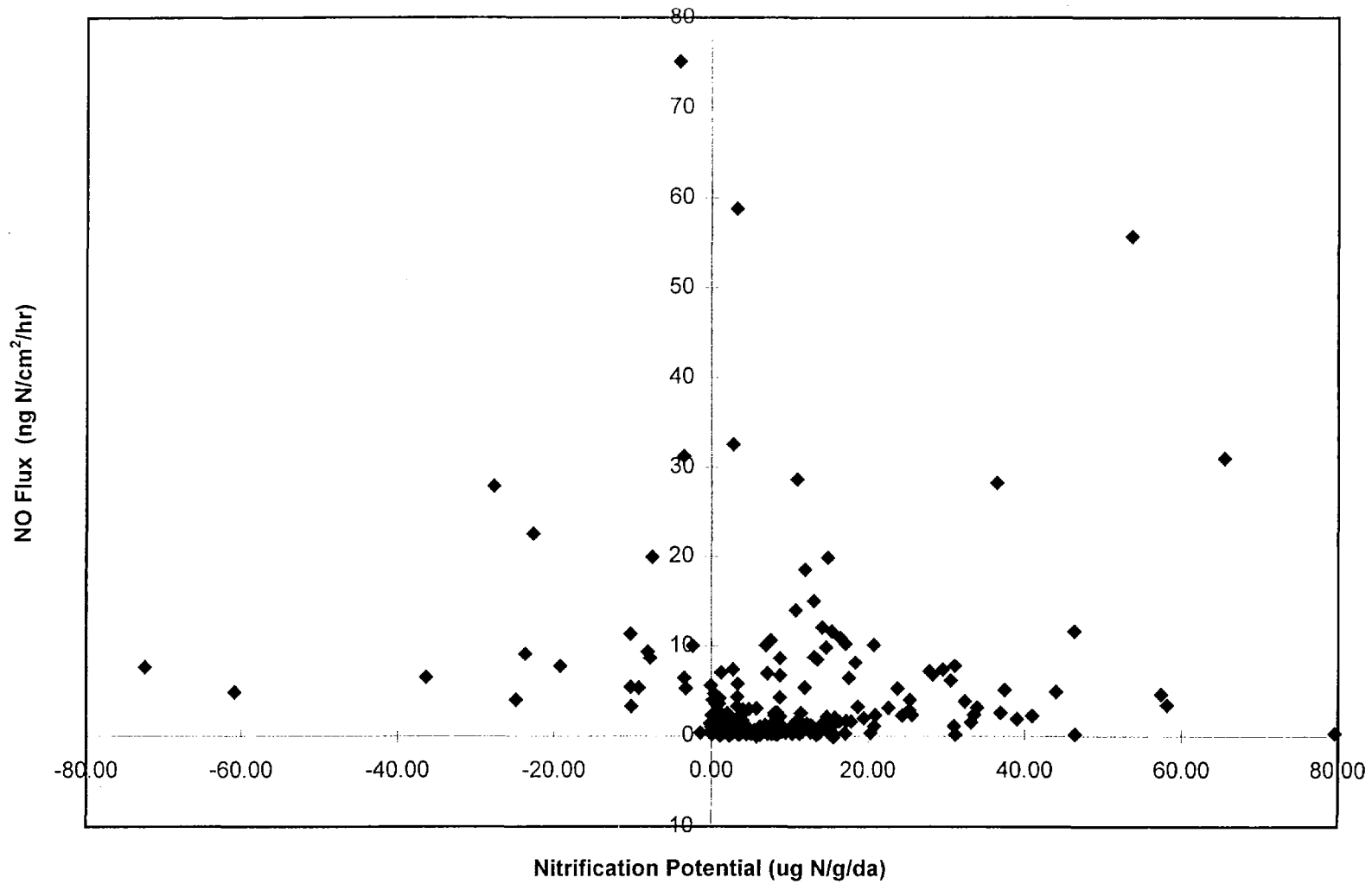


Figure 10. Relationship of NO_x flux to nitrification potential measured in the San Joaquin Valley, July-September, 1995. Each point is one NO_x flux measurement with its corresponding nitrification potential measurement.

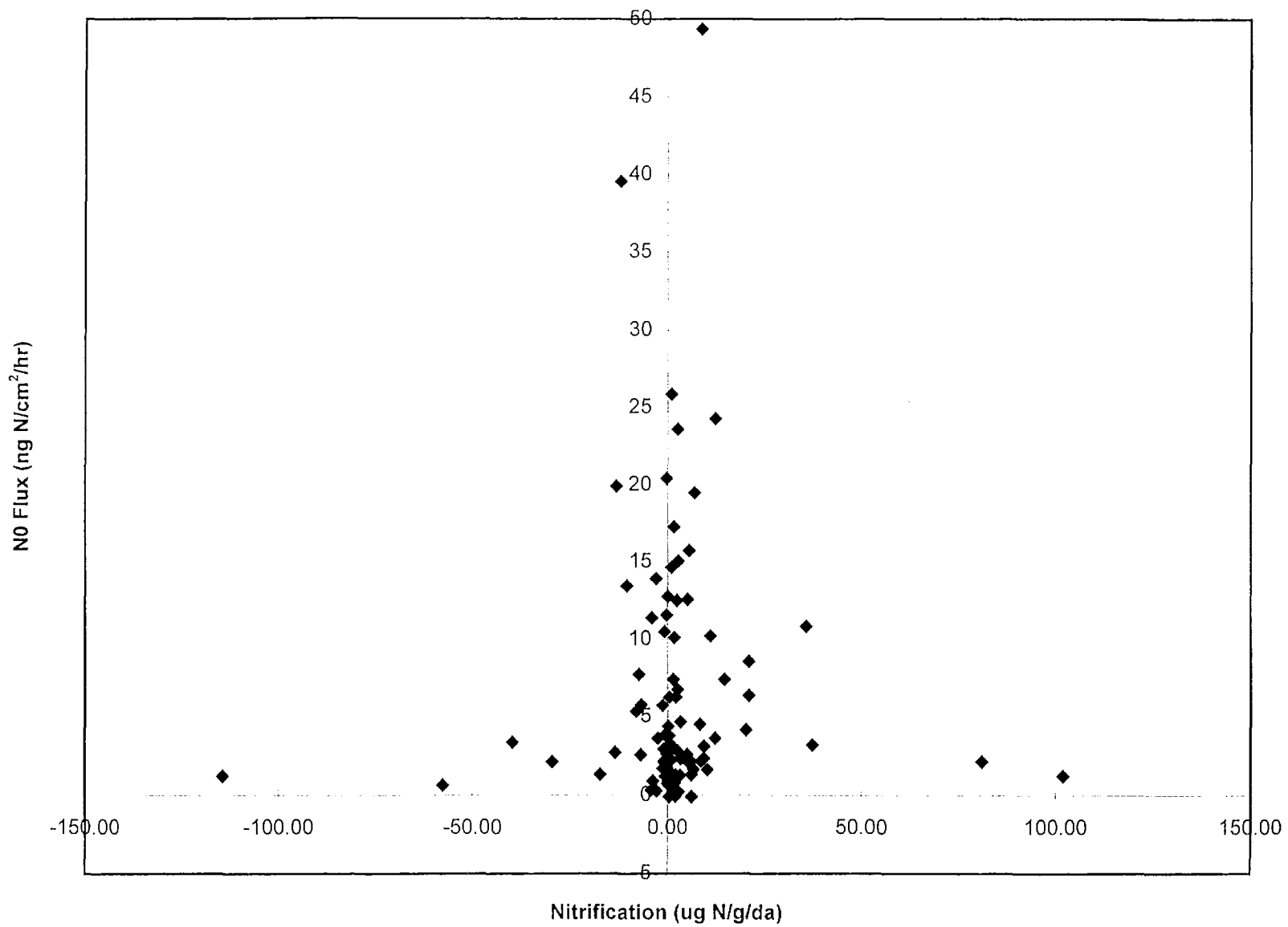


Figure 11. Relationship of NO_x flux to gross nitrate production measured in the San Joaquin Valley, July-September, 1995. Each point is one NO_x flux measurement with its corresponding gross nitrate production measurement.

analytical and statistical approaches taken, and present results of the analyses. We will describe 1) extrapolations using maximum hourly and daily fluxes together with a GIS data base of the crop types in the counties of the San Joaquin Valley; 2) development of statistical models relating NO_x flux to other site and soil variables; 3) comparisons to other models.

2.3.1 Extrapolation Approach.

First and most simply, we have used information on NO_x emissions over time in each crop type times the area of that crop type to calculate total daily, weekly, and monthly fluxes in the San Joaquin Valley during July, August and early September.

2.3.1.1 GIS-Based Crop Maps and Extrapolation Approaches.

Crop distribution maps were produced using ARC/INFO 7.0.3 and ArcView 2.1. The maps are based on data obtained from the Air Resources Board, and the original source of the data was the California Department of Water Resources (DWR). The data covers parts of seven counties in the San Joaquin Valley; no data was available for Stanislaus county. It should be noted that the available data were not comprehensive. Fresno, Kern, Madera, Merced, and Tulare counties are covered only in the center of the Valley; San Joaquin and Kings counties are covered in their entirety. In this analysis, we assume that the non-covered areas were not under agriculture.

It was necessary to make several assumptions while analyzing the data. The DWR data showed a small percentage of the sites (less than 1%) planted in several crops or rotating crops throughout the year. In these instances, the site was assigned a code for only one of the crops. The following order of preference was used: grapes > tropical fruits > deciduous fruits and nuts > truck crops > pasture > field crops > rice > grain. For example, a site which was planted in both tomatoes (a truck crop) and corn (a field crop) would be assigned the code for tomatoes. Therefore, there is a slight bias in the analysis toward crops appearing earlier in the above list.

The DWR data assigned a small percentage of the sites (less than 0.1%) ambiguous codes. These sites were included as "unclassified" for the purposes of this analysis, except for sites assigned a code "W", which were assumed to be water.

The DWR data provided more detailed and specific crop classifications than were represented by our gas and soil sampling, so it was necessary to simplify the data in several ways. For this analysis, if a site was planted with one of the crops identified in Section 2.1.1 (Table 1.) as a dominant San Joaquin Valley crop, it was

assigned a code for that specific crop. Otherwise, the site was assigned a code that only identified the broad category to which the crop belonged.

A few broad categories of data were concatenated. Sites coded as "entry denied", "outside the zone of study" and "not surveyed" were all included as "unclassified" for the purposes of this analysis. Sites coded as "native classes", "native vegetation" and "riparian vegetation" were all included as "native vegetation." Urban classes were not differentiated for this analysis.

The broad category of "Vegetables, as defined in the County Agricultural Commissioners's Report Data (CACRD), was identified as a dominant San Joaquin Valley crop. The DWR data categorized crops somewhat differently. Table 9 below shows the crop components of each category. It should be noted that the CACRD's category "vegetables" is comparable to the DWR's category "truck crops" except for the inclusion of dry beans.

Table 9 Comparison between crop categories used by the 1993 County Agricultural Commissioners' report and the Department of Water Resources Database for the San Joaquin Valley.

1993 County Agricultural Commissioners' Report Categories

<u>Crop Category</u>	<u>Crops Included</u>
Cotton	cotton
Corn	corn
Sugar beets	sugar beets
Alfalfa	alfalfa
Irrigated pasture	non-alfalfa, irrigated pasture
Vegetables	dry beans, green beans, cole crops, carrots, lettuce, melons, peas, peppers, spinach, tomatoes, eggplant
Prunus	almonds, apricots, peaches, nectarines, plums, prunes
Citrus	citrus

Department of Water Resources Categories

<u>Crop Category</u>	<u>Crops Included</u>
Grains	barley, wheat, oats, miscellaneous and mixed grains and hay
Field crops	cotton, safflower, flax, hops, sugar beets, corn, grain sorghum, sudan, castor beans, dry beans, sunflowers, miscellaneous

Pasture	alfalfa, clover, native, turf farms, mixed and miscellaneous
Truck crops	artichokes, asparagus, green beans, cole crops, carrots, celery, lettuce, melons, onions and garlic, peas, potatoes, sweet potatoes, spinach, tomatoes, flowers, tree farms, berries, peppers, mixed and miscellaneous
Deciduous fruits and nuts	apples, pears, cherries, walnuts, pistachios, figs, almonds, apricots, peaches, nectarines, plums, prunes, miscellaneous
Citrus and subtropical fruits	citrus, dates, avocados, olives, kiwis, jojoba, eucalyptus, miscellaneous
Grapes	table, wine, raisin
Idle lands	recently cropped land, land being prepared for cropping
Semi-agricultural lands	farmsteads, livestock feed lots, dairies, poultry, miscellaneous

Once the spatial distribution and area of relevant crop types are available, extrapolation of NO_x flux can utilize measured fluxes ($\text{ng-N cm}^{-2} \text{h}^{-2}$), calculated daily fluxes ($\text{g m}^{-2} \text{day}^{-1}$), calculated monthly fluxes and so on. For this analysis, we choose to present the mean measured hourly fluxes per crop type (Table 8). Our assumption here is that the mean flux of all sites within a type accurately represents the mix of high to low fluxes that are occurring across the valley at any one time and that result from variation in management within that type. This variation includes response to fertilization. Alternatively, we could have extrapolated using the maximum site values to indicate spatial characteristics of flux under field conditions leading to high fluxes.

2.3.1.2 Results.

Table 10 presents the area (in hectares) of each major crop type in the Valley, based on the GIS-based California Department of Water Resources data base. The areas of the different crop types calculated from the GIS-based data base do not agree perfectly with our initial estimates derived from the 1993 County Agricultural Commissioners' Report (Table 1). However, the two area estimates are typically within 85% of each other. It is not within the scope of this project to examine the basis for disagreement in the two estimates; however, differences may have arisen from different definitions of crop classes, from survey errors, or simply

Table 10. Area (ha) occupied by major land use types in San Joaquin Valley counties.
 (Source: California Department of Water Resources, data collected between 1987 and 1993.)

County	Cultivated land								Idle land	Cultivated Area
	Grains	Rice	Field crops	Pasture	Truck crops	Deciduous fruits & nuts	Tropical fruits	Grapes		
Fresno	51384.3	1787.5	175333.5	61240.1	62177.9	44462.9	10964.7	98779.6	5596.3	511726.9
Kern	24972.0	231.2	179413.3	48606.6	27245.5	56449.2	20367.9	39197.3	22145.3	418628.4
Kings	16392.2	0.0	152740.8	26681.7	8245.4	11631.0	557.4	2055.8	28320.2	246624.6
Madera	17924.3	58.3	42834.9	22333.4	2193.8	34926.0	2616.4	36955.8	1953.2	161796.1
Merced	17017.4	4737.2	57504.7	58396.9	6761.6	39275.0	67.6	7064.4	10422.1	201246.9
San Joaquin	25115.8	2192.3	62305.8	47593.3	31899.9	44211.0	203.3	27474.0	14341.8	255337.3
Tulare	42628.2	0.0	103986.7	37317.2	3936.9	46982.1	56917.0	32975.4	1803.7	326547.1
Totals	195434.3	9006.5	774119.8	302169.2	142461.0	277937.2	91694.3	244502.3	84582.7	2121907.3
% of Land	5.4%	0.3%	21.5%	8.4%	4.0%	7.7%	2.5%	6.8%	2.4%	
% of Cultivated Land	9.2%	0.4%	36.5%	14.2%	6.7%	13.1%	4.3%	11.5%	4.0%	

County	Non-cultivated land						Non-Cultivated Area
	Semi-agricultural	Urban	Native vegetation	Water	Barren land	Not surveyed	
Fresno	38639.6	37273.9	123713.4	2817.8	0.0	1832.0	204276.7
Kern	10615.2	29974.2	429207.4	1813.2	0.0	8195.0	479805.0
Kings	4921.6	8152.3	120376.5	3352.3	0.0	10.5	136813.2
Madera	3153.1	4991.6	88059.2	480.1	0.0	3817.5	100501.5
Merced	6706.1	8850.9	155998.4	971.7	0.0	16700.5	189227.6
San Joaquin	16110.4	31026.7	87970.2	10002.3	69.5	11.0	145190.3
Tulare	7848.0	27267.5	179322.9	3449.3	364.1	0.0	218251.9
Totals	87994.0	147537.1	1184648.1	22886.9	433.6	30566.6	1474066.2
% of Land	2.4%	4.1%	32.9%	0.6%	0.0%	0.9%	

from the fact that the survey years differed. For the extrapolations, we will utilize the spatially explicit data provided by the GIS framework.

Total NO_x flux by crop type and county is given in Tables 11a and 11b. Cotton, which had an intermediate mean flux in relation to the other crops (.46 g N ha⁻¹ h⁻¹), had the highest total flux due to the large total acreage. Grapes produced the next largest amount when summed over the Valley.

Expression of NO_x emissions in terms of total fluxes, however, masks the spatial component of the fluxes that may be critical in determining air chemistry. Spatial distributions of measured average NO_x fluxes (g N ha⁻¹ h⁻¹) by county are shown in Figures 12 a-g. The spatial characteristics of fluxes are apparent for Tulare County (Figure 12g, Tables 11a and 11b), in which grapes account for 14.4% of the total area and 21.3% of the total flux. Because of the distribution of crops, highest fluxes are concentrated near the south border of the county.

2.3.2 Statistical Model Development.

2.3.2.1 Approach.

Statistical models were developed to investigate relationships between NO_x flux and various driving variables. First, a widely used empirical model by Williams, et.al., 1992, was investigated by application to the San Joaquin Valley data, and the model's explanatory ability and consistency with Williams' results were analyzed. Then, two new models with greater explanatory power were developed for 1) "point-predictive" purposes, to examine basic mechanisms at the chamber level; and 2) management purposes, to make use of measures for which published spatially explicit data are more widely available. Results of all three models were then compared.

The following model of NO_x flux was previously posed by Williams, et.al., 1992:

$$\text{NO} = A * \exp(cT) \quad \text{where NO} = \text{NO emission [ng-N/m}^2\text{/s]}$$

$$T = \text{soil temperature [degrees C]}$$

$$A, c = \text{constants from log-linear regression}$$

Williams, et.al., 1992, obtained their model fit by observing that NO_x flux is more nearly lognormally distributed, so that a log transform would allow a straight linear regression:

Table 11a. Area occupied by surveyed crops, mean measured mid-day NOx fluxes for each crop weighted by position, and total NOx flux for each crop summed over the 7 San Joaquin Valley counties made July-September 1995 in the San Joaquin Valley. Total NOx flux was calculated by multiplying the total acreage for a crop by the weighted mean mid-day hourly NOx flux for that crop. (Source Crop Acreages: California Department of Water Resources, data collected 1987 and 1993.)

Surveyed Crops	Fresno	Kern	Kings	Madera	Merced	SanJoaquin	Tulare	Total Area (hectares)	Weighted mean	Total NOx flux (g N/h)
									maximum hourly NOx flux (g N/ha/h)	
Cotton	139432.3	140077.9	100312.7	23357.7	23149.8	11926.7	63625.9	501883.0	0.46	232120.90
Sugarbeets	11988.6	4595.5	2465.6	1706.5	7093.5	17120.7	888.0	45858.6	0.17	7782.20
Corn	13322.8	2671.0	10485.6	7957.8	16851.0	26165.6	31528.8	108982.6	0.54	59232.03
Irrigated pasture	9965.0	2252.0	1715.9	6523.4	30287.7	17812.3	4371.8	72928.0	0.91	66225.88
Alfalfa	51264.5	46354.6	24965.8	15810.1	28076.1	29781.0	32945.4	229197.4	0.29	65619.21
Tomatoes	28257.9	2105.3	4774.7	758.7	3210.8	13556.9	299.1	52963.4	0.72	38377.28
Almonds	15757.9	37872.7	1280.8	18599.1	29409.9	19143.3	4801.9	126865.6	0.64	80940.23
Peaches	12133.5	1904.4	2914.3	1211.9	2005.1	1043.1	11816.7	33028.9	0.10	3269.86
Oranges	10061.6	17099.9	25.9	1776.8	36.9	0.0	46075.4	75076.5	0.14	10863.58
Grapes	98779.6	39197.3	2055.8	36955.8	7064.4	27474.0	32975.4	244502.3	0.58	142936.06
Total	390963.6	294130.7	150997.2	114657.8	147185.3	164023.6	229328.3	1491286.3		707367.23

Table 11b. Total NOx flux for each crop within 7 San Joaquin Valley counties. Total fluxes were computed by multiplying the total acreage for a crop (Table 11a) by the weighted mean midday hourly NOx flux for that crop (Table 11a).

Surveyed Crops	Fresno (g N/h)	Kern (g N/h)	Kings (g N/h)	Madera (g N/h)	Merced (g N/h)	SanJoaquin (g N/h)	Tulare (g N/h)
Cotton	64487.4	64786.0	46394.6	10802.9	10706.8	5516.1	29427.0
Sugarbeets	2034.5	779.9	418.4	289.6	1203.8	2905.4	150.7
Corn	7240.9	1451.7	5698.9	4325.1	9158.5	14221.0	17135.9
Irrigated pasture	9049.2	2045.0	1558.2	5923.9	27504.2	16175.4	3970.0
Alfalfa	14677.0	13271.3	7147.7	4526.4	8038.2	8526.3	9432.3
Tomatoes	20475.7	1525.5	3459.8	549.7	2326.5	9823.3	216.7
Almonds	10053.6	24162.8	817.1	11866.2	18763.5	12213.4	3063.6
Peaches	1201.2	188.5	288.5	120.0	198.5	103.3	1169.9
Oranges	1455.9	2474.4	3.8	257.1	5.3	0.0	6667.1
Grapes	57746.6	22914.8	1201.8	21604.4	4129.8	16061.3	19277.4
Total	188421.9	133599.9	66988.8	60265.3	82035.3	85545.4	90510.5

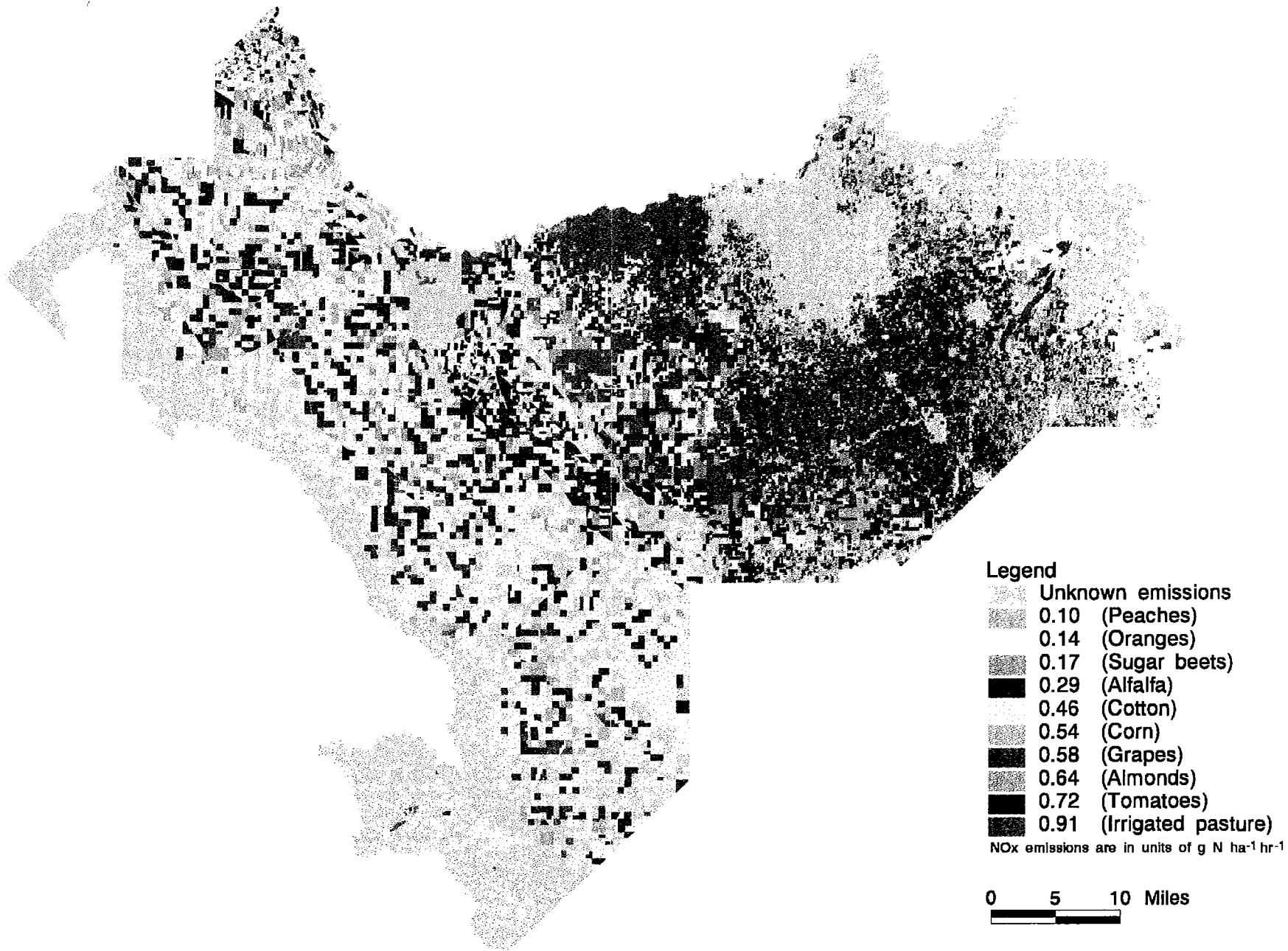


Figure 12a. Estimated NO_x Emissions as a Function of Crop Type in Western Fresno County, California

Crop distribution is based on data provided by the California Department of Water Resources. Data on NO_x emissions was produced and analyzed by the University of California at Berkeley. See accompanying metadata for details. NO_x emissions (g N ha⁻¹ hr⁻¹) for each crop type are the mean values for measurements taken in 1 - 5 fields per crop type.

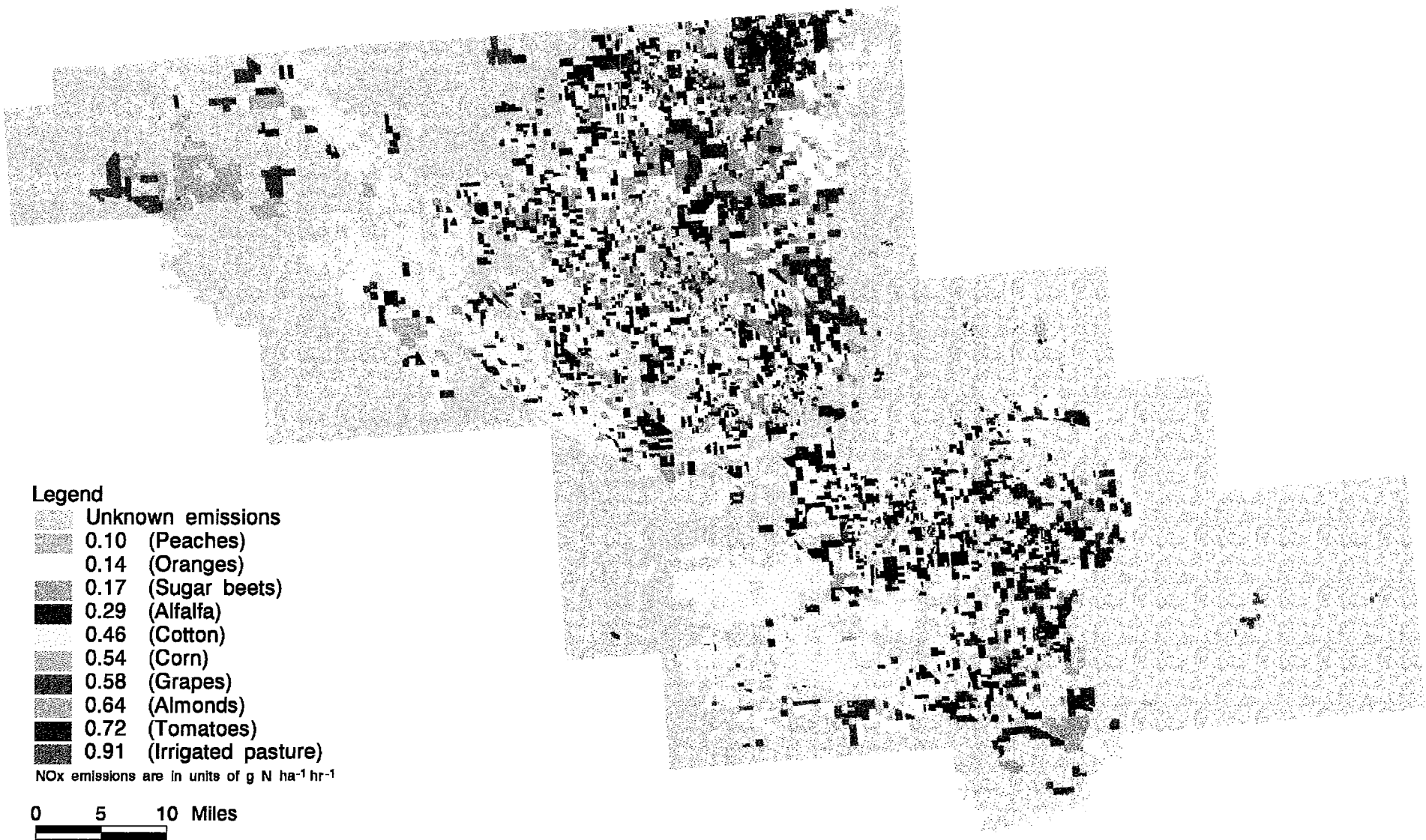

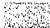











Figure 12b. Estimated NO_x Emissions as a Function of Crop Type in Western Kern County, California

Crop distribution is based on data provided by the California Department of Water Resources. Data on NO_x emissions was produced and analyzed by the University of California at Berkeley. See accompanying metadata for details. NO_x emissions (g N ha⁻¹ hr⁻¹) for each crop type are the mean values for measurements taken in 1 - 5 fields per crop type.

Legend

	Unknown emissions
	0.10 (Peaches)
	0.14 (Oranges)
	0.17 (Sugar beets)
	0.29 (Alfalfa)
	0.46 (Cotton)
	0.54 (Corn)
	0.58 (Grapes)
	0.64 (Almonds)
	0.72 (Tomatoes)
	0.91 (Irrigated pasture)

NO_x emissions are in units of g N ha⁻¹ hr⁻¹

0 5 10 Miles

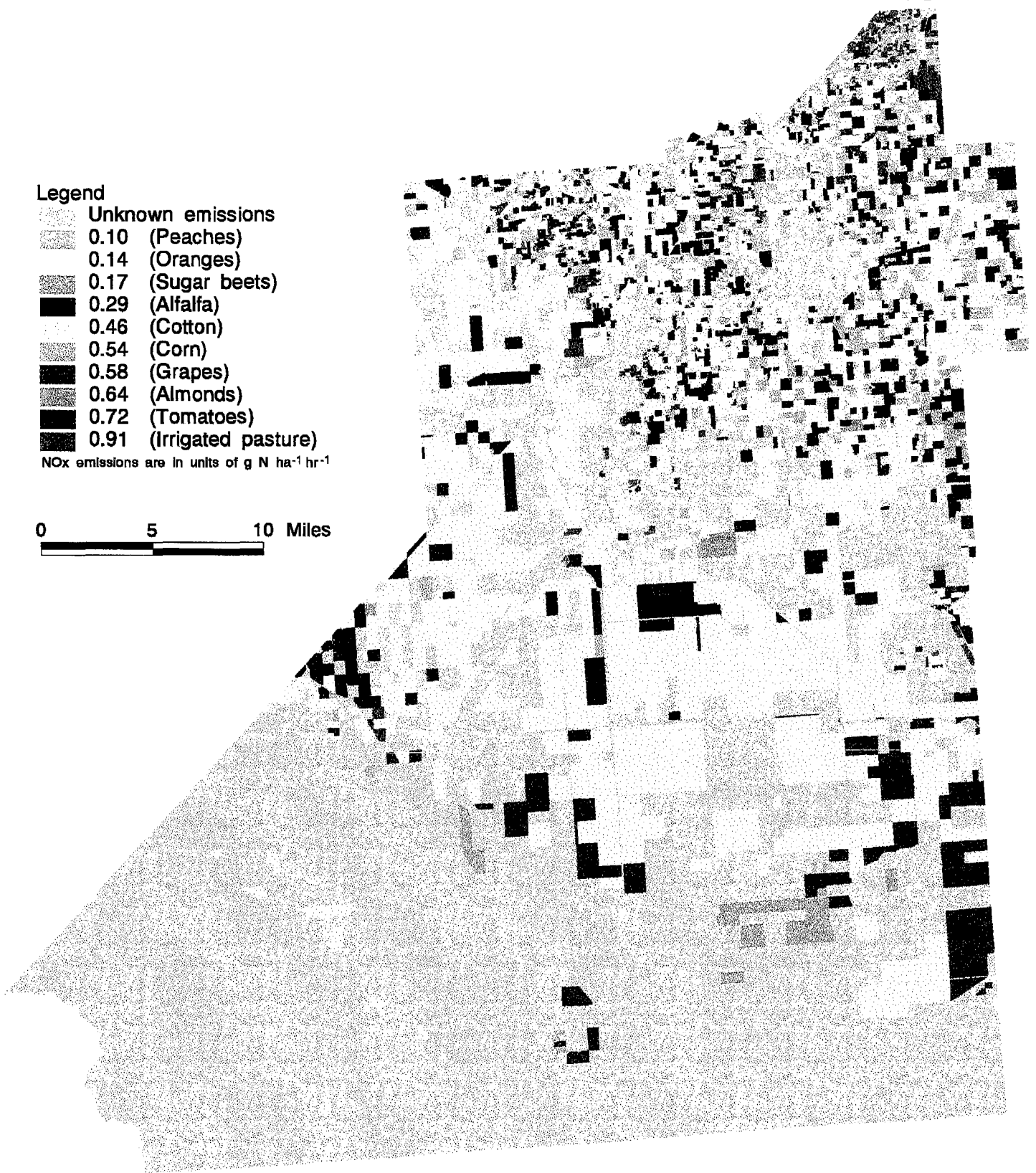


Figure 12c. Estimated NO_x Emissions as a Function of Crop Type in Kings County, California

Crop distribution is based on data provided by the California Department of Water Resources. Data on NO_x emissions was produced and analyzed by the University of California at Berkeley. See accompanying metadata for details. NO_x emissions (g N ha⁻¹ hr⁻¹) for each crop type are the mean values for measurements taken in 1 - 5 fields per crop type.

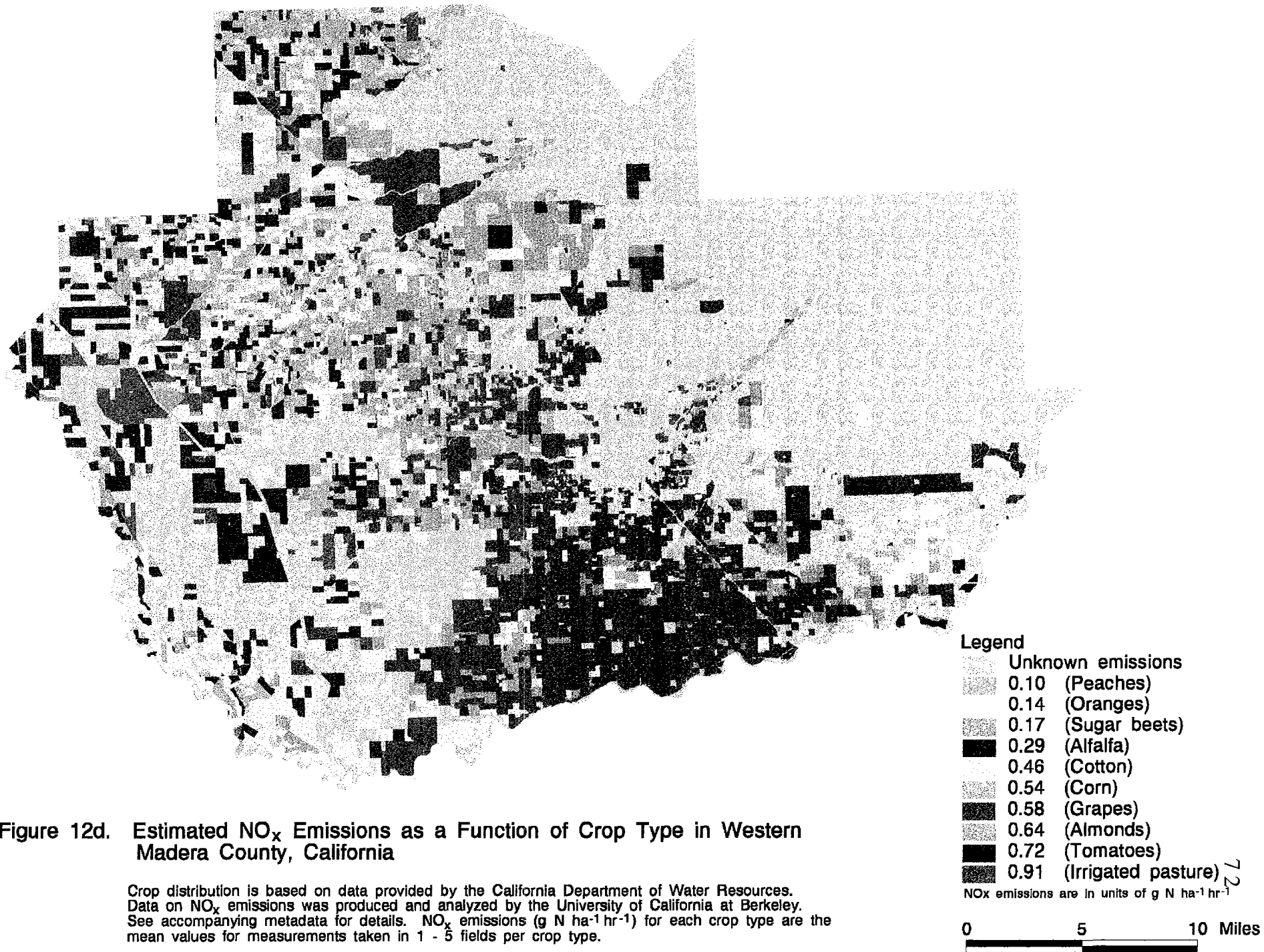


Figure 12d. Estimated NO_x Emissions as a Function of Crop Type in Western Madera County, California

Crop distribution is based on data provided by the California Department of Water Resources. Data on NO_x emissions was produced and analyzed by the University of California at Berkeley. See accompanying metadata for details. NO_x emissions (g N ha⁻¹ hr⁻¹) for each crop type are the mean values for measurements taken in 1 - 5 fields per crop type.

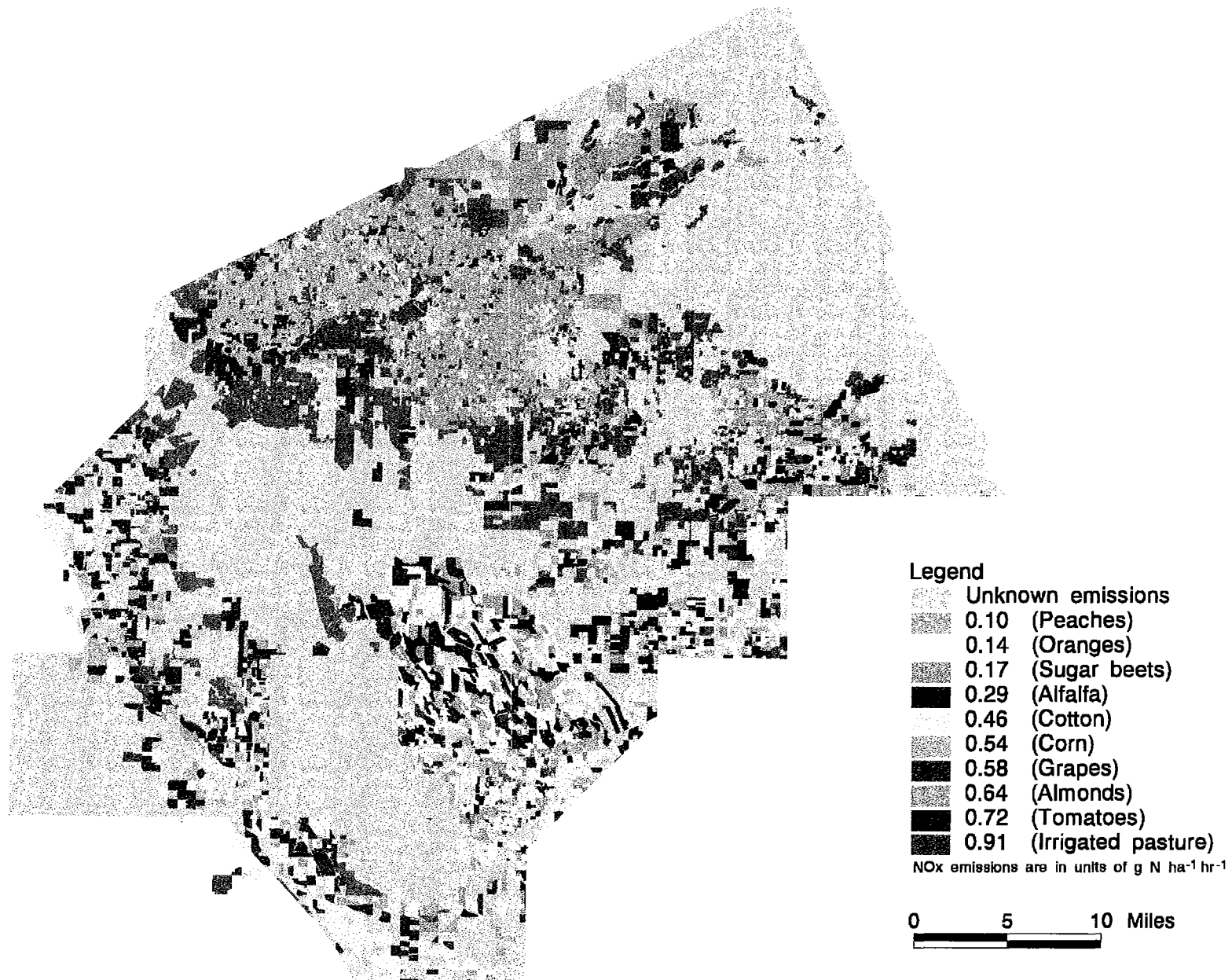


Figure 12e. Estimated NO_x Emissions as a Function of Crop Type in Eastern Merced County, California

Crop distribution is based on data provided by the California Department of Water Resources. Data on NO_x emissions was produced and analyzed by the University of California at Berkeley. See accompanying metadata for details. NO_x emissions (g N ha⁻¹ hr⁻¹) for each crop type are the mean values for measurements taken in 1 - 5 fields per crop type.

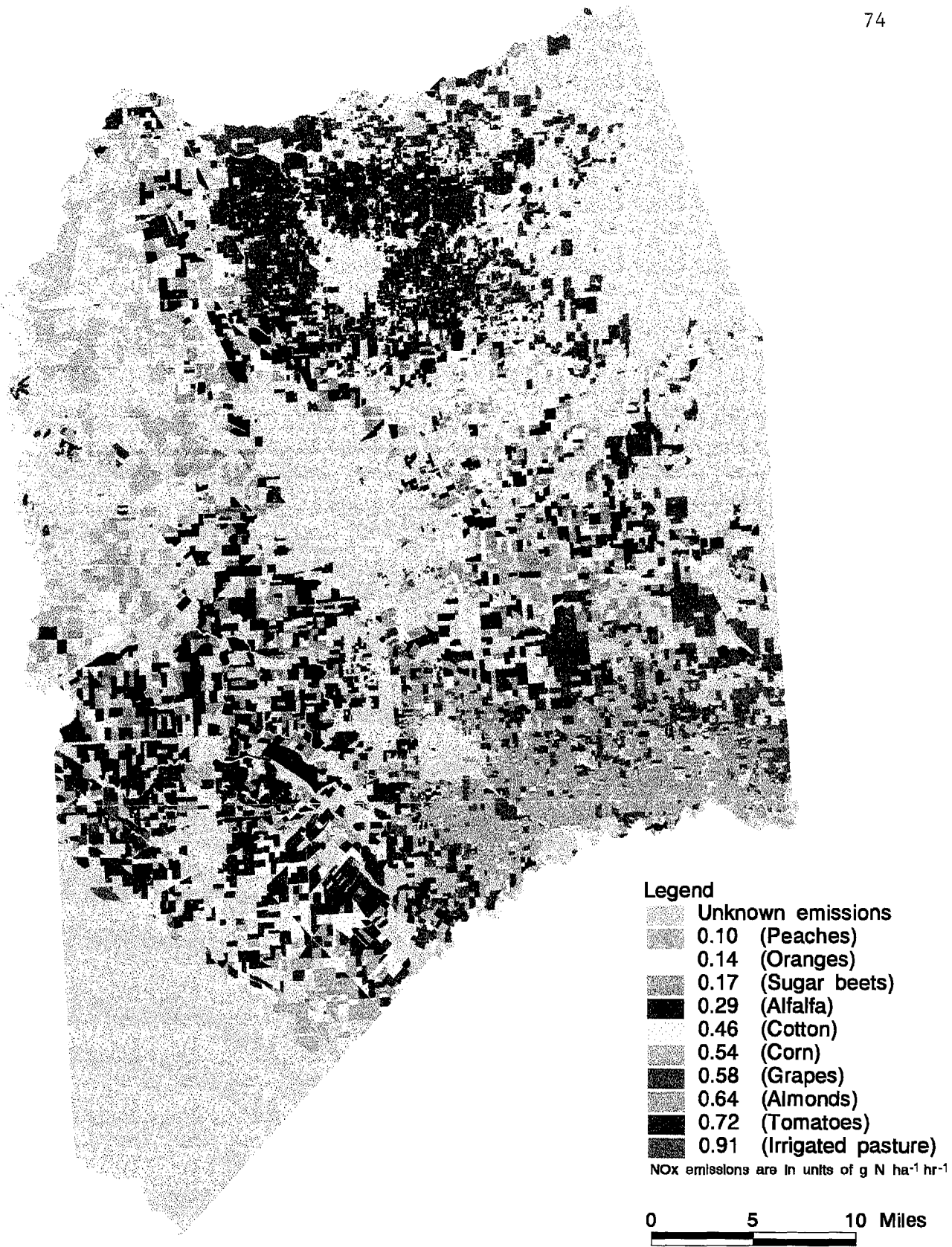


Figure 12f. Estimated NO_x Emissions as a Function of Crop Type in San Joaquin County, California

Crop distribution is based on data provided by the California Department of Water Resources. Data on NO_x emissions was produced and analyzed by the University of California at Berkeley. See accompanying metadata for details. NO_x emissions ($\text{g N ha}^{-1} \text{hr}^{-1}$) for each crop type are the mean values for measurements taken in 1 - 5 fields per crop type.

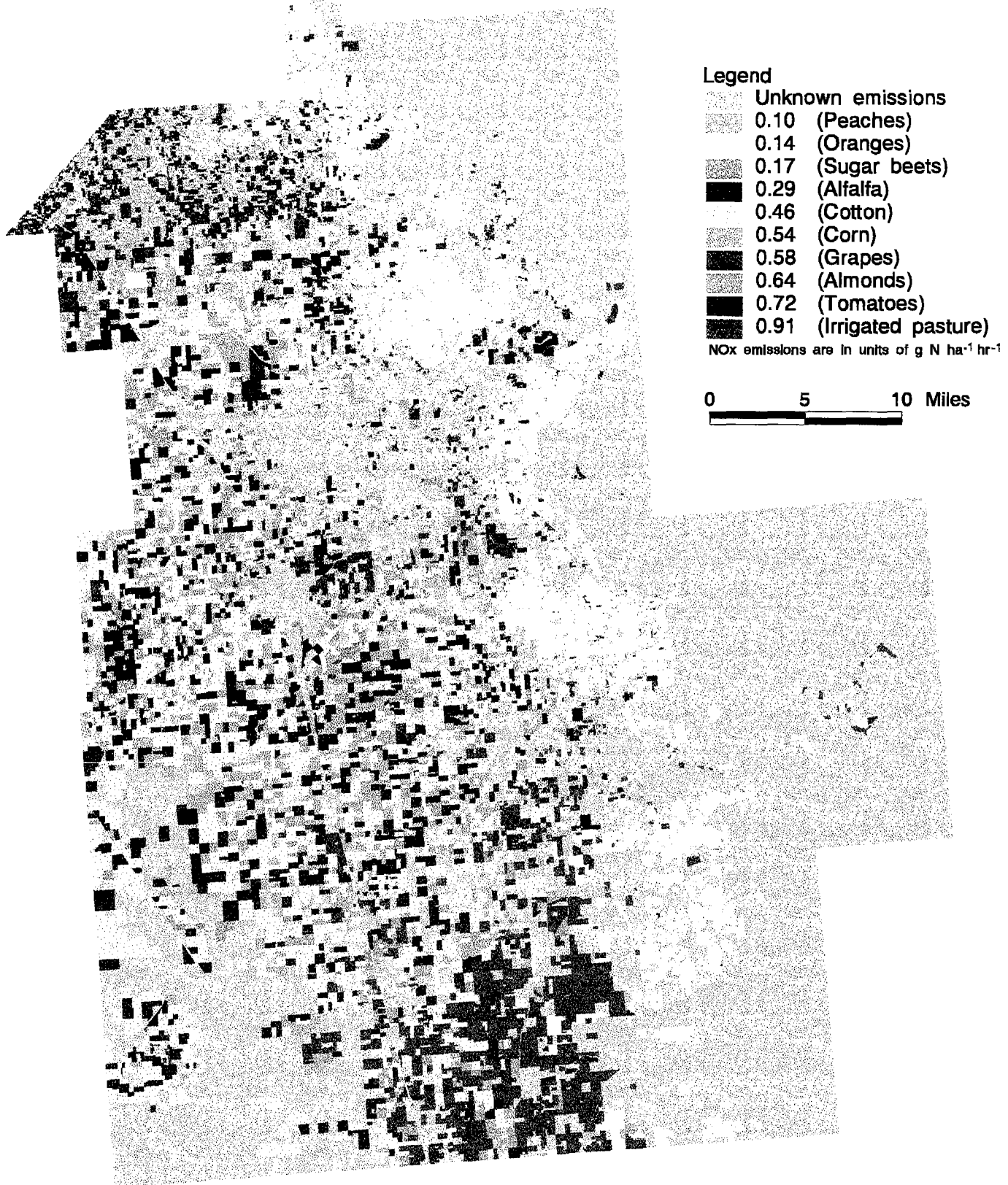


Figure 12g. Estimated NO_x Emissions as a Function of Crop Type in Western Tulare County, California

Crop distribution is based on data provided by the California Department of Water Resources. Data on NO_x emissions was produced and analyzed by the University of California at Berkeley. See accompanying metadata for details. NO_x emissions (g N ha⁻¹ hr⁻¹) for each crop type are the mean values for measurements taken in 1 - 5 fields per crop type.

$$\log(\text{NO}) = cT + \log(A) + \text{error}$$

Any non-soil temperature effects are grossly incorporated in the A coefficient (or $\log(A)$ intercept). Note that since NO_x flux can be zero or negative, it is not strictly lognormally distributed and to date there are no satisfactory transformations to account for zero or negative observations from these "pseudo"-lognormal variables. As will be later shown below, the NO_x fluxes at or below zero exhibit different behaviors from positive fluxes, and so we could model these separately for our Point-predictive and Management models.

We applied the model of Williams, et. al. to the San Joaquin Valley data as they did for their data, using the same units of NO_x flux [$\text{ng-N m}^{-2} \text{s}^{-1}$], and running regressions for individual sites. We used our measures of soil temperature directly, however, rather than using a derivation of soil temperature from air temperature, as Williams did. We then examined the model's explanatory ability and consistency with Williams' results.

For our more detailed Point-predictive and Management models, we utilized variables for which the collected data vary at both the site and chamber levels. The reader should refer again to Table 4 of Section 2.2.1 for a mental picture of the experimental layout. All data types collected are listed in Appendix A-2, and those relevant to a statistical model are outlined below:

Site-level variables:

Crop [categorical]

Soil texture [categorical]

"clayey", "loamy", "sandy"*

Fertilizer type [categorical]

NH_4^+ -fertilizer, mixed fertilizer (both NO_3^- and NH_4^+)

Fertilizer amount [numeric, but does not vary within site]

Days since last fertilizations [numeric]

Organic matter

C content [numeric, but does not vary within site]

N content [numeric, but does not vary within site]

pH [numeric, but does not vary within site]

Air Temperature [one site mean per sampling period]

Chamber-level variables:

Position [categorical]

Temperature

soil temperature [numeric, taken for each NO_x reading]
 Moisture
 water-filled pore space [WFPS]
 [one observation per chamber per sampling period]
 NH₄⁺ content [one observation per chamber per sampling period]
 NO₃⁻ content [one observation per chamber per sampling period]
 NO₂⁻ content [one observation per chamber per sampling period]

The variable sets for the two sets of models were:

Point prediction: response = NO_x flux/hour
 explanatory variables =
 crop, soil texture category, C, N, position,
 soil temperature, WFPS, NH₄⁺, NO₃⁻, NO₂⁻

sub-models: same model as above, but run on subsets of
 the data by crop type

Management: response = mean measured NO_x flux/hour on a day
 (measured between 9:30 a.m. and 3 p.m.)
 explanatory variables =
 crop, soil texture, pH,
 daily mean air temperature at time of flux,
 daily mean WFPS at time of flux,
 amount last fertilized, fertilizer type,
 days since last fertilization

sub-models: same model as above, but run on subsets of
 the data by crop type

*These categories include texture classes from a standard textural triangle (Brady 1974): clayey= clay, sandy clay; loamy= loam, clay loam; sandy= sand, loamy sand, sandy loam, sandy clay loam.

Soil texture was categorized into three broad classes, "clayey", "loamy", and "sandy" as indicators of the porosity of the soil and hence its interaction with soil moisture and its impedance of the

escape of NO_x gas from the soil. None of the soils in our data set were of silty textures, so no category was created for silty soil textures. For other soil characteristics, in the Point model, soil organic matter is indicated by N and C content, and soil chemistry is quantified by NH_4^+ , NO_3^- , and NO_2^- contents.

The management model makes use of NO_x measurements at the site level, since the explanatory variables rely on measures that are mostly obtainable only at the site level. For routine data collected at the chamber level, we took the site means by day of observation. For diel data we took the maximum NO_x flux from the diel curves and the mean air temperature and WFPS for the hours between 9:30 a.m. and 3 p.m. when maximum NO_x flux occurs. The management set of variables include air temperature rather than soil temperature, since air temperature is readily available on an hourly basis from weather stations. While there is a crude linear relationship between soil temperature and air temperature, some modeling of their relationship should be done to take into account soil moisture and canopy effects if it is necessary to convert between the two measures. Soil acidity (pH) is included in the Management model but not in the Point model because one average soil pH value was measured at the site level and expressed as a mean. (The pH values were based on random soil samples collected, rather than the soils collected at chamber positions.) Soil pH is also readily available from soil databases and maps and is easily measured in the field; therefore, we retained our own field-measured pH values to fit the Management model. Fertilizer variables were used to represent the nitrogen variables of the point model, since fertilization data are presumably more available over large spatial scales than are soil N concentrations. Fertilizer types were broadly grouped into two categories: those that are NH_4^+ -based (11-52-0, $(\text{NH}_4)_2\text{SO}_4$, NH_3 , aqua NH_3 , urea) and those that utilize mixes of NO_3^- and NH_4^+ compounds (NH_4NO_3 , CAN17, UN32); there were no sites in this study that received only NO_3^- -based fertilizer. The categories for the NH_4^+ fertilizers and the mixed fertilizers are listed in the bottom of Table 4. Water-filled pore space (WFPS) is one variable that is not generally available, but it was included because it was the best available data to describe soil moisture conditions. For broad application of this model, water-filled pore space may be estimated as a function of irrigation event or precipitation event and soil texture, as has been attempted in the CASA model (Potter, et. al., 1996).

The statistical modeling strategy was to 1) postulate a basic model, 2) run diagnostics on the data to look for nonlinear relations, and 3) use goodness of fit tests to improve the model fit. The general statistical model is of the form:

$$Y = f(x_1, x_2, \dots) + e$$

where $Y = \text{NO}_x \text{ flux [ng-N/cm}^2\text{/hr]}$
 $f = \text{any function, to be determined}$
 $x_1, x_2, \dots = \text{explanatory variables}$
 $e = \text{error (assumed normally distributed)}$

A first pass at determining the function f was to postulate an additive model of the form:

$$t(Y) = a_0 + f_1(x_1) + f_2(x_2) + \dots + e$$

where $a = \text{intercept}$
 $t, f_1, f_2, \dots = \text{transformations of the response and variates, not necessarily linear}$
 $e = \text{error}$

If a variable is categorical, such as crop, then its presence in the equation is like that of a set of dummy variables for each level of the variable, such as alfalfa, almonds, corn, etc. The fitted coefficients to these categorical variables serve as offsets to the intercept in the linear regression equation. Contrasts between levels of a categorical variable can be modeled as linear combinations that maintain relationships between levels. Here, a simple treatment contrast was used, assigning a 0 to the first level and 1 to the other $k-1$ of k variables. Thus the model being fit would be:

$$\begin{aligned} t(Y) &= a_0 + \dots + f_2(x_2) + f_3(x_3) + \dots + e \\ t(Y) &= a_0 + a_{12}[\text{crop}_2] + f_2(x_2) + f_3(x_3) + \dots + e \\ t(Y) &= a_0 + a_{13}[\text{crop}_3] + f_2(x_2) + f_3(x_3) + \dots + e \\ &\dots \text{ continue for each } k-1 \text{ levels of crop for total } k \text{ levels} \end{aligned}$$

To explore the form of the transforming functions, the Alternating Conditional Expectation (ACE) algorithm of Breiman & Friedman (J. Amer. Stat. Assoc., Vol. 80, 1985), available in S-Plus software, was used. This algorithm seeks to maximize correlations between the predictor ($a + f_1(x_1) + \dots$) and $t(Y)$. The plots of the transformed variates provided clues to the form the relations

between the response and the explanatory variables. Regression was performed for the two model sets using a) a straight linear model, and b) an additive model of curve fits to the transformed variates. The Chi-square test then was used to determine the importance of the variables in the model, and analysis of deviance to compare different models' goodness of fit.

In summary, our modeling involved the following:

(1) Application of Williams' simple model to the San Joaquin Valley data to validate or invalidate his model.

(2) Development of more detailed models with more explanatory variables, the chamber-level Point-predictive model and the site-level Management model, through the following procedure:

(a) Using the framework of a general additive model, diagnostics were run on the data with ACE to look for important variables and non-linearities.

(b) A straight log-linear model was fit to the data, with significant reactions retained but no transformations to explanatory variables.

(c) The same model as in (a) was refit with transformations to explanatory variables, as indicated by the ACE transformations; the goodness of fit of this new model was compared to that of the straight log-linear model in (a) through analysis of deviance.

(d) The robustness of the final model in (b) was tested by application to individual crop types.

(3) Comparison of Williams' model, the Point-predictive model, and the Management model results.

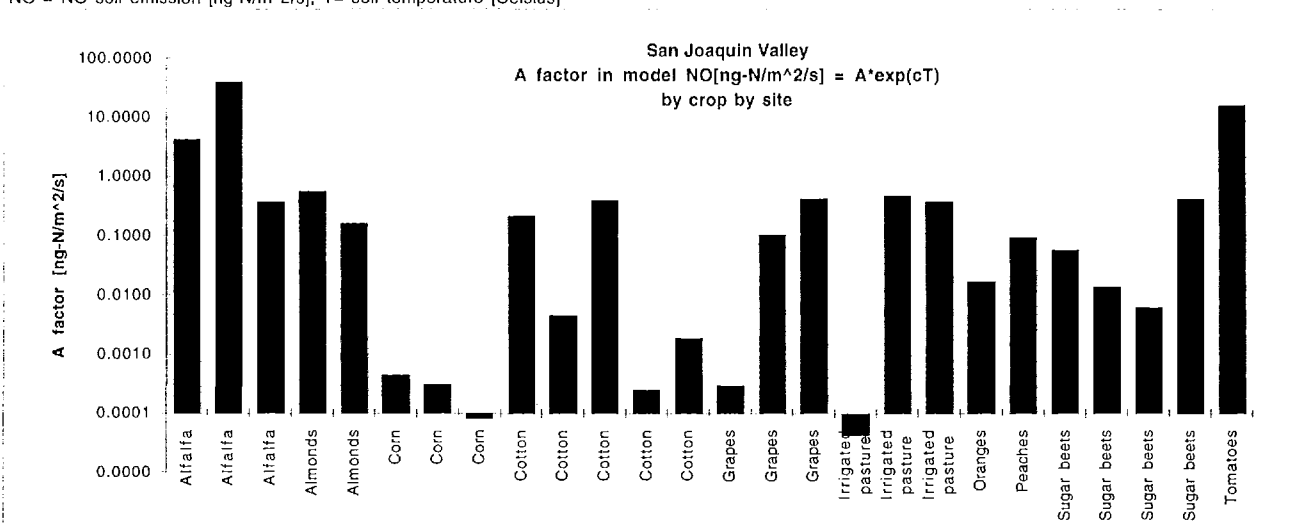
2.3.2.2 Results.

2.3.2.2.1 Application of Williams' Model.

Figures 13a and 13b show the results of refitting Williams' simple $NO = A \cdot \exp(cT)$ model to the San Joaquin Valley data; tables of the fitted parameters are given below the figures of A factors. Figure 13a makes use of the San Joaquin Valley data at the chamber

Figure 13a. "A" factors fitted to San Joaquin Valley NOx data using Williams' model: $NO = A^{\exp(cT)}$, using data collected at individual chambers. NOx emissions and temperatures were measured July-September 1995.

NO = NO soil emission [ng-N/m²/s], T= soil temperature [Celsius]

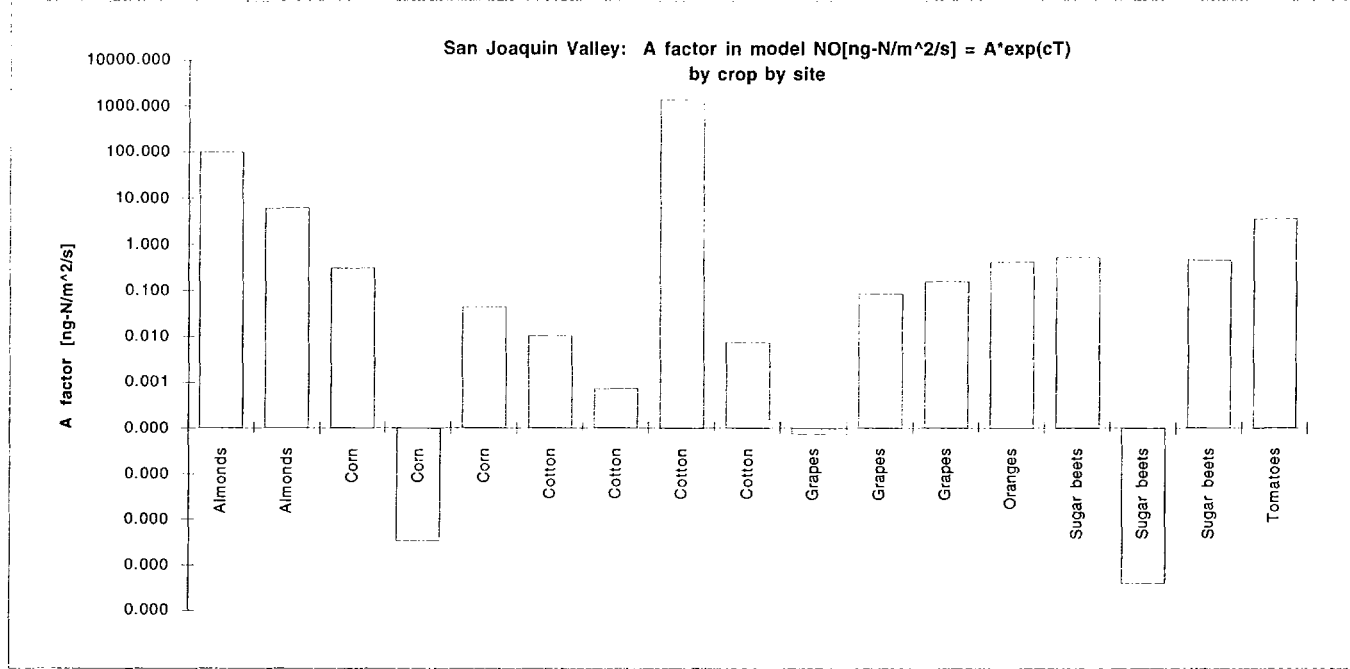


Sites regressed separately: from regression on $\ln(NO>0) = \ln(A) + cT + \text{error}$

crop	site	Location	soil	ln(A)			A			c			null.dev	deviance	%dev red.	numdata
				intcpt	intcpt.se	intcpt.t	A	coeff	coeff.se	coeff.t						
Alfalfa	A	Firebaugh	Sandy Loam	1.451	1.985	0.731	4.2661	-0.034	0.059	-0.569	5.697	5.559	2.4%	15		
Alfalfa	O	Kearney	Hanford Fine Sandy Loam	3.713	1.821	2.039	40.9771	-0.137	0.047	-2.895	19.383	13.226	31.8%	20		
Alfalfa	P	Kearney	Hanford Fine Sandy Loam	-0.969	2.405	-0.403	0.3795	0.024	0.073	0.330	0.614	0.606	1.3%	10		
Almonds	B	Parlier	Hanford Sandy Loam	-0.570	0.326	-1.746	0.5658	-0.016	0.010	-1.662	1737.028	1728.331	0.5%	551		
Almonds	C	Parlier	Sandy Loam	-1.798	0.894	-2.011	0.1656	0.042	0.026	1.642	201.743	193.708	4.0%	67		
Corn	I	Tulare	Loam	-7.698	3.128	-2.461	0.0005	0.184	0.119	1.552	68.183	64.484	5.4%	44		
Corn	J	Plainview	Fine Loam	-8.070	0.441	-18.298	0.0003	0.269	0.016	16.958	510.347	171.846	66.3%	148		
Corn	K	Waukena	Loam	-9.434	2.312	-4.080	0.0001	0.256	0.087	2.940	67.207	57.470	14.5%	53		
Cotton	D	San Joaquin	Sandy Clay Loam	-1.511	0.768	-1.967	0.2208	0.087	0.024	3.613	49.080	39.665	19.2%	57		
Cotton	E	San Joaquin	Sandy Loam	-5.383	1.861	-2.893	0.0046	0.140	0.060	2.345	74.443	63.530	14.7%	34		
Cotton	F	Tranquillity	Clay Loam	-0.900	1.504	-0.598	0.4067	0.018	0.047	0.383	17.795	17.725	0.4%	39		
Cotton	G	Riverdale	Fine Clay Loam	-2.277	2.885	-2.869	0.0003	0.213	0.120	1.771	23.173	18.033	22.2%	13		
Cotton	Y	West Side	Sandy Clay Loam	-6.248	0.442	-14.124	0.0019	0.138	0.016	8.579	1099.908	905.124	17.7%	344		
Grapes	L	Firebaugh	Loamy Sand	-8.123	1.088	-7.464	0.0003	0.256	0.033	7.870	85.589	30.335	64.6%	36		
Grapes	Q	Kearney	Hanford Sandy Loam	-2.239	0.277	-8.076	0.1066	0.045	0.007	6.140	91.982	69.569	24.4%	119		
Grapes	R	Kearney	Hanford Fine Sandy Loam	-0.871	0.163	-5.340	0.4186	0.026	0.005	5.147	283.531	264.731	6.6%	375		
Irrigated pasture	M	Sanger	Sandy Loam	-10.061	6.489	-1.551	0.0000	0.302	0.181	1.667	12.039	8.619	28.4%	9		
Irrigated pasture	W	Bonadelle Ranch	Loam	-0.740	2.424	-0.305	0.4769	0.035	0.080	0.441	62.639	62.173	0.7%	28		
Irrigated pasture	X	Bonadelle Ranch	Loam	-0.956	5.944	-0.161	0.3845	0.010	0.196	0.052	74.877	74.868	0.0%	24		
Oranges	T	Lindcove	San Joaquin Sandy Loam	-4.062	0.930	-4.367	0.0172	0.093	0.030	3.097	166.795	147.430	11.6%	75		
Peaches	V	Clovis	Visalia Sandy Loam Clay	-2.348	1.048	-2.241	0.0956	0.011	0.034	0.317	18.117	18.004	0.6%	18		
Sugar beets	H	Mendota	Sandy Loam	-2.837	0.571	-4.965	0.0586	0.047	0.020	2.358	16.033	13.939	13.1%	39		
Sugar beets	N	Mendota	Loam	-4.273	1.175	-3.637	0.0139	0.089	0.036	2.503	17.649	15.151	14.2%	40		
Sugar beets	S	Corcoran	Sandy Loam partially dreg	-5.076	1.618	-3.138	0.0062	0.052	0.043	1.195	3.751	2.918	22.2%	7		
Sugar beets	U	San Joaquin	Sandy Loam	-0.846	0.583	-1.450	0.4293	0.034	0.017	2.069	16.759	14.977	10.6%	38		
Tomatoes	Z	West Side	Panoche Clay Loam very	2.807	0.815	3.445	16.5655	-0.069	0.023	-2.948	163.242	152.133	6.8%	121		

Figure 13b. "A" factors fitted to San Joaquin Valley NOx data using Williams' model: $NO = A * \exp(cT)$, using site means for all data. NOx emissions and temperatures were measured July-September 1995.

NO = NO soil emission [ng-N/m²/s], T= soil temperature [Celsius]



Sites regressed separately: from regression on $\ln(NO>0) = \ln(A) + cT + \text{error}$
 NO responses are daily mean maximums converted to Williams' units of [ng-N/m²/s].
 Soil temperatures are the mean soil temperatures between 10 a.m. and 3 p.m.

crop	site	Location	soil	ln(A)			A	c		coeff.t	null.dev	deviance	%dev red.	numdat
				intcpt	intcpt.se	intcpt.t		coeff	coeff.se					
Almonds	B	Parlier	Hanford Sandy Loam	4.597	1.790	2.568	99.233	-0.166	0.057	-2.933	52.113	34.599	33.6%	19
Almonds	C	Parlier	Sandy Loam	1.829	2.706	0.676	6.227	-0.050	0.077	-0.654	16.896	15.771	6.7%	8
Corn	I	Tulare	Loam	-1.166	7.158	-0.163	0.311	-0.050	0.274	-0.182	3.654	3.624	0.8%	6
Corn	J	Plainview	Fine Loam	-14.915	2.866	-5.204	0.000	0.492	0.093	5.303	44.867	7.890	82.4%	8
Corn	K	Waukena	Loam	-3.105	1.679	-1.849	0.045	0.021	0.059	0.356	2.008	1.958	2.5%	7
Cotton	D	San Joaquin	Sandy Clay Loam	-4.576	4.245	-1.078	0.010	0.164	0.134	1.230	8.044	5.837	27.4%	6
Cotton	E	San Joaquin	Sandy Loam	-7.201	1.660	-4.339	0.001	0.227	0.054	4.193	2.438	0.249	89.8%	4
Cotton	F	Tranquillity	Clay Loam	7.236	4.300	1.683	1389.210	-0.248	0.134	-1.849	1.371	0.506	63.1%	4
Cotton	Y	West Side	Sandy Clay Loam	-4.887	2.415	-2.024	0.008	0.095	0.087	1.086	11.079	10.088	8.9%	14
Grapes	L	Firebaugh	Loamy Sand	-9.512	3.455	-2.753	0.000	0.301	0.104	2.876	6.407	1.247	80.5%	4
Grapes	Q	Kearney	Hanford Sandy Loam	-2.453	0.590	-4.157	0.086	0.036	0.016	2.265	3.756	2.482	33.9%	12
Grapes	R	Kearney	Hanford Fine Sandy Loam	-1.836	1.430	-1.284	0.159	0.013	0.041	0.315	4.450	4.363	2.0%	7
Oranges	T	Lindcove	San Joaquin Sandy Loam	-0.850	1.086	-0.783	0.427	0.008	0.035	0.214	0.811	0.805	0.8%	8
Sugar beets	H	Mendota	Sandy Loam	-0.625	1.508	-0.414	0.536	-0.046	0.053	-0.862	0.269	0.196	27.1%	4
Sugar beets	N	Mendota	Loam	-17.061	2.897	-5.890	0.000	0.467	0.088	5.312	2.730	0.181	93.4%	4
Sugar beets	U	San Joaquin	Sandy Loam	-0.764	2.132	-0.358	0.466	0.020	0.061	0.335	0.984	0.932	5.3%	4
Tomatoes	Z	West Side	Panoche Clay Loam ver	1.304	3.086	0.423	3.685	-0.051	0.089	-0.573	25.023	24.449	2.3%	16

level, while Figure 13b makes use of the site means of these data at the mean measured NO_x at mid-day.

Williams assumed the c parameter to remain fairly constant, while only the A factor would vary with different crop types and other soil conditions. This is in accord with our strategy here, in which the variables other than soil temperature should account for the magnitudes of the A factor in Williams' model. Ideally, in a log-linear model, the c parameter would remain constant if the soil temperature is additive with other (unknown) terms. However, without other explanatory variables, both c and A may obtain very different values in simple regressions on different data sets, especially if soil temperature is not the main driving variable at a particular site and especially if it is interactive with other driving variables. Both the c and A parameters are equally important in determining the magnitude of the predicted NO_x flux -- much attention to Williams' model has been devoted only to the A parameter. Williams, et.al., recognized the importance of at least some other variables in their efforts to extrapolate the A factor for different crop types and also different fertilizer regimes. Here, we have not averaged the fitted parameters to produce "representative" equations of crop types, because from the A and c values in the table, it is evident that there can be extreme differences between sites with the same crop, such that averaging their fitted parameters will not produce a representative equation. Also, when Williams, et.al., chose an average c parameter, they neglected to account for the standard deviation in the coefficients that were averaged (they calculated a c value of $0.071 \pm .007$, but the smallest standard deviation in one of the c 's used is 0.011).

The fitted parameter values for the San Joaquin Valley data are nowhere near those calculated by Williams for the same crop type. For corn crops, Williams obtained an A factor of $9 \text{ ng-N m}^{-2} \text{ s}^{-1}$, whereas, for the chamber level data we obtained A values of $0.0001\text{-}0.0005 \text{ ng-N m}^{-2} \text{ s}^{-1}$, while for the site means we obtained A values of less than 0.00001 to 0.311 . For cotton, Williams' A value was 4, whereas we found a range of $0.002\text{-}0.4 \text{ ng-N m}^{-2} \text{ s}^{-1}$ for the chamber level data. The c values for cotton range from 0.018 to 0.213, which are close to Williams' value, but in some cases the c value is negative. In Figure 13b, we see how dramatically the A and c parameters can interplay with each other in a single-variable regression, with a negative value of c offsetting a very large value of A (Cotton F). Looking at the model deviances in our applications of the model, we can see that soil temperature is highly variable in its

influence on NO_x flux, accounting for anywhere from nearly 0% to 66% of the deviances of the null model. There must, therefore, be other variables that at different times or places have a strong or stronger influence on NO_x flux. We now investigate some of these.

2.3.2.2.2 Point-Predictive Model.

Alternating Conditional Expectation (ACE) transformations

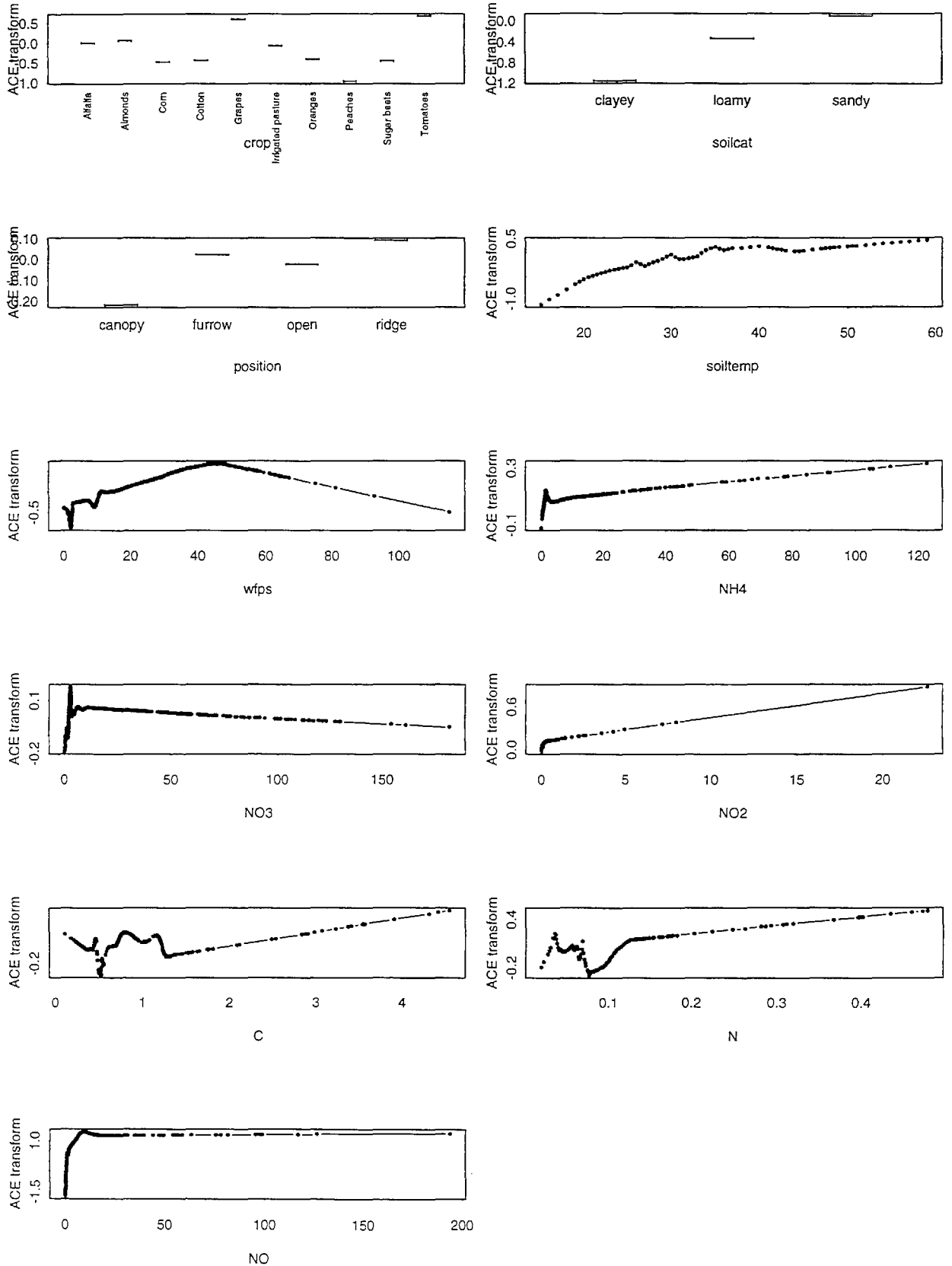
The ACE transformations to NO_x and the Point-predictive model's explanatory variables are shown in Figure 14. Each plot consists of the variable data values on the x-axis and its ACE transformation on the y-axis. The transformation to the response, NO_x , is clearly of a log form over a limited range of about 0-20 $\text{ng-N cm}^{-2} \text{ h}^{-1}$, but at the other interval above 20 and less than or equal to zero NO_x flux, the transformation behavior is very different. These changes in behavior may indicate different processes operating at extreme levels of NO_x flux, and developing different models over specific ranges of NO_x may be the appropriate approach. The transformation of soil temperature appears to be of a log form, also, indicating that it may not be exponentially related to NO_x . Water-filled pore space shows a remarkable trend of increase in NO_x flux over 0-45 percent water-filled pore space and then decrease with higher moisture contents; these trends are in accord with previous evidence of higher nitrification at moderate moisture levels, then shift to denitrification and greater impediment to NO_x escape in more anaerobic soil environments. Other variables appear to be fairly linearly related to the transform of NO_x , but all exhibit a large amount of noise at their low values, which also often include a large fraction of the data. The poor R-squared of 0.4 for the point-predictive model indicates either the high variability of the data or the inappropriateness of a linear or additive model. Also, interaction terms may play an important role; these are produced in model equations later.

The three ranges of different NO_x behaviors are $\text{NO}_x \leq 0$, $0 < \text{NO}_x < 20$, $\text{NO}_x \geq 20$. The transition at the $\text{NO}_x = 20$ point is not so marked, however, and the number of observations above this account for only 2 percent of the data. Given the fairly disjoint nature of the transformations from ACE at $\text{NO}_x = 0$, and since 93 percent of the data occur in the interval $0 < \text{NO}_x$, we modeled the upper two of the three ranges of NO_x flux together and separately from the lower range. (Note that we did not separate these ranges for the diel curve estimations, because there we were merely finding

Figure 14. Alternating Conditional Expectations (ACE) transformations to the variables used in the Point-Predictive Model, developed using NOx emissions and site-level variables.

Data collected in San Joaquin Valley, July-September, 1995.

rsq = 0.423867 Num obs = 2324



mean flux levels, while here we must model the driving variables, which may act differently for NO_x flux above and below zero).

Fitting of Point-Predictive Model

For $\text{NO}_x > 0$, the data are still very noisy, with persistent high variability in the low ranges of some variables, giving an R-squared of only 0.42. We first ran a full model with all interaction terms and used the Chi-square test for analysis of deviance to identify significant terms. Also, plotting out the data by individual crops allowed us to see possible interactions between crop type and other explanatory variables. This resulted in the following model with significant interactions (from now on, coefficients of terms will not be explicitly written but implied in the equations):

$$\begin{aligned}
 (\#) \quad \log(\text{NO}) = & \text{crop} + \text{soilcat} + \text{position} + \text{soiltemp} + \text{WFPS} + \text{NH}_4^+ + \\
 & \text{NO}_3^- \\
 & + \text{NO}_2^- + \text{C} + \text{N} + \text{crop} * \text{soiltemp} + \text{soiltemp} * \text{WFPS} * \text{NH}_4^+ + \\
 & + \text{WFPS} * (\text{NO}_3^- + \text{C}) + \text{NO}_3^- * \text{C} + \text{NO}_2^- * \text{N} + \text{WFPS} * \text{C} * \text{N} \\
 & + \text{NH}_4^+ * \text{NO}_2^- * \text{C} * \text{N}
 \end{aligned}$$

* indicates interaction term

The ACE transformations indicated two non-linear transformations that would improve the model fit: a concave-down transformation for water-filled pore space, and an exponential transformation for soil temperature. Water-filled pore space has been observed to be correlated with increases in NO_x flux from 0 up to around 45 percent water-filled pore space, and then with decreases in NO_x flux at higher water contents. We obtained a concave-down transformation of water-filled pore space through non-linear regression on the ACE transformed output, achieving the following:

$$\text{transformed WFPS} = 0.57 * \sin(\text{WFPS}/17.6 - 1) + 0.04$$

(Note: Future users of the model should constrain the transformed WFPS to the half sine period and extrapolate downward, in cases where observed soil temperature is higher than the maximum in the data here (60 degrees Celsius).

Soil temperature appeared more linearly related to NO_x , and therefore we transformed (to get $\log(\text{NO}_x) = \dots \log(\text{soil temperature}) \dots$):

$$\text{transformed soil temperature} = \log(\text{soil temperature})$$

Model (#) was run with the transformed WFPS and soil temperature, adding transforms one at a time, and the deviances of the original and new model were compared. The models were run both on the entire data set (for $\text{NO}_x > 0$) and also on individual crop types. We found that the above transformations do significantly improve the model fit in their reduction of the deviances, and are therefore closer to the true relationship between NO_x flux and soil temperature and water-filled pore space.

Point-predictive model results

A listing of the final model with significant interactions retained is provided in Table 12. The t values are generally high (>2), except for tomatoes ($t=0.700$), irrigated pasture ($t=1.784$), and peaches ($t=1.714$). Note that the categorical variables' levels listed in parentheses simply have 0 offsets from the intercept, since this was how the contrasts between category levels were modeled. There are still considerable deviances unaccounted for by the model, but the Chi-square test was still able to show the significant variables and interactions.

The Chi-square test, interestingly, consistently showed NO_3^- to be less successful at explaining NO_x flux than NH_4^+ or NO_2^- ; this low significance is likely due to the extreme non-linearities in the relation between NO_x and NO_3^- , which we did not try to model here. Nitrate is known to exhibit high spatial heterogeneity at small scales. Most studies have suggested that nitrification (the conversion of NH_4^+ to NO_3^-) is the primary source for NO_x production in soils, so differences in NH_4^+ may be more closely tied to NO_x emission than are NO_3^- concentrations. This is corroborated by its low significance in the model. Interestingly, however, the interaction between the transformed WFPS and NO_3^- shows high significance and also a tight standard error; the positive coefficient implies that if WFPS is around 45 (when its transformation is a maximum) and NO_3^- content is high, then NO_x flux is promoted.

All of the first-order variables are highly significant in the model. Crop effects show fairly tight standard errors, except for tomatoes. Transformed water-filled pore space, NH_4^+ , and the

Table 12. Parameters for point-predictive model developed using NO_x emissions and site and chamber-level variables measured July-September 1995 in the San Joaquin Valley. Model with significant interactions, transformed soil temperature and transformed water-filled pore space, with interactions between crop and soil temperature.

Variables:**Crop**

"Alfalfa" "Almonds" "Corn"
 "Cotton" "Grapes" "Irrigated pasture"
 "Oranges" "Peaches" "Sugar beets"
 "Tomatoes"

Soil texture category

"clayey" "loamy" "sandy"

Position

"canopy" "open" "furrow" "ridge"

Soil temperature

NH₄, NO₃, NO₂, C, N

Water-filled pore space

```
Call: glm(formula = log(NO) ~ crop * log(soiltemp) + soilcat + position +
twfps + NH4 + NO3 + NO2 + C + N +
log(soiltemp) * twfps * NH4 + twfps * (NO3 + C) +
NO3:C + NO2 * N + twfps:C:N + NH4:NO2:C:N,
data = as.data.frame(cbind(data[index, ],
twfps = pred.wfps1(wfps[index], ))))
```

Deviance Residuals:

Min	1Q	Median	3Q	Max
-6.783	-0.746	0.114	0.900	4.164

Coefficients:

	Value	Std. Error	t value
(Intercept)	10.666	6.758	1.578
	0	7.522	
cropAlmonds	-13.842	6.761	-2.047
cropCorn	-33.908	7.166	-4.732
cropCotton	-33.718	6.920	-4.872
cropGrapes	-18.203	6.781	-2.685
cropIrrigated pasture	-16.161	9.057	-1.784
cropOranges	-22.429	7.473	-3.002
cropPeaches	-14.811	8.641	-1.714
cropSugar beets	-26.954	7.244	-3.721
cropTomatoes	-5.359	7.652	-0.700
soilcatclayey	0	0.387	
soilcatloamy	0.234	0.432	0.541
soilcatsandy	1.189	0.399	2.979
positioncanopy	0	0.420	
positionopen	0.442	0.113	3.923
positionfurrow	2.616	0.573	4.565
positionridge	2.651	0.573	4.624
log(soiltemp)	-3.451	1.894	-1.822
twfps	-2.248	1.929	-1.165
NH ₄	0.136	0.056	2.418
NO ₃	-0.003	0.002	-1.079
NO ₂	-0.104	0.232	-0.451
C	-0.429	0.257	-1.670
N	9.475	2.275	4.165
(cropAlfalfalog(soiltemp))	0	2.585	
cropAlmondslog(soiltemp)	3.975	1.897	2.095

Table 12. Con't. Point-predictive model parameters.

	Value	Std. Error	t value
(Intercept)	10.666	6.758	1.578
cropCornlog(soiltemp)	9.142	2.016	4.535
cropCottonlog(soiltemp)	8.789	1.937	4.538
cropGrapeslog(soiltemp)	4.767	1.894	2.517
cropIrrigated pasturelog(soiltemp)	4.555	2.586	1.762
cropOrangeslog(soiltemp)	6.247	2.115	2.953
cropPeacheslog(soiltemp)	3.708	2.476	1.497
cropSugar beetslog(soiltemp)	6.980	2.024	3.449
cropTomatoeslog(soiltemp)	1.290	2.142	0.602
log(soiltemp):twfps	0.939	0.563	1.667
log(soiltemp):NH4	-0.035	0.017	-2.131
twfps:NH4	0.270	0.124	2.172
twfps:NO3	0.021	0.004	4.852
twfps:C	0.685	0.499	1.372
NO3:C	0.009	0.003	2.812
NO2:N	0.620	2.448	0.253
log(soiltemp):twfps:NH4	-0.069	0.037	-1.878
twfps:C:N	-3.126	1.369	-2.283
NH4:NO2:C:N	-0.010	0.017	-0.603

(Dispersion Parameter for Gaussian family taken to be 1.936568)

Null Deviance: 7305.35 on 2323 degrees of freedom

Residual Deviance: 4421.184 on 2283 degrees of freedom

Analysis of Deviance Table

Gaussian model

Response: log(NO)

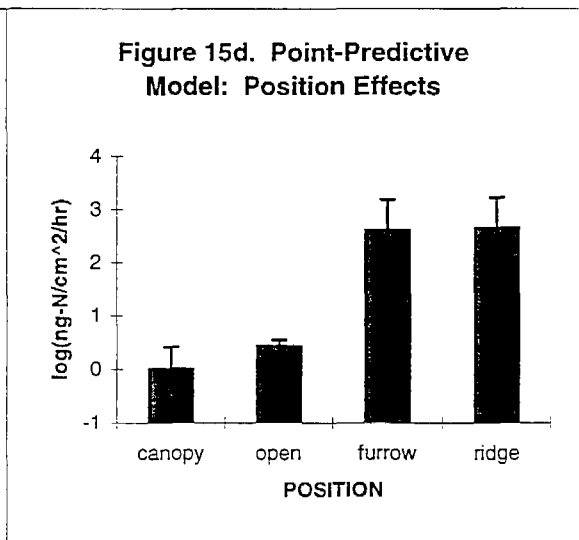
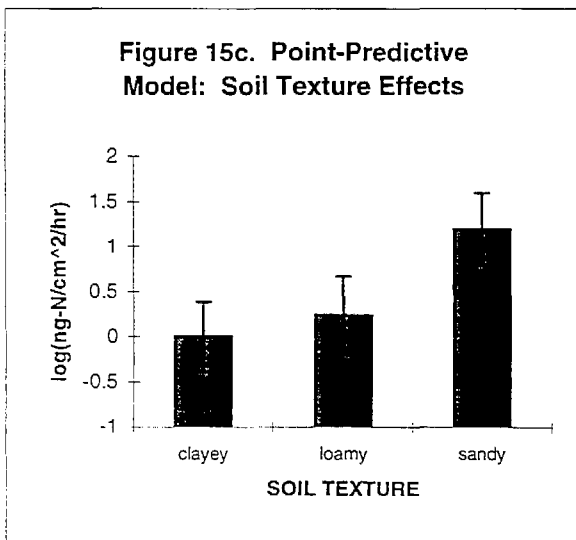
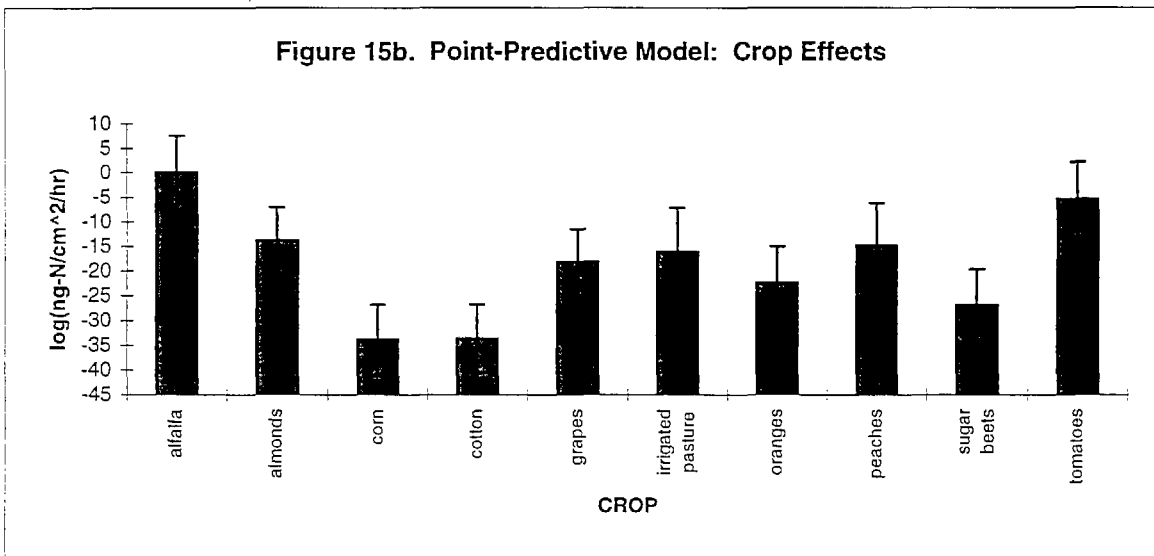
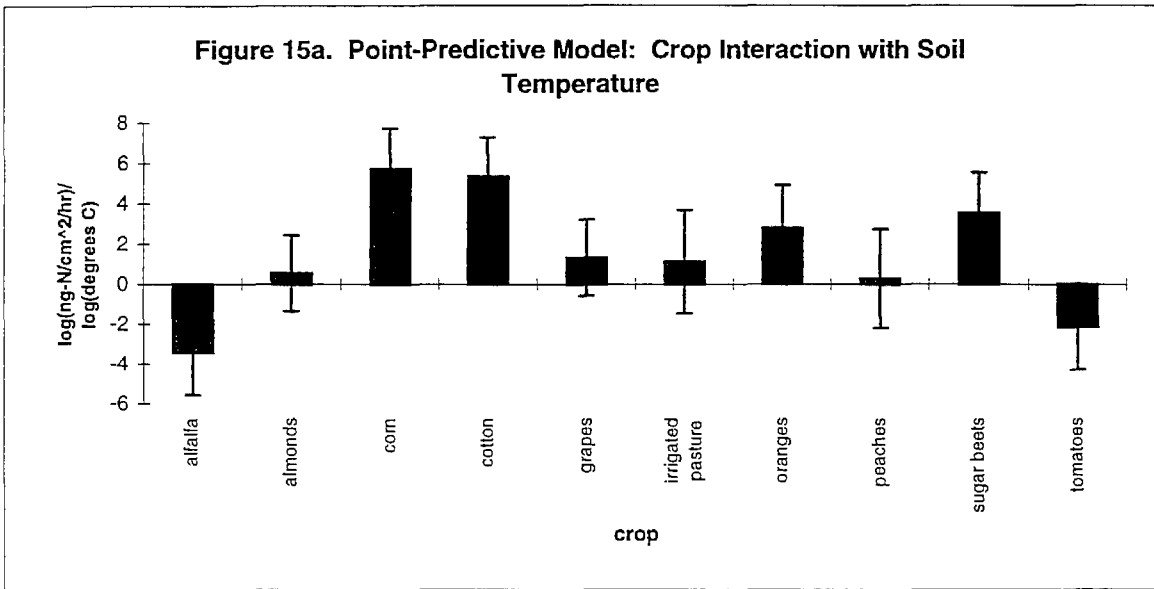
	Df	Deviance	Resid. Df	Resid. Dev	Pr(Chi)
NULL			2323	7305.350	
crop	9	1113.780	2314	6191.570	0.00000
log(soiltemp)	1	326.736	2313	5864.834	0.00000
soilcat	2	26.799	2311	5838.036	0.00000
position	3	56.270	2308	5781.765	0.00000
twfps	1	503.055	2307	5278.711	0.00000
NH4	1	51.293	2306	5227.417	0.00000
NO3	1	1.773	2305	5225.644	0.18296
NO2	1	7.846	2304	5217.798	0.00509
C	1	38.015	2303	5179.783	0.00000
N	1	27.936	2302	5151.847	0.00000
crop:log(soiltemp)	9	574.338	2293	4577.510	0.00000
log(soiltemp):twfps	1	0.629	2292	4576.881	0.42771
log(soiltemp):NH4	1	11.144	2291	4565.736	0.00084
twfps:NH4	1	36.165	2290	4529.571	0.00000
twfps:NO3	1	57.517	2289	4472.054	0.00000
twfps:C	1	12.307	2288	4459.747	0.00045
NO3:C	1	18.676	2287	4441.072	0.00002
NO2:N	1	0.417	2286	4440.655	0.51849
log(soiltemp):twfps:NH4	1	8.922	2285	4431.733	0.00282
twfps:C:N	1	9.845	2284	4421.889	0.00170
NH4:NO2:C:N	1	0.704	2283	4421.184	0.40132

interaction between them are very significant, as is organic matter (C, N), confirming our expectations about the influence of these variables on NO_x flux. The coefficient to WFPS is negative, because it turns out that the interactive effect of WFPS with soil temperature takes over the depressing effect of $\text{WFPS} > 45\%$ on NO_x flux; this interaction is always negatively correlated with WFPS, and the two may switch sign for different data sets. In the full-data model, this interaction appears as not significant, but as we see later, it can often be highly significant within crop types, so it is retained in the model.

The relative effects of crop, soil texture, and position are graphically shown in Figures 15 a, b, c, and d. Note that these are relative effects, with shared additive effects contained in the intercept of the regression equation. Recall that the first level in each category has a zero offset relative to the intercept. The effects are additive in the log model, and therefore multiplicative in the effect on actual NO_x . Corn and cotton crops have lowering effects on NO_x emissions, controlling for the other variables, while almonds reduce NO_x less. The other crops cannot really be differentiated from each other, given the standard errors on their coefficients.

For soil temperature effects, note that there are two coefficients to take into account, that for soil temperature and that for the crop interaction with soil temperature. The crop-soil temperature variable is a dummy variable whose coefficient is added to that for soil temperature to obtain the net soil temperature effect for a crop. The crops in fact have different NO_x flux responses to soil temperature, as shown in Figure 15a. Alfalfa and tomatoes show decreases in NO_x flux with temperature, while corn and cotton show strong increases. The other crops are in between, with more probable increases in NO_x flux with temperature; these crops are not distinguishable from each other.

Clayey and loamy soil textures are no different in their effects on NO_x emissions, but sandy soils appear to produce higher emissions than the other two. Similar results have been found in clay vs. Sandy tropical forest soils (Bakwin, et. al., 1990). Position in a field does not seem to play a major role, since other explanatory variables account for the differences between positions; this variable appears as significant in the model, because canopy/open crops do differ from ridge/furrow crops, but within these types, position makes little difference (besides the soil temperature and WFPS differences).



Point-Predictive Model Robustness

To test the robustness of the model we ran the same model above on each crop individually. Results of these tests are provided in Appendix F. Given our knowledge about the diversity of site and crop effects, the same variables should not have the same level of significance for all crop types. Also, because of the deviances still unaccounted for by the available variables, we expect there to be other unknown variables or non-linear relations. We therefore looked for which variables and interactions were especially important for a particular crop.

The model was able to account for anywhere from 16% (almonds) to 73% (alfalfa) of the deviances of the null model, improving somewhat on Williams' soil temperature model when non-soil temperature variables are also important, but also indicating that there is still unexplained variation. The variables and interactions that showed up as significant most consistently among the crop types were soil temperature, water-filled pore space, the interaction between water-filled pore space and NH_4^+ , and the interaction between water-filled pore space and soil temperature. Other higher-order interactions varied in their importance for different crops. Less frequently, NH_4^+ , NO_3^- , and C, were among the very important explanatory variables.

For alfalfa, soil temperature accounted for 46% of the model deviance, and water-filled pore space accounted for 12%. For corn, the significant interactions in addition to soil temperature and WFPS were organic matter content (C and N percent) ($P < 0.0009$ and $P < 0.002$, respectively), NO_3^- ($P < 0.003$), the interaction between NH_4^+ and WFPS ($P < 0.002$). For cotton, the additionally significant variables were the same as for corn, except that NO_3^- was highly insignificant. For peaches, no higher-order interactions were significant.

The fitted coefficients for the separate regressions vary between crops, meaning that these coefficients are not robust for transfer of the model to other systems. However, the relative differences between crops in terms of the soil temperature-crop interaction are preserved from the full data model. The coefficients for water-filled pore space and for its interaction with soil temperature seem individually inconsistent, but they are consistently opposite in sign, indicating when one of the two variables has greater influence than the other, or when soil temperature switches in effect between crop types to negative or

positive. The interactions $WFPS * NH_4^+$ and $WFPS * NO_3^-$ show good consistency in relative magnitude of their coefficients. The intercept, of course, changes depending on which categorical variable levels are relevant.

2.3.2.2.3 Management Model.

Management Model ACE Transformations

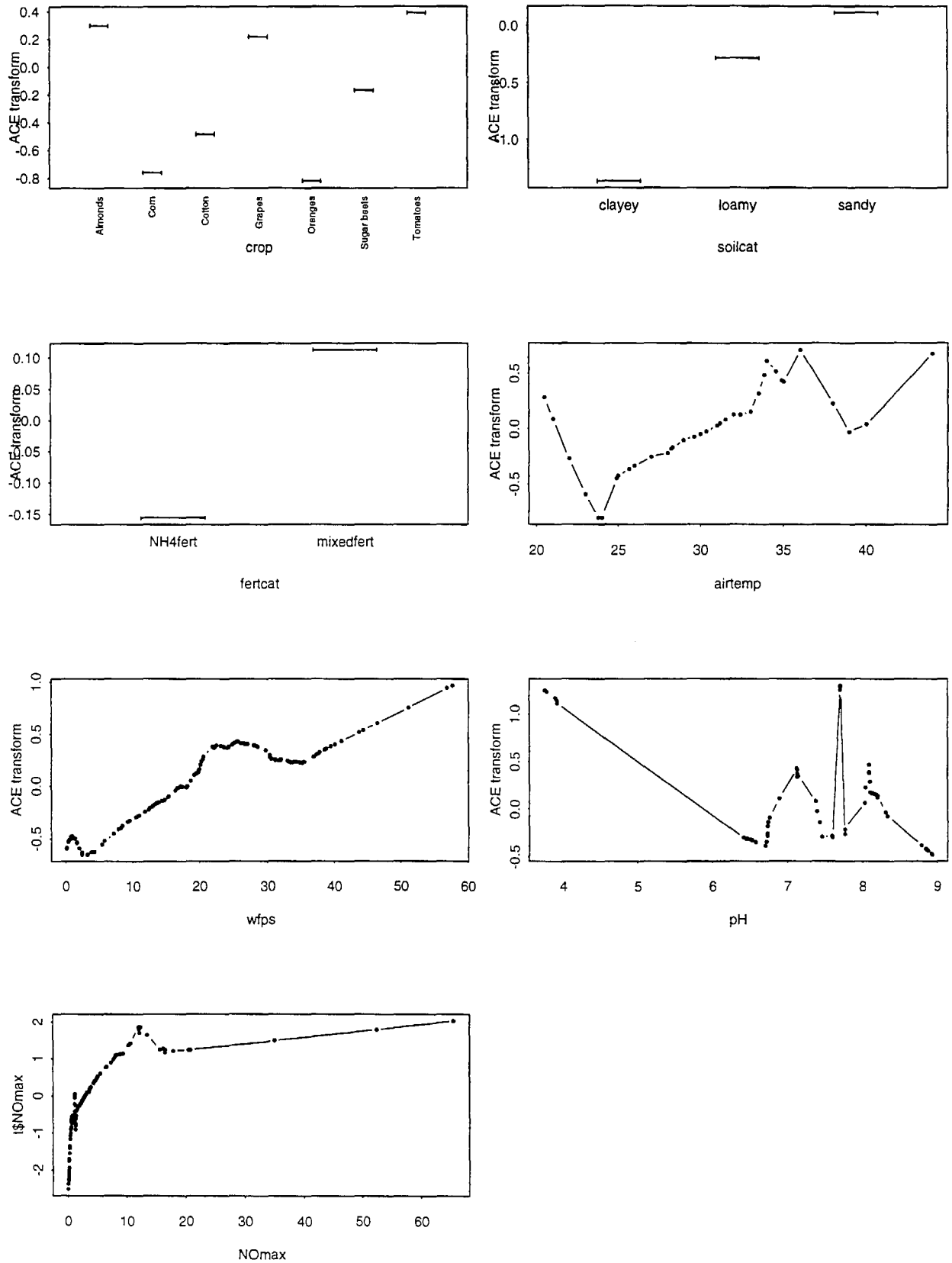
The ACE transformations to the variables of the management model are shown in Figure 16. Fewer observations were available for this model: taking the site means reduced the data set size (but also removed the high variability of the chamber level); fertilizer data are not applicable to irrigated pasture; there were too few days of observations for alfalfa and peaches. Transformations for crop, soil texture, air temperature, and NO_x flux are very like those for the same variables in the point-predictive model (air temperature in the management model in place of soil temperature). Removing the chamber-level variability has greatly reduced the data size and hence increased the uncertainty of estimation and led to some overfitting by ACE. This overfitting is seen in the lack of smoothness in the transformations of air temperature and pH. Cross-validation by modeling from subsets of the data shows that the transformation for air temperature is between a log or linear transformation, such that the exponential relation between temperature and NO_x flux in Williams' model may be adequate, after all. Cross-validation also showed the concave downward trend centered at 45 % WFPS is still preserved here; additionally, the low-WFPS variability that was seen in the point-predictive model now is more distinctly a spike of NO_x flux at $WFPS < 2\%$. This spike at very low WFPS and high temperature has been observed previously (Davidson et. al., 1993).

The pH transformations show some interesting trends. At very low pH (<4.0), there may be extremely high NO_x flux (these low pH levels with high NO_x occurred at site D, cotton on sandy soil with mixed fertilizer, with an air temperature range of 25-38 degrees Celsius). No sites had pH levels between 4 and 6.4, but the ACE transformations indicate much lower NO_x flux at higher pH, with a local peak at pH = 7.5. The time since last fertilization (days) does not have any meaningful relation to NO_x flux here. According to previous experience with fertilization events, the NO_x flux is only affected during a very short time (1-2 weeks) immediately after the fertilization; only three sites here were fertilized during the study period. Fertilizer amount also has little meaningful relationship to

Figure 16. Alternating Conditional Expectations (ACE) transformations to the variables used in the Management Model, developed using NOx emissions and site-level variables.

Data collected in San Joaquin Valley, July-September, 1995.

rsq = 0.679133 Num obs = 139



NO_x flux, because our data do not provide comparisons of several fertilization events on a particular site or crop type. It appears that fertilizer types utilizing a mix of NO_3^- and NH_4^+ tend to promote greater NO_x flux than simple NH_4^+ -based fertilizers, which is contrary to our expectations about nitrification. Again, there may be other confounding interactions, which we investigate in the regression models.

Fitting the Management Model

We ran the management model with all potentially meaningful interactions and looked for significant components, using the Chi-square test (not all interactions of higher orders were tested here, due to the smaller data set for the Management model). The resulting model with significant interactions and selected interactions of interest was (coefficients are implied again for each term):

$$\log(\text{NO}) = \text{crop} + \text{soilcat} + \text{airtemp} + \text{tWFPS} + \text{pH} \\ + \text{crop} * \text{airtemp} + \text{fertcat} * (\text{fertamt} / \text{fertdt})$$

where fertcat = fertilizer category
 fertdt = days since last fertilization
 "*" denotes interaction terms

The transformation of WFPS provided a better model fit than the untransformed WFPS. The log transformation for air temperature, however, was not significantly better than the untransformed variable, and so closer investigation should be done on the relation between air temperature and soil temperature. We did not attempt to model the small spike of NO_x at $\text{WFPS} < 2\%$, but this may be interesting for future work.

For pH, we maintained a linear term in the model, as the small hump in the ACE transformation may be due to site effects in this data set; however, the downward trend in NO_x flux with increasing pH is significant to preserve. Previous studies of tropical soils have found an increase in NO_x flux following an arctan-shaped curve from pH ranging from 4.0 to 6.8 (Motavalli, et.al., 1996), with exceptions for acid soils with high nitrification rates (Stams, et.al., 1990; Parton, et.al., 1996). Our data included a soil with pH slightly less than 4.0, and other soils with pH levels from 6.4 to 9.0. While we use a rough linear term here, it may be desirable in future modeling to fit a transformation piecewise for $\text{pH} < 4.0$, $\text{pH} = 4.0$ to 7.5, and $\text{pH} > 7.5$.

The last term in the equation, $\text{fertcat}:(\text{fertamt}/\text{fertdt})$, expresses the decay in effect of a fertilization event with time, with different responses for NH_4^+ fertilizers versus mixed fertilizers. We did not find it realistic to model the three fertilizer variables as independent, but, combined, they indicate the soil chemistry on the day of a NO_x measurement.

Management Model Results

The regression results for the management model are shown in Table 13. With the chamber-level variation removed, these variables were able to explain 61 percent of the deviances of the model with fewer parameters than the point-predictive model. However, the management model was less able to distinguish the amount of influence of different levels of certain categorical variables.

All terms are highly significant at $P < 0.002$. Unlike in the Point model, the interaction between air temperature and WFPS did not show significance in the Management model, and so this interaction was dropped.

Figures 17 a, b, c, d show the coefficients for the categorical variables. The interaction between air temperature and crop (Figure 17a, sum of airtemp coefficient and $\text{crop}:\text{airtemp}$ coefficients), shows the same pattern as the $\text{crop}:\text{soiltemp}$ interaction of the point-predictive model, which implies that air temperature may be a good proxy for soil temperature in predicting NO_x flux at the site level. The coefficients that resulted for the crops (Figure 17 b) also show similar relative trends as in the point-predictive model; however, the differences are not as pronounced. Almonds, grapes, and tomatoes would tend to show greater NO_x flux than other crops, but their overall effect on NO_x flux, positive or negative, is uncertain due to the size of the standard errors on their coefficients. Note that values are relative effects, since shared effects are contained in the regression equation intercept. If the intercept is taken into account, then it appears that the crops other than almonds, grapes, and tomatoes would tend to have a decreasing effect on NO_x emissions from the soil. The effects of soil texture and fertilizer type are shown in Figures 17 c and d. Soil texture effects show the same trends as in the point-predictive model but are not as clearly different, due to the standard errors in the coefficients; the tendency appears to be that sandy soils promote NO_x emissions the most, which was more confidently differentiated in the point-predictive model.

Table 13. Parameters for management model developed using NOx emissions and site variables measured July-September 1995 in the San Joaquin Valley.

(Model with selected interactions and transformations to air temperature and wfps.)

Variables:

crop

"Alfalfa"(*) "Almonds" "Corn"
 "Cotton" "Grapes" "Irrigated pasture"(*)
 "Oranges" "Peaches"(*) "Sugar beets"
 "Tomatoes"

soil texture category

"clayey" "loamy" "sandy"

fertilizer category

"NH4fert" "mixedfert"

air temperature

water-filled pore space

fertilizer amount

days since last fertilized

response: NO > 0

*Alfalfa and peaches are not included, because there were too few observations at the site level. Irrigated pasture is excluded, because fertilizer type and date are not available.

```
Call: glm(formula = log(NOmax) ~ crop + soilcat + airtemp + twfps + pH
          + crop:airtemp + fertcat:l(fertamt/fertdt),
          data = as.data.frame(cbind(sitemeans[index, ],
          twfps = pred.wfps1(wfps[index], junk1))))
```

Deviance Residuals:

Min	1Q	Median	3Q	Max
-3.304	-0.577	0.113	0.604	2.401

Coefficients:

	Value	Std. Error	t value
(Intercept)	-0.684	3.169	-0.216
(cropAlmonds)	0.000	3.664	
cropCorn	-8.284	3.792	-2.185
cropCotton	-3.679	3.122	-1.178
cropGrapes	0.956	3.826	0.250
cropOranges	-3.901	4.510	-0.865
cropSugar beets	-3.969	3.538	-1.122
cropTomatoes	2.978	3.197	0.931
(soilcatclayey)	0.000	0.911	
soilcatloamy	1.727	0.946	1.825
soilcatsandy	3.000	0.876	3.425
airtemp	0.011	0.092	0.121
twfps	1.843	0.589	3.126
pH	-0.194	0.133	-1.457
(cropAlmondsairtemp)	0.000	0.119	
cropCornairtemp	0.299	0.123	2.425
cropCottonairtemp	0.119	0.101	1.178
cropGrapesairtemp	-0.019	0.121	-0.158
cropOrangesairtemp	0.099	0.156	0.636
cropSugar beetsairtemp	0.117	0.114	1.033
cropTomatoesairtemp	-0.002	0.099	-0.016
fertcatNH4fertl(fertamt/fertdt)	-0.538	0.162	-3.314
fertcatmixedfertl(fertamt/fert	0.000	0.016	-0.023

(Dispersion Parameter for Gaussian family taken to be 1.110171)

Null Deviance: 340.3161 on 138 degrees of freedom

Residual Deviance: 132.1103 on 119 degrees of freedom

Table 13 Cont'd. Management model parameters.

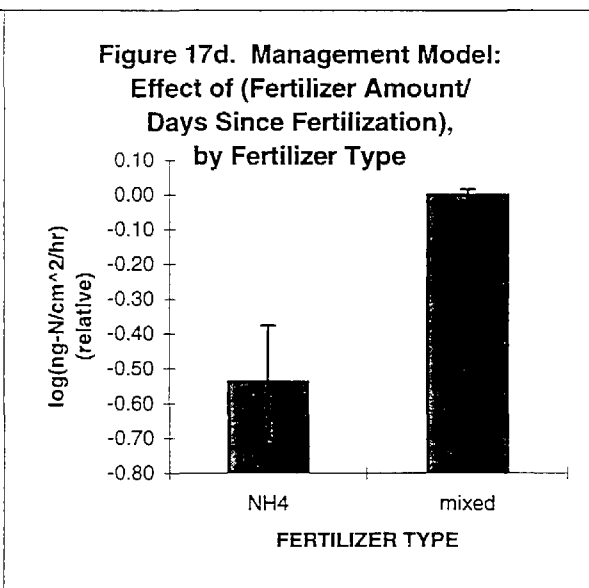
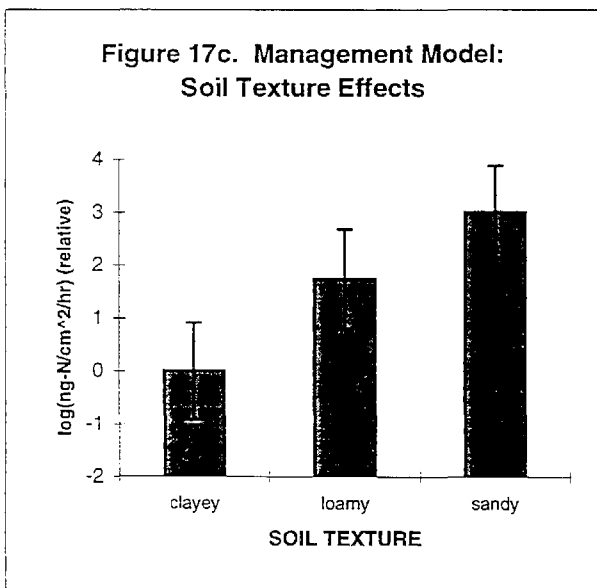
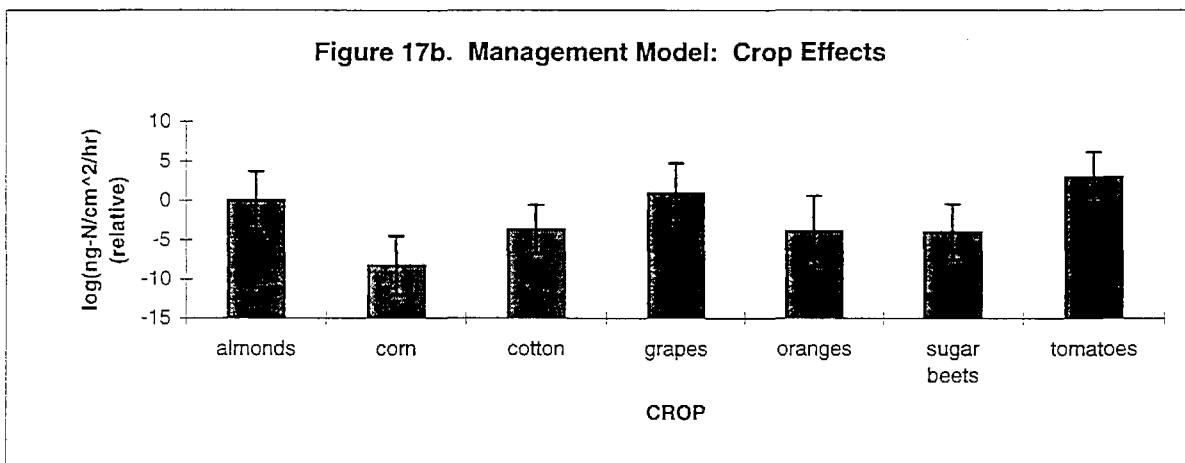
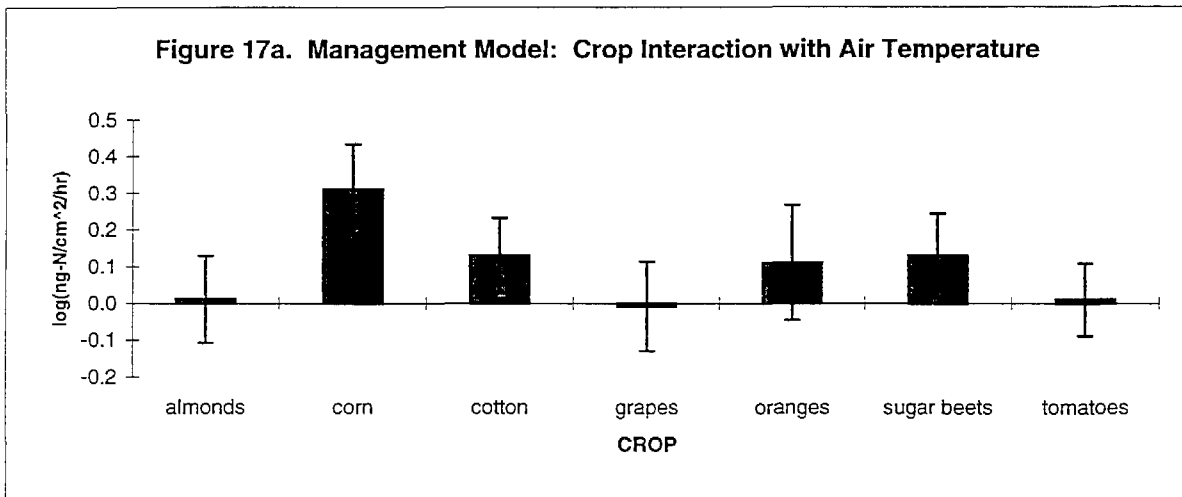
Analysis of Deviance Table

Gaussian model

Response: log(NOmax)

	Df	Deviance	Resid. Df	Resid. Dev	Pr(Chi)
NULL			138	340.316	
crop	6	52.498	132	287.819	0.0000
soilcat	2	12.991	130	274.828	0.0015
airtemp	1	19.245	129	255.583	0.0000
twfps	1	63.505	128	192.078	0.0000
pH	1	17.941	127	174.137	0.0000
crop:airtemp	6	29.447	121	144.690	0.0001
fertcat:l(fertamt/fertdt)	2	12.580	119	132.110	0.0019

Coefficients derived from fitting Management Model to NO_x flux data collected from San Joaquin Valley, July-September, 1995.



The effect of fertamt/fertdt is contrary to our expectations, with strong differentiation between fertilizer categories. NH_4^+ -fertilized crops have lower NO_x emissions (negative coefficient) with increasing fertilizer content, while crops with mixed fertilizer have no or possibly increasing effect on NO_x emissions. Further investigation must be carried out to determine the extent to which these fertilizer measures can be surrogates of soil chemistry.

Transformed water-filled pore space shows a tight standard error, with $t=3.126$. Soil pH has a negative coefficient ($t=-1.457$), implying an overall decline in NO_x flux with increasing pH.

Management Model Robustness

As for the point-predictive model, we applied the management model to subsets of the data by crop to test the robustness and to look for differences in significant terms between crops. Alfalfa, irrigated pasture, and peaches were excluded due to too few observations at the site level, so the crops analyzed were almonds, corn, cotton, grapes, oranges, sugar beets, and tomatoes. Soil pH was excluded for oranges, because there was only one site and hence one pH value for oranges. The model is able to account for from 16% of the variation in NO_x flux at 24 degrees of freedom (d.f.) (almonds) to as high as 96%, 13 d.f. (corn), and 76%, 23 d.f. (cotton).

Which terms are of greatest significance varies between crop types. Air temperature was strongly explanatory for almonds ($P < 0.09$), corn ($P \sim 0$), cotton ($P \sim 0$), and sugar beets ($P < 0.04$), but not so for grapes ($P > 0.20$) or tomatoes ($P > 0.80$). For oranges, the model shows poor P values (>0.60) for all terms, which is the same case for the point model. Water-filled pore space is significant for corn ($P < 0.07$), cotton ($P \sim 0$), grapes ($P < 0.1$), and tomatoes ($P < 0.001$), but not for almonds or sugar beets. Soil pH is significant for almonds ($P < 0.08$), corn ($P < 0.001$), and cotton ($P < 0.02$), but not for the other crops.

The fertilizer indicator, fertamt/fertdt, showed significance only for corn ($P < 0.002$), with coefficients following the trend of the full data management model, lower for NH_4^+ fertilizers, and higher for mixed fertilizers. This low significance means that better measures need to be found to estimate soil chemistry for NO_x prediction at the site level.

The parameter coefficient magnitudes vary considerably among the model fits to different crops. This lack of robustness is due to an inadequate amount of variation in the small data subsets for the different crops. The Management model with the full data set is

consistent with our scientific knowledge of the effects of temperature and WFPS, may provide new insight on pH, but requires better estimators of soil N. The most consistently significant variables continue to be temperature and WFPS.

2.3.2.2.4 Comparison of Models.

We compare now Williams, et.al.'s soil temperature-based model, the point-predictive model, and the management model, and examine where aspects of one model improve on the deficiencies of another. For consistency of comparison, we look at only those crops for which data were fully available for the management model, which had the most limited data set. We will not be exhaustive in our comparison here, but will note important differences between the models. Note that when soil temperature or air temperature are mentioned in relation to the point-predictive and management models, it is their transformation that is being discussed.

With Williams' model (see again Figures 13a and b), the one explanatory variable, soil temperature, derived from air temperature data, was inconsistent at explaining almonds, corn, cotton, grapes, sugar beets, and tomatoes, accounting for less than 7% of the variation in NO_x flux at several sites, while accounting for as much as 80% at other sites within the same crop. For almonds, the point-predictive model shows that WFPS, NO_3^- , the interaction between soil temperature and NH_4^+ , the interaction between WFPS and NH_4^+ are all even more important than soil temperature, which itself is significant at $P < 0.0005$, thus explaining both site differences and the influence of WFPS. In the management model, pH is also an important explanatory variable. For corn, the point-predictive model shows soil temperature to be the most important driving variable but also organic matter, WFPS, and several interactions with WFPS. The management model additionally shows some indicator of remaining fertilizer by type may be important. NO_x flux from tomato crops, for which the Williams model explains less than 7% of the NO_x variation on a chamber basis and less than 3% on a site basis, are consistently shown by both the point-predictive model and the management model to be very strongly explained by WFPS ($P < 0.0001$, 21% variation explained by WFPS alone in the point-predictive model, and 61% by WFPS in the management model).

NO_x flux from orange crops is consistently poorly explained by all three models, although in the point model temperature is

significant (10% of NO_x variation). In Williams' and the point-predictive model, soil temperature is quite evidently important, accounting for 80% of the NO_x variation on a site basis at one site (but only 2% at another in the Williams model). The point-predictive model confirms that WFPS is highly significant, and shows that soil chemistry (soil N parameters) and hence probably fertilizer type, amount, and timing explains site differences.

These statistical models using both direct driving variables and indirect explanatory variables were able to confirm the nature of influence of some soil and environmental conditions on NO_x emissions from soil. Sandy soils consistently promote NO_x emissions more than finer-textured soils. In the point-predictive model, increasing soil temperature effects can be very dependent on crop types and is not necessarily exponentially related to NO_x flux; water-filled pore space is just as important as soil temperature, with a peaking influence at around 45 percent WFPS; the interactions WFPS*soil temperature, WFPS* NH_4^+ , WFPS* NO_3^- , are all frequently important drivers of NO_x emissions, with the first varying in its effect depending on the relative importance of WFPS or soil temperature, and with the latter two being promoters of NO_x emissions. Water-filled pore space alone and its interaction with soil temperature are negatively correlated with each other in their promotion of NO_x flux.

In the management model, air temperature generally works well as an indicator of soil temperature. Water-filled pore space is not significant as often as it is in the point-predictive model, possibly because the spatial heterogeneity within sites has been removed due to using site mean values of the data. Fertilizer amount divided by days since fertilization may be too rough an indicator of fertilizer remaining, i.e. of soil N; however, there is a clear distinction between NH_4^+ -based and mixed fertilizers, the latter surprisingly promoting NO_x flux more than the former.

On a crop basis, it appears from the point-predictive model that alfalfa has less of a tendency to reduce NO_x emissions than other crop types, otherwise the crop effects cannot be distinguished. An interesting finding, however, of both this and the management model is that the crop types do interact differently with soil temperature in influencing NO_x flux: emissions from alfalfa fields apparently decline with increasing temperature, and emissions from corn, cotton, and sugar beets increase with higher temperature. The alfalfa results, however, may have been confounded by a mowing event that occurred between sampling dates (Site A = pre-mowing; Site P = pre-mowing; Site O = post-mowing; Figure 8). When post-mowing

measurements were removed from the analysis, the temperature- NO_x relationship was not significant.

In general, the high variability of NO_x emissions measured on a chamber-level basis limited the ability of point-predictive model to account for more than 40% of the total variation in NO_x fluxes for the whole data set. It would be interesting in future work to apply the point-predictive model to eddy correlation estimates of fluxes at the site level which average over the point level variability.

The management model performed fairly well as a more widely usable version of the point-predictive model on a site basis, given adequate variation in the data; how it falls short of the point-predictive model in explanatory power with respect to the influence of water-filled pore space should be examined further, for example in the legitimacy of using the site mean WFPS. Also, more modeling should be done to make use of information on fertilization and to explain why field with mixed fertilizers should emit more NO_x than those with NH_4^+ -based fertilizers. The mechanisms behind some of the significant interactions must be further analyzed; for example, fine modeling can be done for NO_x fluxes less than or equal to zero and for very low water-filled pore space less than 2%. Further efforts should also be made to derive more mechanistic relations between variables than are currently in this general additive model.

2.3.2.2.5 Comparison of Davidson Model (CASA) and San Joaquin Valley NO_x data.

Figure 9 shows the relationship between NO_x flux and soil WFPS assumed by the CASA model (derived from Davidson, 1991) as an overlay of the actual NO_x fluxes and associated WFPS values from our data base. A simple bar graph of mean maximum NO_x fluxes plotted against WFPS shows a pattern roughly similar to that of the Davidson model (used by CASA). Our NO_x fluxes do show a maximum at about 50% WFPS, decreasing generally with lower WFPS. The summer '95 fluxes show a small spike at very low water content (WFPS = 1-3%). The occurrence of significant NO_x fluxes from very hot and dry central valley soils has been previously reported and discussed (Davidson, et al., 1993a).

2.3.3. Discussion.

Mean fluxes of NO_x , measured during midday when fluxes are highest, ranged from less than 1 to greater than 9 $\text{ng-N cm}^{-2} \text{ h}^{-1}$ across all the crops measured, with peach and orange crops having the lowest fluxes and tomatoes, almonds, and irrigated pastures

having the highest (Figure 7). Values for individual chambers across all sites ranged from -0.9 to 194 ng-N cm⁻² h⁻¹. In comparison with NO_x measurements taken in other crops, the average fluxes measured in the San Joaquin Valley crops fall within the range of values reported for not-recently-fertilized agricultural fields in the temperate zone (from 0.4 to 5 ng-N cm⁻² h⁻¹; conversion of data in Williams et al., 1992b). In contrast, recently fertilized crops generally have much higher fluxes ranging from 4 to 34 ng-N cm⁻² h⁻¹ (Williams et al. 1992b). Matson et al. (1996) measured mean NO_x fluxes of over 100 ng-N cm⁻² h⁻¹ in surface fertilized sugar cane systems in Hawaii, and of over 300 ng-N cm⁻² h⁻¹ in fertilized and irrigated wheat systems in Sonora, Mexico (Matson, pers. comm).

Non-parametric statistics indicated significant differences among crops, but variability among sites within crop types (Figure 8) and even among different days for a single site was extreme. This variability could in many cases be related to soil inorganic nitrogen and water filled pore space (WFPS). This point is reinforced by regression analysis. Analyses using chamber NO_x measurements and soil and site data also indicated the importance of WFPS, NH₄⁺, and the interaction of soil temperature and WFPS.

In our spatial extrapolation, we used a crop data layer in a GIS to extrapolate average mid-day fluxes per crop type. While this presentation indicates potentially important spatial patterns in NO_x fluxes, it is of limited use given the high variance of fluxes within crop types. Nevertheless, this approach indicates that across the seven counties of the San Joaquin Valley which we sampled, a total of 707 kg of NO_x is emitted per hour by the crop types we measured during July and August. These fluxes are spatially heterogeneous, with Fresno county having the highest total flux, and Madera county having the lowest (Calculated from data in Table 11b). Likewise, within counties, NO_x appears to be spatially heterogeneous.

We present no calculations on the proportion of applied fertilizer lost as NO_x. Our temporal sampling window (July-August) was short and because of the sampling period chosen, we had very few sampling dates closely associated with fertilizer application (the period during which NO_x fertilizer loss is likely highest). We conclude that use of our data set for this type of extrapolation would be misleading.

Our analysis indicates that simple algorithms such as produced by Williams et al (1992b) are not appropriate for use in the San Joaquin Valley. Instead of the Williams model, we suggest a management model that utilizes information on water-filled pore space, soil texture, crop type, time since fertilization, and interactions between WFPS X temperature and

crop X temperature. WFPS is clearly a critical factor in this model; we suggest that functions such as the one used in the CASA model can be developed to serve as proxy for measured WFPS.

2.4 Task IV. Integrated Field Measurement Program.

Field experiments designed to evaluate both emissions of NO_x from soil and the fate of NO_x as it moves through plant canopies and enters into boundary layer chemistry are necessary for regional air quality studies. These experiments will require collaborative efforts by atmospheric chemists and modelers as well as ecosystem and microbial ecologists (Matson and Harriss, 1995). These efforts can build on the basic understanding of the spatial and temporal patterns of NO_x emission from soil that have been developed in this study.

These comprehensive studies should include measurement of NO_x fluxes at the soil surface, turbulent transfers at the top of the canopy, concentrations of NO , NO_2 , O_3 , PAN, and hydrocarbons inside and above the canopy, and micrometeorological data to calculate rates of vertical exchange.

Based on our field measurements and spatial extrapolation, it seems reasonable to direct such expensive field set ups to regions with relatively homogeneous distributions of high-flux crops such as irrigated pasture in Merced County or almonds in Merced or Kern counties.

On the other hand, our analysis indicates low fluxes from most crops during these months. If fertilizer use remains limited during these months, it is possible that soil NO_x fluxes may be relatively insignificant in terms of atmospheric chemistry and air pollution events. As a preliminary step to any major multi-disciplinary field study we believe that air quality modeling exercises should use the highest and lowest site means per crop type as well as the overall crop means (Table 8) of hourly mid-day NO_x fluxes in order to evaluate the potential importance of NO_x flux at varying soil conditions. It is worthwhile to note, however, that any changes in management practices that lead to increased application of fertilizer during or immediately preceding this July-August time from may lead to very significant increases in NO_x flux from soils. Thus, the importance of San Joaquin Valley agricultural soils as contributors to air quality in California cannot be assumed to be constant year to year, but rather will change as a function of the fertilizer and irrigation use and timing that are employed in the Valley.

3. Summary and Conclusions

The objective of this study was to estimate emissions of nitric oxide and nitrogen dioxide (together referred to as NO_x) from agricultural systems in the San Joaquin Valley of California during the months of July and August (periods of maximum tropospheric ozone development). We measured NO_x fluxes in agricultural systems representing the most important crop types, and utilizing the dominant fertilizer and irrigation management practices. We used hourly and daily flux data along with a spatial data base of crop types to extrapolate fluxes to the area of the Valley. We also identified the factors that control the rate and timing of NO_x fluxes, and we suggest ways that this information can be used in the development of spatially explicit models.

The project was organized around four sequential tasks. In the following paragraphs, we will summarize the approach and results of each.

Task I. Determine the most important crop/management practices in the San Joaquin Valley (in terms of area extent of crop type and amounts of fertilizer used) and use this information to develop a systematic sampling plan.

Utilizing information from the "1993 Agricultural Commissioners' Report Data" and the "1990 Engineering Science Design Research Planning Final Report to the Environmental Protection Agency (EPA): Leaf Biomass Density and Land Use Data for Estimating Vegetative Emissions", we tabulated crop acreage for the eight San Joaquin Valley counties. We identified nine dominant types, including alfalfa, citrus, corn, cotton, grapes, irrigated pasture, stonefruits, sugar beets, vegetables, and other. We identified 28 agricultural systems representing the most important crop types and the dominant fertilizer and irrigation management practices. Diel measurements (measurements carried out over a 24 hour period) were carried out at least once on 4 agricultural systems; 13 of the 28 were sampled repeatedly over several week periods in order to estimate means and variation in fluxes within sites over time.

Task II. Carry out field studies of soil NO_x fluxes measured simultaneously with measurements of environmental and edaphic (soil) characteristics of importance in regulating NO_x emission, and

carry out laboratory analyses of soil samples collected simultaneously with NO_x flux.

We measured soil surface NO_x fluxes, water-filled pore space (WFPS), soil temperature, air temperature, ammonium and nitrate in the soil, total soil nitrogen and carbon, pH, and soil texture for all of the sites. Soil characteristics were measured for the top 10 cm of soil. In a subset of the sites, we carried out measurements of net and gross nitrogen mineralization and nitrification and nitrification potentials. In general, there was substantial variability in mean midday NO_x fluxes among crops (range 1.0-9.1 ng-N cm⁻² h⁻¹), with irrigated pastures, almonds, and tomatoes having generally high fluxes relative to the other crops (crop mean mid-day fluxes of 9.1, 6.4, and 7.2 ng-N cm⁻² h⁻¹ for pastures, almonds, and tomatoes respectively; range for other crops: 1.0 - 5.8 ng-N cm⁻² h⁻¹). In the case of almonds and irrigated pasture, mean fluxes were consistently high from site to site and date to date. However, for some of the other crops, variation among different fields or sampling dates were very large (e.g., 0.13-17.53 ng-N cm⁻² h⁻¹ for cotton, 0.16-15.69 ng-N cm⁻² h⁻¹ for corn) and appeared to be related to proximity in time of our measurements to a fertilizer event and to water-filled pore space at the time of sampling. Within a given site, mean fluxes for different days varied by over an order of magnitude, apparently as a consequence of changes in soil inorganic N and in water filled pore space. This temporal variation at the scale of individual fields suggests that estimation of fluxes on a daily or hourly basis, as is needed for air quality and chemical transport models, will be difficult without information on the temporal and spatial distribution of fertilizer and irrigation as well as the more easily obtained information on air temperature.

Task III. Develop soils emissions statistical models based on the field and laboratory study data, and develop spatially and temporally explicit estimates of NO_x flux at the soil-air interface for the San Joaquin Valley for the months of July, August and early September, 1995.

We developed two sets of regression models relating NO_x flux to other variables measured in the field.

a) Models that require more detailed soil variables and that will be useful in process modeling frameworks ("Point-predictive model").

e.g. $\text{NO}_x = f(\text{crop type, \%WFPS, soil texture, soil temperature, soil } \text{NO}_3^-, \text{NO}_2^- \text{ and } \text{NH}_4^+ \text{ concentrations, total organic carbon concentration, total organic nitrogen concentration, position within the field -- under canopy/open and furrow/ridge}).$

b) Models that can be applied at a regional scale using spatial data bases of crop type, soils and climate ("Management model"). e.g. $\text{NO}_x = f(\text{crop type, air temperature, soil texture, soil pH, an index of fert amount, type and timing, and mean WFPS}).$

We compared the outputs of our models to those of the Williams model, which uses air temperature as well as an empirically-derived "A value" to drive predictions of NO_x flux. The Point-predictive model and the Management model both substantially improved the prediction of NO_x fluxes across a variety of crops and sites, in contrast to the Williams model. In fact, for most crops, WFPS was as important as temperature in the prediction of NO_x emissions.

We also compared our NO_x flux data to the Davidson model of NO_x flux as a function of soil WFPS (the functional relationship used in the CASA model). There was reasonably good agreement between the summer '95 San Joaquin Valley NO_x flux vs. soil WFPS and that predicted by Davidson. Both show maximum NO_x fluxes occurring at about 50% WFPS; however the San Joaquin Valley data show significant NO_x fluxes occurring at very low water contents (WFPS 1-3 %), a result not predicted by previous models but which has been reported in other measurement studies.

GIS-based data on major crop types in the San Joaquin Valley were used in combination with measured mid-day mean fluxes and calculated daily fluxes for each crop type, in order to calculate hourly and daily NO_x flux by crop type, county, and for the entire San Joaquin Valley area that the GIS data covered. Cotton, which had an intermediate mean mid-day flux in relation to other crops, had the highest Valley-scale flux (232120.9 g/h) due to its large total acreage. Grapes were calculated to have the next largest mid-day hourly flux when summed over the Valley (142936.1 g/h). Among San Joaquin Valley counties, Fresno county had the highest flux summed over the crop types we measured (188422 g-N h⁻¹), while Madera county had the lowest (60265 g-N h⁻¹). The estimated spatial distribution of NO_x flux (which may be an important factor in air chemistry) is presented in map and tabular format.

Task IV. Once the systems with greatest soil fluxes have been identified, begin planning for integrated field studies (to take place

in 1996 or later) in several sites to determine the role of vegetation canopies and boundary layer chemistry and dynamics in controlling the contributions and role of soil NO_x emissions in ozone formation.

Planning for integrated field studies should begin with estimation of the potential role of soil NO_x fluxes via air chemistry modeling. Given the range in variability in fluxes measured in our sites during the July-August period, we suggest that air quality modeling experiments be carried out utilizing the highest and lowest site means measured for the different crops, in addition to the average flux by crop. If such modeling experiments reveal circumstances under which agricultural soils play a critical role in air chemistry, multi-disciplinary studies that couple soil and canopy-scale flux measurements with atmospheric chemistry studies may be appropriate. For such studies, we suggest emphasizing regions with relatively homogeneous expanses of crops with high flux characteristics, such as irrigated pasture or almonds, and as appropriate, with concurrent use of fertilizer.

Overall Conclusions

The San Joaquin Valley is an highly complex agricultural system, composed of at least nine dominant crop types (alfalfa, citrus, corn, cotton, grapes, irrigated pasture, stonefruits, sugar beets, vegetables) as well as other crops, grown on a range of soils and managed under a number of different fertilizer and irrigation management practices. Because NO_x fluxes are potentially influenced by the types of plants growing in the fields as well as by the soils being cropped and by the ways those crops are managed, NO_x fluxes should be expected to show a large degree of spatial and temporal variation within the Valley. The data presented in this document substantiate this expected large range of variation.

The implications of this variability are several. First, it suggests that carrying out a field sampling program that encompasses that variability is a very difficult task. Fluxes change from field to field, crop to crop, and day to day. Therefore, while our flux estimates for given sites and days are accurate, their extrapolation to all sites within a given crop and to all dates within the July-August time-frame must be viewed as rough approximations rather than reality. On the other hand, our data do indicate some consistencies. For example, they indicate that almonds and irrigated pasture have typically higher fluxes than other crops we measured, whereas the other crops have greater ranges in fluxes

from time to time or site to site. Also, our data quite clearly suggest that NO_x fluxes in the San Joaquin Valley in July and August 1995 were not remarkably high in comparison with the range of values published in the literature. (We note, however, that we cannot draw conclusions about the relative importance of agricultural soil NO_x emissions in atmospheric chemistry in the San Joaquin Valley by simply looking at these flux values, and we leave it to air quality modelers within the California Air Resources Board to develop that analysis.)

The large potential for spatial and temporal variability in the Valley agricultural system also suggests that, given the difficulties inherent in NO_x measurements and the cost of the instruments used to measure NO_x flux at the soil-air or canopy-air interface, detailed spatial monitoring of those fluxes (even for a short period) is logistically impossible. We believe a viable alternative for estimation of NO_x in complex systems like the San Joaquin Valley is the development and use of predictive models that can utilize spatially and temporally-varying data on crops, soils, climate/weather, and management. We have developed such models as part of this project. One critical conclusion drawn from the model development task is that accurate prediction for most crop types in the Valley require more than just temperature, the variable used in the only other commonly used NO_x model (Williams et al 1992). Rather, our point-based "Point-predictive model" and the site-based "Management model" both indicate that soil moisture (described here as %WFPS) is at least as important as temperature, and that variables describing either soil inorganic nitrogen concentrations or fertilization activity are also important. Given our process-based understanding of the interactive controls of nitrogen, water, and temperature on NO_x production and emission, we find these results entirely consistent.

While our models are ready for use at the site level, their application at the scale of the Valley will require several additional steps. First, while spatially-explicit data bases on crop type, soil characteristics like texture, organic C, organic N and pH, and meteorological station data such as air temperature and precipitation are generally available, spatially-explicit data bases on fertilizer type, rate, and time of application, and on irrigation use and thus change in water-filled pore space in the soil, are not available. What may be more available are county-wide monthly data on fertilizer use and on allocation of water for irrigation. Short of doing detailed farm-by-farm surveys of fertilizer and water use, we believe it may be possible to develop models of irrigation and fertilizer applications that distribute county totals as a function of crop type and weather

conditions. Once such models have been developed and the NO_x models run at the scale of the Valley, validation through measurements of soil-air and canopy-air exchange of NO_x at select sites would be required. These tasks are outside the scope of this project.

Finally, it is worthwhile to note that our analysis of San Joaquin soils fluxes reflects the current management framework for the Valley, that is, there is relatively little application of fertilizer to crops during the July-August period. Any changes in management practices that lead to increased application of fertilizer during or immediately preceding this July-August time frame may lead to very significant increases in NO_x flux from soils. Thus, the importance of San Joaquin Valley agricultural soils as contributors to air quality in California cannot be assumed to be constant year to year, but rather will change as a function of the crop type, fertilizer and irrigation employed in the valley.

References

- California Department of Food and Agriculture. 1994. Fertilizing Materials Tonnage Report.
- Bakwin, P.S., S.C. Wofsy, S. Fan, M. Keller, S. Trumbore, and J.M. daCosta. 1990. Emissions of nitric oxide (NO) from tropical forest soils and exchange of NO between the forest canopy and atmospheric boundary layers. *J. Geophys. Res.* 95(D10):16755-16764.
- Brady, Nyle C. (1974). *The Nature and Properties of Soils*, 8th Edition, New York: Macmillan Publishing Co., Inc.
- Chambers, J.M. and Hastie, T.J. (1992). *Statistical Models in S*. New York: Chapman and Hall. (Formerly Monterey: Wadsworth and Brooks/Cole).
- Cleveland, W.S., Grosse, E. and Shyu, W.M. 1992. Local regression models, In: Chambers, J.M. and Hastie, T.J. 1992. *Statistical Models in S*. New York: Chapman and Hall. (Formerly Monterey: Wadsworth and Brooks/Cole).
- Davidson, Eric A. 1991. Fluxes of Nitrous Oxide and Nitric Oxide from Terrestrial Ecosystems. In *Microbial Production and Consumption of Greenhouse Gases: Methane, Nitrogen Oxides, and Halomethanes*, ed. John E. Rogers and William B. Whitman, American Society of Microbiology, Washington, D.C.
- Davidson, E.A., D.J. Herman, A. Schuster, and M.K. Firestone. 1993a. Cattle grazing and oak trees as factors affecting soil emissions of nitric oxide from an annual grassland. In *Agricultural Ecosystem Effects on Trace Gases and Global Climate Change*. ASA Special Pub no. 55. Madison WI.
- Davidson, E.A. 1992. Sources of nitric oxide and nitrous oxide following wetting of dry soil. *Soil Science Society of America Journal* 56(1):95-101.
- Davidson, E.A., P.A. Matson, P.M. Vitousek, P.A. Matson, R. Riley, G. Garcia-Mendez, and J.M. Maass. 1993b. Process regulation of soil emissions of NO and N₂O in a seasonally dry tropical forest. *Ecology* 74(1):130-139.
- Davidson, E.A., P.A. Matson, P.M. Vitousek, R. Riley, K. Dunkin, G. Garcia-Mendez, and J.M. Maass. 1991. Soil emissions of nitric oxide in a seasonally dry tropical forest of Mexico. *Journal of Geophysical Research* 96:15439-15445.

- Davidson, E.A., and D.S. Schimel. 1995. Microbial processes of production and consumption of nitric oxide, nitrous oxide, and methane. IN: Matson, P.A. and R.C. Harriss (eds). Biogenic Trace Gases: Exchange between Soils, Sediments, Aquatic Systems and the Atmosphere. Blackwell Scientific Publishing, Cambridge.
- Day, P.R. 1965. Particle fractionation and particle size analysis. In: Methods of soil analysis, physical, mineralogical properties, including statistics of measurement and sampling. American Society of Agronomy, Madison.
- Eichner, M.J. 1990. Nitrous oxide emissions from fertilized soils: summary of available data. J. Environ. Quality 19:272-280.
- Firestone, M.K. and E.A. Davidson. 1989. Microbial basis of NO and N₂O production and consumption in soil. In: M.O. Andreae and D.Schimel. Exchange of Trace Gases between Terrestrial Ecosystems and the Atmosphere. John Wiley and Sons, Chichester.
- Hall, S.J., P.A. Matson, and P. Roth. NO_x emission from soil: Implications for Air Quality Modeling in Agricultural Regions. Annual Review of Energy and Environment, in press.
- Hart, S.C., J.M. Stark, E.A. Davidson, and M.K. Firestone. 1994. Nitrogen mineralization, immobilization and nitrification. In: Methods of Soil Analysis, Part 2. Microbiological and Biochemical Properties. Soil Science Society of America, Madison.
- Hutchinson, G.L. and E.A. Brams. 1992. NO vs. N₂O emissions from an NH₄-amended Bermuda grass pasture. Journal of Geophysical Research 97:9889-9896.
- Hutchinson, G.L. and E.A. Davidson. 1993. Processes for production and consumption of gaseous nitrogen oxides in soil. In: Agricultural Ecosystem Effects on Trace Gases and Global Climate Change.
- Hutchinson, G.L. and G.P. Livingston. 1993. Use of chamber systems to measure trace gas fluxes. In: Harper, L.A., A.R. Mosier, J.M. Duxbury, and D.E. Rolston (eds), Agricultural ecosystem effects on trace gases and global climate change. American Society of Agronomy Special Publication No. 55, Madison, WI.

- Jacob, D.J. and S.C. Wofsy. 1990. Budgets of reactive nitrogen, hydrocarbons, and ozone over the Amazon forest during the wet season. *Journal of Geophysical Research*. 95:16737-16754.
- Johansson, C. and L. Granat. 1984. Emission of nitric oxide from arable land. *Tellus* 36:25-37.
- Keller, M. and P.A. Matson. 1994. Biosphere-atmosphere exchange of trace gases in the tropics: Evaluating the effects of land use change. In R. Prinn (ed) Global Atmospheric-Biospheric Chemistry, Plenum Press, NY.
- Matson, P.A., C. Volkman, K. Copping and W.A. Reiners. 1991. Annual nitrous oxide flux and soil nitrogen characteristics in sagebrush steppe ecosystems. *Biogeochemistry* 14: 1-12.
- Matson, P.A., S.T. Gower, C. Volkman, C. Billow and C.C. Grier. 1992. Soil nitrogen cycling and nitrous oxide flux in Rocky Mountain Douglas-fir forest: effects of fertilization, irrigation and carbon addition. *Biogeochemistry* 18: 11-117.
- Matson, P.A., C. Billow, S. Hall and J. Zachariesson. 1996. Nitrogen trace gas responses to fertilization in sugar cane ecosystems. *Journal of Geophysical Research* 101: 18,533-18,545.
- Matson, P.A. and R.C. Harriss. 1995. Biogenic Trace Gases: Exchange between Soils, Sediments, Aquatic Systems and the Atmosphere. Blackwell Scientific Publishing, Cambridge.
- Melillo, J.M., P.A. Steudler, J.D. Aber, and R.D. Bowden. 1989. Atmospheric deposition and nutrient cycling. In M.O. Andreae and D. Schimel. *Exchange of Trace Gases between Terrestrial Ecosystems and the Atmosphere*. J. Wiley and Sons, Chichester.
- Motavalli, A. R., D.W. Valentine, W. J. Parton, D. S. Ojima, D.S. Schimel, and J.A. Delgado. 1996. "CH₄ and N₂O fluxes in the Colorado shortgrass steppe: 1. Impact of landscape and nitrogen addition," *Global Biogeochemical Cycles*, Vol. 10, No. 3.
- Parton, W.J., A. R. Mosier, D. S. Ojima, D. W. Valentine, D. S. Schimel, K. Weier, and A. E. Kulmala. (1996). "Generalized model for N₂ and N₂O production from nitrification and denitrification," *Global Biogeochemical Cycles*, Vol. 10, No. 3, 401-412.

- Remde, A., F. Slemr and R. Conrad. 1989. Microbial production and uptake of nitric oxide in soil. *FEMS Microbial Ecology* 62:221-230.
- Shepard, M.F., S. Barzetti and D.R. Hastie. 1991. The production of atmospheric NO and N₂O from a fertilized agricultural soil. *Atmo. Environ.* 25:1961-1969.
- Statistical Sciences. 1993. *S-Plus Guide to Mathematical and Statistical Analysis, Version 3.2.* Seattle: StatSci, a division of MathSoft, Inc., 1993.
- Tortoso, A.C. and G.L. Hutchinson. 1990. Contributions of autotrophic and heterotrophic nitrifiers to soil NO and N₂O emissions. *Appl. Environ. Microbiol.* 56:1799-1805.
- Turner, R.E. and N.N. Rabalais. 1991. Changes in Mississippi River water quality this century. *BioScience* 41(3):140-147.
- Vitousek, P.M. and P.A. Matson. 1993. Agriculture, the global nitrogen cycle, and trace gas flux. In: R.S. Oremland (Ed.) *The Biogeochemistry of Global Change: Radiatively Active Trace Gases.* Chapman and Hall, NY.
- Williams, E.J. and E. A. Davidson. 1993. An intercomparison of two chamber methods for the determination of emission of nitric oxide from soil. *Atmospheric Environment* 27A:2107-2113
- Williams, E.J., G.L. Hutchinson and F.C. Fehsenfeld. 1992a. NO_x and N₂O emissions from soil. *Global Biogeochemical Cycles* 6(4): 351-388.
- Williams, E.J., A. Guenther, and F.C. Fehsenfeld. 1992b. "An inventory of nitric oxide emissions from soils in the United States," *Journal of Geophysical Research*, Vol. 97, 7511-7519.
- Williams, E.J., D.D. Parrish, M.P. Buhr and F.C. Fehsenfeld. 1988. Measurement of soil NO_x emissions in central Pennsylvania. *Journal of Geophysical Research* 93:9539-9546.

List of Appendices

Appendix A. San Joaquin Valley data descriptions: point and site level parameters. (See Diskette 1 for master data file: SJVdata.txt)

Appendix B. Farm Advisors and scientists/specialists interviewed and interview information on agricultural practices.

Appendix C. Data on crop distribution for San Joaquin Valley from 1993 County Agricultural Commissioners report.

Appendix D. Schematic of field NO_x measurement apparatus.

Appendix E. Method for calculating diel characteristic curves.

Appendix F. Point predictive model refitted to individual crops.

Appendix G. Management model refitted to individual crops.

Appendix H. Estimating Fluxes from the diel characteristic curves and example page of diel characteristic curves: xy values. (See Diskette 2 for data file: Diel.txt)

Appendix I. Deliverables from original proposal.

Diskettes:

1. San Joaquin Valley data master. File: SJVdata.txt.
2. Diel Characteristic Curves; xy values. File:Diel.txt.

Appendix A. San Joaquin Valley data descriptions: point and site level parameters. (See Diskette 1, Master data file: SJVdata.txt)

S/C*	DATA ITEM	UNITS or VALUES	DESCRIPTION
	Study Location	name	San Joaquin Valley
	Crop	name	plant: Alfalfa, Almonds, Corn, Cotton, Grapes, Irrigated pasture, Oranges, Peaches, Sugar beets, Tomatoes
	Location	name	Firebaugh, Partier, San Joaquin, Tranquillity, Riverdale, Mendota, Tulare, Plainview, Waukena, Sanger, Kearney, Corcoran, Lindcove, Clovis, Bonadelle Ranchos, West Side
	Irrigation	name	method: Drip, Flood, Border Check, Furrow
S	Site code	letter	site distinguished by crop, soil texture, irrigation: A,B,C,...,Z
S	Type	name	measurement freq: Routine (1/day at midday), Diel
S	County	name	Fresno, Kings, Madera, Tulare
	Date	[mm/dd/yy]	date of data observation
S	Fertilization date	[mm/dd/yy]	last date fertilized; information provided by growers
S	Days since fert.	[days]	days since last fertilization
S	amt. last Fert(#/ac)	[lbs/acre]	amount last fertilized; information provided by growers
S	Fert type	name	11-52-0, (NH4)2SO4, CAN-17, CAN17, NH3, NH4NO3, UN32, aqua NH3, urea
	Fert method	name	side dressed, surface application, bandcast, broadcast, water spray, injected, shanked in, side dressed, subsoil injection, subsoil shank, water run, NA's
	Annual fert(#/ac)	[lbs/acre]	information provided by growers
S	Protocol	category	extensive (<=3 visits), intensive (>=4 visits)
	Replicate	count	Replicate: 1,2,3,...,10; 10 per position within a site
C	Position	category	position in field: for tree crops [canopy, open], for row crops [ridge, furrow], for pasture & alfalfa [open]
C	Time of Day	[hh:mm].[h+min/60]	military time; time of day of data observation
C	NO Flux	[ng-N/cm^2/hr]	measured via NO flux chamber
C	Chamber Temperat	[degrees C]	air temperature inside NO flux chamber
S	Air Temperature	[degrees C]	Estimated from chamber temperatures as described in section 2.2.1.1
C	Soil Temperature	[degrees C]	measured at 2 cm depth
S	Soil Type	name	name + other description, e.g. San Joaquin Sandy Loam
S	%Sand/Silt/Clay	[%/%/%]	determined by hydrometer method
S	Total C	[%C]	gravimetric, measured once during the study period
S	Total N	[%N]	gravimetric, measured once during the study period
S	pH	[pH]	site average
S	% Canopy Cover	[%length]	% of cross section between edges of rows that is under canopy
	pos split	[%area]	relative contribution of different positions to total site area
S	Bulk density of repl.	[g/cm^3]	soil bulk density for particular replicate
S	Bulk density mean	[g/cm^3]	mean soil bulk density of 10 replicates
	Freshsoil (g)	[g]	sample weight (used in other calculations)
	Dry soil (g)	[g]	sample weight (used in other calculations)
C	%M/wet	[%wt]	field wetness at the time (10 cm deep) = 100 * (fresh wt - dry wt)/(fresh wt)
C	Grav.h2o	[%wt]	gravimetric moisture = 100 * (fresh wt - dry wt)/(dry wt)
C	WFPS	[%vol]	water-filled pore space = bulkd.m*h2o.grav/(1-bulkd.m/rho), rho=2.65 g/cm^3
C	NH4 ug/g	[ug/g]	Measured per chamber per day of observation
C	NO3 ug/g	[ug/g]	Measured per chamber per day of observation
C	NO2 ug/g	[ug/g]	Measured per chamber per day of observation
C	Nit Pot ug/g/d	[ug/g/day]	nitrification potential = NO3 + NO2 production rate
	Gross nit (ug/g/d)	[ug/g/day]	gross nitrification rate

*S/C: S-site code, C-chamber

Appendix B. Interview information on agricultural practices: San Joaquin county.

Corn	
Distribution:	
	70% west county
	30% central and east county
Fertilization Rate:	
	250 lb/ac
Fertilization Type:	
	UN-32
	33%
	irrigation water, spray, banded
	Aqua NH3
	33%
	shanked in
	Anhydrous NH3
	33%
	bubbled in
Fertilization Timing:	
	30 lb/acre at preplant
	the balance of fertilizer applied when crop is 1 ft high
	planting occurs from early to late spring
Irrigation:	
	furrow
	2 - 3 week cycle
Comments	
	Corn planted in June may be fertilized in July
	Management decision making is by grower, not by region
Sources:	
	Terry Prichard, San Joaquin farm advisor
	Roland Meyer, U.C. Davis

Appendix B. Interview information on agricultural practices: San Joaquin county.

Sugar Beets	
Distribution:	
	50% west county
	50% east county
Fertilization Rate:	120 - 180 lb/ac
Fertilization Types:	
	NPK
	25%
	broadcast
	Anhydrous NH3
	50%
	shanked in
	UN-32
	25%
	shanked in
Fertilization Timing:	
Preplant:	
	36 lb/ac of NPK
	30 d after planting:
	80 - 150 lb/ac of anhydrous NH3 or UN-32
Irrigation:	
	furrow
	14 day cycle
Comments:	
	West of I-5 sugar beets are planted in early spring and harvested in the fall
	East of I-5 sugar beets are planted in May and harvested the following spring
	Delta soils west of I-5 are organic and receive lower N application rates
	Mineral soils east of I-5 receive higher N application rates
	On west side, sugar beets are concentrated from Tracey northward
	On east side, sugar beets are abundant around the area of Mariposa Rd.
Source:	
	Michael Canevari, San Joaquin farm advisor

Appendix B. Interview information on agricultural practices: San Joaquin county.

Almonds	
Distribution:	50% in southern county along Stanislaus River, 50% west side
Fertilization Rate:	200 lb/ac
Fertilizer Types:	UN-32
	Urea
	NH4NO3
Fertilization Timing:	67% April
	33% August
Irrigation:	flood
	50%
	14 - 21 day cycle
	solid set sprinkler
	50%
	14 - 21 day cycle
Comments:	Management decision making is by grower, not region
Source:	Terry Prichard, San Joaquin farm advisor

Appendix B. Interview information on agricultural practices: Stanislaus county.

Irrigated Pasture	
Distribution:	mostly around Oakdale in a band below the hills some near dairies around Turlock and San Joaquin River
Fertilization Rate:	40 - 50% of growers apply 30 lb/ac/yr 50 - 60% of growers apply none
Irrigation:	border 10 day cycle
Comments:	Manure applications in pastures affiliated with dairies could be substantial Irrigated pastures are planted to a grass-clover combination
Source:	Bill van Riet, Stanislaus farm advisor
Vegetable Crops	
Distribution:	west of San Joaquin River
Fertilization Rate:	Tomato: 150 - 180 lb/ac Bean: 60 lb/ac Pepper: 300 - 600 lb/ac
Fertilization Type:	Aqua NH ₃ > 90% injected
Fertilization Timing:	20 - 30 lb/ac preplant the balance at 4 - 5 weeks
Irrigation:	furrow 8 - 10 day cycle
Comments:	Management decision making based on specific crop types
Source:	Jesus Valencia, Stanislaus farm advisor
Stonefruits	
Distribution:	Almonds: East and west of San Joaquin River Peaches: East of San Joaquin River Apricots: West of San Joaquin River Tree crops require well-drained soils
Fertilization Rate:	

Appendix B. Interview information on agricultural practices: Stanislaus county.

	150 - 200 lb/ac			
Fertilization Types:				
	NH ₄ NO ₃			
Fertilization Method:				
	Broadcast			
Irrigation:				
	Flood			
	14 - 21 day cycle			
Source:				
	Cathy Kelly, Stanislaus farm advisor			

Appendix B. Interview information on agricultural practices: Merced county.

Alfalfa			
	Distribution:		
		25% east, 25% central, 50% west county	
	Fertilization Rate:		
		20 - 30 lb/ac	
	Fertilization Types:		
		NH4SO4	
		50%	
		broadcast	
		UN-32	
		50%	
		broadcast	
	Fertilization Timing:		
		planting	
	Irrigation:		
		border check	
		10 day cycle	
Comments:			
		Management decision making is by grower, not by region	
Source:			
		Bill Weir, Merced farm advisor	
Cotton			
	Distribution:		
		predominantly west side	
	Fertilization Rate:		
		150 - 180 lb/ac	
	Fertilization Type:		
		UN-32	
		>90%	
		side-dressed	
	Fertilization Timing:		
		33% winter	
		67% May	
	Irrigation:		
		furrow	
		10 - 14 day cycle	
Source:			
		Bill Weir, Merced farm advisor	

Appendix B. Interview information on agricultural practices: Merced county.

Corn	
Distribution:	75% east, 25% central county
Fertilization Rate:	200 - 250 lb/ac
Fertilization Types:	Anhydrous NH3
	20%
	shanked in
	Aqua NH3
	50%
	shanked in
	UN-32
	30%
	water
Fertilization Timing:	30 lb/ac at preplant
	most of the rest side-dressed when knee-high
	some is applied late, bubbled into irrigation water
Irrigation:	furrow
	10 day cycle
Comments:	Management decision making is by grower, not by region
Source:	Bill Weir, Merced farm advisor

Appendix B. Interview information on agricultural practices: Madera county.

Cotton	Distribution:	Predominantly west
	Fertilization Rate:	200 - 280 lb/ac
	Fertilization Type:	UN-32
		side dressed
		aqua NH3
		side dressed
		urea
		side dressed
	Fertilization Timing:	33% winter
		67% May
	Irrigation:	> 90% furrow
		10 - 14 day cycle
Source:		Ron Vargas, Madera farm advisor
Grapes	Distribution:	South of Madera and west of 99
	Fertilization Rate:	40 - 60 lb/ac
	Fertilization Types:	UN-32
		NH4NO3
	Fertilization Timing:	Mostly late winter - early spring, right around fruit-set
	Irrigation:	flood
		3 week cycle
Comments		Most of the plantations are on Hanford soils.
		Within the last 20 years, the Madera and San Joaquin sandy loams, which have iron-silica hardpans, have been ripped before planting, and planted with grapes
Source:		George Levitt, Madera farm advisor

Appendix B. Interview information on agricultural practices: Madera county.

Stonefruits			
Distribution:			
Along west side of 99			
Foothills			
Fertilization Rate:			
150 - 250 lb/ac			
Fertilization Types:			
UN-32			
50%			
Shanked in flood-irrigated soils			
CAN-17			
50%			
water-run in low-volume irrigation			
Fertilization Timing:			
UN-32 in Spring			
CAN-17 may be applied weekly			
Irrigation:			
Flood:			
50%			
12 - 14 day cycle			
Low-volume:			
50%			
3 - 7 day cycle			
Comments:			
Older plantations are on the well-drained alluvial fan sandy loam soils, flood irrigated			
Newer plantations are on the Madera-San Joaquin & Tujunga-Graingeville associations			
and are on low-volume irrigation (they would water-log on flood irrigation)			
Madera-San Joaquin association is clayey, with Fe-Si hardpan ripped			
Tujunga-Graingeville association is sandy, with Fe-Si hardpan ripped			
Brent Holtz may be able to help us line up almond growers			
Source:			
Brent Holtz, Madera farm advisor			

Appendix B. Interview information on agricultural practices: Fresno county.

Sugar beets	
Distribution:	
Fertilizer Rates:	80 - 120 lb/ac
Fertilization Type:	>90% urea side dressed
Fertilization Timing:	no preplant most at post-emergence
Irrigation:	> 95% furrow 10 - 14 day cycle
Source:	Bill Fischer, Fresno farm advisor
Stonefruits	
Distribution:	Alluvial fan soils, well drained, pH 6 - 7
Fertilization Rate:	150 - 300 lb/ac
Fertilization Types:	NH ₄ NO ₃ > 90% broadcast on flood-irrigated soils CAN-17 < 10% water-run in low-volume irrigation
Irrigation	
Furrow:	> 90% 14 - 21 day cycle
Low-volume:	< 10% 3 day cycle
Comments:	There may be more low-volume irrigation around Bakersfield.
Source:	Scott Johnson, Kearney extension specialist

Appendix B. Interview information on agricultural practices: Fresno county.

Cotton	
Distribution:	from Kerman - Raisin City - Caruthers on east to the foothills on the west.
Fertilization Rate:	180 lb/ac
Fertilization Type:	UN-32
	50%
	side-dressed
	Aqua NH3
	30%
	water run
	Anhydrous NH3
	20%
	water run
Fertilization Timing:	Mostly prior to first irrigation Some anhydrous NH3 is water-run late season
Irrigation:	far west of I-5: sprinkler > 90% furrow 10 day cycle on lighter soils in the east 28 day cycle on heavy flood plain soils
Comments:	Heavy clay loam soils are abundant on fans along Coast Range About 30% of furrow irrigation is "border check", but is applied in furrows; whereas border check in Kings County is applied across flat land. "Border check" is more common in lighter soils of eastern county Fertilization rates are fairly constant throughout the county Dan Munk may be interested in collaboration on his West Side plots
Source:	Dan Munk, Fresno farm advisor
Grapes	
Distribution:	Mostly east and central some west
Fertilization Rates:	40 - 60 lb/ac
Fertilization Type:	> 75% UN-32
Fertilization Timing:	Spring
Irrigation:	> 75% flood, 2 - 3 week cycle

Appendix B. Interview information on agricultural practices: Fresno county.

	< 25% drip, 2 - 3 day cycle		
Source:			
	Michael Costello, Fresno farm advisor		

Appendix B. Interview information on agricultural practices: Tulare county.

Citrus	
Distribution:	mostly east county
Fertilization Rate:	110-140 lb/ac
Fertilization Types:	dry (NH ₄ NO ₃ , CaNO ₃ , urea):
	70%
	mostly applied from late Jan - mid Mar
	liquid (CAN-17, UN-32):
	30%
	mostly applied from mid Feb - Aug
Fertilization Methods:	
dry:	broadcast
liquid:	irrigation water
Fertilization Timing:	
through June 1:	60%
after June 1:	40%
Irrigation Method:	
low volume:	70%
	4 - 7 day cycle
furrow and flood:	30%
	7 - 10 day cycle
Comments:	
	About 5% of acreage receives about 25% of its N as foliar application
	Management decision making is by grower, not by region.
Source:	
	Neal O'Connell, Tulare farm advisor

Appendix B. Interview information on agricultural practices: Tulare county.

Cotton	Distribution	67% west of 99 sandy loams 33% east of 99 sandy loams
	Fertilization Rate:	120 - 180 lb/ac
	Fertilization Type:	UN-32 side-dressed Anhydrous NH3 side-dressed
	Fertilization Timing:	Early June
	Irrigation:	furrow 2 week cycle
Source:		Steve Wright, Tulare farm advisor
Corn	Distribution	67% west of 99 sandy loams 33% east of 99 sandy loams
	Fertilization Rate:	200 - 250 lb/ac
	Fertilization Type:	UN-32 side-dressed Anhydrous NH3 side-dressed
	Fertilization Timing:	End of March through mid-July
	Irrigation:	furrow 2 week cycle
Source:		Steve Wright, Tulare farm advisor

Appendix B. Interview information on agricultural practices: Kings county.

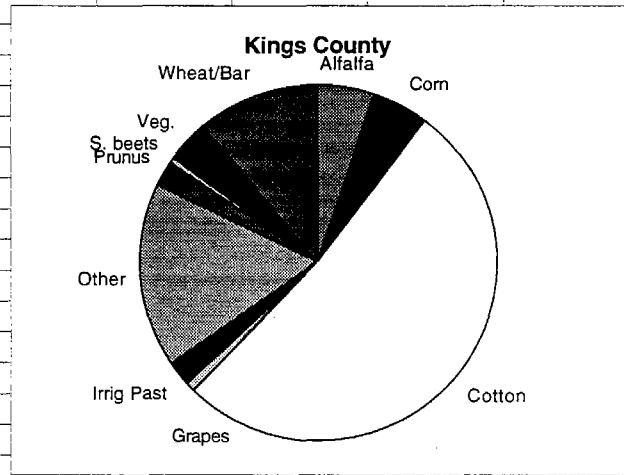
Cotton				
	Distribution:			
		throughout county		
	Fertilization Rate:			
		150 lb/ac		
	Fertilization Type:			
		Anhydrous NH3		
		75%		
		Shanked in		
		UN-32		
		25%		
		water		
	Fertilization Timing:			
		75% Anhydrous NH3 shanked in prior to first irrigation, late May - early June		
		25% UN-32 liquid water run, late June - early July		
	Irrigation:			
		50% furrow, 10 - 14 day cycle		
		50% border check, 3 - 4 week cycle		
Source:				
		Bruce Roberts, Kings farm advisor		
Alfalfa				
	Distribution:			
		seed: southern third		
		forage: northern two-thirds		
	Fertilization Rate:			
		none		
	Irrigation:			
		border check		
		4 week cycle on heavy soils		
		2 week cycle on light soils		
Source:				
		Bruce Roberts, Kings farm advisor		

Appendix B. Interview information on agricultural practices: Kern county.

Cotton:		
	Fertilization Rate:	
	200 lb/ac	
	Fertilization Types:	
	Anhydrous NH3	
		33%
		side dressed
	Urea	
		33%
		side dressed
	UN-32	
		33%
		side dressed
	Fertilization Timing:	
	25% Nov - Feb	
	75% May - June	
	Irrigation:	
	50% furrow	
	50% flood	
	25% sprinkler	
	10 - 14 day cycle	
Source:		
	Doug Munier, Kern farm advisor	
Almonds		
	Fertilization Rate:	
	200 - 300 lb/ac	
	Fertilization Types:	
	liquid	
		90%
		surface applied
	anhydrous	
		10%
		water run
	Fertilization Timing:	
	Feb: 100 - 150 lb/ac	
	May: 40 - 60 lb/ac	
	Jun - Jul: 20 - 40 lb/ac	
	Oct: 40 - 60 lb/ac	
Source:		
	Radian Survey	

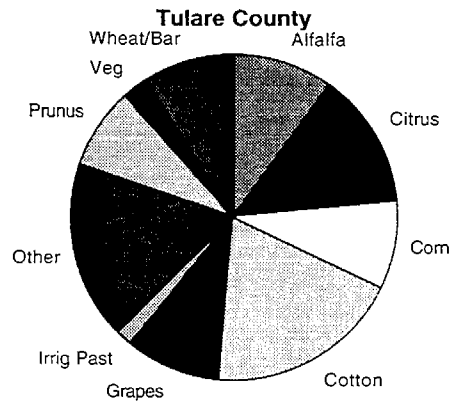
Appendix C. Data on crop distribution for San Joaquin Valley from 1993 County Agricultural Commissioners Report: Kings county.

			Alfalfa	27457
HAY, ALFALFA	27457	A	Corn	25598
SUGARBEETS	3221	B	Cotton	266315
COTTON LINT, UPLAND	233980	C	Grapes	3905
COTTON LINT, PIMA	27835	C	Irrig Past	11000
SEED, COTTON FOR PLANTING	4500	C	Other	88118
GRAPES, RAISIN	1475	G	Prunus	10111
GRAPES, TABLE	718	G	S. beets	3221
GRAPES, WINE	1712	G	Veg.	20894
CORN FOR SILAGE	25348	N	Wheat/Bar	56330
CORN, SWEET ALL	250	N		
PASTURE, IRRIGATED	11000	P		
PASTURE, RANGE	100000	P		
PASTURE, MISC. FORAGE	31777	P		
ALMONDS, ALL	1907	S		
ALMOND HULLS		S		
APRICOTS, ALL	251	S		
NECTARINES	2034	S		
PEACHES, CLINGSTONE	1289	S		
PEACHES, FREESTONE	2685	S		
PLUMS	1945	S		
BEANS, UNSPEC. DRY EDIBLE	2401	V		
BROCCOLI, FR MKT	1398	V		
BROCCOLI, PROC		V		
MELON, CANTALOUPE	925	V		
TOMATOES, FRESH MARKET	775	V		
TOMATOES, PROCESSING	11000	V		
VEGETABLES, UNSPECIFIED	4395	V		
SEED WHEAT	9309	W		
BARLEY, UNSPECIFIED	16423	W		
WHEAT ALL	30598	W		
COTTONSEED		Z		
HAY, GRAIN	1238	Z		
SAFFLOWER	46485	Z		
FIELD CROPS, UNSPEC.	20438	Z		
SEED, VEG & VINECROP	4327	Z		
SEED BARLEY	1514	Z		
SEED, VEG & VINECROP	137	Z		
NURSERY, FLOWERS SEEDS		Z		
APPLES, ALL	502	Z		
KIWIFRUIT	303	Z		
OLIVES	1114	Z		
PISTACHIOS	5596	Z		
POMEGRANATES	340	Z		
WALNUTS, ENGLISH	5797	Z		
FRUITS & NUTS, UNSPEC.	327	Z		



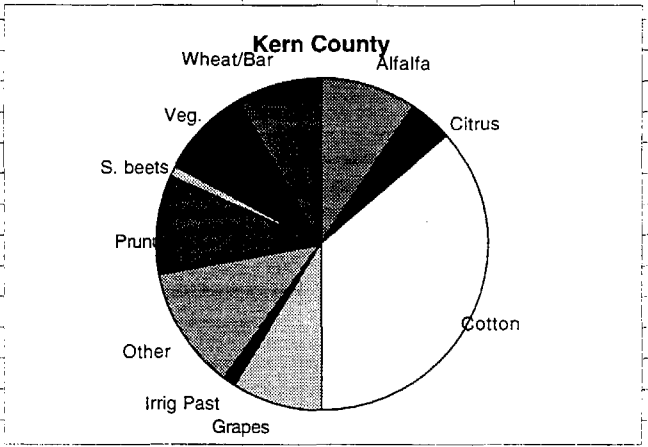
Appendix C. Data on crop distribution for San Joaquin Valley from 1993 County Agricultural Commissioners Report: Tulare county.

			Alfalfa	76900
HAY, ALFALFA	76900	A	Citrus	103357
SUGARBEETS	3220	B	Corn	70700
COTTON LINT, UNSPEC	144600	C	Cotton	148065
SEED, COTTON FOR PLANTING	3465	C	Grapes	73580
GRAPES, RAISIN	13178	G	Irrig Past	12400
GRAPES, TABLE	35151	G	Other	137405
GRAPES, WINE	25251	G	Prunus	63915
GRAPEFRUIT, ALL	639	I	Veg	19677
LEMONS, ALL	4067	I	Wheat/Bar	70261
ORANGES, NAVAL	67777	I		
ORANGES, VALENCIAS	29257	I		
TANGERINES & MANDARINS	1617	I		
CORN FOR GRAIN	14600	N		
CORN FOR SILAGE	56100	N		
PASTURE, IRRIGATED	12400	P		
PASTURE, RANGE	701000	P		
ALMONDS, ALL	10866	S		
APRICOTS, ALL	775	S		
NECTARINES	13767	S		
PEACHES, CLINGSTONE	1376	S		
PEACHES, FREESTONE	9841	S		
PLUMS	20782	S		
PRUNES, DRIED	6508	S		
BEANS, UNSPEC. DRY EDIBLE	7970	V		
BROCCOLI, UNSPECIFIED	2005	V		
CAULIFLOWER, UNSPECIFIED	1236	V		
CUCUMBERS	285	V		
TOMATOES, FRESH MARKET	172	V		
VEGETABLES, UNSPECIFIED	8009	V		
SEED WHEAT	4461	W		
BARLEY, UNSPECIFIED	24200	W		
WHEAT ALL	41600	W		
SILAGE	44300	z		
SORGHUM, GRAIN	1610	z		
FIELD CROPS, UNSPEC.	35900	z		
SEED, OTHER (NO FLOWERS)	1031	z		
APPLES, ALL	2129	z		
AVOCADOS, ALL	865	z		
CHERRIES, SWEET	244	z		
KIWIFRUIT	1802	z		
OLIVES	15238	z		
PEARS, UNSPECIFIED	632	z		
PECANS	770	z		
PERSIMMONS	893	z		
PISTACHIOS	5462	z		
POMEGRANATES	1129	z		
WALNUTS, ENGLISH	25087	z		
FRUITS & NUTS, UNSPEC.	313	z		



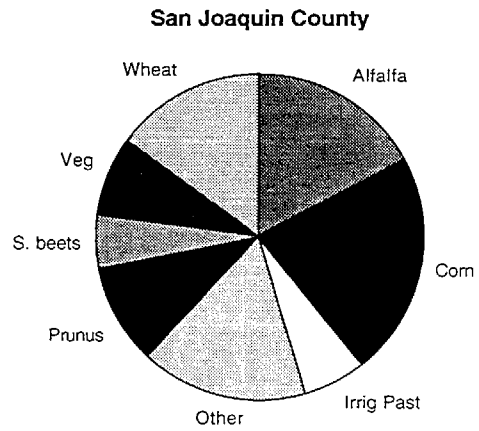
Appendix C. Data on crop distribution for San Joaquin Valley from 1993 County Agricultural Commissioners Report: Kern county.

HAY, ALFALFA	78568 A	Alfalfa	78568
SUGARBEETS	9779 B	Citrus	34835
COTTON LINT, UPLAND	248354 C	Cotton	300759
COTTON LINT, PIMA	29134 C	Grapes	73719
SEED, COTTON FOR PLANTING	23271 C	Irrig Past	10000
GRAPES, TABLE	29058 G	Other	99631
GRAPES, RAISIN	4493 G	Prunus	79453
GRAPES, WINE	40168 G	S. beets	9779
GRAPEFRUIT, ALL	851 I	Veg.	74093
LEMONS, ALL	3061 I	Wheat/Bar	68111
ORANGES, NAVEL	22881 I		
ORANGES, VALENCIAS	6985 I		
TANGELOS	1057 I		
CORN, SWEET ALL	605 N		
PASTURE, IRRIGATED	10000 P		
PASTURE, RANGE	2236475 P		
ALMONDS, ALL	71574 S		
ALMOND HULLS	S		
APRICOTS, ALL	669 S		
NECTARINES	1837 S		
PEACHES, UNSPECIFIED	2189 S		
PLUMS	3184 S		
BEANS, UNSPEC. DRY EDIBLE	6340 V		
MELON, CANTALOUPE	1775 V		
CARROTS, FR MKT	45290 V		
LETTUCE, HEAD	4340 V		
MELON, UNSPECIFIED	1044 V		
PEPPERS, BELL	1679 V		
TOMATOES, FRESH MARKET	1425 V		
TOMATOES, PROCESSING	3600 V		
MELON, WATER MELONS	3903 V		
VEGETABLES, UNSPECIFIED	4697 V		
BARLEY, UNSPECIFIED	22664 W		
WHEAT ALL	44447 W		
APPLES, ALL	4985 z		
KIWIFRUIT	626 z		
OLIVES	2017 z		
PISTACHIOS	19713 z		
WALNUTS, ENGLISH	1612 z		
FRUITS & NUTS, UNSPEC.	2403 z		
HAY, GRAIN	6000 z		
HAY, OTHER UNSPECIFIED	3500 z		
SAFFLOWER	13510 z		
SILAGE	11000 z		
ASPARAGUS, UNSPECIFIED	613 z		
GARLIC, ALL	3938 z		
ONIONS	8789 z		
POTATOES, IRISH ALL	20925 z		



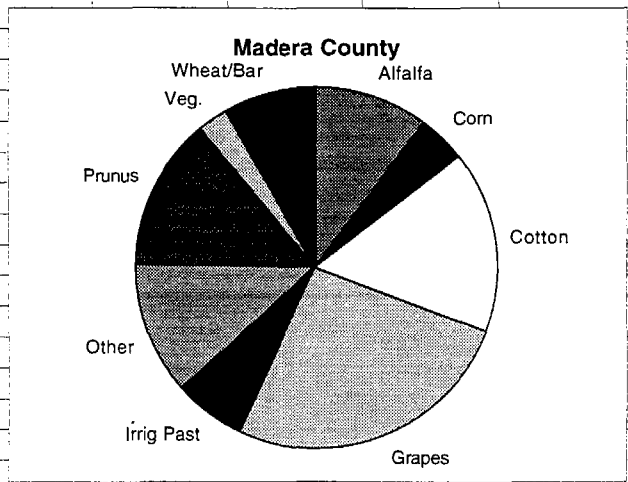
Appendix C. Data on crop distribution for San Joaquin Valley from 1993 County Agricultural Commissioners Report: San Joaquin county.

HAY, ALFALFA	64000 A	Alfalfa	64000
SUGARBEETS	20600 B	Corn	81600
GRAPES, TABLE	G	Irrig Past	23700
GRAPES, WINE	G	Other	62126
CORN FOR GRAIN	56200 N	Prunus	36100
CORN FOR SILAGE	25400 N	S. beets	20600
CORN, SWEET ALL	N	Veg	28624
OATS FOR GRAIN	1000 O	Wheat	56070
PASTURE, IRRIGATED	23700 P		
PASTURE, RANGE	144000 P		
ALMONDS, ALL	36100 S		
ALMOND HULLS	S		
APRICOTS, ALL	S		
PEACHES, CLINGSTONE	S		
PEACHES, FREESTONE	S		
BEANS, BLACKEYE (PEAS)	3380 V		
BEANS, RED KIDNEY	15600 V		
LIMA BEANS, UNSPECIFIED	4726 V		
BEANS, GARBANZO	800 V		
SEED BEANS	4118 V		
BROCCOLI, UNSPECIFIED	z		
CAULIFLOWER, UNSPECIFIED	V		
CUCUMBERS	V		
MELON, WATER MELONS	V		
MELON, UNSPECIFIED	V		
PEPPERS, BELL	V		
PUMPKINS	V		
TOMATOES, FRESH MARKET	V		
TOMATOES, PROCESSING	V		
VEGETABLES, UNSPECIFIED	V		
BARLEY, UNSPECIFIED	7070 W		
WHEAT ALL	49000 W		
HAY, OTHER UNSPECIFIED	15500 z		
RICE, FOR MILLING	5040 z		
SAFFLOWER	21900 z		
SILAGE	16700 z		
SUNFLOWER SEED	970 z		
FIELD CROPS, UNSPEC.	230 z		
SEED, MISC FIELD CROP	250 z		
POTATOES, SEED	934 z		
SEED, VEG & VINECROP	282 z		
SEED, GRASS. UNSPECIFIED	320 z		



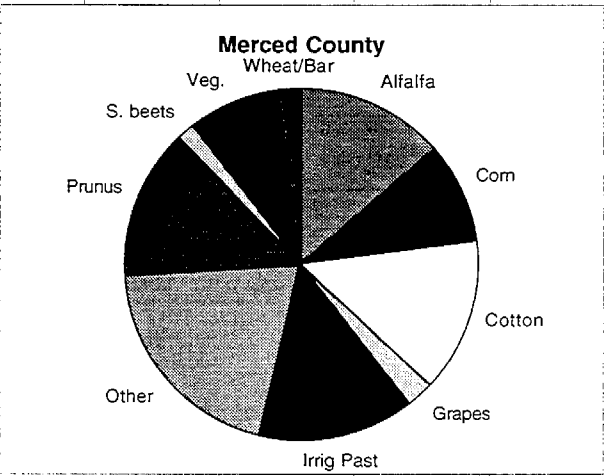
Appendix C. Data on crop distribution for San Joaquin Valley from 1993 County Agricultural Commissioners Report: Madera county.

HAY, ALFALFA	31800	A	Alfalfa	31800
SUGARBEETS	780	B	Corn	12800
COTTON LINT, UNSPEC	51400	C	Cotton	51400
GRAPES, RAISIN	25883	G	Grapes	81644
GRAPES, WINE	50308	G	Irrig Past	20000
GRAPES, TABLE	5453	G	Other	37039
ORANGES, UNSPECIFIED	4161	I	Prunus	42454
CORN FOR GRAIN	8700	N	Veg.	7991
CORN FOR SILAGE	4100	N	Wheat/Bar	26300
PASTURE, IRRIGATED	8000	P		
PASTURE, RANGE	393000	P		
PASTURE, MISC. FORAGE	20000	P		
ALMONDS, ALL	39176	S		
ALMOND HULLS		S		
NECTARINES	790	S		
PEACHES, FREESTONE	1260	S		
PLUMS	1228	S		
BEANS, UNSPEC. DRY EDIBLE	1550	V		
VEGETABLES, UNSPECIFIED	6441	V		
BARLEY, UNSPECIFIED	4300	W		
SILAGE	1050	Z		
COTTONSEED		Z		
HAY, GRAIN	2000	Z		
WHEAT ALL	22000	W		
FIELD CROPS, UNSPEC.	6441	Z		
SEED, OTHER (NO FLOWERS)	1055	Z		
APPLES, ALL	2250	Z		
FIGS, DRIED	6690	Z		
OLIVES	1781	Z		
PISTACHIOS	16884	Z		
WALNUTS, ENGLISH	981	Z		
FRUITS & NUTS, UNSPEC.	2207	Z		



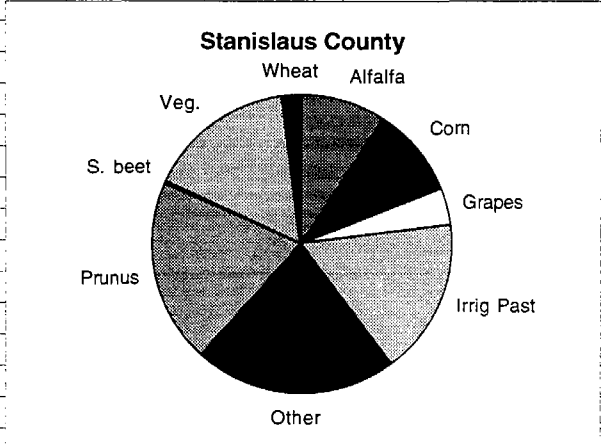
Appendix C. Data on crop distribution for San Joaquin Valley from 1993 County Agricultural Commissioners Report: Merced county.

HAY, ALFALFA	75220	A	Alfalfa	75220
SUGARBEETS	8900	B	Corn	50540
COTTON LINT, UNSPEC	79200	C	Cotton	79200
GRAPES, RAISIN	1190	G	Grapes	14338
GRAPES, WINE	13148	G	Irrig Past	80000
CORN FOR GRAIN	5540	N	Other	110796
CORN FOR SILAGE	45000	N	Prunus	76711
PASTURE, MISC. FORAGE	9700	P	S. beets	8900
PASTURE, IRRIGATED	80000	P	Veg.	46600
PASTURE, RANGE	553000	P	Wheat/Bar	11850
PLUMS	180	S		
NECTARINES	203	S		
PEACHES, FREESTONE	1667	S		
APRICOTS, ALL	1997	S		
PRUNES, DRIED	2096	S		
PEACHES, CLINGSTONE	4049	S		
ALMONDS, ALL	66519	S		
ALMOND HULLS		S		
PEAS, GREEN, PROCESSING	210	V		
PEPPERS, BELL	600	V		
MELON, WATER MELONS	1170	V		
BEANS, GREEN LIMAS	2580	V		
LIMA BEANS, UNSPECIFIED	2850	V		
BEANS, UNSPEC. DRY EDIBLE	2900	V		
MELON, UNSPECIFIED	3200	V		
VEGETABLES, UNSPECIFIED	3560	V		
TOMATOES, FRESH MARKET	7430	V		
TOMATOES, PROCESSING	10900	V		
MELON, CANTALOUPE	11200	V		
KIWIFRUIT	37	z		
SORGHUM, GRAIN	60	z		
HAY, SUDAN	690	z		
OATS FOR GRAIN	2700	z		
SEED, OTHER (NO FLOWERS)	3304	z		
FIGS, DRIED	3345	z		
SAFFLOWER	3760	z		
PISTACHIOS	4133	z		
FRUITS & NUTS, UNSPEC.	4352	z		
RICE, FOR MILLING	4390	z		
SWEET POTATOES	5500	z		
WALNUTS, ENGLISH	6435	z		
BARLEY, UNSPECIFIED	6590	z		
WHEAT ALL	11850	W		
HAY, GRAIN	18200	z		
SILAGE	47300	z		



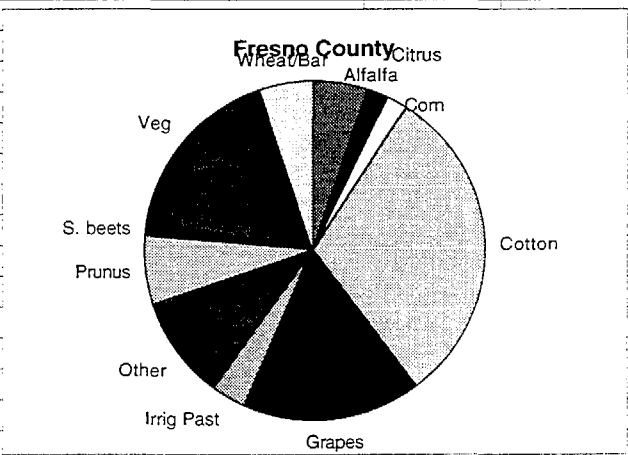
Appendix C. Data on crop distribution for San Joaquin Valley from 1993 County Agricultural Commissioners Report: Stanislaus county.

Commodity	Acres		Alfalfa	40200
SUGARBEETS	720	B	Corn	42700
GRAPES, WINE	17200	G	Grapes	17200
CORN FOR SILAGE	41700	N	Irrig Past	75500
CORN FOR GRAIN	1000	N	Other	96218
PASTURE, RANGE	358800	P	Prunus	88100
PASTURE, IRRIGATED	75500	P	S. beet	720
ALMONDS, ALL	70000	S	Veg.	69905
PEACHES, CLINGSTONE	10000	S	Wheat	10300
APRICOTS, ALL	6600	S		
PEACHES, FREESTONE	1400	S		
NECTARINES	100	S		
TOMATOES, PROCESSING	12400	V		
BEANS, GREEN LIMAS	8500	V		
BEANS, LIMAS, LG. DRY	8200	V		
BEANS, BLACKEYE (PEAS)	7600	V		
BEANS, LIMAS, BABY DRY	5000	V		
MELON, HONEYDEW	3300	V		
BEANS, UNSPECIFIED SNAP	3100	V		
MELON, UNSPECIFIED	2900	V		
PEAS, GREEN, PROCESSING	2500	V		
MELON, CANTALOUPE	2500	V		
CAULIFLOWER, UNSPECIFIED	2300	V		
BEANS, UNSPEC. DRY EDIBLE	2100	V		
MELON, WATER MELONS	2000	V		
PUMPKINS	1420	V		
BROCCOLI, UNSPECIFIED	1400	V		
VEGETABLES, UNSPECIFIED	1200	V		
SPINACH UNSPECIFIED	1190	V		
TOMATOES, FRESH MARKET	1175	V		
PEPPERS, BELL	1120	V		
WHEAT ALL	7400	W		
HAY, ALFALFA	40200	A		
SILAGE	28500	z		
HAY, GRAIN	26500	z		
WALNUTS, ENGLISH	25800	z		
BARLEY, UNSPECIFIED	2900	W		
RICE, FOR MILLING	2700	z		
SEED, MISC FIELD CROP	2000	z		
HAY, OTHER UNSPECIFIED	2000	z		
FIELD CROPS, UNSPEC.	1700	z		
CHERRIES, SWEET	1600	z		
APPLES, ALL	1400	z		
SWEET POTATOES	1300	z		
FRUITS & NUTS, UNSPEC.	961	z		
ONIONS	900	z		
SQUASH	380	z		
SEED, VEG & VINECROP	277	z		
KIWIFRUIT	200	z		



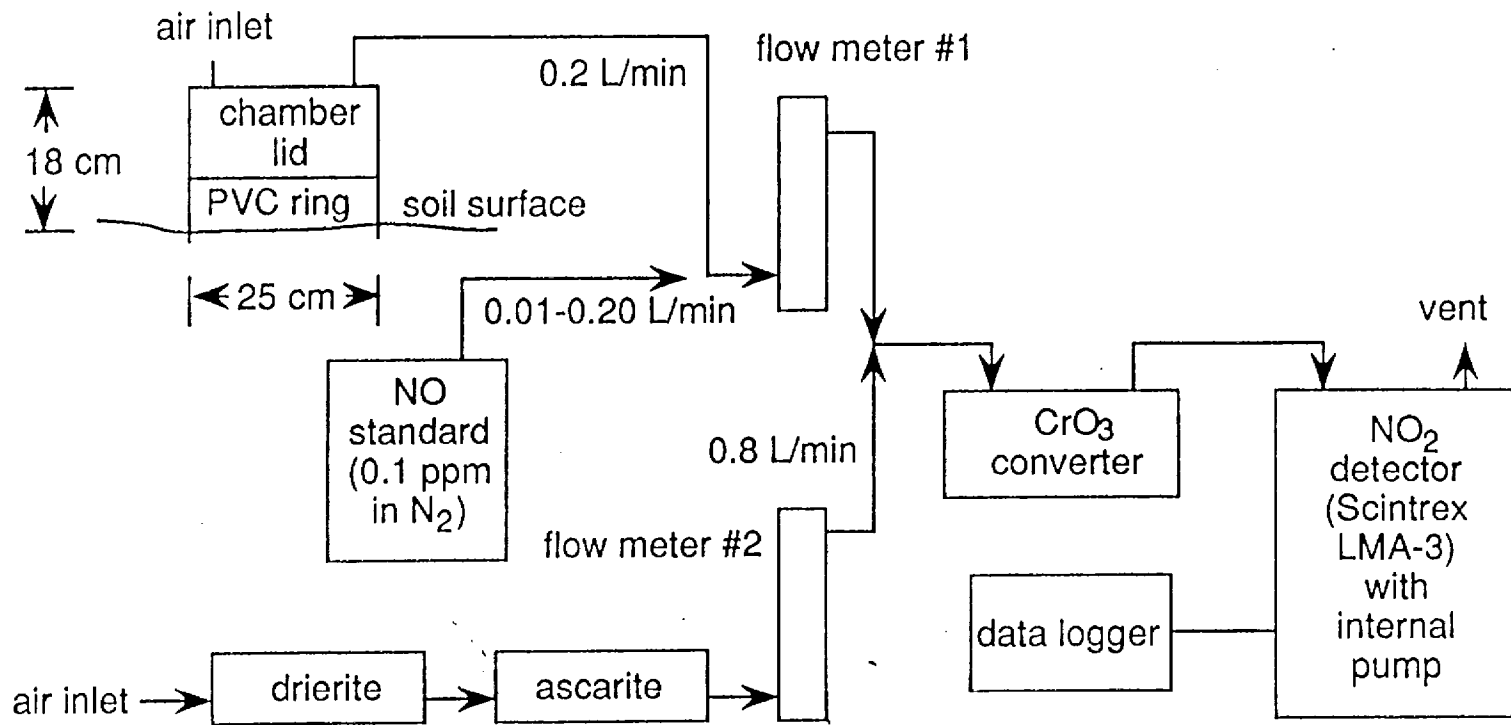
Appendix C. Data on crop distribution for San Joaquin Valley from 1993 County Agricultural Commissioners Report: Fresno county.

Commodity	Acres	Alfalfa	66000
HAY, ALFALFA	66000 A	Citrus	23218
SUGARBEETS	17000 B	Corn	24200
COTTON LINT, UPLAND	338000 C	Cotton	377700
COTTON LINT, PIMA	33500 C	Grapes	208228
SEED, COTTON FOR PLANTING	6200 C	Irrig Past	40000
GRAPES, TABLE	11690 G	Other	121075
GRAPES, WINE	61022 G	Prunus	80586
GRAPES, RAISIN	135516 G	S. beets	17000
LEMONS, ALL	991 I	Veg	209045
ORANGES, NAVEL	16885 I	Wheat/Bar	66500
ORANGES, VALENCIAS	4742 I		
CITRUS, UNSPECIFIED	600 I		
CORN FOR GRAIN	3900 N		
CORN FOR SILAGE	18000 N		
CORN, SWEET ALL	2300 N		
PASTURE, MISC. FORAGE	17300 P		
PASTURE, IRRIGATED	40000 P		
PASTURE, RANGE	850000 P		
ALMONDS, ALL	36503 S		
APRICOTS, ALL	829 S		
NECTARINES	12396 S		
PEACHES, CLINGSTONE	1730 S		
PEACHES, FREESTONE	11634 S		
PLUMS	16065 S		
PRUNES, DRIED	1429 S		
BEANS, UNSPEC. DRY EDIBLE	17900 V		
PEPPERS, BELL	1500 V		
BROCCOLI, UNSPECIFIED	6800 V		
CARROTS, UNSPECIFIED	610 V		
EGGPLANT, ALL	770 V		
LETTUCE, HEAD	18200 V		
MELON, CANTALOUPE	37000 V		
MELON, HONEYDEW	4200 V		
MELON, UNSPECIFIED	1750 V		
MELON, WATER MELONS	550 V		
VEGETABLES, ORIENTAL, ALL	2000 V		
TOMATOES, CHERRY	1000 V		
TOMATOES, FRESH MARKET	9600 V		
TOMATOES, PROCESSING	96000 V		
VEGETABLES, UNSPECIFIED	11165 V		
BARLEY, UNSPECIFIED	16000 W		
WHEAT ALL	28000 W		
SEED WHEAT	22500 W		
ONIONS	22000 z		
SEED, VEG & VINECROP	20800 z		
GARLIC, ALL	18400 z		
SAFFLOWER	15700 z		



Appendix C. Data on crop distribution for San Joaquin Valley from 1993 County Agricultural Commissioners Report: Fresno county.

HAY, GRAIN	10200	z		
RICE, FOR MILLING	7200	z		
FIELD CROPS, UNSPEC.	4270	z		
FIGS, DRIED	3319	z		
PISTACHIOS	2858	z		
WALNUTS, ENGLISH	2502	z		
APPLES, ALL	2484	z		
SEED, VEG & VINECROP	2000	z		
SEED BARLEY	1450	z		
SWEET POTATOES	1320	z		
OLIVES	1127	z		
SQUASH	940	z		
POMEGRANATES	929	z		
SEED, MISC FIELD CROP	819	z		
STRAWBERRIES, UNSPECIFIED	620	z		
FRUITS & NUTS, UNSPEC.	591	z		
PEARS, UNSPECIFIED	577	z		
KIWIFRUIT	377	z		
PERSIMMONS	313	z		
PECANS	279	z		
COTTONSEED		z		
CHRISTMAS TREES/CUT GRNS		z		
NURSERY, HERBAC. PRRNLS		z		
NURSERY, WOODY ORNAMNTALS		z		
NURSERY, NON-BRG FR,VN,NT		z		
CATTLE, BEEF BRDNG COWS		z		
CATTLE, BEEF BRDNG BULLS		z		
CATTLE, STOCKERS,FEEDERS		z		
CATTLE, CALVES ONLY		z		
CATTLE, FED STEERS,HEFRS		z		
CATTLE, CULL BEEF COWS		z		
CATTLE, DAIRY BRDNG COWS		z		
CATTLE, CULL MILK COWS		z		
CATTLE, VEAL CALVES		z		
HOGS & PIGS, UNSPECIFIED		z		
SHEEP, LAMBS		z		
SHEEP, CULL EWES		z		
TURKEYS, UNSPECIFIED		z		
MINK		z		
POULTRY, UNSPECIFIED		z		
MANURE		z		
MILK, MANUFACTURING		z		
MILK, FLUID MKT		z		
WOOL		z		
EGGS, UNSPECIFIED		z		
APIARY PROD, HONEY		z		
APIARY PROD, BEESWAX		z		
APIARY PROD, POLLIN. FEES		z		



Appendix D. Schematic of field NO_x measurement apparatus.

Appendix E. Method for calculating diel characteristic curves.

The following page of plots illustrates how the diel characteristic curves were calculated, using almonds, site B, as an example. The strategy was to assume that, for a particular crop type and position, the overall shape of the diel pattern of NO flux is approximately the same on different days, but the amplitude and maximum may differ, stretching or flattening the curve. The ratio of the amplitude to the maximum was assumed to remain constant; this assumption is considered reasonable, as inspection of the data showed the amplitude of the diel flux to be approximately proportional to the maximum flux. Thus, the diel curve can be predicted if only the maximum NO flux is known for a particular day.

A. Local regression, spline, lower bounds

The first three plots (from left to right, going down the page) are of the curves fitted to diel data (here, for almonds, Site B, canopy position, different days; days 07/06/95-07/07/95 were grouped together, since these consecutive days had similar NO fluxes). The curves were fit by local regression, as explained in more detail in the text in Section 2.2.1.4. For hours without data, NO flux values were interpolated. The rules followed for interpolation were as follows:

1. The NO flux is known to be periodic on daily cycles, and it is assumed that adjacent days have similar absolute NO fluxes. Therefore, repeating the loess curves from the available data in cycles of 3 consecutive days allows splining in of the missing hours.
2. If the fitted loess curve is very steep, the splined NO values may drop very low, yielding an unrealistic interpolation. In such cases, the lowest predicted value from the loess fit of the data (or zero, whichever is largest) is used as a lower bound for NO flux.
3. When splined values (i.e. no data taken during those hours) fall during the night-time hours of 11 pm to 5 am, the interpolated NO flux is held to the minimum of the fitted data, or zero, whichever is larger.

B. Normalization of each daily curve

Each diel curve was normalized to a range [0, 1]. These normalized curves from different days are shown plotted together on the same graph in the fourth figure. The amplitude/maximum ratio was also calculated.

C. Confidence intervals of normalized curves

The confidence intervals to the normalized curves were calculated by scaling (with the normalization of the curve) the mean confidence interval for the original curve. Overlaying these confidence intervals for different days gives a sense for how well the diel curve shapes are in agreement with each other (fifth plot).

D. Diel characteristic curve

The final characteristic diel curve for almonds, canopy, is shown in the last plot, with its propagated 95% confidence envelope. The final curve is achieved by taking the average of the normalized curves and rescaling this by the average of their amplitude/maximum ratio:

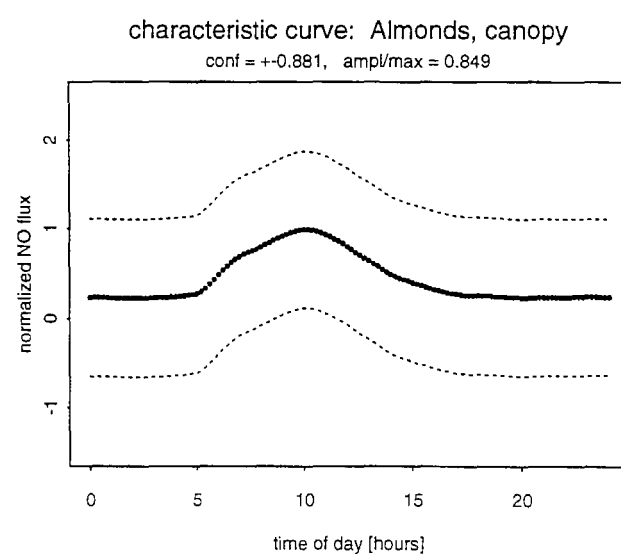
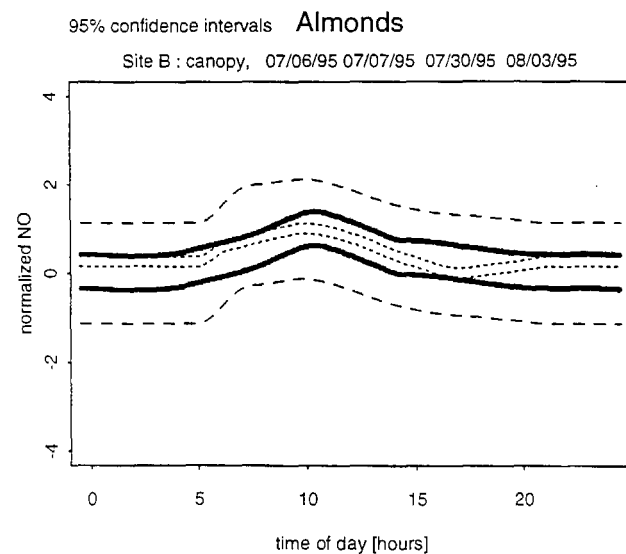
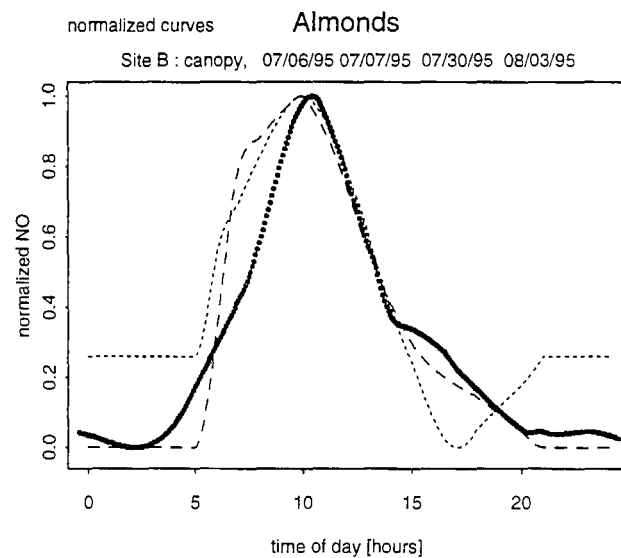
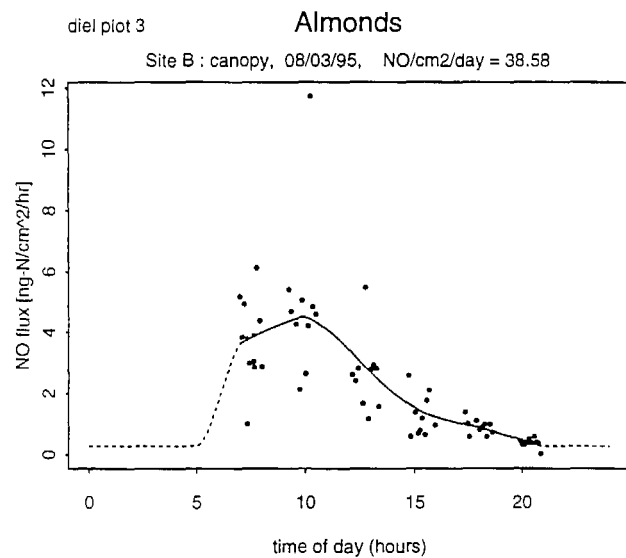
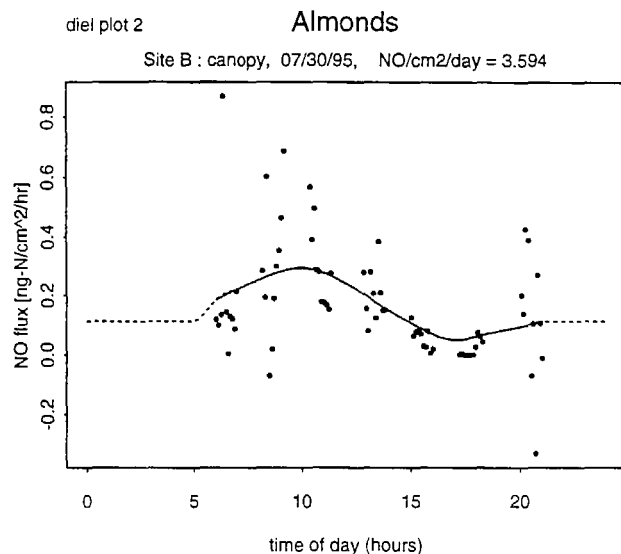
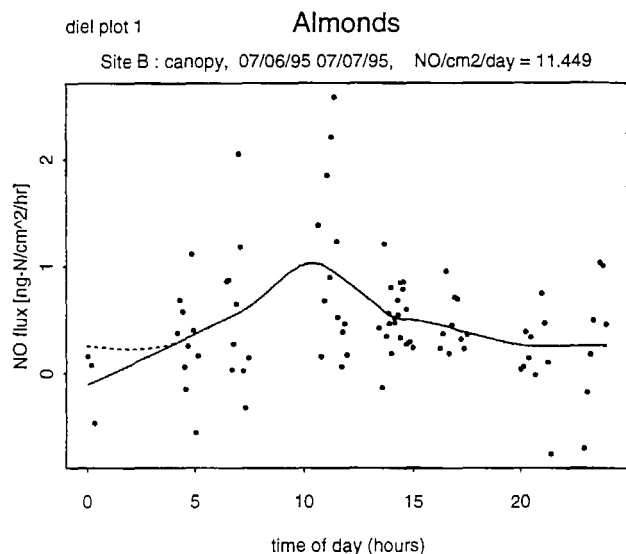
$$\begin{aligned} \text{characteristic normalized NO} \\ = \text{average normalized} * \text{ratio} + 1 - \text{ratio} \end{aligned}$$

Note that the curve is not merely rescaled for amplitude but also translated up so that its maximum is at 1.

Thus, to estimate diel curves for a day on which only the maximum NO flux is known, one merely multiplies the characteristic curve by the new maximum NO value and thus obtains a new, estimated diel curve.

Appendix E. Method for calculating diel characteristic curves

Locally fitted curves by date, normalized curves, normalized confidence intervals, and final characteristic curve



Appendix F. Point-predictive model refitted to individual crops.

```
[1] "Alfalfa"
[1] "sandy"
[1] "open"
[1] 4
```

```
Call: glm(formula = log(NO) ~ log(soiltemp) + twfps + NH4 + NO3 + NO2 + C + N
+ log(soiltemp) * twfps * NH4 + twfps * (NO3 + C) + NO3:C + NO2 * N +
twfps:C:N + NH4:NO2:C:N, data = newdata, model = T)
```

Deviance Residuals:

Min	1Q	Median	3Q	Max
-2.161946	-0.2185778	0.02156267	0.3409101	0.9980896

Coefficients:

	Value	Std. Error	t value
(Intercept)	7.07258152	12.7237195	0.5558580
log(soiltemp)	-1.88899759	3.5327852	-0.5347049
twfps	-26.40321014	33.5158186	-0.7877835
NH4	6.34379173	14.4475986	0.4390897
NO3	-0.08612367	0.1169894	-0.7361665
NO2	-25.93129386	60.3628288	-0.4295904
C	-1.11490809	0.9273963	-1.2021916
N	11.24323069	15.7322539	0.7146612
log(soiltemp):twfps	7.41314466	9.4661608	0.7831205
log(soiltemp):NH4	-1.84323632	4.1099702	-0.4484792
twfps:NH4	14.83276565	34.3528872	0.4317764
twfps:NO3	-0.06027273	0.1716654	-0.3511058
twfps:C	2.48500463	5.2669041	0.4718151
NO3:C	0.27278001	0.3227869	0.8450778
NO2:N	409.94450362	966.2479945	0.4242643
log(soiltemp):twfps:NH4	-4.18576964	9.8158205	-0.4264309
twfps:C:N	13.70757760	74.8867463	0.1830441
NH4:NO2:C:N	-5.09030220	27.4628747	-0.1853521

(Dispersion Parameter for Gaussian family taken to be 0.5613226)

Null Deviance: 57.61692 on 44 degrees of freedom

Residual Deviance: 15.15571 on 27 degrees of freedom

Number of Fisher Scoring Iterations: 1
Analysis of Deviance Table

Gaussian model

Response: log(NO)

Terms added sequentially (first to last)

	Df	Deviance	Resid.	Df	Resid. Dev	Pr (Chi)
NULL				44	57.61692	
log(soiltemp)	1	26.43604		43	31.18088	0.0000003

twfps	1	6.92431	42	24.25657	0.0085032
NH4	1	0.61330	41	23.64327	0.4335482
NO3	1	2.95897	40	20.68431	0.0854026
NO2	1	0.01626	39	20.66805	0.8985417
C	1	0.09447	38	20.57358	0.7585637
N	1	0.52474	37	20.04883	0.4688258
log(soiltemp):twfps	1	1.69787	36	18.35096	0.1925667
log(soiltemp):NH4	1	0.03913	35	18.31183	0.8431832
twfps:NH4	1	0.02165	34	18.29019	0.8830339
twfps:NO3	1	0.40342	33	17.88677	0.5253284
twfps:C	1	1.49611	32	16.39066	0.2212709
NO3:C	1	1.05096	31	15.33969	0.3052856
NO2:N	1	0.06793	30	15.27177	0.7943787
log(soiltemp):twfps:NH4	1	0.07904	29	15.19272	0.7785971
twfps:C:N	1	0.01773	28	15.17500	0.8940823
NH4:NO2:C:N	1	0.01928	27	15.15571	0.8895540

```
[1] "-----"
[1] "Almonds"
[1] "sandy"
[1] "canopy" "open"
[1] 3
```

```
Call: glm(formula = log(NO) ~ position + log(soiltemp) + twfps + NH4 + NO3 +
NO2 + C +
N + log(soiltemp) * twfps * NH4 + twfps * (NO3 + C) + NO3:C + NO2 * N +
twfps:C:N + NH4:NO2:C:N, data = newdata, model = T)
```

Deviance Residuals:

Min	1Q	Median	3Q	Max
-7.096909	-0.9461991	0.1431127	1.148614	3.86622

Coefficients:

	Value	Std. Error	t value
(Intercept)	-2.630332e-01	1.57490263	-0.16701556
position	6.069765e-01	0.14798583	4.10158507
log(soiltemp)	-1.923446e-02	0.47099037	-0.04083832
twfps	4.635637e+00	3.87875482	1.19513542
NH4	4.765753e-02	0.12342521	0.38612476
NO3	8.608424e-03	0.01606890	0.53571949
NO2	-2.663277e+01	11.94526926	-2.22956611
C	5.535002e-01	0.97672261	0.56669132
N	4.245006e-01	8.99680571	0.04718348
log(soiltemp):twfps	-1.068955e+00	1.13173165	-0.94453002
log(soiltemp):NH4	-5.822732e-03	0.03804803	-0.15303638
twfps:NH4	2.216576e-02	0.28531966	0.07768747
twfps:NO3	5.472907e-02	0.03194343	1.71331227
twfps:C	-1.321719e+00	4.68008053	-0.28241379
NO3:C	-2.466037e-02	0.02795064	-0.88228271
NO2:N	4.965828e+02	235.66658637	2.10714115
log(soiltemp):twfps:NH4	1.225929e-02	0.08803288	0.13925808
twfps:C:N	-9.582614e+00	57.38735585	-0.16698128
NH4:NO2:C:N	5.281123e+01	29.99610026	1.76060314

(Dispersion Parameter for Gaussian family taken to be 2.775019)

Null Deviance: 1970.276 on 617 degrees of freedom

Residual Deviance: 1662.236 on 599 degrees of freedom

Number of Fisher Scoring Iterations: 1

Analysis of Deviance Table

Gaussian model

Response: log(NO)

Terms added sequentially (first to last)

	Df	Deviance	Resid.	Df	Resid. Dev	Pr(Chi)
NULL				617	1970.276	
position	1	20.4509		616	1949.825	0.0000061
log(soiltemp)	1	12.3610		615	1937.464	0.0004384
twfps	1	112.5945		614	1824.870	0.0000000
NH4	1	0.8867		613	1823.983	0.3463855
NO3	1	45.8441		612	1778.139	0.0000000
NO2	1	0.3855		611	1777.754	0.5346555
C	1	3.9598		610	1773.794	0.0466006
N	1	0.1170		609	1773.677	0.7323216
log(soiltemp):twfps	1	10.5198		608	1763.157	0.0011810
log(soiltemp):NH4	1	21.6741		607	1741.483	0.0000032
twfps:NH4	1	54.3841		606	1687.099	0.0000000
twfps:NO3	1	8.4023		605	1678.697	0.0037476
twfps:C	1	0.8098		604	1677.887	0.3681736
NO3:C	1	2.3475		603	1675.539	0.1254828
NO2:N	1	4.6593		602	1670.880	0.0308861
log(soiltemp):twfps:NH4	1	0.0046		601	1670.875	0.9458713
twfps:C:N	1	0.0374		600	1670.838	0.8467176
NH4:NO2:C:N	1	8.6018		599	1662.236	0.0033583

[1] "-----"
[1] "Corn"
[1] "loamy"
[1] "furrow" "ridge"
[1] 3

Call: glm(formula = log(NO) ~ position + log(soiltemp) + twfps + NH4 + NO3 + NO2 + C + N + log(soiltemp) * twfps * NH4 + twfps * (NO3 + C) + NO3:C + NO2 * N + twfps:C:N + NH4:NO2:C:N, data = newdata, model = T)

Deviance Residuals:

Min	1Q	Median	3Q	Max
-5.500015	-0.5002014	0.122416	0.709231	2.939799

Coefficients:

	Value	Std. Error	t value
(Intercept)	8.13124302	7.84858775	1.0360135
position	0.36378996	0.16648322	2.1851449
log(soiltemp)	-2.23232334	1.75083755	-1.2750031
twfps	-52.36787885	19.75245405	-2.6512087
NH4	-37.20196326	10.09761831	-3.6842315
NO3	-0.09952070	0.19533916	-0.5094764

NO2	0.36786493	1.00400063	0.3663991
C	1.06839891	3.80688320	0.2806492
N	-26.56490180	11.84649647	-2.2424269
log(soiltemp):twfps	20.84943446	4.18954844	4.9765350
log(soiltemp):NH4	10.49978837	2.86411779	3.6659765
twfps:NH4	61.39626732	16.75569853	3.6642022
twfps:NO3	0.05974942	0.08743069	0.6833918
twfps:C	-21.15602328	9.52110081	-2.2220144
NO3:C	0.07632937	0.15584085	0.4897905
NO2:N	-6.07992021	8.54254056	-0.7117227
log(soiltemp):twfps:NH4	-17.32230893	4.75394114	-3.6437786
twfps:C:N	73.40762575	22.06419350	3.3270024
NH4:NO2:C:N	0.02717517	0.03104280	0.8754098

(Dispersion Parameter for Gaussian family taken to be 1.498334)

Null Deviance: 880.3753 on 244 degrees of freedom

Residual Deviance: 338.6234 on 226 degrees of freedom

Number of Fisher Scoring Iterations: 1

Analysis of Deviance Table

Gaussian model

Response: log(NO)

Terms added sequentially (first to last)

	Df	Deviance	Resid.	Df	Resid. Dev	Pr(Chi)
NULL				244	880.3753	
position	1	9.9355		243	870.4397	0.0016212
log(soiltemp)	1	350.4433		242	519.9964	0.0000000
twfps	1	20.4140		241	499.5825	0.0000062
NH4	1	2.3799		240	497.2025	0.1229027
NO3	1	8.7042		239	488.4983	0.0031747
NO2	1	2.5522		238	485.9461	0.1101420
C	1	15.2431		237	470.7030	0.0000945
N	1	9.4942		236	461.2089	0.0020613
log(soiltemp):twfps	1	74.2854		235	386.9235	0.0000000
log(soiltemp):NH4	1	1.7968		234	385.1268	0.1801034
twfps:NH4	1	8.8215		233	376.3053	0.0029771
twfps:NO3	1	0.4420		232	375.8633	0.5061432
twfps:C	1	0.5777		231	375.2856	0.4472217
NO3:C	1	0.7857		230	374.4999	0.3753975
NO2:N	1	0.4486		229	374.0513	0.5030137
log(soiltemp):twfps:NH4	1	17.2995		228	356.7518	0.0000319
twfps:C:N	1	16.9802		227	339.7716	0.0000378
NH4:NO2:C:N	1	1.1482		226	338.6234	0.2839186

[1] "-----"

[1] "Cotton"

[1] "sandy" "loamy" "clayey"

[1] "furrow" "ridge"

Call: glm(formula = log(NO) ~ soilcat + position + log(soiltemp) + twfps + NH4 + NO3 +

NO2 + C + N + log(soiltemp) * twfps * NH4 + twfps * (NO3 + C) + NO3:C + NO2 * N + twfps:C:N + NH4:NO2:C:N, data = newdata, model = T)

Deviance Residuals:

	Min	1Q	Median	3Q	Max
	-4.784721	-0.8368273	0.07714343	1.022508	3.856622

Coefficients:

	Value	Std. Error	t value
(Intercept)	-14.121763780	1.936906305	-7.2908864
soilcatloamy	0.323372502	0.534518593	0.6049790
soilcatsandy	1.448246059	0.450155076	3.2172159
position	0.375803051	0.155985339	2.4092203
log(soiltemp)	2.835121585	0.545443192	5.1978311
twfps	-20.639782814	5.057991567	-4.0806282
NH4	-2.475875083	1.135478421	-2.1804686
NO3	0.005024431	0.008540621	0.5882981
NO2	1.596577577	2.703516439	0.5905559
C	2.118126031	0.807695124	2.6224326
N	10.781686823	8.350992024	1.2910666
log(soiltemp):twfps	7.438595317	1.545364066	4.8134905
log(soiltemp):NH4	0.745508451	0.318004325	2.3443343
twfps:NH4	8.971245509	2.937293024	3.0542562
twfps:NO3	0.007643477	0.009899688	0.7720927
twfps:C	-7.762329096	3.070999636	-2.5276229
NO3:C	-0.009467456	0.013265581	-0.7136857
NO2:N	-21.982168956	40.521043380	-0.5424877
log(soiltemp):twfps:NH4	-2.655806265	0.850431778	-3.1228916
twfps:C:N	36.337844824	20.866300953	1.7414608
NH4:NO2:C:N	1.348786037	3.543209502	0.3806679

(Dispersion Parameter for Gaussian family taken to be 2.098458)

Null Deviance: 2100.872 on 486 degrees of freedom

Residual Deviance: 977.8816 on 466 degrees of freedom

Number of Fisher Scoring Iterations: 1

Analysis of Deviance Table

Gaussian model

Response: log(NO)

Terms added sequentially (first to last)

	Df	Deviance	Resid.	Df	Resid. Dev	Pr(Chi)
NULL				486	2100.872	
soilcat	2	116.5058		484	1984.367	0.0000000
position	1	31.0243		483	1953.342	0.0000000
log(soiltemp)	1	471.6614		482	1481.681	0.0000000
twfps	1	230.7846		481	1250.896	0.0000000
NH4	1	108.2462		480	1142.650	0.0000000
NO3	1	0.0040		479	1142.646	0.9498615

NO2	1	0.1845	478	1142.462	0.6675138
C	1	53.3808	477	1089.081	0.0000000
N	1	45.4598	476	1043.621	0.0000000
log(soiltemp):twfps	1	23.9545	475	1019.666	0.0000010
log(soiltemp):NH4	1	3.2580	474	1016.408	0.0710773
twfps:NH4	1	2.4087	473	1014.000	0.1206590
twfps:NO3	1	1.9489	472	1012.051	0.1627002
twfps:C	1	5.8493	471	1006.201	0.0155828
NO3:C	1	0.7697	470	1005.432	0.3803147
NO2:N	1	0.0034	469	1005.428	0.9533629
log(soiltemp):twfps:NH4	1	20.5714	468	984.857	0.0000057
twfps:C:N	1	6.6712	467	978.186	0.0097984
NH4:NO2:C:N	1	0.3041	466	977.882	0.5813337

[1] "-----"

[1] "Grapes"

[1] "sandy"

[1] "furrow" "ridge"

[1] 3

Call: glm(formula = log(NO) ~ position + log(soiltemp) + twfps + NH4 + NO3 + NO2 + C + N + log(soiltemp) * twfps * NH4 + twfps * (NO3 + C) + NO3:C + NO2 * N + twfps:C:N + NH4:NO2:C:N, data = newdata, model = T)

Deviance Residuals:

Min	1Q	Median	3Q	Max
-4.76598	-0.4782958	0.0637618	0.6069113	1.929435

Coefficients:

	Value	Std. Error	t value
(Intercept)	-0.685708491	1.084578167	-0.6322352
position	-0.406627888	0.096774906	-4.2017906
log(soiltemp)	0.485508203	0.311091728	1.5606593
twfps	-4.230571173	4.213670963	-1.0040108
NH4	2.752168972	1.395786623	1.9717691
NO3	0.011108411	0.006536798	1.6993659
NO2	3.610543967	3.377440796	1.0690177
C	-0.618592779	0.571900010	-1.0816450
N	7.546946015	5.298654717	1.4243136
log(soiltemp):twfps	0.632759194	1.173371480	0.5392659
log(soiltemp):NH4	-0.830502799	0.414464827	-2.0037956
twfps:NH4	8.596296970	3.564018157	2.4119678
twfps:NO3	0.019897114	0.007839538	2.5380468
twfps:C	8.683494959	3.732138699	2.3266807
NO3:C	-0.003833573	0.011452684	-0.3347314
NO2:N	-18.615132764	42.496578066	-0.4380384
log(soiltemp):twfps:NH4	-2.545197523	1.053371881	-2.4162383
twfps:C:N	-59.861747700	27.724229307	-2.1591853
NH4:NO2:C:N	-9.666564557	16.178666832	-0.5974883

(Dispersion Parameter for Gaussian family taken to be 0.7083266)

Null Deviance: 496.3951 on 529 degrees of freedom

Residual Deviance: 361.9549 on 511 degrees of freedom

Number of Fisher Scoring Iterations: 1
 Analysis of Deviance Table

Gaussian model

Response: log(NO)

Terms added sequentially (first to last)

	Df	Deviance	Resid.	Df	Resid. Dev	Pr(Chi)
NULL				529	496.3951	
position	1	49.55124		528	446.8439	0.0000000
log(soiltemp)	1	2.36163		527	444.4823	0.1243519
twfps	1	29.81140		526	414.6709	0.0000000
NH4	1	0.32924		525	414.3416	0.5661042
NO3	1	15.79577		524	398.5459	0.0000706
NO2	1	10.90135		523	387.6445	0.0009609
C	1	1.22680		522	386.4177	0.2680299
N	1	3.55636		521	382.8614	0.0593176
log(soiltemp):twfps	1	3.41464		520	379.4467	0.0646205
log(soiltemp):NH4	1	1.21864		519	378.2281	0.2696283
twfps:NH4	1	0.36966		518	377.8584	0.5431906
twfps:NO3	1	4.86255		517	372.9959	0.0274458
twfps:C	1	0.94410		516	372.0518	0.3312246
NO3:C	1	0.43619		515	371.6156	0.5089678
NO2:N	1	0.23594		514	371.3796	0.6271541
log(soiltemp):twfps:NH4	1	5.90537		513	365.4743	0.0150948
twfps:C:N	1	3.26648		512	362.2078	0.0707090
NH4:NO2:C:N	1	0.25287		511	361.9549	0.6150634

```
[1] "-----"
[1] "Irrigated pasture"
[1] "sandy" "loamy"
[1] "open"
[1] 2
```

```
Call: glm(formula = log(NO) ~ soilcat + log(soiltemp) + twfps + NH4 + NO3 +
NO2 + C +
N + log(soiltemp) * twfps * NH4 + twfps * (NO3 + C) + NO3:C + NO2 * N +
twfps:C:N + NH4:NO2:C:N, data = newdata, model = T)
```

Deviance Residuals:

Min	1Q	Median	3Q	Max
-4.610977	-0.6416017	0.01557415	0.7183327	3.688135

Coefficients:

	Value	Std. Error	t value
(Intercept)	-7.845938983	16.53069636	-0.47462846
soilcat	0.216292705	1.08636593	0.19909747
log(soiltemp)	2.042267237	4.82666743	0.42312160
twfps	5.267125353	34.96791185	0.15062739
NH4	0.098740367	0.81943020	0.12049881
NO3	0.022145647	0.18329102	0.12082232
NO2	0.416420339	6.94849918	0.05992954
C	0.138781596	1.56405372	0.08873199
N	3.929760454	15.47004505	0.25402385

```

log(soiltemp):twfps -1.111168100  9.63367700 -0.11534205
log(soiltemp):NH4 -0.024854616  0.23019066 -0.10797404
twfps:NH4 -0.691315433  1.60462943 -0.43082560
twfps:NO3 -0.022953490  0.06841874 -0.33548542
twfps:C 0.620709627  3.48039217  0.17834474
NO3:C -0.001092653  0.05872624 -0.01860588
NO2:N -3.858134406  35.77870652 -0.10783326
log(soiltemp):twfps:NH4 0.209974135  0.45196687  0.46457860
twfps:C:N -3.281631992  6.31491324 -0.51966383
NH4:NO2:C:N 0.022246133  0.09283679  0.23962625

```

(Dispersion Parameter for Gaussian family taken to be 2.863401)

Null Deviance: 167.422 on 60 degrees of freedom

Residual Deviance: 120.2629 on 42 degrees of freedom

Number of Fisher Scoring Iterations: 1
Analysis of Deviance Table

Gaussian model

Response: log(NO)

Terms added sequentially (first to last)

	Df	Deviance	Resid.	Df	Resid. Dev	Pr(Chi)
NULL				60	167.4220	
soilcat	1	5.71613		59	161.7059	0.0168098
log(soiltemp)	1	0.93214		58	160.7738	0.3343075
twfps	1	2.36019		57	158.4136	0.1244673
NH4	1	20.18560		56	138.2280	0.0000070
NO3	1	0.43435		55	137.7936	0.5098620
NO2	1	0.00418		54	137.7894	0.9484698
C	1	3.34457		53	134.4449	0.0674272
N	1	0.21124		52	134.2336	0.6457936
log(soiltemp):twfps	1	0.12050		51	134.1131	0.7284944
log(soiltemp):NH4	1	0.02984		50	134.0833	0.8628607
twfps:NH4	1	2.10713		49	131.9762	0.1466137
twfps:NO3	1	0.12492		48	131.8512	0.7237558
twfps:C	1	8.76998		47	123.0813	0.0030623
NO3:C	1	1.04607		46	122.0352	0.3064141
NO2:N	1	0.19278		45	121.8424	0.6606129
log(soiltemp):twfps:NH4	1	0.76258		44	121.0798	0.3825232
twfps:C:N	1	0.65256		43	120.4273	0.4191992
NH4:NO2:C:N	1	0.16442		42	120.2629	0.6851206

[1] "-----"

[1] "Oranges"

[1] "sandy"

[1] "canopy" "open"

[1] 3

Call: glm(formula = log(NO) ~ position + log(soiltemp) + twfps + NH4 + NO3 + NO2 + C + N + log(soiltemp) * twfps * NH4 + twfps * (NO3 + C) + NO3:C + NO2 * N +

twfps:C:N + NH4:NO2:C:N, data = newdata, model = T)
 Deviance Residuals:

Min	1Q	Median	3Q	Max
-5.912709	-0.5146489	0.01146303	0.6721933	3.151048

Coefficients:

	Value	Std. Error	t value
(Intercept)	-13.3953329	8.14847803	-1.64390612
position	-0.1935021	0.41486642	-0.46642025
log(soiltemp)	3.8250843	2.09492645	1.82587999
twfps	10.7789933	20.06347560	0.53724457
NH4	-6.6093063	7.05120429	-0.93733014
NO3	-0.1254525	0.10930321	-1.14774785
NO2	0.7303322	2.06924355	0.35294647
C	1.0775173	6.19193447	0.17401949
N	0.9730768	31.86516155	0.03053733
log(soiltemp):twfps	-3.7163540	5.57889077	-0.66614569
log(soiltemp):NH4	1.9739904	2.10691453	0.93691055
twfps:NH4	28.2681942	19.26052017	1.46767553
twfps:NO3	0.1403419	0.08709275	1.61140696
twfps:C	24.0153116	27.89703794	0.86085525
NO3:C	0.2140853	0.39872615	0.53692313
NO2:N	7.9731481	34.06182643	0.23407870
log(soiltemp):twfps:NH4	-7.3749437	5.48164215	-1.34538948
twfps:C:N	-417.4691349	341.17929977	-1.22360628
NH4:NO2:C:N	-28.0621431	17.87291609	-1.57009315

(Dispersion Parameter for Gaussian family taken to be 2.079862)

Null Deviance: 166.7951 on 74 degrees of freedom

Residual Deviance: 116.4723 on 56 degrees of freedom

Number of Fisher Scoring Iterations: 1

Analysis of Deviance Table

Gaussian model

Response: log(NO)

Terms added sequentially (first to last)

	Df	Deviance	Resid.	Df	Resid. Dev	Pr(Chi)
NULL				74	166.7951	
position	1	2.69110		73	164.1040	0.1009101
log(soiltemp)	1	17.24459		72	146.8594	0.0000329
twfps	1	0.31225		71	146.5472	0.5763050
NH4	1	0.83365		70	145.7135	0.3612193
NO3	1	1.09905		69	144.6145	0.2944745
NO2	1	2.47201		68	142.1425	0.1158894
C	1	0.40377		67	141.7387	0.5251502
N	1	0.03701		66	141.7017	0.8474476
log(soiltemp):twfps	1	1.11924		65	140.5825	0.2900824
log(soiltemp):NH4	1	1.33715		64	139.2453	0.2475380
twfps:NH4	1	3.33495		63	135.9104	0.0678226

	twfps:NO3	1	7.70175	62	128.2086	0.0055167
	twfps:C	1	0.81114	61	127.3975	0.3677828
	NO3:C	1	1.16584	60	126.2316	0.2802574
	NO2:N	1	1.20895	59	125.0227	0.2715394
log(soiltemp):twfps:	NH4	1	1.60278	58	123.4199	0.2055094
	twfps:C:N	1	1.82039	57	121.5995	0.1772673
	NH4:NO2:C:N	1	5.12726	56	116.4723	0.0235529

[1] "-----"
 [1] "Peaches"
 [1] "Sugar beets"
 [1] "sandy" "loamy"
 [1] "open" "furrow" "ridge"

Call: glm(formula = log(NO) ~ soilcat + position + log(soiltemp) + twfps + NH4 + NO3 + NO2 + C + N + log(soiltemp) * twfps * NH4 + twfps * (NO3 + C) + NO3:C + NO2 * N + twfps:C:N + NH4:NO2:C:N, data = newdata, model = T)

Deviance Residuals:

Min	1Q	Median	3Q	Max
-1.321444	-0.4177301	-0.03896702	0.4609592	1.883339

Coefficients:

	Value	Std. Error	t value
(Intercept)	-2.659150696	2.731361803	-0.97356223
soilcat	-1.172851946	0.784465247	-1.49509739
positionopen	-3.533229493	0.498043997	-7.09421159
positionridge	0.062788743	0.144873013	0.43340538
log(soiltemp)	1.766027091	0.543339280	3.25032103
twfps	5.937138258	8.096886588	0.73326188
NH4	0.043721292	1.037676650	0.04213383
NO3	0.006716225	0.013658784	0.49171471
NO2	4.075000879	3.112434046	1.30926497
C	-3.048895521	1.412734885	-2.15815122
N	-5.909149474	9.317730761	-0.63418332
log(soiltemp):twfps	-0.507306726	2.224462092	-0.22805816
log(soiltemp):NH4	0.028007893	0.286266111	0.09783866
twfps:NH4	2.949853674	5.524618569	0.53394703
twfps:NO3	-0.007601268	0.008139592	-0.93386352
twfps:C	-8.984962265	4.920139203	-1.82616017
NO3:C	-0.021325059	0.027680708	-0.77039428
NO2:N	-6.294085501	49.123279362	-0.12812837
log(soiltemp):twfps:NH4	-0.940163585	1.614895242	-0.58218240
twfps:C:N	41.813922090	26.976447461	1.55001589
NH4:NO2:C:N	-36.542820009	27.403678496	-1.33350054

(Dispersion Parameter for Gaussian family taken to be 0.4802536)

Null Deviance: 170.458 on 123 degrees of freedom

Residual Deviance: 49.46612 on 103 degrees of freedom

Number of Fisher Scoring Iterations: 1

Analysis of Deviance Table

Gaussian model

Response: log(NO)

Terms added sequentially (first to last)

	Df	Deviance	Resid.	Df	Resid. Dev	Pr(Chi)
NULL				123	170.4580	
soilcat	1	7.64609		122	162.8119	0.0056895
position	2	42.74773		120	120.0641	0.0000000
log(soiltemp)	1	34.51630		119	85.5478	0.0000000
twfps	1	13.92578		118	71.6220	0.0001902
NH4	1	1.98603		117	69.6360	0.1587568
NO3	1	0.74950		116	68.8865	0.3866359
NO2	1	4.43807		115	64.4485	0.0351459
C	1	11.08787		114	53.3606	0.0008689
N	1	0.00039		113	53.3602	0.9842866
log(soiltemp):twfps	1	0.01967		112	53.3405	0.8884709
log(soiltemp):NH4	1	0.32112		111	53.0194	0.5709366
twfps:NH4	1	0.58452		110	52.4349	0.4445474
twfps:NO3	1	0.31178		109	52.1231	0.5765869
twfps:C	1	0.08711		108	52.0360	0.7678902
NO3:C	1	0.64385		107	51.3922	0.4223199
NO2:N	1	0.06788		106	51.3243	0.7944457
log(soiltemp):twfps:NH4	1	0.06443		105	51.2598	0.7996329
twfps:C:N	1	0.93973		104	50.3201	0.3323482
NH4:NO2:C:N	1	0.85400		103	49.4661	0.3554237

```
[1] "-----"  
[1] "Tomatoes"  
[1] "loamy"  
[1] "furrow" "ridge"  
[1] 3
```

```
Call: glm(formula = log(NO) ~ position + log(soiltemp) + twfps + NH4 + NO3 +  
NO2 + C +  
N + log(soiltemp) * twfps * NH4 + twfps * (NO3 + C) + NO3:C + NO2 * N +  
twfps:C:N + NH4:NO2:C:N, data = newdata, model = T)
```

Deviance Residuals:

Min	1Q	Median	3Q	Max
-2.545258	-0.6149222	0.005321983	0.6187332	2.304916

Coefficients:

	Value	Std. Error	t value
(Intercept)	12.69046015	8.57004397	1.48079289
position	0.05883044	0.18748418	0.31378884
log(soiltemp)	-3.01906232	2.38996197	-1.26322609
twfps	-31.44087938	21.08131199	-1.49140999
NH4	-1.15623885	6.16634396	-0.18750800
NO3	-0.02362091	0.06761561	-0.34934115
NO2	-8.84127171	8.73372887	-1.01231351
C	-2.14772731	3.32708387	-0.64552846
N	1.38100998	18.84587310	0.07327917
log(soiltemp):twfps	9.48792262	5.66101975	1.67600946
log(soiltemp):NH4	0.31632201	1.71551343	0.18438912
twfps:NH4	14.82803734	18.82941524	0.78749325

twfps:NO3	0.03625852	0.03209076	1.12987424
twfps:C	-1.24451001	14.69282728	-0.08470187
NO3:C	0.04464490	0.11691885	0.38184517
NO2:N	198.73089089	110.36841038	1.80061387
log(soiltemp):twfps:NH4	-4.10237143	5.25232025	-0.78105889
twfps:C:N	13.13862539	75.97176831	0.17294089
NH4:NO2:C:N	-58.27159760	31.39609248	-1.85601433

(Dispersion Parameter for Gaussian family taken to be 0.9148189)

Null Deviance: 163.2424 on 120 degrees of freedom

Residual Deviance: 93.31153 on 102 degrees of freedom

Number of Fisher Scoring Iterations: 1

Analysis of Deviance Table

Gaussian model

Response: log(NO)

Terms added sequentially (first to last)

	Df	Deviance	Resid.	Df	Resid. Dev	Pr(Chi)
NULL				120	163.2424	
position	1	0.34403		119	162.8984	0.5575142
log(soiltemp)	1	11.54663		118	151.3518	0.0006787
twfps	1	34.98247		117	116.3693	0.0000000
NH4	1	0.04062		116	116.3287	0.8402767
NO3	1	4.21671		115	112.1120	0.0400278
NO2	1	1.19487		114	110.9171	0.2743491
C	1	0.21730		113	110.6998	0.6411044
N	1	0.16531		112	110.5345	0.6843110
log(soiltemp):twfps	1	6.47202		111	104.0625	0.0109586
log(soiltemp):NH4	1	0.63234		110	103.4301	0.4264966
twfps:NH4	1	2.47842		109	100.9517	0.1154180
twfps:NO3	1	0.22015		108	100.7316	0.6389247
twfps:C	1	0.00000		107	100.7316	0.9992068
NO3:C	1	0.39669		106	100.3349	0.5288047
NO2:N	1	1.86641		105	98.4685	0.1718869
log(soiltemp):twfps:NH4	1	1.88906		104	96.5794	0.1693084
twfps:C:N	1	0.11651		103	96.4629	0.7328495
NH4:NO2:C:N	1	3.15136		102	93.3115	0.0758638

[1] "-----"

[1] "-----"

Appendix G. Management model refitted to individual crops.
 3rd-order interactions excluded
 Irrigated pasture not included because fertilizer type unknown.
 Alfalfa and peaches excluded due to too few data points.

```
[1] "Almonds"
[1] "sandy"
[1] "mixedfert"
[1] 4
```

```
Call: glm(formula = log(NOmax) ~ log(airtemp) + fertdt +
log(airtemp) * twfps, data = newdata, model = T)
```

Deviance Residuals:

Min	1Q	Median	3Q	Max
-2.360552	-1.090174	0.0145722	0.8682951	2.766292

Coefficients:

	Value	Std. Error	t value
(Intercept)	27.922884821	12.92937635	2.1596467
log(airtemp)	-7.908692346	3.80644936	-2.0777085
fertdt	0.002817022	0.02277347	0.1236975
twfps	-66.498191305	29.70269773	-2.2387930
log(airtemp):twfps	19.801680266	8.72122920	2.2705148

(Dispersion Parameter for Gaussian family taken to be 1.995286)
 Null Deviance: 75.48935 on 28 degrees of freedom
 Residual Deviance: 47.88688 on 24 degrees of freedom

Analysis of Deviance Table

Gaussian model

Response: log(NOmax)

	Df	Deviance	Resid.	Df	Resid. Dev	Pr(Chi)
NULL				28	75.48935	
log(airtemp)	1	13.42943		27	62.05992	0.0002477
fertdt	1	3.21107		26	58.84885	0.0731415
twfps	1	0.67580		25	58.17305	0.4110367
log(airtemp):twfps	1	10.28618		24	47.88688	0.0013403

```
[1] "-----"
[1] "Corn"
[1] "loamy"
[1] "mixedfert" "NH4fert"
[1] 3
```

```
Call: glm(formula = log(NOmax) ~ log(airtemp) + fertcat * fertdt +
log(airtemp) * twfps, data = newdata, model = T)
```

Deviance Residuals:

Min	1Q	Median	3Q	Max
-0.6949064	-0.3411285	-0.03584551	0.3251346	0.8565682

Coefficients:

	Value	Std. Error	t value
(Intercept)	-39.9927669	14.86389959	-2.690597
log(airtemp)	7.7088936	4.20300023	1.834141
fertcat	20.4947128	4.77930035	4.288224
fertdt	0.1344762	0.04596445	2.925656
twfps	46.5409555	28.60607848	1.626960
fertcat:fertdt	-0.3232902	0.05543966	-5.831388
log(airtemp):twfps	-14.5020488	8.51670709	-1.702777

(Dispersion Parameter for Gaussian family taken to be 0.2721376)
Null Deviance: 83.03473 on 19 degrees of freedom
Residual Deviance: 3.537789 on 13 degrees of freedom

Analysis of Deviance Table

Gaussian model

Response: log(NOmax)

	Df	Deviance	Resid. Df	Resid. Dev	Pr(Chi)
NULL			19	83.03473	
log(airtemp)	1	50.36429	18	32.67044	0.0000000
fertcat	1	6.10025	17	26.57019	0.0135163
fertdt	1	9.33815	16	17.23203	0.0022443
twfps	1	3.29663	15	13.93541	0.0694222
fertcat:fertdt	1	9.60857	14	4.32684	0.0019367
log(airtemp):twfps	1	0.78905	13	3.53779	0.3743879

[1] "-----"
[1] "Cotton"
[1] "sandy" "loamy" "clayey"
[1] "NH4fert" "mixedfert"

Call: glm(formula = log(NOmax) ~ soilcat + log(airtemp) + fertcat * fertdt +
log(airtemp) * twfps, data = newdata, model = T)

Deviance Residuals:

Min	1Q	Median	3Q	Max
-1.264332	-0.3253451	0.04534393	0.2773339	1.727372

Coefficients:

	Value	Std. Error	t value
(Intercept)	-17.4761792	3.73134913	-4.6836087
soilcatloamy	3.5849565	1.31640268	2.7232977
soilcatsandy	5.0663282	1.36742518	3.7050131
log(airtemp)	3.9518570	1.28737247	3.0697076
fertcat	13.1782986	6.81418613	1.9339505
fertdt	-0.0287368	0.01664165	-1.7268001
twfps	10.3614841	12.43734911	0.8330943
fertcat:fertdt	-0.2035077	0.11635329	-1.7490501
log(airtemp):twfps	-2.3181023	3.83597690	-0.6043056

(Dispersion Parameter for Gaussian family taken to be 0.4448036)
Null Deviance: 71.06634 on 31 degrees of freedom
Residual Deviance: 10.23048 on 23 degrees of freedom

Analysis of Deviance Table

Gaussian model

Response: log(NOmax)

	Df	Deviance	Resid.	Df	Resid. Dev	Pr(Chi)
NULL				31	71.06634	
soilcat	2	6.23625		29	64.83009	0.0442401
log(airtemp)	1	14.62196		28	50.20813	0.0001314
fertcat	1	27.48018		27	22.72795	0.0000002
fertdt	1	7.61511		26	15.11284	0.0057881
twfps	1	2.71577		25	12.39707	0.0993610
fertcat:fertdt	1	2.00415		24	10.39292	0.1568694
log(airtemp):twfps	1	0.16244		23	10.23048	0.6869238

```
[1] "-----"
[1] "Grapes"
[1] "sandy"
[1] "mixedfert" "NH4fert"
[1] 3
```

```
Call: glm(formula = log(NOmax) ~ log(airtemp) + fertcat * fertdt +
log(airtemp) * twfps, data = newdata, model = T)
```

Deviance Residuals:

Min	1Q	Median	3Q	Max
-1.172111	-0.4992582	-0.06099875	0.6069734	1.172111

Coefficients:

	Value	Std. Error	t value
(Intercept)	301.226295	232.192845	1.2973108
log(airtemp)	-2.678818	8.862299	-0.3022712
fertcat	-291.207753	209.599110	-1.3893559
fertdt	-1.656414	1.191164	-1.3905846
twfps	58.135350	86.196803	0.6744490
fertcat:fertdt	1.640514	1.189771	1.3788476
log(airtemp):twfps	-16.763959	25.458313	-0.6584866

(Dispersion Parameter for Gaussian family taken to be 0.667515)

Null Deviance: 24.15827 on 23 degrees of freedom

Residual Deviance: 11.34776 on 17 degrees of freedom

Analysis of Deviance Table

Gaussian model

Response: log(NOmax)

	Df	Deviance	Resid.	Df	Resid. Dev	Pr(Chi)
NULL				23	24.15827	
log(airtemp)	1	0.096809		22	24.06146	0.7556935
fertcat	1	8.953944		21	15.10752	0.0027687
fertdt	1	1.164282		20	13.94324	0.2805793
twfps	1	1.216229		19	12.72701	0.2701021
fertcat:fertdt	1	1.089816		18	11.63719	0.2965119
log(airtemp):twfps	1	0.289438		17	11.34776	0.5905811

```
[1] "-----"
[1] "Oranges"
[1] "sandy"
[1] "NH4fert"
[1] 4
```

```
Call: glm(formula = log(NOmax) ~ log(airtemp) + fertdt + log(airtemp) * twfps,
          data = newdata, model = T)
```

Deviance Residuals:

```
      106      107      108      109      110      111      112
-0.3651759 0.4696469 0.02932317 -0.1687685 0.2533953 -0.3750102 0.03719553
      113
0.1193936
```

Coefficients:

	Value	Std. Error	t value
(Intercept)	0.854119973	9.46464376	0.09024322
log(airtemp)	0.086795427	2.87574646	0.03018188
fertdt	-0.007778973	0.06014702	-0.12933266
twfps	-24.439225762	33.95769802	-0.71969619
log(airtemp):twfps	7.564274868	10.44812927	0.72398366

(Dispersion Parameter for Gaussian family taken to be 0.2012481)

Null Deviance: 0.8111489 on 7 degrees of freedom

Residual Deviance: 0.6037444 on 3 degrees of freedom

Analysis of Deviance Table

Gaussian model

Response: log(NOmax)

	Df	Deviance	Resid. Df	Resid. Dev	Pr(Chi)
NULL			7	0.8111489	
log(airtemp)	1	0.0769690	6	0.7341799	0.7814478
fertdt	1	0.0225943	5	0.7115856	0.8805168
twfps	1	0.0023565	4	0.7092291	0.9612832
log(airtemp):twfps	1	0.1054847	3	0.6037444	0.7453445

```
[1] "-----"
[1] "Sugar beets"
[1] "sandy" "loamy"
[1] "NH4fert" "mixedfert"
```

```
Call: glm(formula = log(NOmax) ~ soilcat + log(airtemp) + fertcat * fertdt +
          log(airtemp) * twfps, data = newdata, model = T)
```

Deviance Residuals:

```
      61      62      63      64      87      88      89      90
0.25041 0.240278 -0.25041 -0.240278 -0.8131631 -0.4601821 0.8131631 0.4601821
      114      115      116      117
```

0.8400164 -0.01133392 -0.8400164 0.01133392

Coefficients:

	Value	Std. Error	t value
(Intercept)	30.5976294	371.121116	0.08244648
soilcat	-21.5268881	53.771044	-0.40034350
log(airtemp)	-0.7787807	29.085154	-0.02677588
fertcat	-48.4117307	256.799162	-0.18851982
fertdt	-0.1321044	5.393956	-0.02449118
twfps	56.3923575	283.673086	0.19879347
fertcat:fertdt	0.7249347	4.830080	0.15008751
log(airtemp):twfps	-18.4655920	83.747829	-0.22049040

(Dispersion Parameter for Gaussian family taken to be 0.8495983)

Null Deviance: 12.23285 on 11 degrees of freedom
Residual Deviance: 3.398393 on 4 degrees of freedom

Analysis of Deviance Table

Gaussian model

Response: log(NOmax)

	Df	Deviance	Resid. Df	Resid. Dev	Pr(Chi)
NULL			11	12.23285	
soilcat	1	1.333849	10	10.89900	0.2481216
log(airtemp)	1	3.862705	9	7.03630	0.0493707
fertcat	1	3.067223	8	3.96907	0.0798858
fertdt	1	0.000570	7	3.96850	0.9809459
twfps	1	0.420012	6	3.54849	0.5169310
fertcat:fertdt	1	0.108794	5	3.43970	0.7415213
log(airtemp):twfps	1	0.041304	4	3.39839	0.8389521

[1] "-----"
[1] "Tomatoes"
[1] "loamy"
[1] "NH4fert"
[1] 4

Call: glm(formula = log(NOmax) ~ log(airtemp) + fertdt + log(airtemp) * twfps,
data = newdata, model = T)

Deviance Residuals:

Min	1Q	Median	3Q	Max
-1.036982	-0.3848827	0.06332942	0.3768815	0.7568117

Coefficients:

	Value	Std. Error	t value
(Intercept)	20.69391692	16.99791743	1.2174384
log(airtemp)	-5.40108801	3.90617281	-1.3827059
fertdt	-0.02617291	0.08402222	-0.3114999
twfps	-69.79900031	38.21544393	-1.8264605
log(airtemp):twfps	20.82640313	10.45921711	1.9912010

(Dispersion Parameter for Gaussian family taken to be 0.3582146)

Null Deviance: 25.22238 on 15 degrees of freedom
Residual Deviance: 3.940361 on 11 degrees of freedom

Analysis of Deviance Table
Gaussian model
Response: log(NOmax)

	Df	Deviance	Resid.	Df	Resid. Dev	Pr(Chi)
NULL				15	25.22238	
log(airtemp)	1	1.21915		14	24.00323	0.2695270
fertdt	1	3.26613		13	20.73710	0.0707244
twfps	1	15.37646		12	5.36064	0.0000881
log(airtemp):twfps	1	1.42028		11	3.94036	0.2333576

Appendix H. Estimating fluxes from the diel characteristic curves.

See Diskette 2 for the text file: DIEL.TXT, containing the xy values of the eight diel characteristic curves for:

Corn, furrow position	x = time of day [hours]
Corn, ridge	
Grapes, furrow	y = normalized NOx [unitless,
max=1]	
Grapes, ridge	
Almonds, canopy	
Almonds, open	
Cotton, furrow	
Cotton, ridge	

Because the curves are obtained by a combination of local regression on data and interpolation, their xy values rather than the functions that are their piecewise curve fits are provided here as tables from which users can more easily make estimations.

To make estimations of hourly or daily NOx flux, choose the curve whose crop type and position match the crop being estimated.

A. To make estimations of hourly NOx flux at a given time of day:

1. Use linear interpolation to calculate the characteristic curve value y at time of day x (maximum y value is 1).
2. Given a daily maximum NOx flux, M [ng-N/cm²/hr], calculate the hourly NOx flux:

$$\text{NOx flux at time } x = y * M$$

B. To make estimations of daily NOx flux:

1. Estimate a diel curve, Y, in absolute NOx flux units [ng-N/cm²/hr]. Given a daily maximum NOx flux, M [ng-N/cm²/hr], for all values of y provided for the characteristic curve, calculate:

$$Y = y * M$$

2. Integrate along the estimated curve Y from x = 0 hours to 24 hours to get the total daily NOx flux. Stepsizes may be chosen at the user's discretion.

Appendix I. Deliverables for San Joaquin Valley NO_x Project.

I. Emissions Estimates

1) Extrapolation Approach: We will sample NO_x emissions intensively in 14 fields representing the major crop/soil/management combinations (types) in the Valley, as well extensively (one-time sampling) in other fields. From this data, we will estimate NO_x emissions for the Valley by the following:

flux/type x area of type x time (modified by diel variability)

Using this approach, we can calculate flux on an hourly, daily, weekly, and monthly basis.

Limitations to the approach:

- a) We assume that our sites are representative of all sites within a given type. Sampling in the extensive site will provide a test of this assumption.
- b) temporal resolution issues:
 - Hourly resolution will have to be estimated on the basis of several diel curves for each crop type. We cannot sample diel variability routinely.
 - While we will provide excellent data on daily temporal variability for the 13 types, we cannot assume that fluxes in all the fields within each type are the same on any given day. Because irrigation and fertilization regimes will be critical in determining fluxes, we expect a portion of the spatial and temporal variability in flux across the Valley to be controlled simply by when farmers irrigate or fertilize. Given that we do not have fine resolution data on those activities, temporal and spatial distributions of those activities will have to be modelled. We do not propose to do so, but expect that the ARB emissions modellers or other consultants will do so.

2. Total fluxes as a proportion of fertilizer applied

For crops receiving fertilization during the study period, we will calculate flux per unit of fertilizer applied. This value can then be multiplied times the fertilizer amounts utilized in those crop types during the whole summer period. For example, if we find that 2% of

fertilizer is lost as NO_x in corn crops, we can calculate total fluxes on the basis of fertilizer use.

3. Algorithm Development

We will develop equations relating NO_x flux to other variables measured in the field. We expect to develop two types of algorithms:

a) Those that require more detailed soil variables and that will be useful in process modelling frameworks.

e.g. $NO_x = f(\%WFPS, \text{soil texture, soil temp, air temp, soil } NO_3, \text{ soil } NH_4, \text{ organic matter content, instantaneous nitrification rates, etc})$

b) Those that can be applied directly to spatial data bases of crop type, soils and climate.

e.g. $NO_x = f(\text{soil texture, est. soil moisture, crop type, fert amount and type})$

Limitations: We do not propose to develop simulation models of flux. For example, soil moisture itself needs to be modelled on the basis of soil texture, precip and irrigation inputs, and evapotranspiration. We do not propose to develop such models, but the data base we will provide will aid other groups in doing so.

2. Provision of Data

These data will be available in Microsoft Exel 4.0 format and will be given to the ARB after they have been quality assured in our laboratories (they will be provided no later than the date of final report).

At each NO_x measurement point:

NO_x
air temp in the shade
soil temp at 2 cm depth
% soil water (0-10 cm increment for this and for all soil variables)
% water filled pore space
NH₄⁺-N ug/g dry weight of soil



NO₃⁻-N ug/g dry weight of soil
NO₂⁻-N ug/g dry weight soil
position in the field (e.g., interrow, furrow, crop row, etc)
proportion of plant cover
date
time

For each field, average values of:

soil bulk density
soil texture
%C and Organic matter
%N
time since irrigation
time since fertilization
type and amount of fertilizer

3. Final Report

The final report will include the following sections.

- a) Executive Summary
- b) Distribution of soils, crops, and management practices in the Valley and a description of our approach for selecting study sites.
- c) Study site descriptions
- d) Methods
- e) Tabulation and presentation of results for each crop combination(including all variables listed above (part 2)).
- f) Discussion of results for intensive and extensive sites, limitations to data.
- g) Emissions estimates using the three approaches listed above.